COMBINING CAMERA AND TELEMETRY DATA TO UNDERSTAND THE DYNAMICS OF WHITE-TAILED DEER IN SOUTH FLORIDA

by

LYDIA LENORA STIFFLER MARGENAU

(Under the Direction of Richard B. Chandler)

ABSTRACT

White-tailed deer (*Odocoileus virginianus*) are the primary prey of the endangered Florida panther (*Puma concolor coryi*) in South Florida, USA where reports of deer population declines have caused stakeholders concern. I used camera and GPS-telemetry data collected from January 2015 through December 2017 to evaluate the distribution, abundance, and demography of deer in the Big Cypress National Preserve and Florida Panther National Wildlife Refuge. I developed a generalized spatial-mark-resight (SMR) model, which revealed density was highest in the drier, western portion (4.3 females/km^2) and lowest in the wetter, eastern region (1.3 females/km^2). Temporal variation in density was driven primarily by seasonal environmental conditions. Long-term SMR trend estimates were negative at all sites, but the rate of decline was only significant at one site (β_1 = -0.074); annual decline was 1.92 females/km^2/yr. Using spatial-mark-resight models and objective weighting, I identified the optimal monitoring design for future long-term, camera-based studies of deer in the region. The most effective use of available resources involves a camera design with 40 on-trail cameras spaced a minimum of 250 m apart within a 25-km^2 area. I assessed deer population viability by calculating population growth and growth rate sensitivity using vital rates and density estimates from pre- and post-panther genetic

restoration. Although I found evidence that the deer population growth has declined since the panther restoration ($\lambda = 0.845$), estimates of population growth suggest the deer population was already declining prior to restoration efforts in 1995 ($\lambda = 0.957$), which is consistent with results from aerial monitoring. This suggests that other factors such as poor soil fertility, hydrology, the predator community, and hunting regulations may have negatively affected the population. While our results do not support the conclusion that panthers have caused the deer population declines, they do indicate that predator restoration has sped up the declines, which could threaten the long-term viability of the panther population unless either management can intervene to bolster the prey population, or cyclic predator-prey dynamics allow the deer population to recover.

INDEX WORDS: Camera, Population density, South Florida, Spatial mark-resight, Telemetry, Unmarked, White-tailed deer, Viability

COMBINING CAMERA AND TELEMETRY DATA TO UNDERSTAND THE DYNAMICS OF WHITE-TAILED DEER IN SOUTH FLORIDA

by

LYDIA LENORA STIFFLER MARGENAU

B.S., Clemson University, 2010

B.S., Clemson University, 2010

M.S., West Virginia University, 2017

A Dissertation Submitted to the Graduate Faculty of The University of Georgia in Partial Fulfillment of the Requirements for the Degree

DOCTOR OF PHILOSOPHY

ATHENS, GEORGIA

2021

COMBINING CAMERA AND TELEMETRY DATA TO UNDERSTAND THE DYNAMICS OF WHITE-TAILED DEER IN SOUTH FLORIDA

by

LYDIA LENORA STIFFLER MARGENAU

Major Professor:	Richard B. Chandler
Committee:	Karl V. Miller
	Michael J. Cherry
	Nathan P. Nibbelink

Electronic Version Approved:

Ron Walcott
Dean of the Graduate School
The University of Georgia
May 2021

DEDICATION

For my husband, Eric, who spent years believing and supporting me from miles away.

I can’t wait to start our adventure together.

ACKNOWLEDGEMENTS

I thank the Florida Fish and Wildlife Conservation Commission (FWC) for providing research funding. I also thank the US Fish and Wildlife Service, US National Park Service, and the Warnell School of Forestry at the University of Georgia for their incredible support. My research was only part of a large-scale deer research project that came to be known as the South Florida Deer Study. I am extremely grateful and honored to have been a part of such an extraordinary collaborative project. I thank all of the women and men at the FWC who provided technical and logistical support. I thank Elina Garrison of the FWC Fish and Wildlife Research Institute for her steadfast commitment to the success of the project through technical and logistical support. I thank the women and men of the National Park Service aviation team who were pivotal to the success of our deer capture efforts. I thank the entire staff at the Florida Panther National Wildlife Refuge for their accommodating cooperation and ensuring I made it out of the swamp every day. I want to acknowledge all my fellow graduate students on the project: Daniel Crawford, Brian Kelly, Kristen Engebretsen, Hunter Ellsworth, and Heather Abernathy. You each paved the way for me to successfully wrap up the study and I'm proud to call you colleagues, friends, and scientists. I want to acknowledge the countless field technicians on the project and their relentless hard work and commitment to quality data. I thank Heather Gaya for her statistical support in navigating the Bayesian world. I thank Michael Cherry for exposing me to the complexities of predator-prey relationships and igniting a passion for studying disturbance landscapes. I thank Karl V. Miller for welcoming this birder into the UGA Deer Lab. His passion for deer management assisted me in making connections between my

quantitative research and real-world application. I thank my Advisory member Nathan Nibbelink for his critical evaluation of my research methods and resulting inferences. Finally, I express my gratitude for my committee chair, Richard Chandler, for his mentorship and guidance through my graduate career. I will forever be thankful that you took a chance in responding to the email of an aspiring quantitative ecologist.

TABLE OF CONTENTS

Page

LIST OF TABLES

Page

LIST OF FIGURES

Page

LIST OF APPENDICES

Page

CHAPTER 1

RESEARCH OVERVIEW

INTRODUCTION

In South Florida, white-tailed deer (*Odocoileus virginianus*) are an important economic and recreational resource, and an integral component of one of North America's most unique ecosystems. Hunter expenditures exceed $700 million annually and almost 80% of Florida's 242,000 hunters partake in deer hunting, making deer the most popular game species in the state (U.S. Dept. of the Interior et al. 2011). In South Florida, deer are the dominant herbivore and they are the primary prey of the endangered Florida panther (*Puma concolor coryi*; Maehr et al. 1990, Fleming et al. 1994, Caudill et al. 2019). Aerial surveys and hunter harvest data suggest that since 2000, deer populations have declined in the southernmost units of the Big Cypress National Preserve (BCNP), while other units have experienced fluctuating population trends (Garrison et al. 2011). Although these declines have coincided with changing hydrological regimes, habitat conditions, predator communities, and hunting regulations, the magnitude to which these variables have impacted the deer population remains unknown, raising concerns about the long-term viability of deer in South Florida.

In recent years, South Florida has undergone major hydrological restoration efforts following the authorization of the multi-billion-dollar, 30-year Comprehensive Everglades Restoration Plan (CERP) to restore, protect, and preserve the greater Everglades ecosystem (Sklar et al. 2005, Wiederholt et al. 2020). To reestablish the pre-drainage hydrology, alterations must be made to water flow, depths, timing, and distribution. With the predicted increase in

water levels, the deer population may experience negative effects through reduced survival and recruitment and alterations in habitat use (Loveless 1959, Labisky et al. 1999, MacDonald-Beyers and Labisky 2005, Paudel et al. 2020). These effects may be compounded by the already low population density, low productivity, high fawn morality, and small body size in the South Florida deer population (Harlow and Jones 1965, Richter and Labisky 1985, Labisky et al. 1991, Boulay 1992, Heffelfinger 2011). Seasonal fluctuations in hydrology and fire coupled with low soil fertility influence the distribution and succession of plant communities thereby altering resource availability for deer (Harlow and Jones 1965, Klein et al. 1970, Duever 1984, Kilgo and Labisky 1995, Duever 2005). Alongside hydrological restoration, managers are attempting to restore the historical fire regime with shifts in the intensity of wildfires and frequency of prescribed fire thereby reversing decades of fire suppression (Cherry et al. 2018, Noss 2018).

The primary change in the predator community has been the increase in the panther population. By the 1920's panthers only existed in Central and South Florida. In 1967, they were listed as an Endangered Species, yet the population continued to decline with their range contracting to a few areas in South Florida (Onorato et al. 2010). Following successful genetic reintroduction efforts, legal protection, and habitat and prey conservation, the Florida panther population has steadily increased since 1995 to estimates exceeding 200 individuals (McClintock et al. 2015, Florida Fish and Wildlife Conservation Commission 2017, van de Kerk et al. 2019). Prior to genetic reintroduction efforts, panther predation of deer was nominal, with wild pigs (*Sus scrofa*) being the dominant prey (Maehr et al. 1990). During this time, bobcats (*Lynx rufus*) were the primary predators of fawns and adult deer (Boulay 1992, Labisky and Boulay 1998). However, following panther genetic rescue efforts, bobcat and wild pig abundances declined, although the relative role of changes in hydrology, hunting regulations, and predation remains

unclear (Roberts and Crimmins 2010, Caudill et al. 2019). Additionally, black bear (*Ursus americanus*) populations have increased, coyotes (*Canis latrans*) have colonized, and invasive Burmese pythons (*Python bivittatus*) have become established in this region, further limiting mammalian prey species (Wilson et al. 2010, Dorcas et al. 2012, Telesco 2012, Humm et al. 2017, McCleery et al. 2015).

In addition to top-down predation pressures, deer are subjected to hunter harvest. Deer hunting in South Florida has a long-standing tradition supporting both subsistence and recreational hunters. Historically, access to BCNP was unlimited with hunters able to reach most remote areas using airboats and swamp buggies. However, concerns over excessive harvest in recent decades led to several regulation changes designed to limit access, reduce hunting pressure and harvest, and protect fawns and female deer (Schortemeyer et al. 1991). Within BCNP, an extensive trail system was established and off-road vehicle (ORV) use was limited to designated trails. Antlerless harvest was prohibited in the private properties surrounding BCNP, with BCNP instituting additional antlered regulations to protect young males and limit or exclude harvest in areas with significant declining populations (Garrison et al. 2011). The impact of these regulations and hunter harvest on current deer population dynamics is needed.

Given concerns about deer population declines, reliable techniques for estimating deer population dynamics within the rapidly changing landscape are needed to guide management actions. The most commonly employed monitoring technique for white-tailed deer in South Florida is aerial surveying. The National Parks Service conducts aerial count surveys, while Florida Fish and Wildlife Conservation Commission implements aerial line transect distance sampling (Buckland et al. 2001). Aerial surveys allow for more maneuverability in sampling large regions that are difficult to access but are inherently dangerous and expensive to perform

(Caughley 1997, DeYoung 2011). The precision and accuracy of estimates from distance sampling are often highly variable and dependent on the vegetation structure, time of day, flying altitude, observer skill, and population density within an area (Graves et al. 1972, Rice and Harder, 1977, Beasom 1979, Beasom et al. 1986, Pollock and Kendall 1987, Dunn et al. 2002). Closed canopy habitats, such as pine and cypress that are prevalent in portions of South Florida, tend to result in low detectability, suggesting aerial surveys may be ill suited for monitoring populations within these areas (Dunn et al. 2002, Potvin et al. 2004, DeYoung 2011).

Camera-based surveys are an alternative to aerial surveys, as they are relatively non-invasive and can be used to monitor wildlife communities (Kucera and Barrett 2011). Data from camera surveys can be used to estimate abundance, density, and activity patterns (Karanth 1995, Jacobson et al. 1997, Karanth and Nichols 1998, Bridges et al. 2004, Dodd et al. 2004, Kucera and Barrett 2011, Caravaggi et al. 2017). In camera trapping studies, remote cameras are often situated along trails or baited stations, and individual animals are photographed and identified either manually or using specialized software through the use of distinguishing characteristics (Kucera and Barrett 2011). Traditional protocols for estimating population size of white-tailed deer from camera trapping are based on individual recognition of the majority of males within a sampled area based on antler characteristics (Jacobson et al. 1997, Weckel et al. 2011). These estimates are derived from ratios of photographic occurrences of branch-antlered males, spike males, females, and fawns from baited surveys (Jacobson et al. 1997). Major limitations to this technique is that it does not provide measures of uncertainty surrounding the parameter estimates, often requires a high density of baited cameras, and extensive time devoted to identifying unique antlered males. Although modifications using bootstrapping have addressed

this deficiency (Weckel et al. 2011, Gulsby et al. 2015), the Jacobson method still relies upon the assumption of equal detection between all age-sex groups.

Modern approaches to density estimation from camera data use spatial capture-recapture (SCR) or spatial mark-resight (SMR) models, which are individual-based, spatially explicit models of population dynamics (Chandler and Clark 2014, Royle et al. 2013, Chandler et al. 2018). These hierarchical models provide direct estimates of density and population size within explicit spatial regions by modeling capture probability as a function of the distance between camera locations and individual activity centers, which are modeled as outcomes of a spatial point process model (Efford 2004, Borchers and Efford 2008, Royle and Young 2008, Royle et al. 2009). Although unobserved, individual activity centers can be estimated using the spatial coordinates of the camera traps in which individuals are detected. Few studies have applied SMR models to camera data on white-tailed deer. Beaver et al. (2017) demonstrated that standard SMR models could be fitted to data on male deer that have been uniquely identified by their antler characteristics. Chandler et al. (2018) developed an SMR model to estimate white-tailed deer fawn survival and recruitment. Their model requires that all detected fawns can be uniquely identified based on spot patterns. Although these methods were shown to be highly effective, they are labor intensive because they can involve manual interpretation and cross-referencing of thousands of images. Moreover, adult female deer lack unique markings, prohibiting the use of standard SMR models (Johnson 2019). Recent extensions of SCR models have relaxed the requirement of individual recognition, now allowing for concepts to be applied to studies of unmarked or partially-marked populations, which may prove effective for monitoring deer in South Florida (Chandler and Royle 2013, Sollmann et al. 2013, Whittington et al. 2018).

STUDY AREA AND DESIGN

The Big Cypress Basin in South Florida is characterized by hot, wet summers (May–October) with dry, cool winters (November–April; Hela 1952, Duever et al. 1986). This region consists of a mosaic of vegetative community types influenced by seasonal fluctuations in hydrology (McPherson 1974). A secondary influence on the ecosystem is fire, which controls the structure and composition of plant species (Duever et al. 1986). Within the Big Cypress Basin, primary vegetation communities were dominated by pine forests, cypress forests, and freshwater marshes, interspersed with hammock forests and wet prairies (McPherson 1974, Duever et al. 1986). Pine and hammock forests are found at higher elevations than the surrounding cypress forests and wet prairies (McPherson 1974).

Pine forests may become inundated following heavy rainfall and can persist in this state for months during the wet season. These areas occur atop mineral soils and are dominated by slash pine (*Pinus elliottii*) with an understory of cabbage palm (*Sabal palmetto*), saw palmetto (*Serenoa repens*), and evergreen shrubs. Islands of hammock forests occur on bedrock outcrops and are comprised of hardwoods, palms, ferns, and shrubs and occur among or along the edges of lower elevation, herbaceous or forested wetlands (McPherson 1974, Duever et al. 1986).

The low elevation of cypress forests results in almost year-round inundation. These areas consist of organic soils on top of limestone bedrock and can vary in composition from large, open stands of cypress (*Taxodium distichm*) to mixed swamps with dense tangles of trees, vines, shrubs, and epiphytes (Duever et al. 1986). Wet prairies and marshes are seasonally inundated communities dominated by emergent vegetation. During the wet season, wet prairies become inundated, but usually dry out during the dry season. Marshes have deeper standing water, but may infrequently dry out. These areas consist of organic soils dominated by sawgrass (*Cladium*

mariscus) and rushes (*Juncus* spp.) with alligator flag (*Thalia geniculata*) in deeper depressions (McPherson 1974, Duever et al. 1986).

The study occurred within the primary range of the Florida panther and consisted of the Bear Island (BI) and North Addition Lands (AL) units of the Big Cypress National Preserve (BCNP) and the adjacent Florida Panther National Wildlife Refuge (FPNWR; Figure 1.1). The areas of BI, AL, and FPNWR encompassed approximately 190 km^2, 271 km^2, and 107 km^2, respectively. These study sites were selected based on availability of historical data, presence of GPS-collared panthers, existing camera grids, access and feasibility, consultation with area biologists and managers, and variation in hydrological gradient and hunting regulations.

RESEARCH OBJECTIVES

Using infrared-triggered camera trap data and GPS-telemetry relocation data, I investigated the population dynamics of white-tailed deer in the Big Cypress Basin, Florida to address three objectives:

1. Develop a suite of generalized spatial capture-recapture models that combine telemetry and camera data for spatio-temporal inferences about density in a partially marked population of white-tailed deer.
2. Assess the optimal camera survey design for monitoring white-tailed deer in South Florida using objective weighting between density estimation precision and logistical costs.
3. Evaluate the viability of the South Florida white-tailed deer population using a stage-structured population model.

DISSERTATION FORMAT

This dissertation is presented in manuscript format. Chapter 1 provides a research overview incorporating an introduction and background of relevant studies, motivation for my research, and description of the research study area. Chapter 2 focuses on the development of a quantitative framework for monitoring partially-marked wildlife population using camera and telemetry data and its estimation of white-tailed deer abundances and densities. Chapter 3 presents an investigation of optimal camera trap survey design using objective weighting between model precision and logistical costs for monitoring white-tailed deer within Big Cypress Basin. Chapter 4 focuses on the development of a stage-structured population model for white-tailed deer within the Big Cypress Basin to forecast population viability pre- and post-panther genetic restoration efforts. Chapter 5 provides general conclusions, management recommendations, and prospective topics for future research.

LITERATURE CITED

Beasom, S. L. 1979. Precision in helicopter censusing of white-tailed deer. Journal of Wildlife Management 43:777–780.

Beasom, S. L., F. G. Leon III, and D. R. Synatzske. 1986. Accuracy and precision of counting white-tailed deer with helicopters at different sampling intensities. Wildlife Society Bulletin 14:364–368.

Beaver, J. T., C. A. Harper, L. I. Muller, P. S. Basinger, M. J. Goode, and F. T. Van Manen. 2016. Current and spatially explicit capture-recapture analysis methods for infrared triggered camera density estimation of white-tailed deer. Journal of the Southeastern Association of Fish and Wildlife Agencies 3:195–202.

Borchers, D. L. and M. G. Efford. 2008. Spatially explicit maximum likelihood methods for capture-recapture studies. Biometrics 64:377–385.

Boulay, M.C. 1992. Mortality and recruitment of white-tailed deer fawns in the wet prairie/tree island habitat of the Everglades. Thesis. University of Florida, Gainesvilles, Florida.

Bridges, A. S., M. R. Vaughan, and S. Klenzendorf. 2004. Seasonal variation in American black bear *Ursus americanus* activity patterns: quantification via remote photography. Wildlife Biology 10:277–284.

Buckland, S. T., E. A. Rexstad, T. A. Marques, and C. S. Oedekoven. 2001. Introduction to distance sampling: estimating abundance of biological populations. Oxford University Press, New York, New York, USA.

Caravaggi, A., P. B. Banks, A. C. Burton, C. M. V. Finlay, P. M. Haswell, M. W. Hayward, M. J. Rowcliffe, and M. D. Wood. 2017. A review of camera trapping for conservation behaviour research. Remote Sensing in Ecology and Conservation 3:109–122.

Caudill, G., D. P. Onorato, M. W. Cunningham, D. Caudill, E. H. Leone, L. M. Smith, and D. Jansen. 2019. Temporal trends in Florida panther food habits. Human–Wildlife Interactions, 13:87–97.

Caughley, G. 1977. Sampling in aerial survey. Journal of Wildlife Management 41:605–615.

Chandler, R. B., and J. D. Clark. 2014. Spatially explicit integrated population models. Methods in Ecology and Evolution 5:1351–1360.

Chandler, R. B., K. Engebretsen, M. J. Cherry, E. P. Garrison, K. V. Miller. 2018. Estimating recruitment from capture–recapture data by modeling spatio-temporal variation in birth and age-specific survival rates. Methods in Ecology and Evolution 9: 2115–2130.

Chandler, R. B., and J. A. Royle. 2013. Spatially explicit models for inference about density in unmarked or partially marked populations. Annuals of Applied Statistics 7:936–954.

Cherry, M. J., R. B. Chandler, E. P. Garrison, D. A. Crawford, B. D. Kelly, D. B. Shindle, K. G. Godsea, K. V. Miller, and L. M. Conner. 2018. Wildfire affects space use and movement of white-tailed deer in a tropical pyric landscape. Forest Ecology and Management 409:161–169.

DeYoung, C. A. 2011. Population dynamics. Pages 147–180 *in* D. G. Hewitt (ed.) Biology and management of white-tailed deer. CRC Press, Boca Raton, Florida, USA.

Dodd, K. C. Jr. W. J. Barichivich, and L. L. Smith. 2004. Effectiveness of a barrier wall and culverts in reducing wildlife mortality on a heavily traveled highway in Florida. Biological Conservation 118:619–631.

Dorcas, M. E., J. D. Wilson, R. N. Reed, R. W. Snow, M. R. Rochford, M. A. Miller, W. E. Meshaka Jr., P. T. Andreadis, F. J. Mazzotti, C. M. Romagosa, and K. M. Hart. 2012. Severe mammal declines coincide with proliferation of invasive Burmese pythons in Everglades National Park. Proceedings of the National Academy of Science of the United States of America 109:2418–2422.

Duever, M. J. 1984. Environmental factors controlling plant communities of the Big Cypress Swamp. Pages 127–137 *in* P. J. Gleason (ed.) Environments of South Florida: Past and Present II. Miami Geological Society, Miami, Florida, USA.

Duever, M. J. 2005. Big Cypress regional ecosystem conceptual ecological model. Wetlands 25:843–853.

Duever, M. J., J. E. Carlson, J. F. Meeder, L. C. Duever, L. H. Gunderson, L. A. Riopelle, T. R. Alexander, R. F. Myers, and D. P. Spangler. 1986. The Big Cypress National Preserve. National Audubon Society Research Report No. 8, New York, New York, USA.

Dunn, W. C., J. P. Donnelly, and W. K. Krausmann. 2002. Using thermal infrared sensing to count elk in the southwestern United States. Wildlife Society Bulletin 30:963–967.

Efford, M. 2004. Density estimation in live-trapping studies. Oikos 106:598–610.

Fleming, M., J. Schortemeyer, and J. Ault. 1994. Distribution, abundance, and demography of white-tailed deer in the Everglades. Pages 147–180 *in* D. Jordan (ed.). Proceedings of the Florida Panther Conference. Fort Myers, Florida, USA. U.S. Fish and Wildlife Service, Gainesville, Florida, USA.

Florida Fish and Wildlife Conservation Commission. 2017. Annual report on the research and management of Florida panthers: 2016-2017. Fish and Wildlife Research Institute and Division of Habitat and Species Conservation, Naples, Florida, USA.

Garrison, E., E. Leone, K. Smith, T. Bartareau, J. Bozzo, R. Sobczak, and D. Jansen. 2011. Analysis of hydrological impacts on white-tailed deer in the Stairsteps Unit, Big Cypress National Preserve. Fish and Wildlife Research Institute Technical Report US National Park Service, Gainesville, Florida, USA.

Graves, H. B., E. D. Bellis, and W. M. Knuth. 1972. Censusing white-tailed deer by airborne thermal infrared imagery. Journal of Wildlife Management 36:875–884.

Gulsby, W. D., C. H. Killmaster, J. W. Bowers, J. D. Kelly, B. N. Sacks, M. J. Statham, and K. V. Miller. 2015. White-tailed deer fawn recruitment before and after experimental coyote removals in central Georgia. Wildlife Society Bulletin 39:248–255.

Harlow, R. F., and F. K. Jones (eds). 1965. The white-tailed deer in Florida. Florida Game and Fresh Water Fish Commission Technical Bulletin No. 9, Tallahassee, Florida, USA.

Heffelfinger, J. R. 2011. Taxonomy, evolutionary history, and distribution. Pages 3–39 *in* D. G. Hewitt (ed.) Biology and management of white-tailed deer. CRC Press, Boca Raton, Florida, USA.

Hela, I. 1952. Remarks on the climate of southern Florida. Bulletin of Marine Science of the Gulf and Caribbean 2:438–447.

Hooten, M. B., D. S. Johnson, E. M. Hanks, and J. H. Lowry. 2010. Agent-based inference for animal movement and selection. Journal of Agricultural, Biological, and Environmental Statistics 15:523–538.

Humm, J. M., J. W. McCown, B. K. Scheick, and J. D. Clark. 2017. Spatially explicit population estimates for black bears based on cluster sampling. Journal of Wildlife Management 81:1187–1201.

Jacobson, H. A., J. C. Kroll, R. W. Browning, B. H. Koerth, and M. H. Conway. 1997. Infrared-triggered cameras for censusing white-tailed deer. Wildlife Society Bulletin 25:547–556.

Johnson, J. T. 2019. White-tailed deer camera surveys: Density estimation and spatiotemporal dynamics. Dissertation, University of Georgia, Athens, Georgia, USA.

Karanth, K. U. 1995. Estimating tiger *Panthera tigris* populations from camera trap data using capture-recapture models. Biological Conservation 71:333–338.

Karanth, K. U., and J. D. Nichols. 1998. Estimation of tiger densities in India using photographic captures and recaptures. Ecology 79:2852–2862.

Kautz, R., R. Kawula, T. Hoctor, J. Comiskey, D. Jansen, D. Jennings, J. Kasbohm, F. Mazzotti, R. McBride, L. Richardson, and K. Root. 2006. How much is enough? Landscape-scale conservation for the Florida panther. Biological Conservation 130: 118–133.

Kilgo, J. C. and R. F. Labisky. 1995. Nutritional quality of three major deer forages in pone flatwoods of northern Florida. Florida Scientist 58:320–326.

Klein, H., W. J. Schneider, B. F. McPherson, and T. J. Buchanan. 1970. Some hydrologic and biologic aspects of the Big Cypress Swamp drainage area. United States Geological Survey, Washington, DC, USA.

Kucera, T. E., and R. H. Barrett. 2011. A history of camera trapping. Pages 9–26 *in* A. F. O'Connell, J. D. Nichols, and K. U. Karanth (eds.). Camera traps in animal ecology methods and analyses. Springer, New York, New York, USA.

Labisky, R. F., and M. C. Boulay. 1998. Behaviors of bobcats preying on white-tailed deer in the Everglades. American Midland Naturalist 139:275–281.

Labisky, R. F., D. E. Fritzen, and J. C. Kilgo. 1991. Population ecology and management of white-tailed deer in the Osceola National Forest, Florida. Final Report to Florida Game and Fresh Water Fish Commission, Department of Wildlife and Range Sciences, University of Florida, Gainesville, Florida, USA.

Labisky, R. F., K. E. Miller, and C. S. Hartless. 1999. Effect of Hurricane Andrew on survival and movements of white-tailed deer in the Everglades. Journal of Wildlife Management 83:872–879.

Loveless, C.M. 1959. The Everglades deer herd life history and management. Florida Game and Fresh Water Fish Commission. Technical Bulletin No. 6, Tallahassee, Florida, USA.

MacDonald-Beyers, K., and R. F. Labisky. 2005. Influence of flood waters on survival, reproduction, and habitat use of white-tailed deer in the Florida Everglades. Wetlands 25:659-666.

Maehr, D. S., R. C. Belden, E. D. Land, and L. Wilkins. 1990. Food habits of panthers in southwest Florida. Journal of Wildlife Management 54:420–423.

McCleery, R. A., A. Sovie, R. N. Reed, M. W. Cunningham, M. E. Hunter, and K. M. Hart. 2015. Marsh rabbit mortalities tie pythons to the precipitous decline of mammals in the Everglades. Proceedings of the Royal Society B 282:20150120.

McClintock, B. T., D. P. Onorato, and J. Martin. 2015. Endangered Florida panther population size determined from public reports of motor vehicle collision mortalities. Journal of Applied Ecology 52:893–901.

McPherson, B. F. 1974. The Big Cypress Swamp. Environments of South Florida: present and past. Miami Geological Society, Miami, Florida, USA.

Noss, R. F. 2018. Fire ecology of Florida and the Southeastern Coastal Plain. University Press of Florida, Gainesville, Florida, USA.

Onorato, D. P., R. Belden, M. Cunningham, D. Land, R. McBride, and M. E. Roelke. 2010. Long-term research on the Florida panther (*Puma concolor coryi*): historical findings and future obstacles to population persistence. Pages 453–469 *in* D. Macdonald and A. Loveridge (eds). Biology and conservation of wild felids. Oxford University Press, Oxford, United Kingdom.

Paudel, R. T. Van Lent, G. M. Naja, Y. Khare, R. Wiederholt, and S. E. Davis III. 2020. Assessing the hydrologic response of key restoration components to Everglades

ecosystem. Journal of Water Resource Planning and Management 146:04020084. DOI: 10.1061/(ASCE)WR.1943-5452.0001283.

Pollock, K. H. and W. L. Kendall. 1987. Visibility bias in aerial surveys: a review of estimation procedures. Journal of Wildlife Management 51:502–510.

Potvin, F., L. Breton, and L.-P. Rivest. 2004. Aerial surveys for white-tailed deer with the double-count technique in Québec: two 5-year plans completed. Wildlife Society Bulletin 32:1099–1107.

Rice, W. R., and J. D. Harder. 1977. Application of multiple aerial sampling to a mark-recapture census of white-tailed deer. Journal of Wildlife Management 41:197–206.

Richter, A. R. and R. F. Labisky. 1985. Reproductive dynamics among disjunct whit-tailed deer herds in Florida. Journal of Wildlife Management 49:964–971.

Roberts, N. M. and S. M. Crimmins. 2010. Bobcat population status and management in North America: Evidence of large-scale population increase. Journal of Fish and Wildlife Management 1:169–174.

Royle, J. A., J. D. Nichols, K. U. Karanth, and A. M. Gopalaswamy. 2009. A hierarchical model for estimating density in camera-trap studies. Journal of Applied Ecology 46:118–127.

Royle, J. A. R. B. Chandler, R. Sollmann, and B. Gardner. 2013. Spatial capture-recapture. Academic Press, Waltham, Massachusetts, USA.

Royle, J. A., and K. V. Young. 2008. A hierarchical model for spatial capture-recapture data. Ecology 89:2281–2289.

Schortemeyer, J. L. D. S. Maehr, J. W. McCown, E. D. Land, and P. D. Manor. 1991. Prey management for the Florida panther: a unique role for wildlife managers. Transactions of the North American Wildlife and Natural Resources Conference 56:512–526.

Sklar, F.H., M. J. Chimney, S. Newman, P. McCormick, D. Gawlik, S. Miao, C. McVoy, W. Said, J. Newman, C. Coronado, and G. Crozier. 2005. The ecological–societal underpinnings of Everglades restoration. Frontiers in Ecology and the Environment 3:161–169.

Sollmann, R., B. Gardner, R. B. Chandler, D. B. Shindle, D. P. Onorato, J. A. Royle, and A. F. O'Connell. 2013. Using multiple data sources provides density estimates for endangered Florida panther. Journal of Applied Ecology 50:961–968.

Telesco, D. 2012. Florida black bear removed from list of state threatened species. International Bear News 27:10–11.

U.S. Department of the Interior, U.S. Fish and Wildlife Service, and U.S. Department of Commerce, U.S. Census Bureau. 2011 National Survey of Fishing, Hunting, and Wildlife-Associated Recreation. https://www.arcgis.com/home/item.html?id=6edf33864f3c4f18a3eb0fd01887c88e.

U.S. Fish and Wildlife Service, Florida Fish and Wildlife Conservation Commission, and Wildlife Research Institute. 2018. Florida Panther Focus Area [GIS data].

van de Kerk, M., D. P. Onorato, J. A. Hostetler, B. M. Bolker, and M. K. Oli. 2019. Dynamics, persistence, and genetic management of the endangered Florida panther population. Wildlife Monographs 2013: 3–35.

Weckel, M., R. F. Rockwell, F. Secret. 2011. A modification of Jacobson et al.'s (1997) individual branch-antlered male method for censusing white-tailed deer. Wildlife Society Bulletin 35:445–451.

Whittington, J., M. Hebblewhite, R. B. Chandler. 2018. Generalized spatial mark-resight models with an application to grizzly bears. Journal of Applied Ecology 55:157–168.

Wiederholt, R., G. A. Stainbeck, R. Paudel, Y. Khare, M. Naja, S. E. Davis III, and T. Van Lent. 2020. Economic valuation of the ecological response to hydrologic restoration in the Greater Everglades ecosystem. Ecological Indicators 117:106678. DOI: 10.1016/j.ecolind.2020.106678

Wilson, J. D., M. E. Dorcas, and R. W. Snow. 2011. Identifying plausible scenarios for the establishment of invasive Burmese pythons (*Python molurus*) in Southern Florida. Biological Invasions 13:1492–1504.

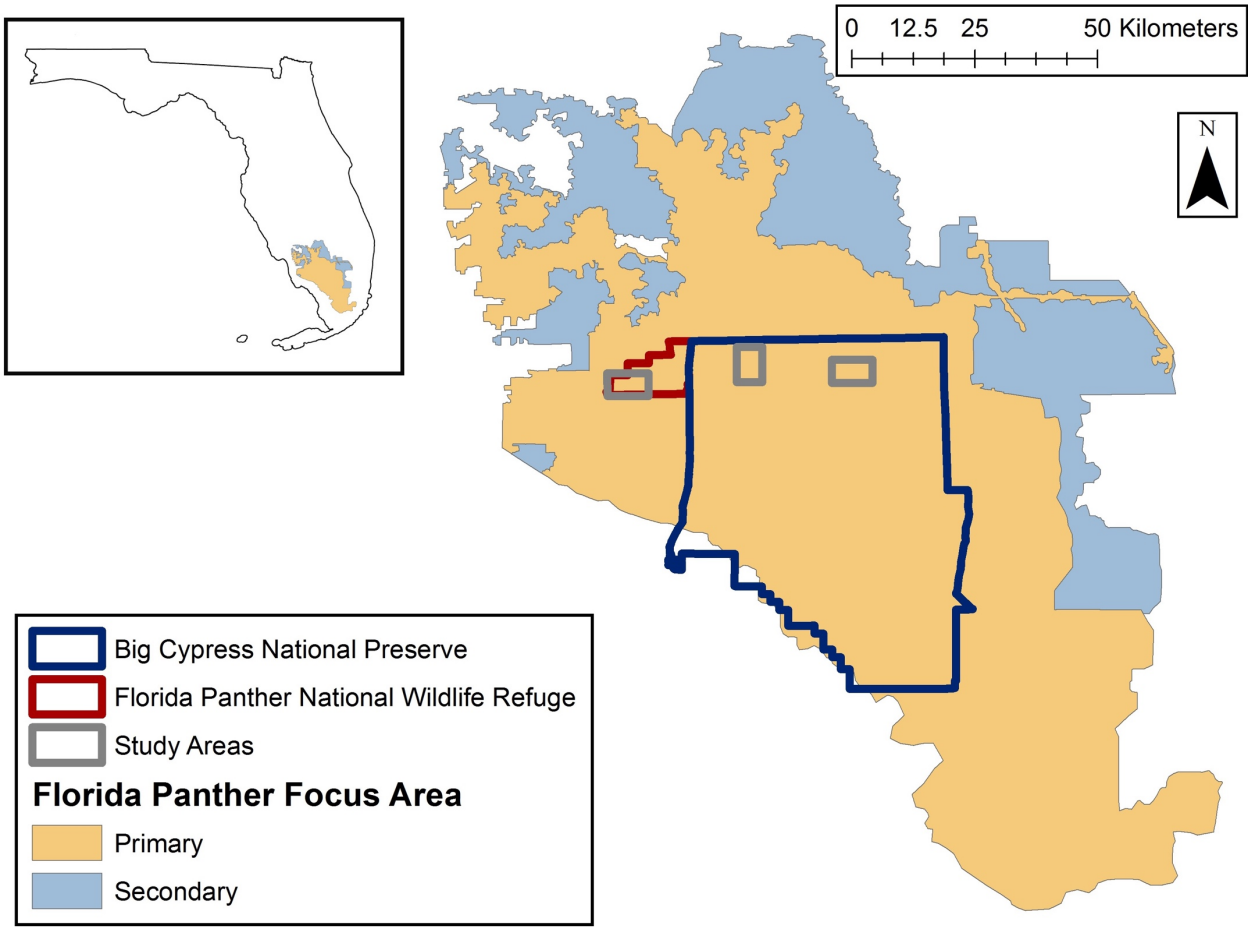

Figure 1.1 The study area with respect to the Florida panther primary and secondary habitat focus areas (Kautz et al. 2006, USFWS 2018). The central (Bear Island) and eastern (North Addition Lands) camera grids were located in Big Cypress National Preserve. The western grid was located in the Florida Panther National Wildlife Refuge.

CHAPTER 2

MONITORING PARTIALLY-MARKED POPULATIONS USING CAMERA AND TELEMETRY DATA[1]

[1] Margenau, L. L. S., M. J. Cherry, K. V. Miller, E. P. Garrison, and R. B. Chandler. Submitted to *Ecological Applications*, 1/25/2021

ABSTRACT

Long-term monitoring is a critical component of effective wildlife conservation. However, many of the available methods for estimating density are too costly or difficult to implement over large spatial and temporal extents. Recently developed spatial mark-resight (SMR) models are increasingly being applied as a cost-effective method to estimate density when data include detections of both marked and unmarked individuals. We developed a generalized SMR model that can accommodate long-term camera data and auxiliary telemetry data for improved spatio-temporal inference in monitoring efforts. The model can be applied in two-stages, with detection parameters estimated in the first stage using telemetry data and camera detections of instrumented individuals. Density is estimated in the second stage using camera data, with all individuals treated as unmarked. Serial correlation in detection and density parameters is accounted for using time-series models. The two-stage approach reduces computational demands and facilitates the application to large datasets from long-term monitoring initiatives. We applied the model to three years (2015-2017) of white-tailed deer (*Odocoileus virginianus*) data collected in three areas of the Big Cypress Basin, Florida, USA. Fifty-nine females marked with ear-tags and fitted with GPS-telemetry collars were detected along with unmarked females on 180 remote cameras. Density estimates were higher in the western portion of the study area and lower in the eastern region. Most of the temporal variation in density was driven by seasonal fluctuations, but one study area exhibited a slight long-term population decline. Modern technologies such as camera traps provide novel possibilities for long-term monitoring, but the resulting massive datasets, which are subject to unique sources of observation error, have posed analytical challenges. The two-stage spatial mark-resight framework provides a solution with lower computational demands than joint SMR models,

allowing for easier implementation in practice. In addition, after detection parameters have been estimated, the model may be used to estimate density even if no synchronous auxiliary information on marked individuals is available, which is often the case in long-term monitoring.

INTRODUCTION

Long-term monitoring is critical to effective wildlife conservation. Monitoring methods that allow for inferences about abundance are preferred over methods that yield simple indices because information about abundance is critical for understanding the drivers of population dynamics (Yoccoz et al., 2001; Williams et al., 2002; Nichols & Williams, 2006). However, many of the available abundance-estimation methods are too costly or difficult to implement over large spatial and temporal extents (Buckland et al., 2001; Williams et al., 2002; Giudice et al., 2010). Consequently, studies of population dynamics and long-term monitoring efforts have often been viewed as distinct endeavors (Williams et al., 2018). Emerging technologies such as camera traps coupled with recently developed hierarchical modeling techniques provide an opportunity to narrow the divide between studies of population dynamics and long-term monitoring efforts to produce reliable estimates at appropriate scales (Royle & Dorazio, 2008; Williams et al., 2018).

Capture-recapture (CR) methods are widely used for estimating abundance. Traditional CR methods require physically capturing and marking individuals within the population followed by repeated sampling. The information from the recapture of individuals and the proportions of marked and unmarked individuals captured during sampling periods allows for inferences about population size and demographic rates such as survival and recruitment (Pollock et al., 1990). Although these methods often result in reliable inferences, they can be

impractical due to the logistical costs and difficulty in trapping individuals. Traditional live-capture methods are also more invasive than modern methods such as camera trapping (Karanth, 1995; Karanth & Nichols, 1998; Royle, Chandler, Sollmann, & Gardner, 2013), DNA sampling (Mowat & Strobeck, 2000; Kéry et al., 2010; Augustine et al., 2019), and acoustic recording (Dawson & Efford, 2009; Royle, 2018). Additionally, traditional CR analyses do not allow for inferences on spatial variation in population and detection parameters.

For species with unique natural characteristics (e.g., pelage, scars, antlers), spatial capture-recapture (SCR) models can use camera data to make inferences about density and other population parameters. These hierarchical models provide direct estimates of density and population size within explicit spatial regions by modeling capture probability as a function of the distance between trap locations and individual activity centers, which are modeled as outcomes of a spatial point process (Efford, 2004; Borchers & Efford, 2008; Royle & Young, 2008; Royle et al., 2009). Although unobserved, individual activity centers can be estimated using the spatial coordinates of the traps where individuals are detected. However, many species lack natural markings, making it impossible to use standard SCR techniques. Recent extensions of SCR models have relaxed the requirement of individual recognition, allowing for inferences about abundance and density to be drawn from camera data on unmarked or partially marked populations (Chandler & Royle, 2013; Sollmann, Gardner, Chandler, et al., 2013). These approaches work best when ancillary information about detection probability is available, such as when a subset of the population is marked or accompanying telemetry data is available (Sollmann, Gardner, Parsons, et al., 2013; Ramsey et al., 2015; Augustine et al., 2018).

Spatial mark-resight (SMR) models can be applied to estimate density when data include detections of both marked and unmarked individuals (Chandler & Royle, 2013; Royle, Chandler,

Sollmann, & Gardner, 2013; Sollmann, Gardner, Chandler, et al., 2013; Royle et al., 2018; Jimenez et al., 2018; Whittington et al., 2018). Recent extensions of these models relax the assumption that marked and unmarked individuals have the same detection parameters (Whittington et al., 2018; Efford & Hunter, 2018; Augustine et al., 2019), and several studies have demonstrated the benefits of including telemetry data in mark-resight models (Royle et al., 2009; Gopalaswamy et al., 2012; Royle, Chandler, Sun, & Fuller, 2013; Tenan et al., 2017; Linden et al., 2018; Tourani et al., 2020). When telemetry data and camera data are collected concurrently, telemetry data can be used to estimate activity center locations, which can greatly increase the precision of detection parameters while providing a more accurate representation of spatial variation in density and space use (Raabe et al., 2013; Sollmann, Gardner, Parsons, et al., 2013; Jimenez et al., 2018; Whittington et al., 2018). These methods have only been applied to data from short time periods when populations can be assumed to be closed.

In this paper, we extend generalized spatial mark-resight models to accommodate long-term camera data and auxiliary telemetry data for improved spatio-temporal inferences in monitoring efforts. The proposed framework consists of consecutive, closed population periods linked by a time series model of density. The modeling framework attempts to balance model complexity with computational demands and logistical constraints ubiquitous to long-term monitoring initiatives. We demonstrate the approach using camera data and GPS-telemetry data collected continuously on white-tailed deer (*Odocoileus virginianus*) over a three-year period in the Big Cypress Basin, Florida, USA. Using the density estimates, we assessed deer population trends within the region.

METHODS

GENERALIZED SMR MODEL

The proposed model is a two-stage SMR model in which temporal variation in the detection parameters is estimated in the first stage using telemetry data and camera detections of instrumented individuals, and density is estimated in the second stage using camera data, with all individuals treated as unmarked. Temporal variation in density is described with a time series model, and a conditional SCR model is used to describe the spatial distribution of individuals and their detection parameters during each primary sampling period, $t = 1, \dots, T$. Any time series model could be used for density ($D_1, \dots, D_T$), with the simplest option being a first-order autoregressive (AR(1)) process for the error terms of a linear model on a link scale:

$$f(D_t) = X_t' \beta_t + \varepsilon_t$$

$$\varepsilon_t \sim \text{Normal}(\alpha \varepsilon_{t-1}, \tau^2)$$

where f() is the link function, X_t is a vector of covariates, β_t is a vector of coefficients, ε_t is the error term, α is the autocorrelation parameter, and τ^2 is the variance of the error terms.

A closed-population 'unmarked SCR' model links density to the observed data during each primary period (Chandler & Royle, 2013). Bayesian inference can be achieved using a data augmentation approach in which, rather than putting a prior directly on abundance (N_t), we specify an augmented population size M_t, with $M_t \gg N_t$, in order to fix the dimensions of the parameter space (Royle et al., 2007). In this formulation, abundance during each primary period is modeled as $N_t = \sum_{i=1}^{M_t} z_{it}$ where $z_{it} \sim \text{Bernoulli}(\psi_t)$ and $\psi_t = E\,(N_t)/M_t = D_t\,A/M_t$, with A being the area of the spatial region within which the N_t individuals occur. The latent variables z_{it} indicate if an individual of the augmented population is a member of the actual population during each primary period. This model implies the distribution for abundance is marginally

$N_t \sim \text{Binomial}(M_t, \psi_t)$, which when M_t is large, is equivalent to the standard Poisson assumption commonly used in point process models.

Unlike existing population models, SCR (Gardner et al., 2010; Whittington et al., 2018; Efford and Schofield, 2020; Milleret et al., 2020), we do not model individual-level survival and recruitment because the unmarked individuals cannot be tracked over time, and therefore we do not retain individual identities among primary periods in the model. While it would be possible to model the latent survival and recruitment processes at the individual level, there is limited information within the unmarked camera data for the estimation to be worth the increased computational demands.

The spatial distribution of individuals during a primary time period is modeled as an outcome of a spatial point process. Each individual is assumed to have an activity center denoted by $s_{i,t}$ within the two-dimensional spatial region S. The activity centers are distributed in proportion to a density surface $\mu(s)$, which could be modeled as a function of spatial covariates or a spatial random field. However, if density is assumed to be spatially uniform, the distribution of activity centers is $s_{it} \sim \text{Uniform}(S)$. The spatial region S should be large enough to ensure that the encounter probability for individuals with activity centers near the boundaries of the region is negligible (Borchers and Efford 2008).

A robust design is used to improve inferences by allowing for K secondary sampling periods during each primary time period when abundance and distribution are assumed to remain constant (Pollock, 1982; Gardner et al., 2010). The expected number of detections (λ_{ijkt}) of individual i ($i = 1, \dots, M_t$) at camera j ($j = 1, \dots, J_t$) on secondary sampling occasion $k (k = 1, \dots, K_t)$ during primary period t is assumed to decrease with Euclidean distance (d_{ijt}) between the activity center and the traps, whose locations are denoted by $x_1, \dots, x_J$. A common

encounter rate function is $\lambda_{ijkt} = \lambda_{0,t} e^{-d_{ijt}^2/2\sigma_t^2}$, where $\lambda_{0,t}$ is the expected number of detections on a single secondary sampling occasion for an individual when the distance between its activity center and a trap is zero. The spatial scale parameter σ_t determines the rate at which detection probability decreases with distance.

If all individuals are marked, we would observe individual-level encounter histories that could be modeled with a Poisson distribution or with a Bernoulli distribution if the counts are converted to binary detection events: $y_{ijkt} \sim \text{Bernoulli}\left(1 - exp\left(-\lambda_{ijkt} z_{it}\right)\right)$. However, many species lack natural markings or individually-distinguishing features, and thus the data (n_{jkt}) are counts of individuals, or binary values indicating if at least one individual was detected at each camera on each occasion. Under the assumption that the number of independent detections of each individual is Poisson distributed, the model for the binary data becomes: $n_{jkt} \sim \text{Bernoulli}(1 - e^{-\Lambda_{jkt}})$ where $\Lambda_{jkt} = \sum_{i=1}^{M} \lambda_{ijkt} z_{it}$.

Without individual-level encounter histories, the binary camera data provide little information about the detection parameters (Chandler & Royle, 2013). However, telemetry data from a subset of individuals can provide valuable information about these parameters. Telemetry data provide direct information about the location of an individual's activity center (s_i) and the probability that a camera detects the individual, which is a function of $\lambda_{0,t}$ and σ_t. A challenge when combining data on marked and unmarked individuals is that the two groups of individuals will have different spatial distributions, except when marked individuals are a random subset of the population with natural markings (Whittington et al., 2018; Efford & Hunter, 2018). To account for the differences in detection parameters between marked and unmarked individuals, generalized spatial mark-resight models have been developed that include a submodel for the marking process.

The generalized SMR approach could be used here, but it would be very computationally demanding when data are from long-term studies spanning large spatial regions. We therefore propose a two-stage analysis in which the detection parameters are estimated in stage one, and their posterior distributions are used as prior distributions in stage two. Specifically, in the first stage, only the marked individuals are included in the analysis, and no effort is made to estimate abundance. In each primary time period, an SCR model is fit to camera data on the individuals that are uniquely identifiable, and possibly outfitted with telemetry devices. A simple bivariate normal model could be used for the telemetry locations: $u_{ikt} \sim \text{Normal}(s_{it}, \sigma_t^2 I)$. A time series model for the detection parameters could be incorporated into stage one of the model to account for the temporal variation between primary periods. We choose to use an first-order autoregressive (AR(1)) process model on the detection parameters and a logarithmic link to account for temporal autocorrelation. The joint posterior distribution for $\lambda_{0,t}$ and σ_t obtained from the first stage of the analysis on marked individuals is used as a prior distribution in the second-stage analysis of the binary camera data. Because all individuals are treated as unmarked in the second stage, there is no need to model different spatial distributions of marked and unmarked individuals.

APPLICATION TO WHITE-TAILED DEER STUDY

White-tailed deer play important cultural, economic, and ecological roles throughout their range, and reliable techniques are needed to monitor deer population dynamics and to guide management decisions. Remote cameras have become increasingly popular monitoring methods for white-tailed deer due to their low-cost and non-invasive nature (Jacobson et al., 1997;

Roberts et al., 2006; Curtis et al., 2009; Chitwood et al., 2017; Keever et al., 2017; Johnson, 2019).

We applied the two-stage SMR models to three years of female white-tailed deer data (2015–2017) collected in the Big Cypress Basin, Florida, USA. Within the Big Cypress Basin, sampling occurred in the Big Cypress National Preserve (BCNP) and the adjacent Florida Panther National Wildlife Refuge (FPNWR; Figure 2.1). In BCNP, sampling was conducted in the Bear Island (BI) and North Addition Lands (AL) management units.

Capture Procedure

During 2015-2017, we captured 145 adult female white-tailed deer via aerial pursuit in open canopy habitats on BCNP and via chemical immobilization and rocket-netting in closed canopy habitats within FPNWR. We captured deer following protocols accepted by University of Georgia IACUC permit A2014 07-009-Y3-A1. We ear-tagged each individual with a set of unique identifiers and fitted individuals with an ATS Model G2110E GPS-telemetry collar (Advanced Telemetry Systems, Isante, MN) programmed to record and store one location every 3-4 h. All data were stored onboard the collar, uploaded to the ATS Server via Iridium satellite (Iridium Communications Inc., McLean, VA), and were remotely accessible. Collars were dropped off at the completion of battery life or remotely triggered to drop off if signal transmission became irregular.

We recorded 410,236 telemetry locations for 145 female deer. We excluded GPS telemetry data recorded within two weeks after capture to avoid the influence of atypical behaviors related to capture. Telemetry locations 7-20 September 2017 were excluded from the analysis due to irregular deer movements relating to Hurricane Irma (Abernathy et al., 2019).

Additional telemetry data processing was needed for a set of collars that experienced a software bug that caused a temporal drift in data uploaded to the Iridium network. For affected collars that we were able to recover, we corrected the errors by downloading the data that was logged on the collar. For unrecovered collars, we excluded locations acquired after the time-bug occurred. We corrected dates for a set of collars that improperly recorded Julian dates in the years following the 2016 leap year. Finally, we selected the subset of female deer located within the camera array and surrounding buffer zone. After processing, we had a total of 280,894 locations for 59 female deer.

Trail camera monitoring

We deployed 180 infrared motion-triggered white-flash cameras (HCO Outdoor Products, model SG565FV, Norcross, GA, USA) continuously from 1 January 2015 – 31 December 2017, such that each study site contained 60 cameras within a 29 km^2 rectangular region (Crawford et al., 2019; Figures 2.A1–2.A3). Of the 60 cameras within each site, 40 cameras were placed along outdoor recreation vehicle (ORV) trails. The remaining 20 cameras on each site were placed approximately 250 m from the nearest on-trail camera. The spatial extent of each camera array was 6.57km x 3.78km for BI, 6.55km x 3.80km for AL, and 6.68km x 4.05km for FPNWR.

We visited each camera approximately once per month for data retrieval and camera maintenance. In the event of a wildfire or prescribed burn, we preemptively removed cameras when access was available and replaced cameras once the area was safe. We processed all camera images using Media Pro software (Phase One, Version 2.1.0.161, Copenhagen, Denmark). We inspected each photograph for white-tailed deer group size, the presence of spots

on fawns, and the sex of adult deer. Additionally, white-tailed deer with ear-tags and/or GPS-collars were identified to the individual-level based on a combination of ear tag number and color combination, unique GPS-collar identifiers, and GPS movements.

Model Specification

We used the binary form of the model described above for both the individual encounter histories in stage one, and for the camera detection data in stage two. We defined the state-space using a 1 km buffer around each camera array. We assumed population closure during 14-day periods (fortnights), as female white-tailed deer daily survival has been observed to be high (Bled et al. *In Review*) and recruitment has been observed to be low (Chandler et al., 2018) over the course of 14 days. The analysis varied in the number of fortnights used for each camera array to allow for the overlap of camera and telemetry datasets. The analysis was conducted for 76 fortnights (29 January 2015 – 27 December 2017) for BI and AL and 70 (23 April 2015 – 27 December 2017) for FPNWR. For the first stage of the analysis using data on GPS-collared deer, we made inferences using 10,000 posterior samples after an adaptive phase of 100 iterations and a burn-in of 15,000 iterations. We fit the first stage of the model to the GPS-collared deer using the package *rjags* (Plummer et al., 2018) in program R (R Core Team, 2019). The second stage of the analysis for unmarked deer was conducted using NIMBLE in program R in order to increase computational efficiency (de Valpine, 2017; Ponisio et al., 2020; Turek et al., 2021). Within the model, we incorporated an AR(1) with a temporal trend and an identity link with a positivity constraint on density (Appendix 2.B). Inferences from the second stage of the analysis were made using 50,000 posterior samples drawn from 3 Markov chains after discarding 5,000 burn-in iterations and thinning by 2. We monitored convergence by visual inspection of the

MCMC chains and using the Gelman-Rubin convergence statistic ($\hat{R}$; Gelman & Rubin, 1992). Posterior means are presented with 95% credible intervals.

RESULTS

During the three-year study, trail cameras recorded 11,549 female white-tailed deer photographs in AL, 14,315 female white-tailed deer photographs in BI, and 35,471 female white-tailed deer photographs in FPNWR (Table 2.1). These values reflect deer that could be reliably identified as either spotted fawns or adults and classified by sex. Female deer displayed spatio-temporal heterogeneity in photographic detection rates within and among the three sites (Appendix 2.C).

Stage One - Detection Parameter Estimation

For the AL site, we used detection histories and telemetry locations from 10 GPS-collared female deer to estimate the detection parameters (Figures 2.2, 2.D1). The estimate of the mean spatial scale parameter ($\overline{\sigma}$) was 302.6 (233.8-387.8; Table 2, Figure 2.3). The estimate of the mean baseline encounter rate parameter ($\overline{\lambda_0}$) was 0.072 (0.020-0.154; Figure 2.4). In the latter half of 2017, estimates of σ and λ_0 were influenced by the sole remaining GPS-collared female on the camera grid. For BI, we used detection histories and telemetry locations from 31 GPS-collared female deer (Figures 2.2, 2.D2). The estimate of $\overline{\sigma}$ was 249.3 (198.1-324.7; Figure 2.3). The estimate of $\overline{\lambda_0}$ was 0.061 (0.029-0.108; Figure 2.4). Throughout the three-year study, estimates of σ and λ_0 remained relatively stable. For FPNWR, we used detection histories and telemetry locations from 18 GPS-collared female deer (Figures 2.2, 2.D3). The analysis of the data on GPS-collared deer resulted in an estimate of 218.2 (160.5-271.9) for $\overline{\sigma}$ (Figure 2.3) and

0.115 (0.029-0.239) for $\overline{\lambda_0}$ (Figure 2.4). While estimates of σ were relatively stable, estimates of λ_0 were highly variable. All sites exhibited similar levels of positive temporal autocorrelation in detection parameters (Appendix 2.E).

Stage Two - Abundance/Density Estimation

In stage two of the model, we used posterior distributions for detection parameters as prior distributions in the analysis of the camera data on unmarked individuals to estimate abundance (Appendix 2.F). For AL, we excluded from the analysis July - December 2017 due to skewed prior distributions influenced by a single individual. In AL, mean female deer abundance across the three-year study within the 49.23 km^2 area was 63 (45-83) individuals, equating to 1.3 (0.9-1.7) females/km^2 (Figure 5). The lowest fortnight-specific density estimate was 1.0 females/km^2, while the highest fortnight estimate was 1.5 females/km^2 (Tables 2.G1–G2) The mean variability in density estimates for consecutive fortnight periods was -0.004 (-0.140, 0.143) females/km^2. AL had the weakest autocorrelation in density estimates (α = 0.353), but did exhibit a temporal trend in density across the three-year study (β_1 = -0.003; Table 2.3), with a posterior probability of 0.83 that the trend was negative. The temporal trend parameter predicted a yearly density decline of 0.078 females/km^2. AL exhibited an initial decline in annual mean fortnight density estimates from 1.37 females/km^2 in 2015 to 1.21 females/km^2 in 2016, but remained stable during the first six months of 2017 at 1.26 females/km^2 (Figure 6).

At BI, average female deer abundance across the three-year study within the 49.47 km^2 area was 152 (86-232) individuals, equating to 3.1 (1.7-4.7) females/km^2 (Figure 2.5). The lowest fortnight-specific estimate was 1.5 females/km^2, while the highest fortnight estimate was 4.5 females/km^2 (Tables 2.G3–G4) The mean variability in density estimates for consecutive

fortnight periods was 0.007 (-0.516, 0.390) females/km^2. The population trend estimate suggested a slight decline in density across the three years (β_1 = -0.010; Table 2.3), with a posterior probability of 0.79 that the trend was negative. The temporal trend parameter predicted a yearly density decline of 0.26 females/km^2. BI exhibited an initial decline in annual mean fortnight density estimates from 3.69 females/km^2 in 2015 to 2.75 females/km^2 in 2016, but remained stable the following year in 2017 at 2.76 females/km^2 (Figure 2.6).

In FPNWR, average female deer abundance across the three-year study within the 52.49 km^2 was 228 (88-431) individuals, equating to 4.3 (1.7-8.2) females/km^2 (Figure 2.5). Density estimates across the study were highly variable with the lowest fortnight estimate at 1.7 females/km^2 and the highest mean fortnight estimate at 8.0 females/km^2 (Tables 2.G5–G6). The mean variability in density estimates for consecutive fortnight periods was -0.087 (-0.834, 0.496) females/km^2. FPNWR had the strongest autocorrelation in density estimates (α = 0.937) and exhibited a decline in density during the study (β_1 = -0.074; Table 2.3), with a posterior probability of 1.00 that the trend was negative. The temporal trend parameter predicted a yearly density decline of 1.92 females/km^2. Annual mean fortnight density estimates were similar for FPNWR between 2015 and 2016 (4.62 and 4.84 females/km^2), but declined in 2017 to 3.62 females/km^2 (Figure 2.6).

DISCUSSION

Long-term monitoring of wildlife relies on novel cost-effective sampling methods alongside computationally efficient statistical modeling techniques. We developed a two-stage spatial mark-resight model for long-term monitoring data, which in our case consisted of camera data collected over a three-year period and auxiliary telemetry data for improved spatio-temporal

inferences. The framework consists of a time series model for density, which is conditionally linked to closed-population spatial mark-resight models. The two-stage spatial mark-resight framework is less computationally demanding than joint SMR models would be, which should make it easier to implement in practice. In addition, the model may be used independently for density estimation when no synchronous auxiliary information on marked individuals is available, which is often the case in long-term monitoring.

An alternative method for long-term monitoring of wildlife populations is aerial transects sampling. Aerial surveying paired with distance sampling or sightability models can be advantageous when sampling large spatial extents with rough terrain or in remote locations as only a small portion of individuals within the study area need be detected and temporal replication of surveys is not required (Buckland et al., 2001; Bart et al., 2004). However, aerial transect surveying may not be a viable option in landscapes characterized by visual obstructions. For example, in South Florida, aerial distance sampling is impeded by heterogeneity of forest cover, which renders animals difficult to observe from the air. Aerial transect surveying is inherently dangerous and expensive to conduct, and the precision and accuracy of estimates are highly variable and dependent on time of day, flying altitude, observer skill, and population density within the area (Graves et al., 1972; Caughley, 1974; Rice & Harder, 1977; Beasom, 1979; Beasom et al., 1986; Samuel et al., 1987; Caughley, 1997; Dunn et al., 2002; DeYoung, 2011).

In lieu of aerial transect sampling, camera surveys have become popularized for density estimation. The recently developed Random Encounter Model (REM) allows for estimating density without the need for individual recognition within camera data by assuming individuals encounter cameras randomly (Rowcliffe et al., 2008). The REM uses independent estimates of

travel speed, group size, active time for each day, and the area of the detection zone of each camera to infer density from camera photos. The REM performed comparatively to distance sampling and sight-resight methods (Cusack et al., 2015). However, this model assumes random placement of cameras with respect to animal movements, which is often difficult to achieve for most species and results in increased logistical costs and sparse data (Rowcliffe et al., 2008; Foster & Harmsen, 2012). Additionally, the REM relies on independent estimation of camera detection zone, which may vary spatio-temporally based on environmental conditions (Cusack et al., 2015). An extension of REM is the Random Encounter and Staying Time Model (REST), which describes the relationship among staying time of an individual within the detection area, trapping rate, and density (Nakashima et al., 2018). The REST model assumes random camera placement relative to animal movements and that cameras sample habitats proportional to their availability. The REST model has resulted in unbiased density estimates and may be a viable alternative method for density estimation (Nakashima et al., 2018; Garland et al., 2020; Nakashima et al., 2020). However, the REST model may be less precise for species that exhibit long periods of inactivity because cameras rarely capture animals resting. Additionally, the REST model still relies upon independent estimation of camera detection zone.

Traditional protocols for estimating population size of white-tailed deer from camera surveys are based on individual recognition of adult males within a sampled area based on antler characteristics (Jacobson et al., 1997; Weckel et al., 2011). These estimates are derived from ratios of photographic occurrences of branch-antlered bucks, spike bucks, does, and fawns from baited surveys (Jacobson et al., 1997). A major limitation to this technique is that it does not provide measures of uncertainty surrounding the parameter estimates. Although modifications using nonparametric bootstrapping of camera stations have addressed this deficiency (Weckel et

al., 2011; Gulsby et al., 2015), this method still relies upon the assumption of equal detection between all age-sex groups.

Few studies have applied SMR models to camera data on white-tailed deer. Beaver et al. (2017) demonstrated that standard SMR models could be fitted to data on male deer that have been uniquely identified by their antler characteristics. Chandler et al. (2018) developed an SMR model to estimate white-tailed deer fawn survival and recruitment. Their model requires that all detected fawns can be uniquely identified based on spot patterns. Although these methods were shown to be highly effective, they are labor intensive because they can involve manual interpretation and cross-referencing of thousands of images. Moreover, adult female deer lack unique markings, prohibiting the use of standard SMR models (Johnson, 2019). Partially-marking the adult female population within our study area allowed for a cost-effective sampling method that balanced the tradeoffs between density estimation and logistical constraints.

Using our two-stage spatial mark-resight model, we detected spatial variation in parameter estimates for adult female white-tailed deer across our study area. The estimates of the baseline encounter rate ($\overline{\lambda_0}$) followed a longitudinal gradient, being highest in FPNWR and lowest in AL. The estimates of the spatial scale parameter ($\overline{\sigma}$) displayed a reverse gradient, being highest in AL and lowest in FPNWR. The inverse relationship in responses at sites between $\overline{\lambda_0}$ and $\overline{\sigma}$ was expected as these parameters tend to exhibit negative covariance. As sigma increases with home range size, $\overline{\lambda_0}$ decreases because animals are less likely to be detected near the center of their range (Efford & Mowat, 2014). Estimates of the $\overline{\sigma}$ remained relatively constant throughout the three-year period with the exception of the expansion in AL in 2017 caused by a single female. The narrow credible intervals $\overline{\sigma}$ are a result of including telemetry data from

marked GPS-collared females within the model for inferences on space use. In contrast, all sites displayed temporal variation in $\overline{\lambda_0}$, with FPNWR having the highest variability.

We detected spatio-temporal variation in density across our study area. Density estimates were highest in FPNWR and lowest in AL, perhaps due to the structural relationship between home range size and population density (Efford et al., 2016). Density experiences an inverse-square relationship with home range size, and within the SCR framework, the spatial scale parameter ($\overline{\sigma}$) is often an index of home range size. Thus, in FPNWR where $\overline{\sigma}$ was the lowest, density was highest. Additionally, the density estimates could reflect a habitat quality gradient with higher densities in the drier, western portion of the study area and lower density estimates in the wetter, eastern region of the study.

Highly dynamic systems often require long-term data to understand population dynamics and conservation status of species in order to make informed management decisions. Long-term studies allow for the observation and understanding of temporal variation in population processes (Reinke et al., 2019). While most of the temporal variation in deer density was driven by seasonal fluctuations, one study area exhibited a slight long-term population decline. Both AL and BI exhibited initial declines in density from 2015 to 2016, which stabilized during 2016 and 2017. While the temporal trend parameter for both areas suggested declining populations, the 95% credible intervals provided weak support. In contrast, FPNWR had the strongest negative trend parameter, indicating a potential long-term population decline. This population trend behavior may be a result from having a large initial population density estimate coupled with high temporal variation. When autocorrelation in density estimates is high within an autoregressive model, the ability to detect trends becomes harder and longer time series data are needed. While our study occurred continuously for three years, >10 years of monitoring is often

required to detect long-term population trends at high statistical power (Gerrodette, 1987; Dixon et al., 1998; White, 2018). Gradual long-term trends in density could be detected by applying our camera trapping methodology and statistical modeling framework to monitoring data collected over longer periods. We suggest continually monitoring these deer populations to determine whether the short-term declines coincide with a persistent long-term declining trend.

While our model was able to detect spatio-temporal variation in density, there are potential future improvements towards a more robust model design that can enhance the precision of density estimation. Transitioning the SMR model from the closed population model using fortnights to a three-year open population model or integrated population model would allow for the incorporation of demographic processes (Gardner et al., 2010; Chandler & Clark, 2014; Gardner et al., 2018). Incorporating survival (Bled et al. *In Review*) and recruitment processes (Chandler et al., 2018) would provide more precise estimates of population trends and aid in understanding the mechanisms underlying density trends. However, the transition to an open population model comes with increased model complexity and computational demands due to daily computations of demographic parameters, which may outweigh potential improvements to density estimation.

Long-term monitoring studies enable the observation of population responses to environmental stressors and management actions by accounting for spatio-temporal heterogeneity. These long-term monitoring efforts are often faced with tradeoffs in density estimation and logistical and financial constraints. The development of novel statistical frameworks that address these tradeoffs can provide management agency analysts with the tools to understand the driving forces of population dynamics.

LITERATURE CITED

Abernathy, H. N., Crawford, D. A., Garrison, E. P., Chandler, R. B., Conner, M. L., Miller, K. V., & Cherry, M. J. (2019). Deer movement and resource selection during Hurricane Irma: implications for extreme climatic events and wildlife. *Proceedings of the Royal Society B, 286,* 20192230. http://doi.org/10.1098/rspb.2019.2230

Augustine, B. C., Royle, J. A., Kelly, M. J., Satter, C. B., Alonso, R. S., Boydston, E. E., & Crooks, K. R. (2018). Spatial capture-recapture with partial identity: An application to camera traps. *Annals of Applied Statistics, 12,* 67–95.

Augustine, B. C., Royle, J. A., Murphy, S. M., Chandler, R. B., Cox, J. J., & Kelly, M. J. (2019). Spatial capture-recapture for categorically marked populations with an application to genetic capture-recapture. *Ecosphere, 10,* e02627.

Bart, J., Droege, S., Geissler, P., Peterjohn, B. & Ralph, C. J. (2004). Density estimation in wildlife surveys. *Wildlife Society Bulletin, 32,* 1242–1247.

Beasom, S. L. (1979). Precision in helicopter censusing of white-tailed deer. *Journal of Wildlife Management, 43,* 777–780.

Beasom, S. L., Leon, F. G. III, & Synatzske, D. R. (1986). Accuracy and precision of counting white-tailed deer with helicopters at different sampling intensities. *Wildlife Society Bulletin, 14,* 364–368.

Beaver, J. T., Harper, C. A., Muller, L. I., Basinger, P. S., Goode, M. J., & Van Manen, F. T. (2017). Current and spatially explicit capture-recapture analysis methods for infrared triggered camera density estimation of white-tailed deer. *Journal of the Southeastern Association of Fish and Wildlife Agencies, 3,* 195–202.

Bled, F., M. J. Cherry, E. P. Garrison, K. V. Miller, L. M. Conner, H. N. Abernathy, W. H. Ellsworth, L. L. S. Margenau, D. A. Crawford, K. N. Engebretsen, B. D. Kelly, D. B. Shindle, and R. B. Chandler. 2021. Impacts of large carnivore restoration on prey species with high economic and cultural value: A case study of Florida panther and white-tailed deer. Manuscript in review.

Borchers, D. L., & Efford, M. G. (2008). Spatially explicit maximum likelihood methods for capture-recapture studies. *Biometrics, 64,* 377–385.

Buckland, S. T., Rexstad, E. A., Marques, T. A., & Oedekoven, C. S. (2001). Introduction to distance sampling: estimating abundance of biological populations. Oxford University Press, New York, New York, USA.

Caughley, G. (1974). Bias in aerial survey. *Journal of Wildlife Management, 38,* 921–933.

Caughley, G. (1977). Sampling in aerial survey. *Journal of Wildlife Management, 41,* 605–615.

Chandler, R. B., & Royle, J. A. (2013). Spatially explicit models for inference about density in unmarked or partially marked populations. *Annals of Applied Statistics, 7,* 936–954.

Chandler, R. B., & Clark, J. D. (2014). Spatially explicit integrated population models. *Methods in Ecology and Evolution, 5,* 1351–1360.

Chandler, R. B., Engebretsen, K., Cherry, M. J., Garrison, E. P., & Miller, K. V. (2018). Estimating recruitment from capture–recapture data by modelling spatio-temporal variation in birth and age-specific survival rates. *Methods in Ecology and Evolution, 9,* 2115–2130.

Chitwood, M. C., Lashley, M. A., Kilgo, J. C., Cherry, M. J., Conner, L. M., Vukovich, M., Ray, H. S., Ruth, C., Warren, R. J., DePerno, C. S., & Moorman, C. E. (2017). Are camera

surveys useful for assessing recruitment in white-tailed deer? *Wildlife Biology, 17,* wlb.00178. https://doi.org/10.2981/wlb.00178.

Crawford, D. A., Cherry, M. J., Kelly, B. D., Garrison, E. P., Shindle, D. B., Conner, L. M., Chandler, R. B., & Miller, K. V. (2019). Chronology of reproductive investment determines predation risk aversion in a felid-ungulate system. *Ecology and Evolution, 9,* 3264–3275.

Curtis, P. D., Boldgiv, B., Mattison, P. M., & Boulanger, J. R. (2009). Estimating deer abundance in suburban areas with infrared-triggered cameras. *Human-Wildlife Conflicts, 3,* 116–128.

Cusack, J. J., Swanson, A., Coulson, T., Packer, C., Carbone, C., Dickman, A. J., Kosmala, M., Lintott, C., & Rowcliffe, J. M. (2015). Applying a random encounter model to estimate lion density from camera traps in Serengeti National Park, Tanzania. *Journal of Wildlife Management, 79,* 1014–1021.

Dawson, D. K., & Efford, M. G. (2009). Bird population density estimated from acoustic signals. *Journal of Applied Ecology, 46,* 1201–1209.

de Valpine, P., Turek, D., Paciorek, C., Anderson-Bergman, C., Temple Lang, D., & Bodik, R. (2017). Programming with models: writing statistical algorithms for general model structures with NIMBLE. *Journal of Computational and Graphical Statistics, 26,* 403-413.

DeYoung, C. A. (2011). Population dynamics. Pages 147–180 *in* D. G. Hewitt (ed.) Biology and management of white-tailed deer. CRC Press, Boca Raton, Florida, USA..

Dixon, P. M., Olsen, A. R., & Kahn, B. M. (1998). Measuring trends in ecological resources. *Ecological Applications, 8,* 225–227.

Dunn, W. C., Donnelly, J. P., & Krausmann, W. K. (2002). Using thermal infrared sensing to count elk in the southwestern United States. *Wildlife Society Bulletin, 30,* 963–967.

Efford, M. (2004). Density estimation in live-trapping studies. *Oikos, 106,* 598–610.

Efford, M. G., Dawson, D. K., Jhala, Y. V., & Quershi. Q. (2016). Density-dependent home-range size revealed by spatially explicit capture-recapture. *Ecography, 39,* 676–688.

Efford, M., & Hunter, C. M. (2018). Spatial capture-mark-resight estimation of animal population density. *Biometrics, 74,* 411–420.

Efford, M. G., & Mowat, G. (2014). Compensatory heterogeneity in spatially explicit capture-recapture data. *Ecology, 95,* 1341–1348.

Efford, M. G., & Schofield, M. R. (2020). A spatial open-population capture-recapture model. *Biometrics, 76,* 392–402.

Foster, R. J., & Harmsen, B. J. (2012). A critique of density estimation from camera-trap data. *Journal of Wildlife Management, 76,* 224–236.

Gardner, B., Reppucci, J., Lucherini, M., & Royle, J. A. (2010). Spatially explicit inference for open populations: estimating demographic parameters from camera-trap studies. *Ecology, 91,* 3376–3383.

Gardner, B., Sollmann, R., Kumar, N. S., Jathanna, D., & Karanth, K. U. (2018). State space and movement specification in open population spatial capture-recapture models. *Ecology and Evolution, 8,* 10336–10344.

Garland, L. Neilson, E., Avgar, T., Bayne, E., & Boutin, S. (2020). Random encounter and staying time model testing with human volunteers. *Journal of Wildlife Management, 84,* 1179–1184.

Gelman, A., & Rubin, D. B. (1992). Inference from iterative simulation using multiple sequences. *Statistical Science, 7,* 457–511.

Gerrodette, T. (1987). A power analysis for detecting trends. *Ecology, 68,* 1364–1372.

Giudice, J. H., Fieberg, J. R., Zicus, M. C., Rave, D. P., & Wright, R. G. (2010). Cost and precision function for aerial quadrat surveys: a case study of ring-necked ducks in Minnesota. *Journal of Wildlife Management, 74,* 342–349.

Gopalaswamy, A. M., Royle, J. A., Delampady, M., Nichols, J. D., Karanth, K. U., & Macdonald, D. W. (2012). Density estimation in tiger populations: combining information for strong inference. *Ecology, 93,* 1741–1751.

Graves, H. B., Bellis, E. D., & Knuth, W. M. (1972). Censusing white-tailed deer by airborne thermal infrared imagery. *Journal of Wildlife Management, 36,* 875–884.

Gulsby, W. D., Killmaster, C. H., Bowers, J. W., Kelly, J. D., Sacks, B. N., Statham, M. J., & Miller, K. V. (2015). White-tailed deer fawn recruitment before and after experimental coyote removals in central Georgia. *Wildlife Society Bulletin, 39,* 248–255.

Jacobson, H. A., Kroll, J. C., Browning, R. W., Koerth, B. H., & Conway, M. H. (1997). Infrared-triggered cameras for censusing white-tailed deer. *Wildlife Society Bulletin, 25,* 547–556.

Jimenez, J., Chandler, R., Tobajas, J., Descalzo, E., Mateo, R., & Ferreras, P. (2018). Generalized spatial mark-resight models within incomplete identification: An application to red fox density estimates. *Ecology and Evolution, 9,* 4739–4748.

Johnson, J. T. (2019). White-tailed deer camera surveys: Density estimation and spatio-temporal dynamics. Dissertation, University of Georgia, Athens, Georgia, USA.

Karanth, K. U. (1995). Estimating tiger *Panthera tigris* populations from camera trap data using capture-recapture models. *Biological Conservation, 71,* 333–338.

Karanth, K. U., & Nichols, J. D. (1998). Estimation of tiger densities in India using photographic captures and recaptures. *Ecology, 79,* 2852–2862.

Keever, A. C., McGowan, C. P., Ditchkoff, S. S., Acker, P. K., Grand, J. B., & Newbolt, C. H. (2017). Efficacy of N-mixture models for surveying and monitoring white-tailed deer populations. *Mammalogy Research, 62,* 413–422.

Kéry, M., Gardner, B., Stoeckle, T., Weber, D., & Royle, J. A. (2010). Use of spatial capture-recapture modeling and DNA data to estimate densities of elusive animals. *Conservation Biology, 25,* 356–364.

Linden, D. W., Sirén, A. P. L., & Pekins, P. J. (2018). Integrating telemetry data into spatial capture-recapture modifies inferences on multi-scale resource selection. *Ecosphere, 9,* e02203.

Milleret, C., Dupont, P., Chipperfield, J., Turek, D., Brøseth, H., Gimenez, O., de Valpine, P., & Bischof, R. (2020). Estimating abundance with interruptions in data collection using open population spatial capture-recapture models. *Ecosphere, 11,* e03172. https://doi.org/10.1002/ecs2.3172.

Mowat, G., & Strobeck, C. (2000). Estimating population size of grizzly bears using hair capture, DNA profiling, and mark-recapture analysis. *Journal of Wildlife Management, 64,* 183–193.

Nakashima, Y., Fukasawa, K., & Samejima, H. (2018). Estimating animal density without individual recognition using information derivable exclusively from camera traps. *Journal of Applied Ecology, 55,* 735–744.

Nakashima, Y., Hongo, S., & Akomo-Okoue, E. F. (2020). Landscape-scale estimation of forest ungulate density and biomass using camera traps: Applying the REST model. *Biological Conservation, 241,* 108381. https://doi.org/10.1016/j.biocon.2019.108381

Nichols, J. D., & Williams, B. K. (2006). Monitoring for conservation. *Trends in Ecology and Evolution, 21,* 668–673.

Plummer, M. (2018). rjags: Bayesian Graphical Models using MCMC. R package version 4-8. https://CRAN.R-project.org/package=rjags.

Pollock, K. H. (1982). A capture-recapture design robust to unequal probability of capture. *Journal of Wildlife Management, 46,* 757–760.

Pollock, K. H., Nichols, J. D., Brownie, C., & Hines, J. E. (1990). Statistical inference for capture-recapture experiments. *Wildlife Monographs, 107,* 3–97.

Ponisio, L. C., de Valpine, P., Michaud, N., & Turek, D. (2020). One size does not fit all: Customizing MCMC methods for hierarchical models using NIMBLE. *Ecology and Evolution, 10,* 2385–2416.

R Core Team. (2019). R: A language and environment for statistical computing. R Foundation for Statistical Computing, Vienna, Austria. https://www.R-project.org/

Raabe, J. K., Gardner, B., & Hightower, J. E. (2013). A spatial capture-recapture model to estimate fish survival and location from linear continuous monitoring arrays. *Canadian Journal of Fisheries and Aquatic Sciences, 71,* 120–130.

Ramsey, D. S., Caley, P. A., & Robley, A. (2015). Estimating population density from presence–absence data using a spatially explicit model. *Journal of Wildlife Management, 79,* 491–499.

Reinke, B. A., Miller, D. A. W., & Janzen, F. J. (2019). What have long-term field studies taught us about population dynamics? *Annual Review of Ecology, Evolution, and Systematics, 50,* 261–278.

Rice, W. R., & Harder, J. D. (1977). Application of multiple aerial sampling to a mark-recapture census of white-tailed deer. *Journal of Wildlife Management, 41,* 197–206.

Roberts, C. W., Pierce, B. L., Braden, A. W., Lopez, R. R., Silvy, N. J., Frank, P. A., & Ransom, D. Jr. (2006). Comparison of camera and road survey estimates for white-tailed deer. *Journal of Wildlife Management, 70,* 263–267.

Rowcliffe, J. M., Field, J., Turvey, S. T., & Carbone, C. (2008). Estimating animal density using camera traps without the need for individual recognition. *Journal of Applied Ecology, 45,* 1228–1236.

Royle, J. A. (2018). Modeling sound attenuation in heterogeneous environments for improved bioacoustic sampling of wildlife populations. *Methods in Ecology and Evolution, 9,* 1939–1947.

Royle, J. A., & Dorazio, R. M. (2008). Hierarchical modeling and inference in ecology: the analysis of data from populations, metapopulations, and communities. Academic Press, Boston, Massachusetts.

Royle, J. A., & Young, K. V. (2008). A hierarchical model for spatial capture-recapture data. *Ecology, 89,* 2281–2289.

Royle, J. A., Dorazio, R. M., & Link, W. A. (2007). Analysis of multinomial models with unknown index using data augmentation. *Journal of Computation and Graphical Statistics, 16,* 67–85.

Royle, J. A., Nichols, J. D., Karanth, K. U., & Gopalaswamy, A. M. (2009). A hierarchical model for estimating density in camera-trap studies. *Journal of Applied Ecology, 46,* 118–127.

Royle, J. A., Chandler, R. B., Sollmann, R., & Gardner, B. (2013). Spatial Capture-Recapture. Academic Press, Boston, Massachusetts, USA.

Royle, J. A., Chandler, R. B., Sun, C. C., & Fuller, A.K. (2013). Integrating resource selection information with spatial capture-recapture. *Methods in Ecology and Evolution, 4,* 520–530.

Royle, J. A., Fuller, A. K., & Sutherland, C. (2018). Unifying population and landscape ecology with spatial capture-recapture. *Ecography, 41,* 444–456.

Samuel, M. D., Garton, E. O., Schlegel, M. W., & Carson, R. G. (1987). Visibility bias during aerial surveys of elk in Northcentral Idaho. *Journal of Wildlife Management, 51,* 622–630.

Sollmann, R., Gardner, B., Chandler, R. B., Shindle, D. B., Onorato, D. P., Royle, J. A., & O'Connell, A. F. (2013). Using multiple data sources provides density estimates for endangered Florida panther. *Journal of Applied Ecology, 50,* 961–968.

Sollmann, R., Gardner, B., Parsons, A. W., Stocking, J. J., McClintock, B. T., Simons, T. R., Pollock, K. H., & O'Connell, A. F. (2013). A spatial mark-resight model augmented with telemetry data. *Ecology, 94,* 553–559.

Tenan, S., Pedrini, P., Bragalanti, N., Groff, C., & Sutherland, C. (2017). Data integration for inference about spatial processes: A model-based approach to test and account for data inconsistency. *PLoS ONE, 12,* e0185588.

Tourani, M., Dupont, P., Nawaz, M. A., & Bischof, R. (2020). Multiple observation processes in spatial capture-recapture models: How much do we gain? *Ecology,* e03030. https://doi.org/10.1002/ecy.3030

Turek, D., Milleret, C., Ergon, T., Brøseth, H., Dupont, P., & de Valpine, P. (2021). Efficient estimation of large-scale spatial capture-recapture models. *Ecosphere, 12,* e03385. https://doi.org/10.1002/ecs2.3385.

Weckel, M., Rockwell, R. F., & Secret, F. (2011). A modification of Jacobson et al.'s (1997) individual branch-antlered male method for censusing white-tailed deer. *Wildlife Society Bulletin, 35,* 445–451.

White, E. R. (2018). Minimum time required to detect population trends: the need for long-term monitoring programs. *BioScience, 69,* 40–46.

Whittington, J., Hebblewhite, M., & Chandler, R. B. (2018). Generalized spatial mark-resight models with an application to grizzly bears. *Journal of Applied Ecology, 55,* 157–168.

Williams, B. K., Nichols, J. D., & Conroy, M. J. (2002). Analysis and management of animal populations. Academic Press, San Diego, California, USA.

Williams , P. J., Hooten, M. B., Womble, J. N., Essliner, G. G., & Bower, M. R. (2018). Monitoring dynamic spatio-temporal ecological processes optimally. *Ecology, 99,* 524–535.

Yoccoz, N. G., Nichols, J. D., & Boulinier, T. (2001). Monitoring of biological diversity in space and time. *Trends in Ecology and Evolution, 16,* 446–453.

Table 2.1. Female white-tailed deer detections at trail cameras in the North Addition Lands and Bear Island management units of Big Cypress National Preserve, and the Florida Panther National Wildlife Refuge (FPNWR) during January 2015 – December 2017.

Site	**2015**	**2016**	**2017**	**Total**
North Addition Lands	4268	4913	2368	11549
Bear Island	6140	4395	3780	14315
FPNWR	13112	12442	9917	35471

Table 2.2. Posterior summary statistics for the detection parameter estimation model (stage one) using marked GPS-collared white-tailed deer. Mean, median, standard deviation (SD) and 95% credible intervals (CI) are reported for the average across all fortnights.

	Mean	Median	SD	LowerCI	UpperCI
North Addition Lands					
$\overline{\lambda_0}$	0.072	0.069	0.037	0.020	0.154
$\overline{\sigma}$	302.6	305.9	43.48	233.8	387.8
Bear Island					
$\overline{\lambda_0}$	0.061	0.059	0.020	0.029	0.108
$\overline{\sigma}$	249.3	245.5	31.04	198.1	324.7
Florida Panther National Wildlife Refuge					
$\overline{\lambda_0}$	0.115	0.108	0.057	0.029	0.239
$\overline{\sigma}$	218.2	215.3	30.06	160.5	271.9

Table 2.3. Posterior summary statistics for the AR(1) density estimation model (stage two) for each camera array. Mean, median, standard deviation (SD) and 95% credible intervals (CI) are reported. Detection parameters are averages across all fortnights.

	Mean	Median	SD	LowerCI	UpperCI
North Addition Lands					
α	0.353	0.499	0.541	-0.773	0.989
β_0	1.396	1.397	0.119	1.164	1.617
β_1	-0.003	-0.003	0.004	-0.010	0.005
$\overline{\lambda_0}$	0.079	0.078	0.029	0.027	0.141
$\overline{\sigma}$	307.7	314.1	43.36	235.4	401.2
Bear Island					
α	0.745	0.769	0.157	0.369	0.973
β_0	3.349	3.399	0.546	2.052	4.465
β_1	-0.010	-0.010	0.012	-0.037	0.015
$\overline{\lambda_0}$	0.068	0.066	0.020	0.034	0.113
$\overline{\sigma}$	247.3	242.4	28.20	204.2	318.5
Florida Panther National Wildlife Refuge					
α	0.937	0.946	0.044	0.829	0.996
β_0	7.321	7.416	1.281	4.981	9.250
β_1	-0.074	-0.073	0.025	-0.118	-0.033
$\overline{\lambda_0}$	0.129	0.119	0.063	0.047	0.293
$\overline{\sigma}$	217.6	214.9	29.14	161.4	269.6

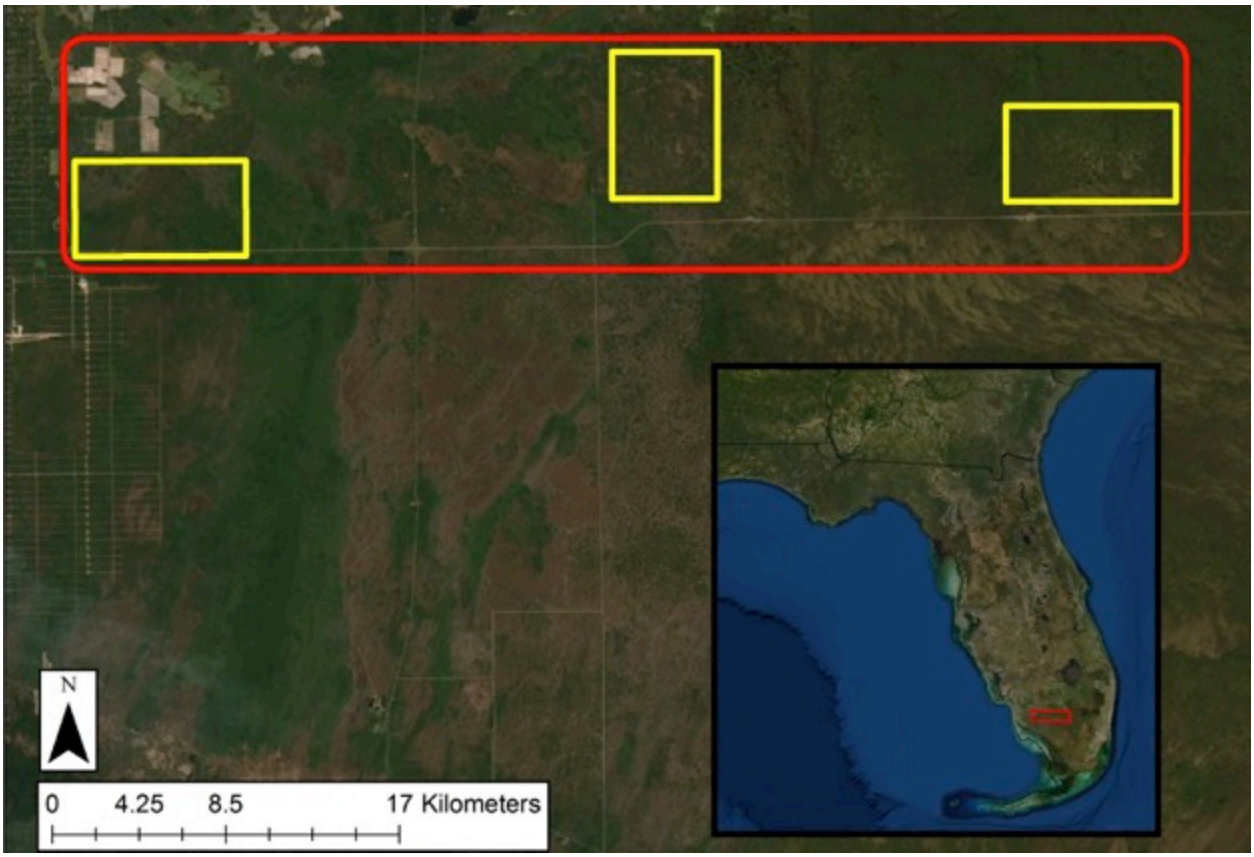

Figure 2.1. South Florida white-tailed deer study area (red boundary line) and camera trapping arrays (yellow boundary lines). The central (Bear Island) and eastern (North Addition Lands) grids were located in Big Cypress National Preserve. The western grid was located in the Florida Panther National Wildlife Refuge.

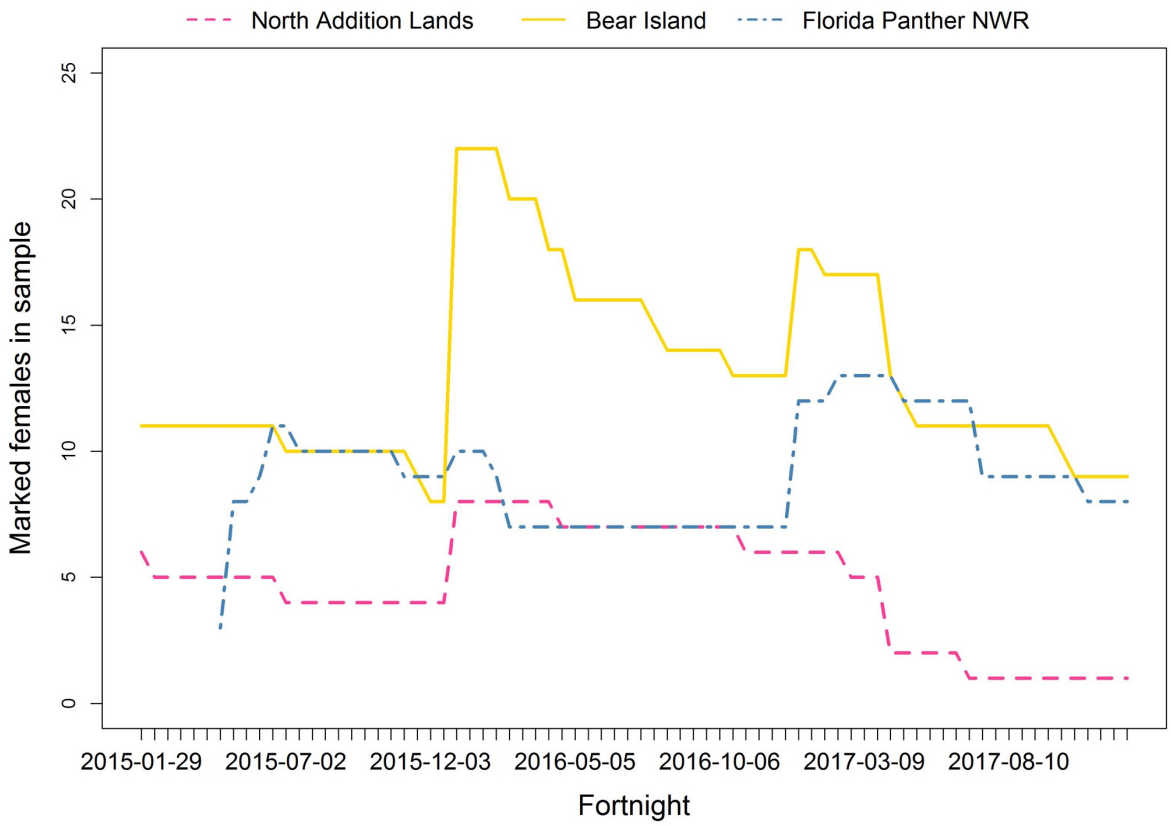

Figure 2.2. Biweekly sample size of marked female white-tailed deer within the North Addition Lands, Bear Island, and Florida Panther National Wildlife Refuge camera grids. Increases in sample size are a reflection of capturing, ear-tagging, and GPS-collaring new individuals.

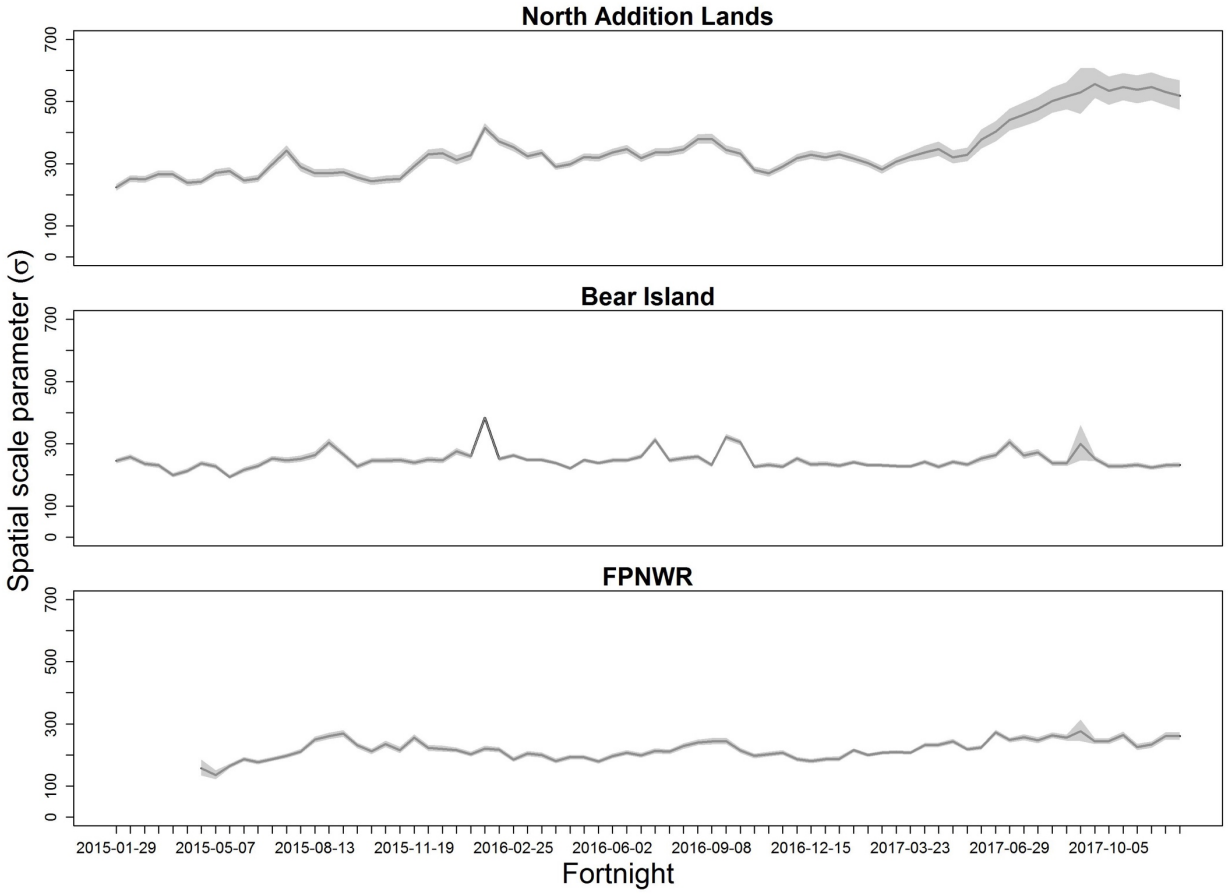

Figure 2.3. Biweekly estimates and 95% credible intervals of the spatial scale parameter (σ) for GPS-collared female deer on North Addition Lands, Bear Island, and Florida Panther National Wildlife Refuge (FPNWR).

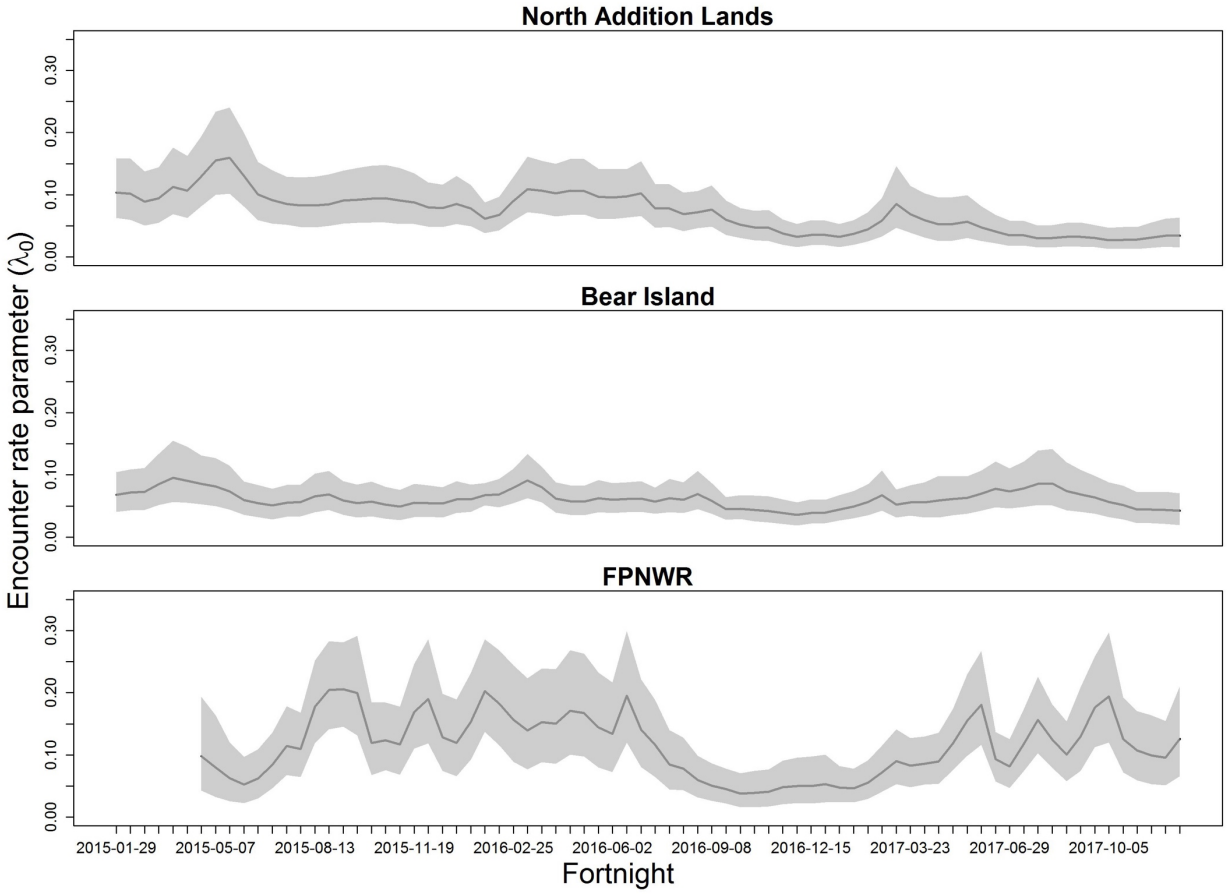

Figure 2.4. Biweekly estimates and 95% credible intervals of the baseline encounter rate parameter (λ_0) for GPS-collared female deer on North Addition Lands, Bear Island, and Florida Panther National Wildlife Refuge (FPNWR).

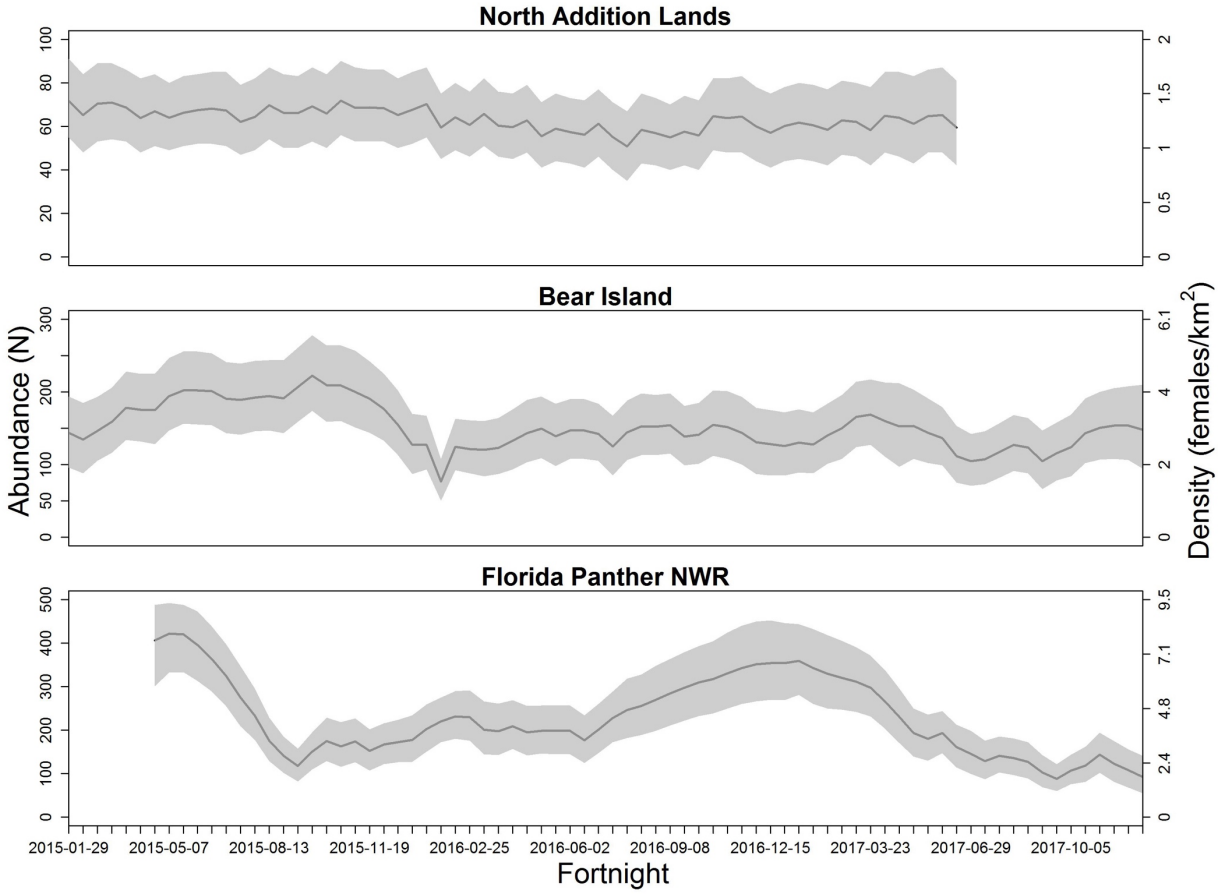

Figure 2.5. Biweekly estimates and 95% credible intervals of abundance and density for female white-tailed deer on North Addition Lands during January 2015 – June 2017, Bear Island during January 2015 – December 2017, and the Florida Panther National Wildlife Refuge during April 2015 – December 2017.

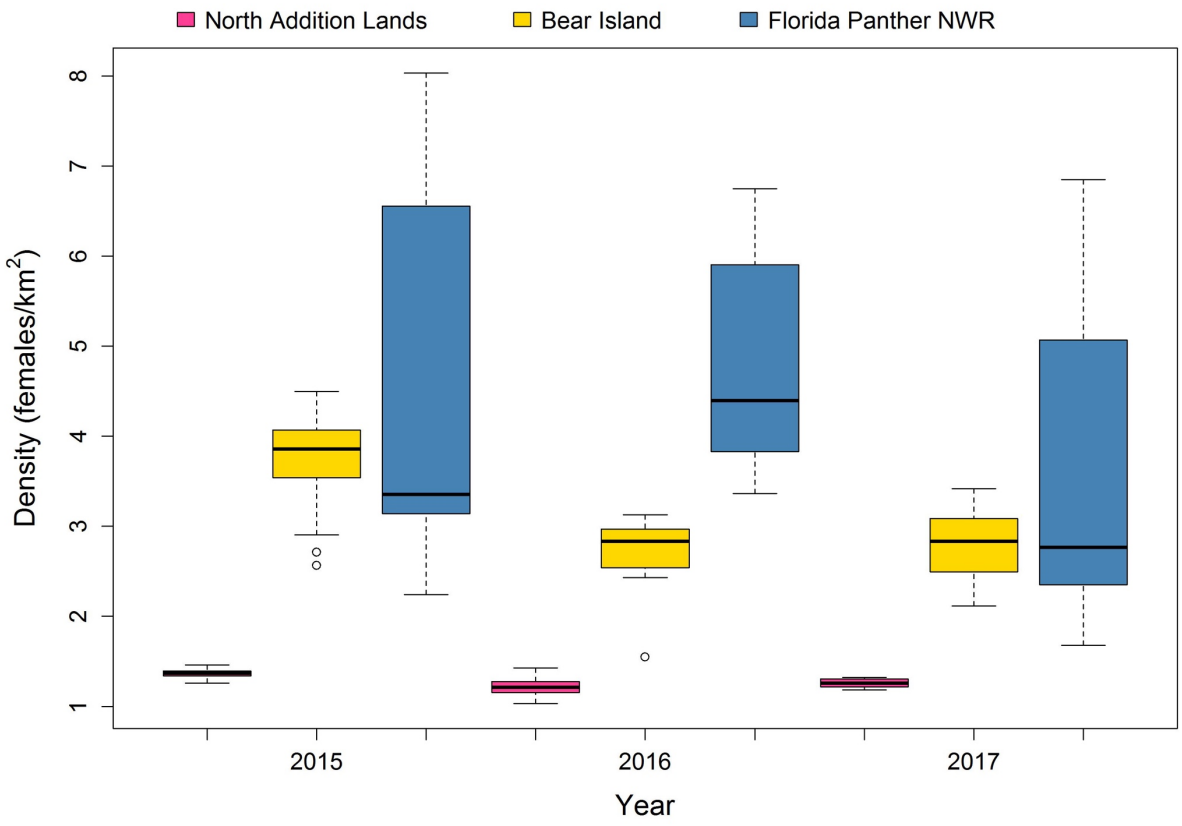

Figure 2.6. Annual fortnight density estimates for female white-tailed deer on North Addition Lands during January 2015 – June 2017, Bear Island during January 2015 – December 2017, and the Florida Panther National Wildlife Refuge during April 2015 – December 2017.

APPENDICES

Appendix 2.A. Camera trapping arrays

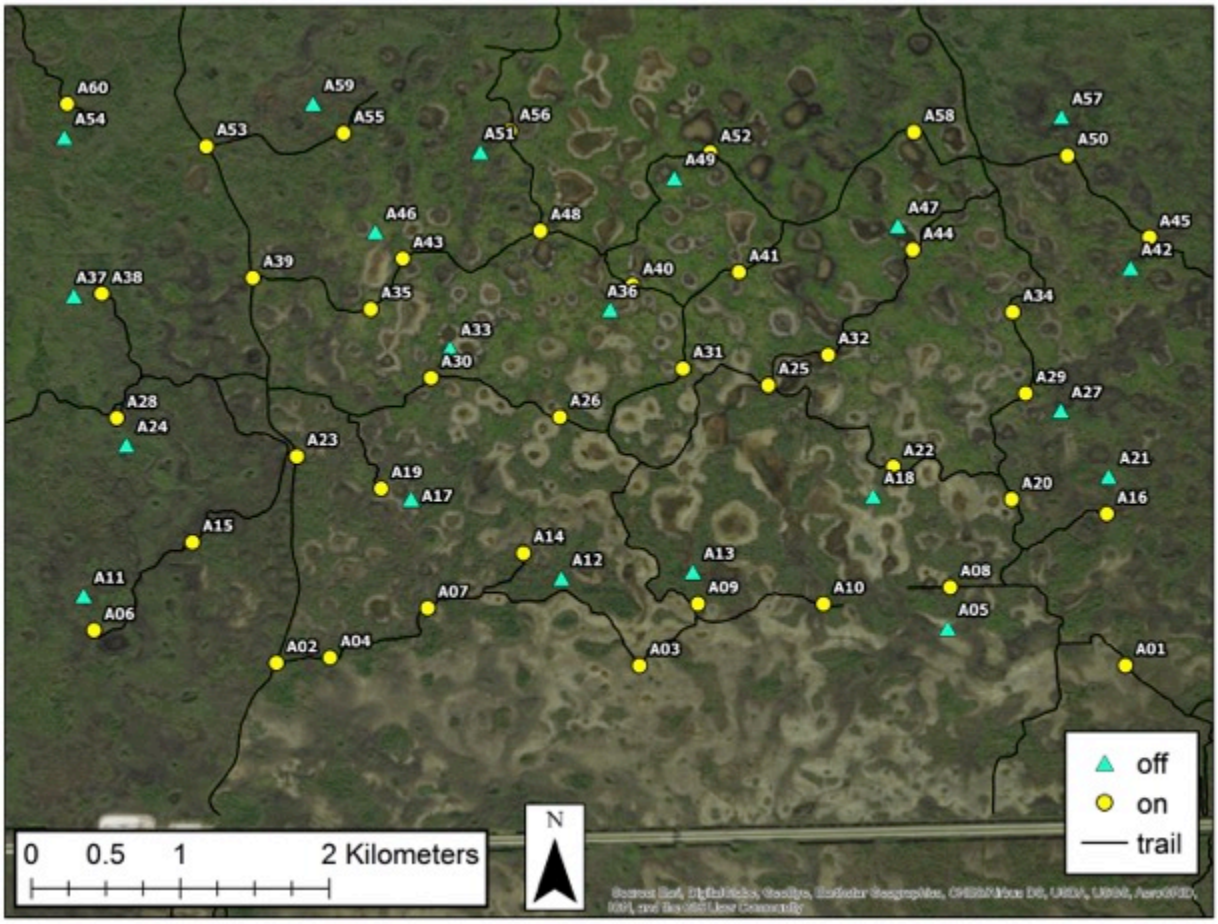

Figure 2.A1. Locations of the 60 cameras used to monitor white-tailed deer between January 2015 – December 2017 within the North Addition Lands study site in Big Cypress National Preserve. Yellow circles indicate on-trail cameras, and blue triangles indicate off-trail cameras.

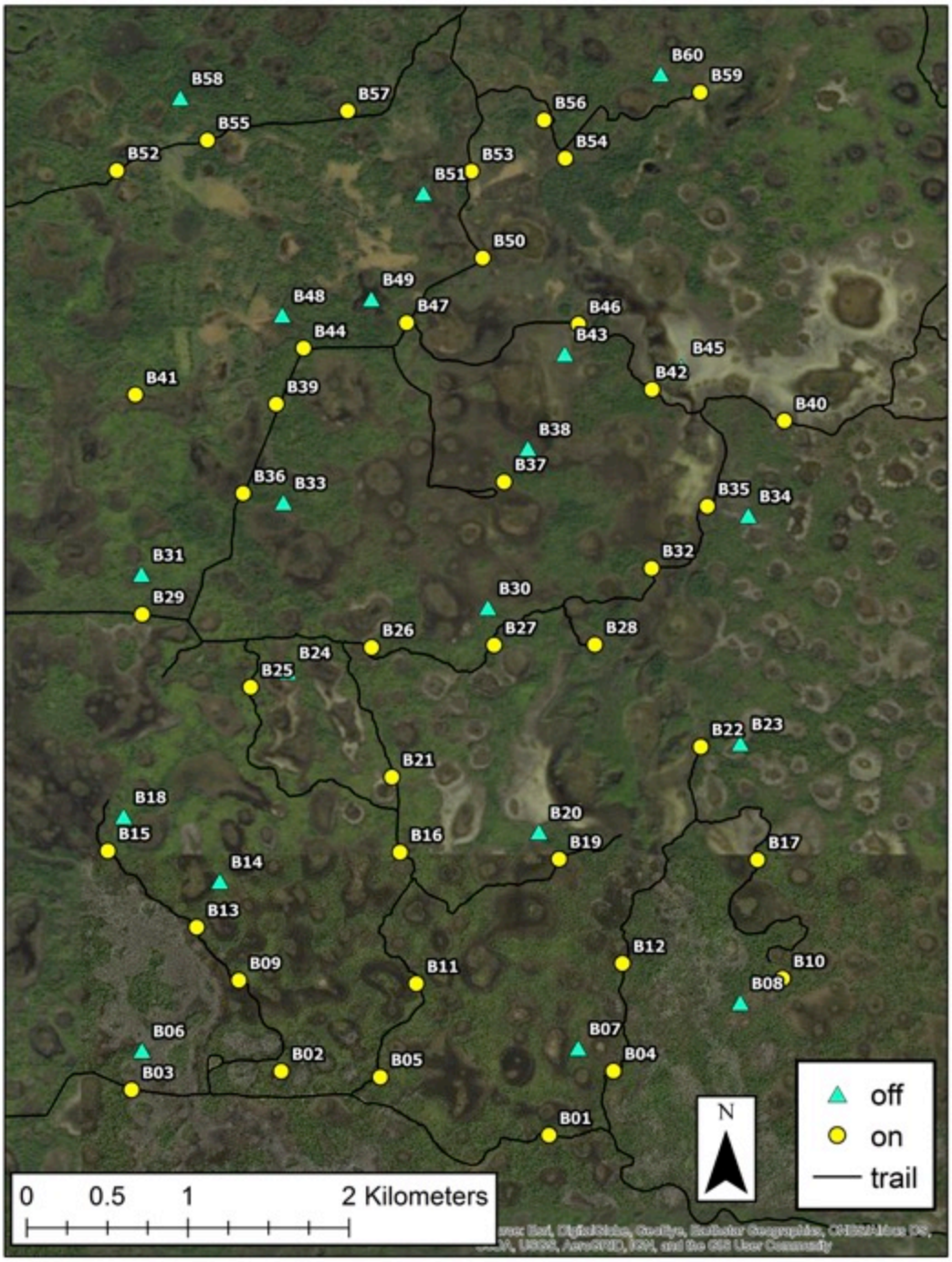

Figure 2.A2. Location of the 60 cameras used to monitor white-tailed deer between January 2015 – December 2017 within the Bear Island study site in Big Cypress National Preserve. Yellow circles indicate on-trail cameras, and blue triangles indicate off-trail cameras.

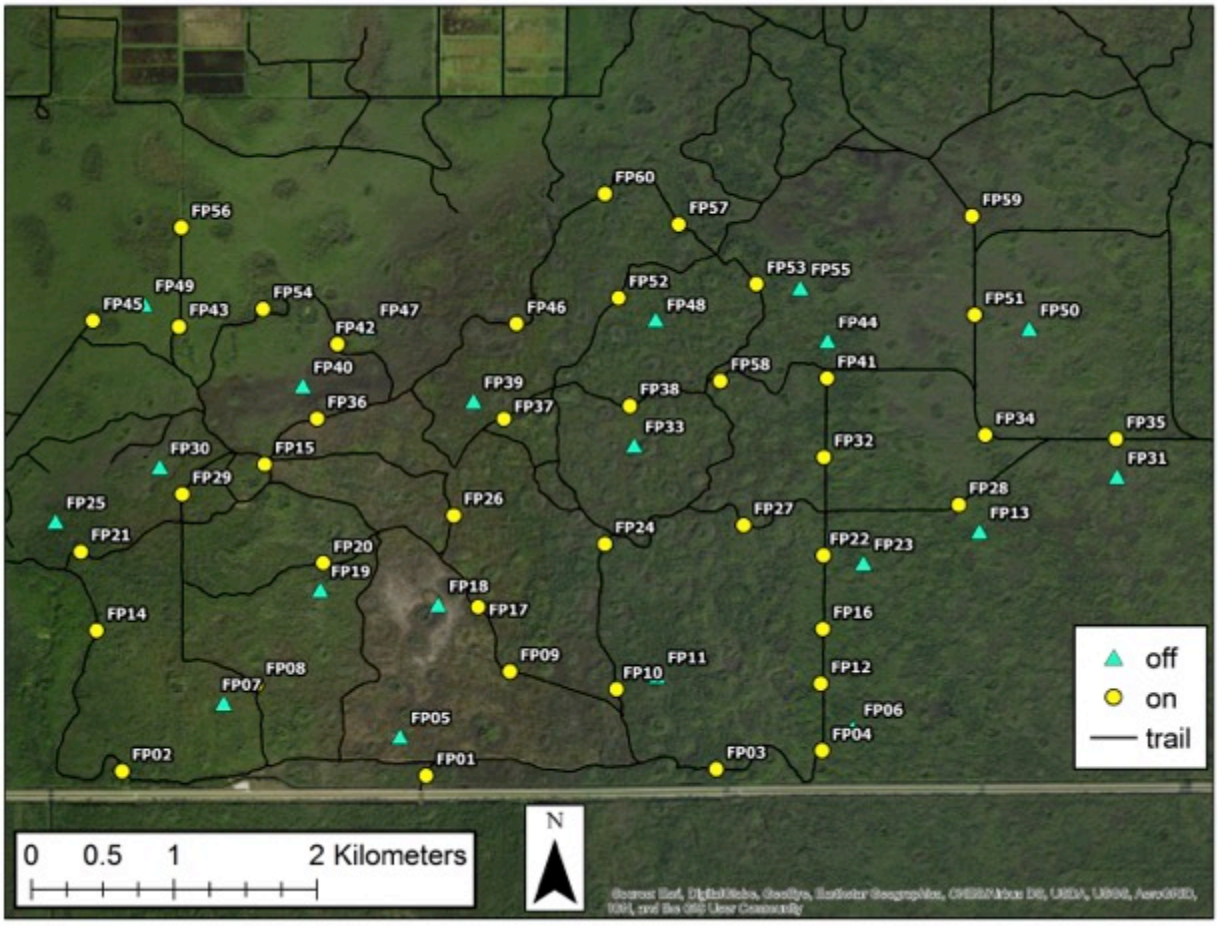

Figure 2.A3. Location of the 60 cameras used to monitor white-tailed deer between January 2015 – December 2017 within the Florida Panther National Wildlife Refuge. Yellow circles indicate on-trail cameras, and blue triangles indicate off-trail cameras.

Appendix 2.B. Autoregressive Unmarked SCR model

```
densityNimble <- nimbleCode({

 ### Prior Distributions
 # Autoregressive estimation
 for(t in 1:T) {
  # Use the posterior estimates from the marked population as informative
  # priors for the unmarked population
  # Multivariate normal distribution
  log_sig_lam0[1:2,t] ~ dmnorm(prior_means[t,1:2], cov=prior_vcov[t,1:2,1:2])
  sigma[t] <- exp(log_sig_lam0[1,t])
  lam0[t] <- exp(log_sig_lam0[2,t])
 }

 beta0.ED ~ dnorm(5, sd = 2.5)  # intercept of ED
 beta1.ED ~ dnorm(0, sd = 0.1)  # slope of ED
 eps.sd ~ dunif(0, 2) ## SD of density noise
 alpha ~ dunif(-1, 1) ## AR1 correlation
 epsilon[1] ~ dnorm(0, sd=eps.sd) # density noise
 ED[1] <- max(beta0.ED + beta1.ED*1 + epsilon[1], 0) # left truncated glm
 EN[1] <- ED[1]*Area # convert ED to EN
 psi[1] <- EN[1]/M # proportion of population in sample

 for(t in 2:T){
  epsilon[t] ~ dnorm(alpha*epsilon[t-1], sd=eps.sd) # autoregression on noise
  ED[t] <- max(beta0.ED + beta1.ED*t + epsilon[t], 0)
  EN[t] <- ED[t]*Area
  psi[t] <- EN[t]/M
 }

 ###Unmarked SCR
 for(t in 1:T){ # loop over each fortnight
  for(i in 1:M){ # loop over each individual
   z[i,t] ~ dbern(psi[t]) # probability of being a member of the population
   # activity centers probabilities assumed uniform
   s[i,1,t] ~ dunif(xlim[1], xlim[2])
   s[i,2,t] ~ dunif(ylim[1], ylim[2])
   for(j in 1:J){ # loop over each trap location
    # calculate distance from activity center to trap location
    d[i,j,t] <- sqrt((s[i,1,t]-x[j,1])^2 + (s[i,2,t]-x[j,2])^2)
    # calculate encounter rate
    lambda[i,j,t] <- lam0[t]*exp(-d[i,j,t]^2 / (2*sigma[t]^2))
   }
  }
  for(j in 1:J) { # loop over each trap location
   Lambda[j,t] <- inprod(lambda[1:M,j,t] , z[1:M,t]) # trap-time specific encounter rate
   p[j,t] <- 1-exp(-Lambda[j,t]) # convert to encounter probability
   nsum[j,t] ~ dbin(p[j,t], K[j,t])
  }
  N[t] <- sum(z[1:M,t]) # abundance
  D[t] <- N[t]/Area # density
 }
})
```

Appendix 2.C. Spatio-temporal trends in the white-tailed deer camera detections

We used two summary statistics to characterize spatio-temporal trends in the raw camera data from 1 January 2015 – 31 December 2017. First, we calculated the daily detection rates at each of the three study sites for adult female white-tailed deer. Daily detection rates were calculated by dividing the total number of detections at a site by the number of cameras that were operational on that day. In most cases, all 60 cameras were operational at each site on each day, but cameras occasionally failed, and in one instance, cameras were removed from a site that was threatened by wildfire. Daily detection rates provided a useful summary of trends in the camera data, but can be influenced by high levels of variability caused by animals that spent long periods of time in front of a camera and were repeatedly photographed. To reduce the influence of these bursts of photographs, we calculated a second summary statistic: the daily proportion of cameras that had a least one detection of female white-tailed deer. To visualize both spatial and temporal heterogeneity, we mapped 6-month averages of the detection rates at each camera.

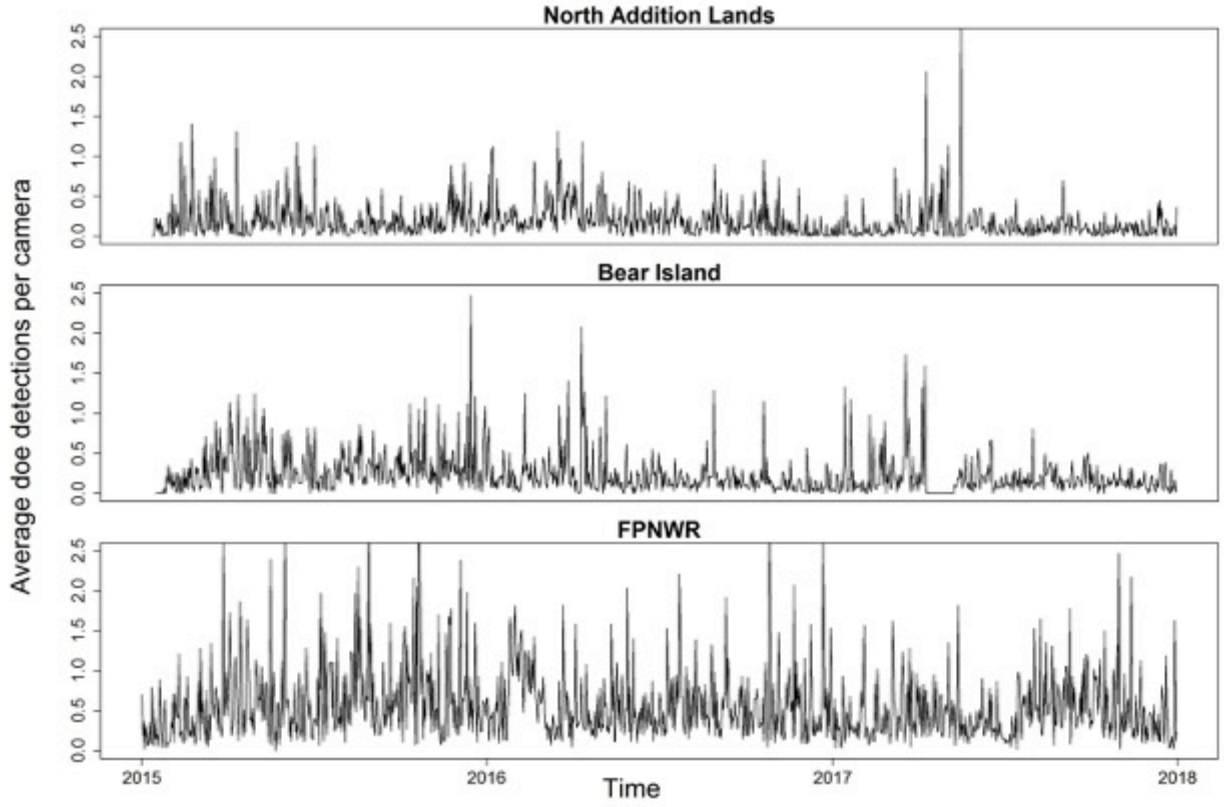

Figure 2.C1. Daily female white-tailed detections per trail camera day across the three trail camera sites in North Addition Lands, Bear Island, and Florida Panther National Wildlife Refuge (FPNWR) from 1 January 2015 – 31 December 2017. We removed cameras from Bear Island during April - May 2017 due to wildfires.

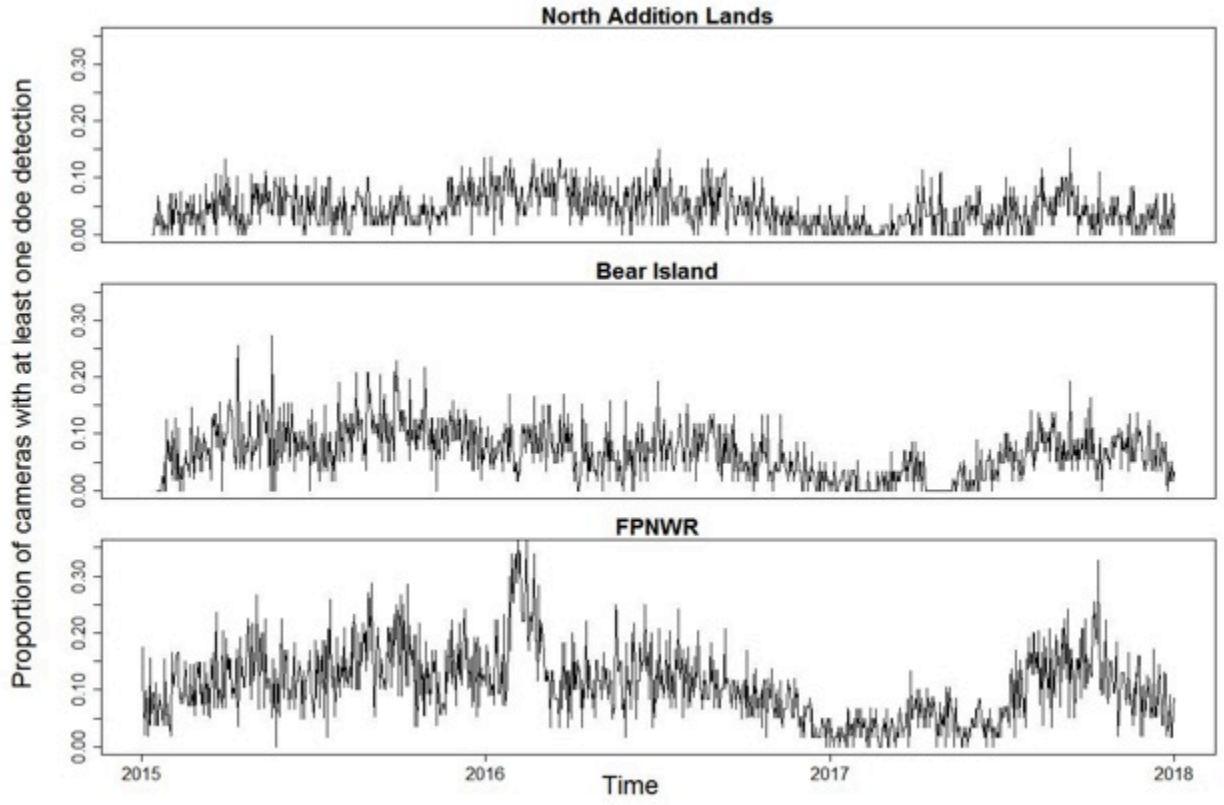

Figure 2.C2. The proportion of trail cameras with at least one female white-tailed deer detection on each day from January 2015 – December 2017 at the three trail camera sites in North Addition Lands, Bear Island, and Florida Panther National Wildlife Refuge (FPNWR). We removed cameras from Bear Island during April – May 2017 due to wildfires.

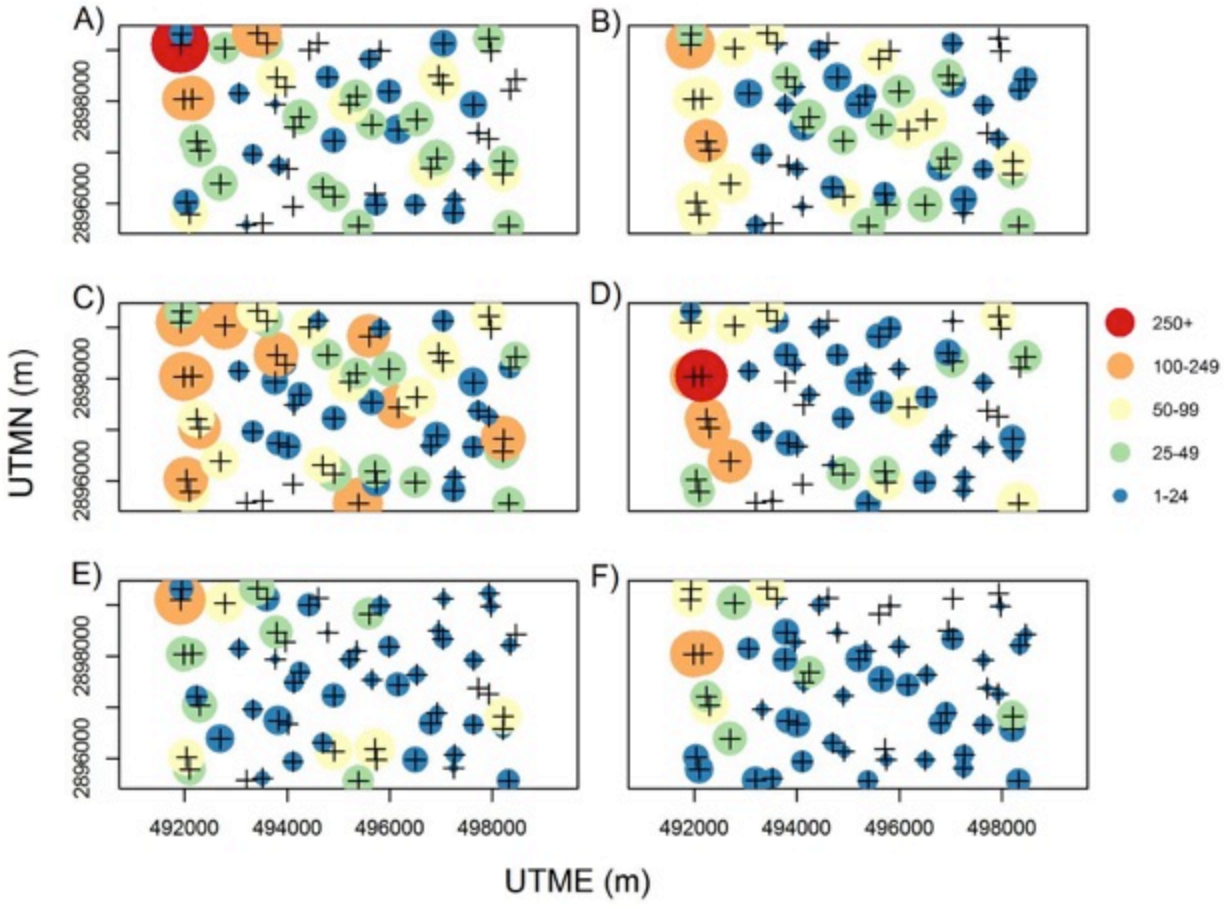

Figure 2.C3. Maps of female white-tailed deer camera detections for 6-month periods on North Addition Lands. The size of each point reflects the number of detections. A) January - June 2015; B) July - December 2015; C) January - June 2016; D) July - December 2016; E) January - June 2017; F) July - December 2017.

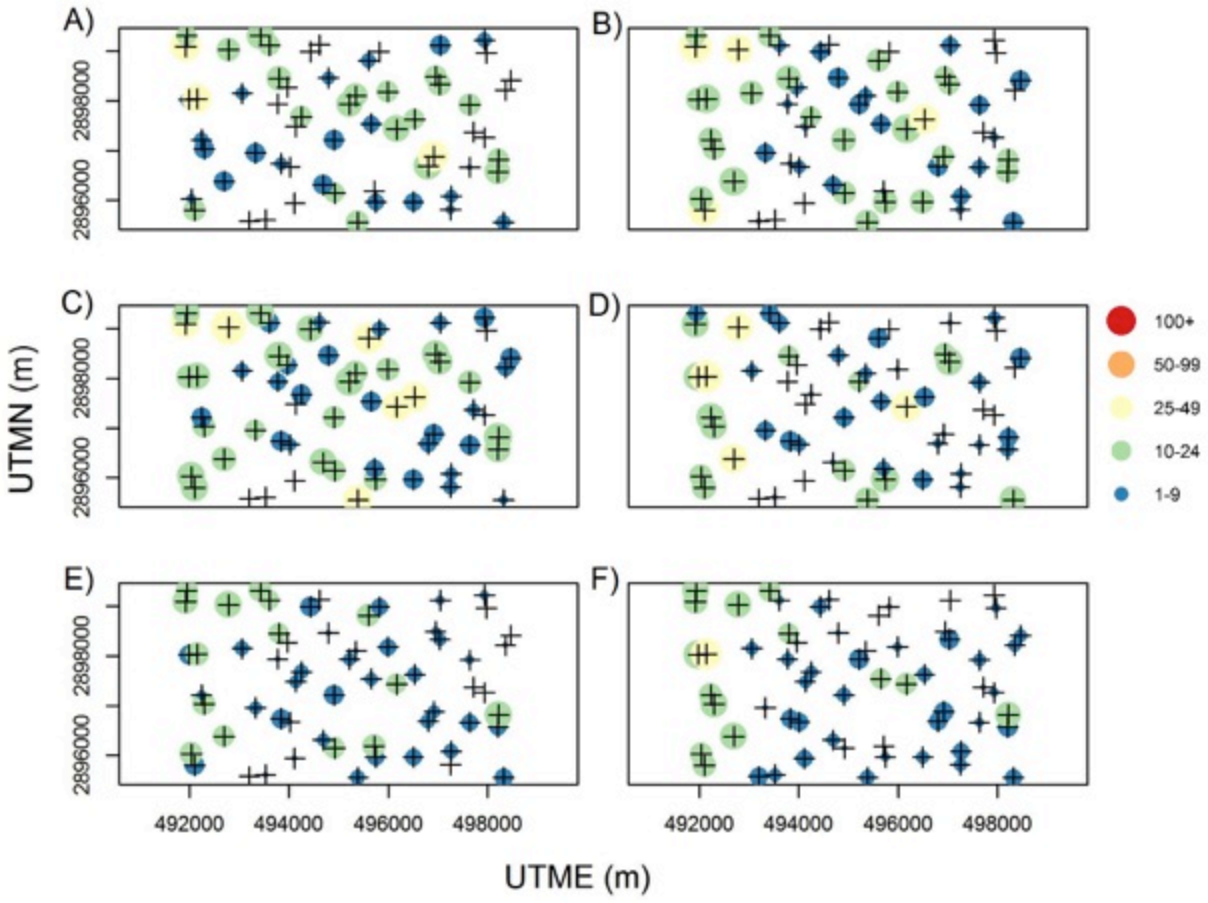

Figure 2.C4. Maps of female white-tailed deer daily occurrences for 6-month periods on North Addition Lands. An occurrence is defined as the detection of at least one deer at a camera during a 24 h sampling occasion. The size of each point reflects the number of daily occurrences. A) January - June 2015; B) July - December 2015; C) January - June 2016; D) July - December 2016; E) January - June 2017; F) July - December 2017.

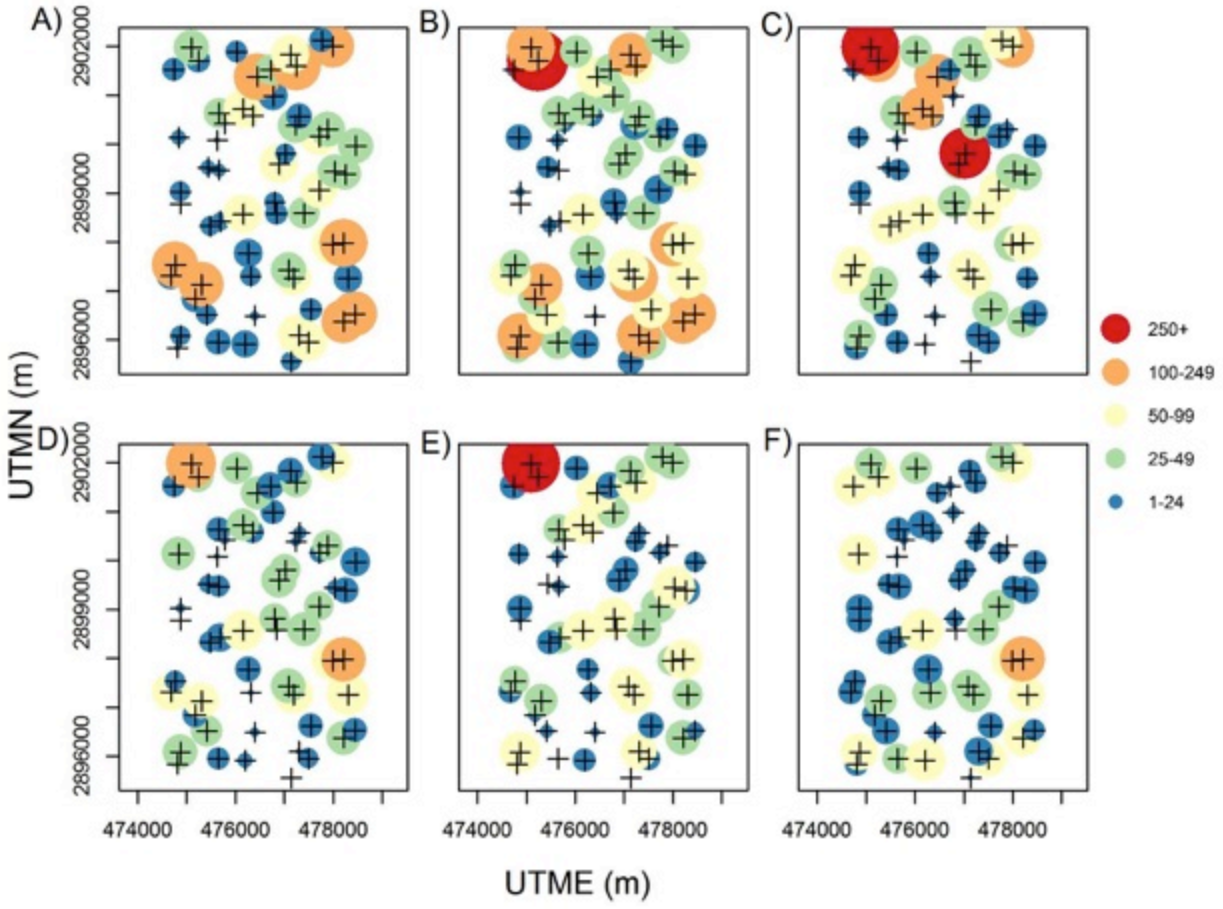

Figure 2.C5. Maps of female white-tailed deer camera detections for 6-month periods on Bear Island. The size of each point reflects the number of detections. A) January - June 2015; B) July - December 2015; C) January - June 2016; D) July - December 2016; E) January - June 2017; F) July - December 2017.

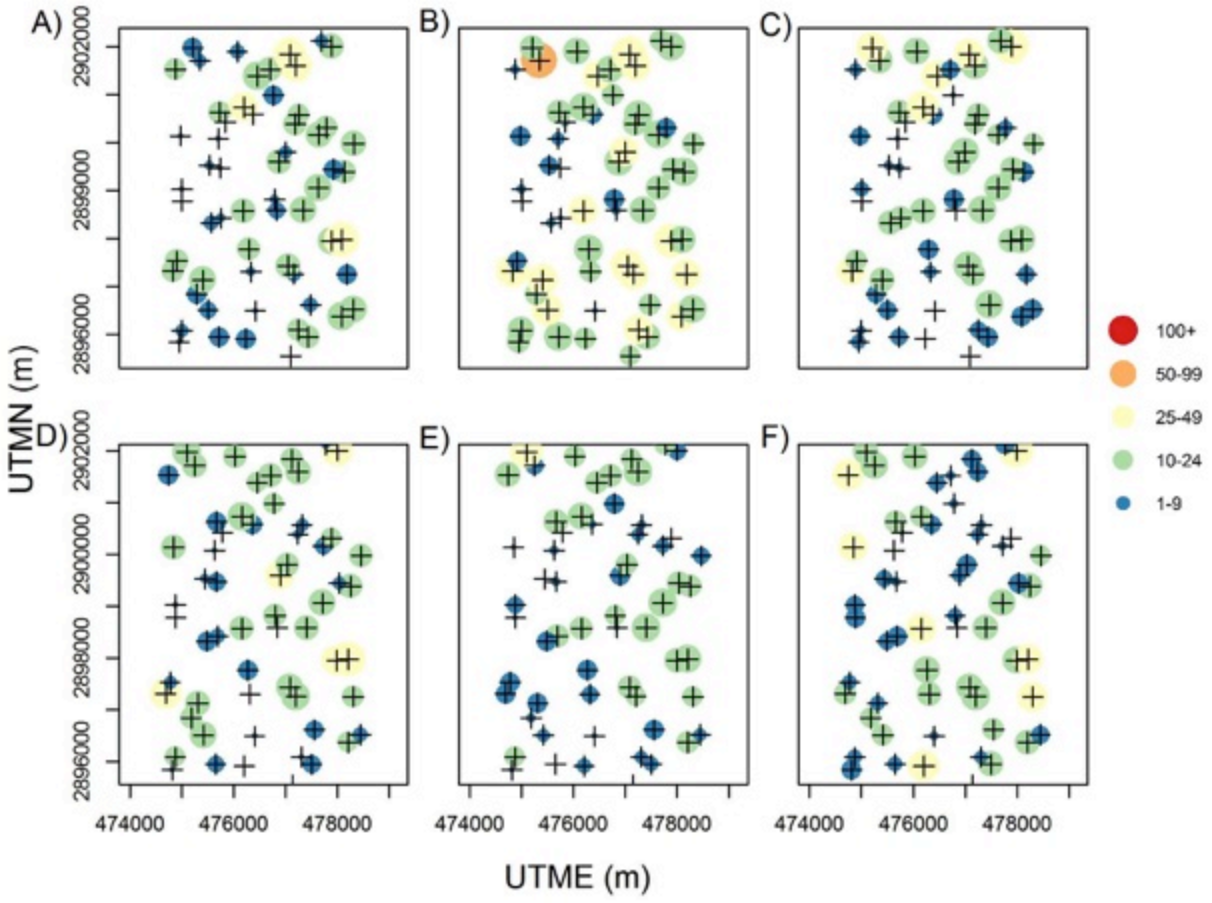

Figure 2.C6. Maps of female white-tailed deer daily occurrences for 6-month periods on Bear Island. An occurrence is defined as the detection of at least one deer at a camera during a 24 h sampling occasion. The size of each point reflects the number of daily occurrences. A) January - June 2015; B) July - December 2015; C) January - June 2016; D) July - December 2016; E) January - June 2017; F) July - December 2017.

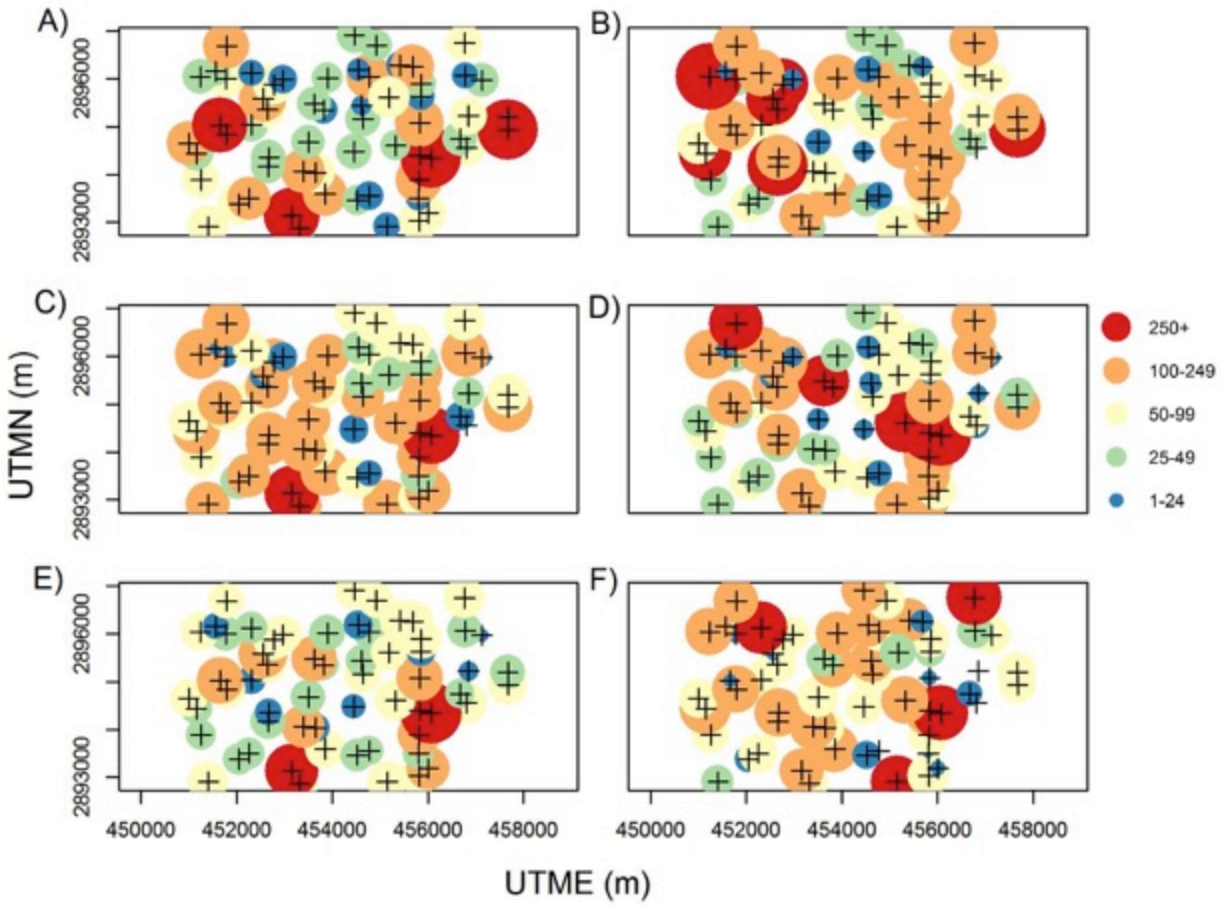

Figure 2.C7. Maps of female white-tailed deer camera detections for 6-month periods on Florida Panther National Wildlife Refuge. The size of each point reflects the number of detections. A) January - June 2015; B) July - December 2015; C) January - June 2016; D) July - December 2016; E) January - June 2017; F) July - December 2017.

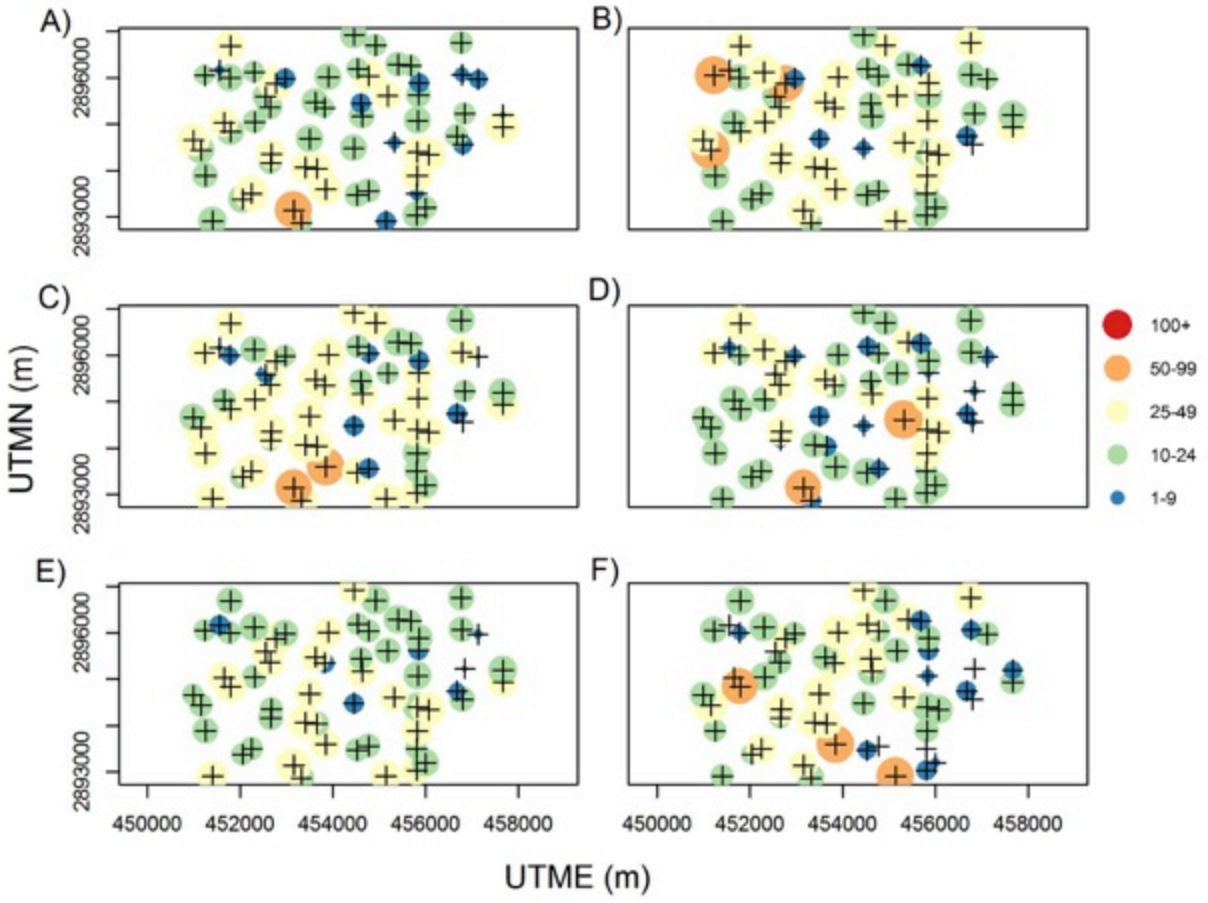

Figure 2.C8. Maps of female white-tailed deer daily occurrences for 6-month periods on Florida Panther National Wildlife Refuge. An occurrence is defined as the detection of at least one deer at a camera during a 24 h sampling occasion. The size of each point reflects the number of daily occurrences. A) January - June 2015; B) July - December 2015; C) January - June 2016; D) July - December 2016; E) January - June 2017; F) July - December 2017.

Appendix 2.D. Telemetry locations of GPS-collared female white-tailed deer on camera grids

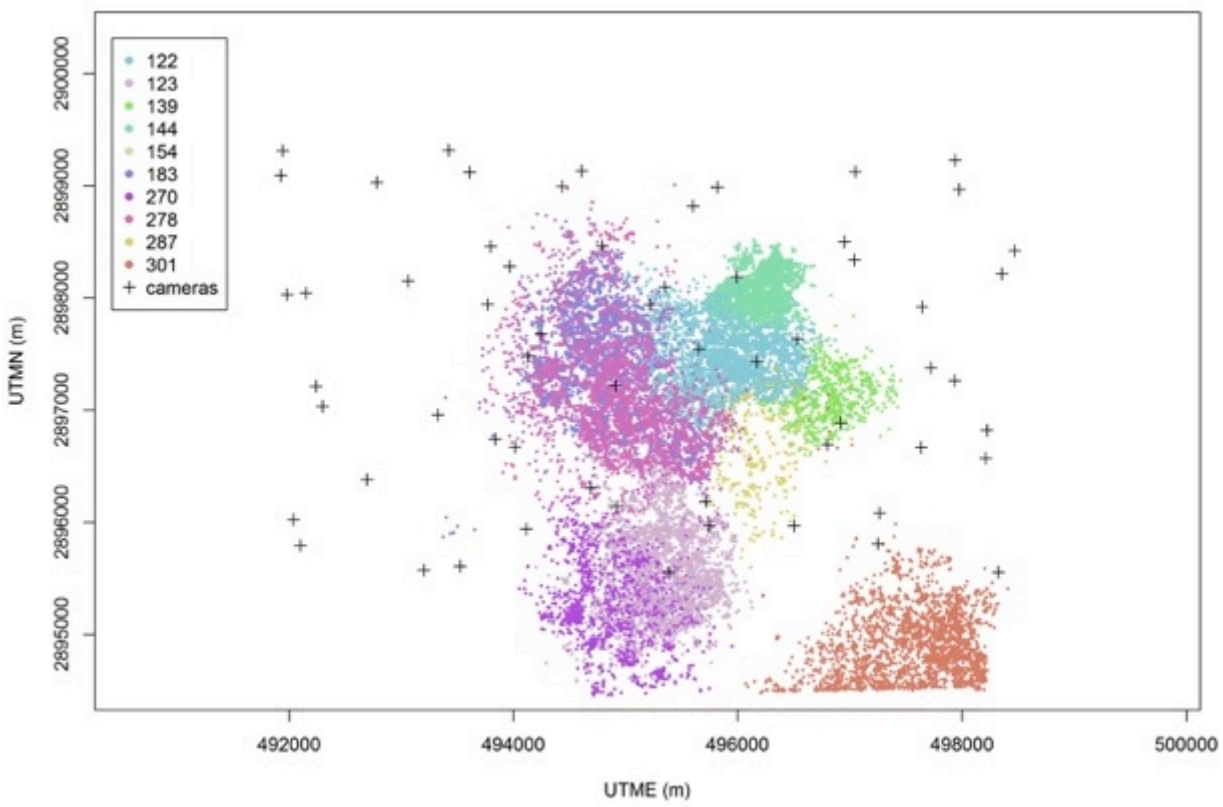

Figure 2.D1. Telemetry locations of 10 GPS-collared white-tailed deer females during January 2015 – December 2017 on North Addition Lands in Big Cypress National Preserve used to estimate the detection probability parameters for the spatial capture-recapture model.

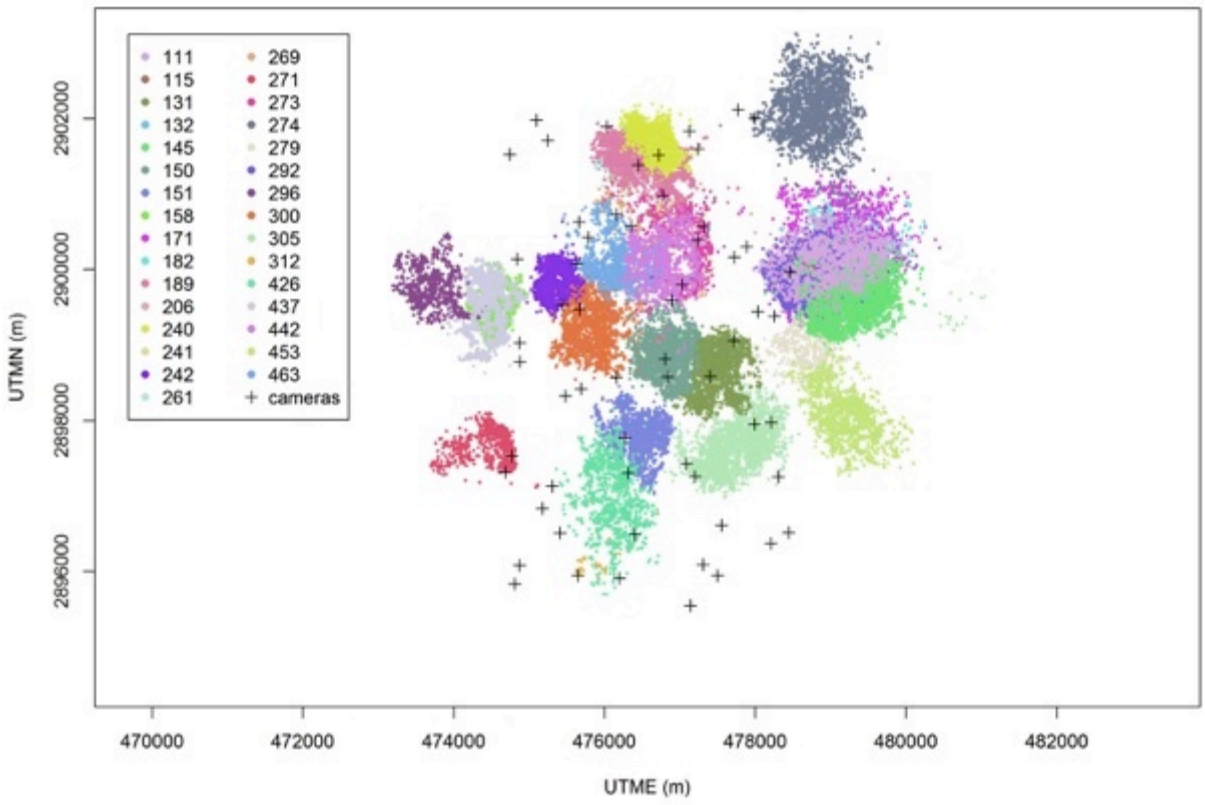

Figure 2.D2. Telemetry locations of 31 GPS-collared female white-tailed deer on Bear Island, Big Cypress National Preserve, used to estimate the detection probability parameters for the spatial capture-recapture model during January 2015 – December 2017.

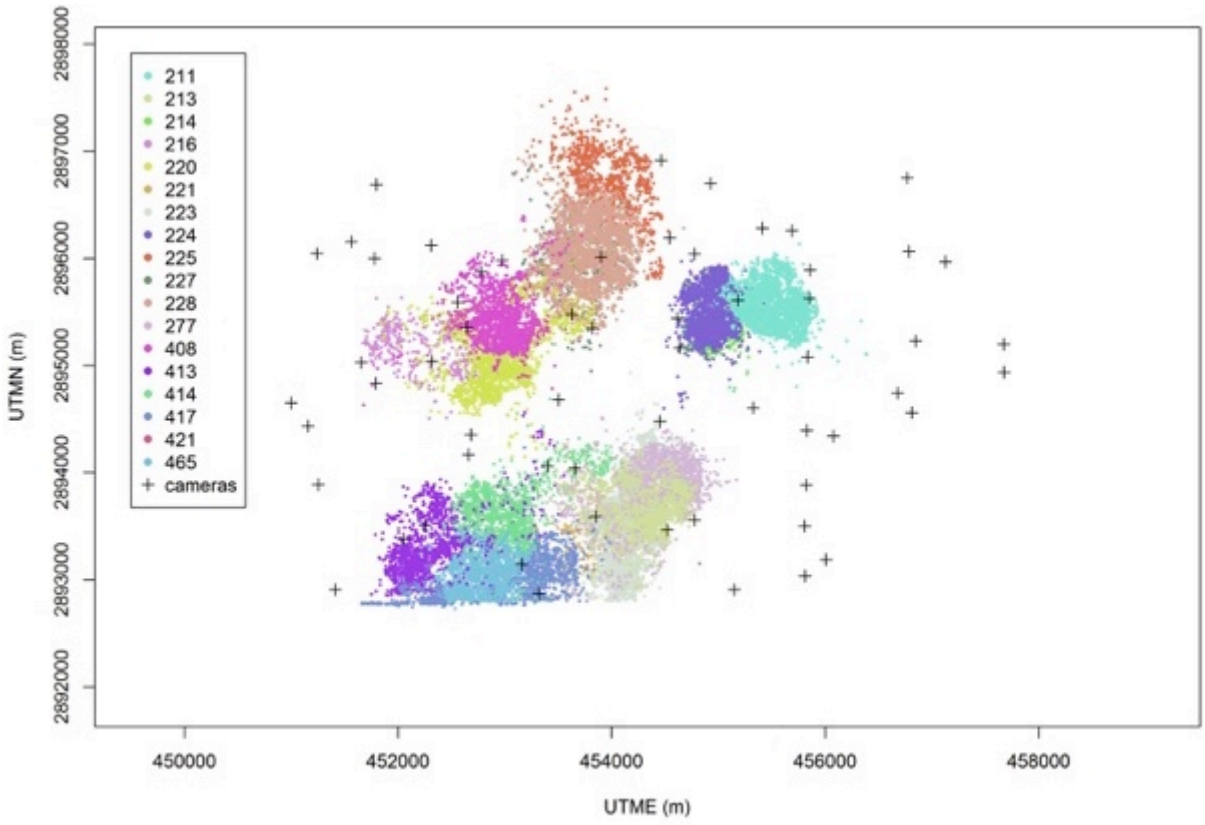

Figure 2.D3. Telemetry locations of 18 GPS-collared female white-tailed deer on Florida Panther National Wildlife Refuge (FPNWR) during April 2015 – December 2017, used to estimate the detection probability parameters for the spatial capture-recapture model.

Appendix 2.E. Posterior summary statistics of AR(1) encounter rate estimation model

Table 2.E1. Posterior summary statistics for the marked GPS-collared Gaussian AR(1) encounter rate estimation model (stage one) for each camera array. Mean, median, standard deviation (SD) and 95% credible intervals (CI) are reported for the average across all fortnights. Estimates for β are back-transformed from log-means.

	Mean	Median	SD	LowerCI	UpperCI
North Addition Lands					
α^{λ_0}	0.704	0.734	0.184	0.279	0.965
$\beta_0^{\lambda_0}$	0.124	0.122	0.028	0.075	0.187
$\beta_1^{\lambda_0}$	0.983	0.983	0.006	0.968	0.994
α^{σ}	0.855	0.857	0.066	0.717	0.973
β_0^{σ}	219.6	218.9	17.56	183.1	253.4
β_1^{σ}	1.010	1.010	0.001	1.008	1.013
Bear Island					
α^{λ_0}	0.710	0.741	0.182	0.242	0.969
$\beta_0^{\lambda_0}$	0.071	0.069	0.015	0.046	0.111
$\beta_1^{\lambda_0}$	0.995	0.996	0.005	0.984	1.004
α^{σ}	0.999	0.999	0.001	0.997	1.000
β_0^{σ}	142.1	141.9	1.46	139.3	146.2
β_1^{σ}	1.121	1.121	0.001	1.119	1.122
Florida Panther National Wildlife Refuge					
α^{λ_0}	0.798	0.812	0.106	0.551	0.965
$\beta_0^{\lambda_0}$	0.106	0.099	0.037	0.054	0.203
$\beta_1^{\lambda_0}$	1.000	1.000	0.008	0.981	1.014
α^{σ}	0.766	0.768	0.089	0.580	0.929
β_0^{σ}	167.2	165.5	10.80	151.1	201.0
β_1^{σ}	1.005	1.006	1.001	1.003	1.007

Appendix 2.F. Prior and posterior distribution comparisons for σ and λ_0

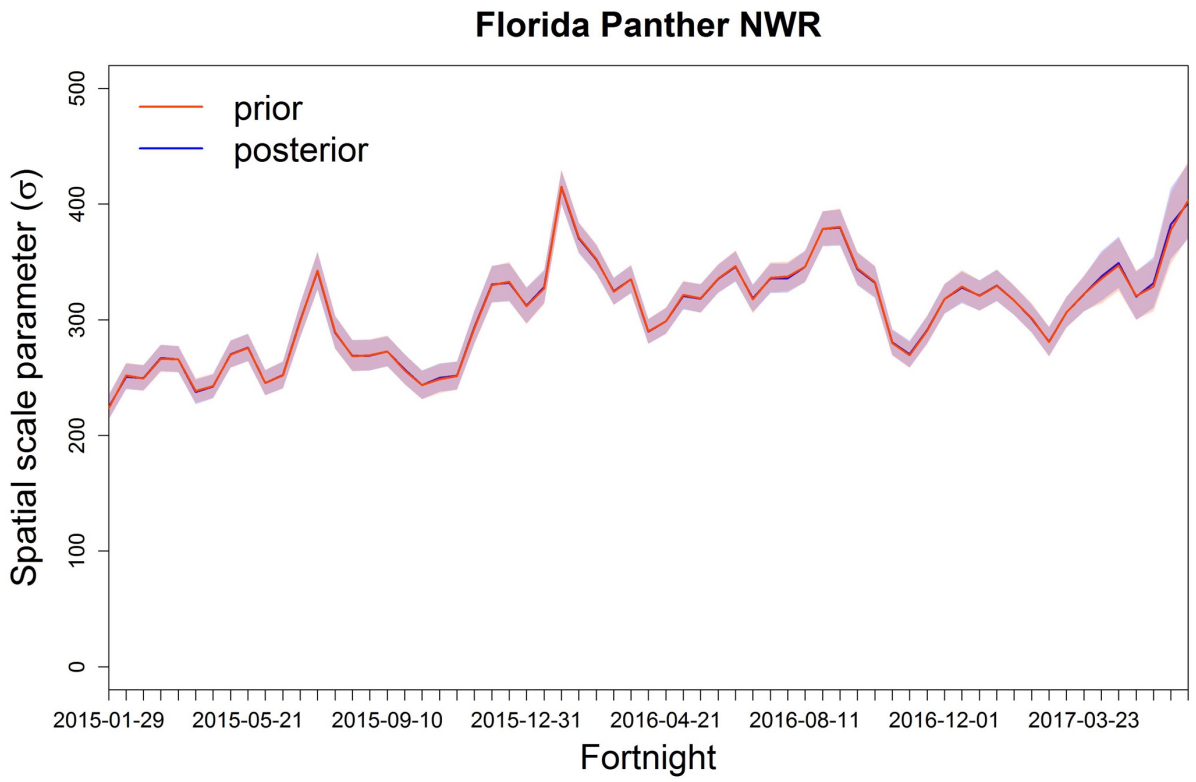

Figure 2.F1. Biweekly estimates and 95% credible intervals of the spatial scale parameter (σ) for the prior and the posterior distribution for the unmarked female white-tailed deer population model in North Addition Lands. The prior distribution for the unmarked model is defined by the posterior distribution from the marked population model.

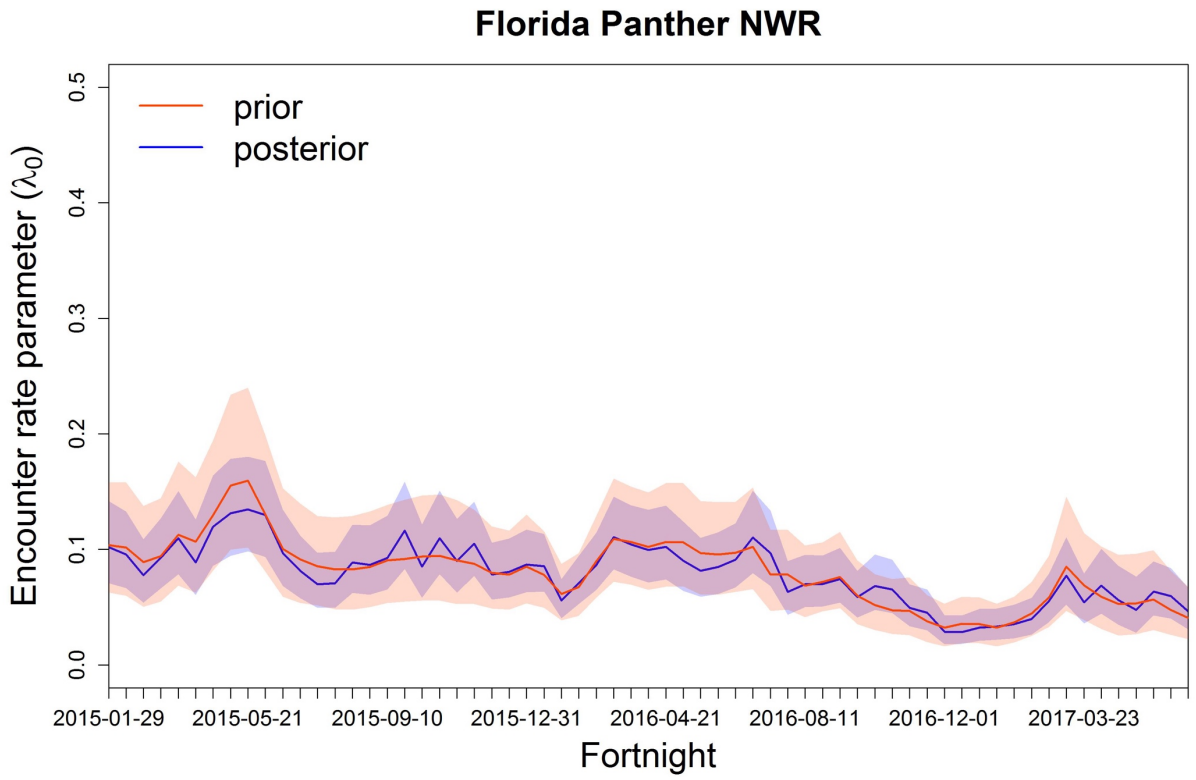

Figure 2.F2. Biweekly estimates and 95% credible intervals of the encounter rate parameter (λ_0) for the prior and the posterior distribution for the unmarked female white-tailed deer population model in North Addition Lands. The prior distribution for the unmarked model is defined by the posterior distribution from the marked population model.

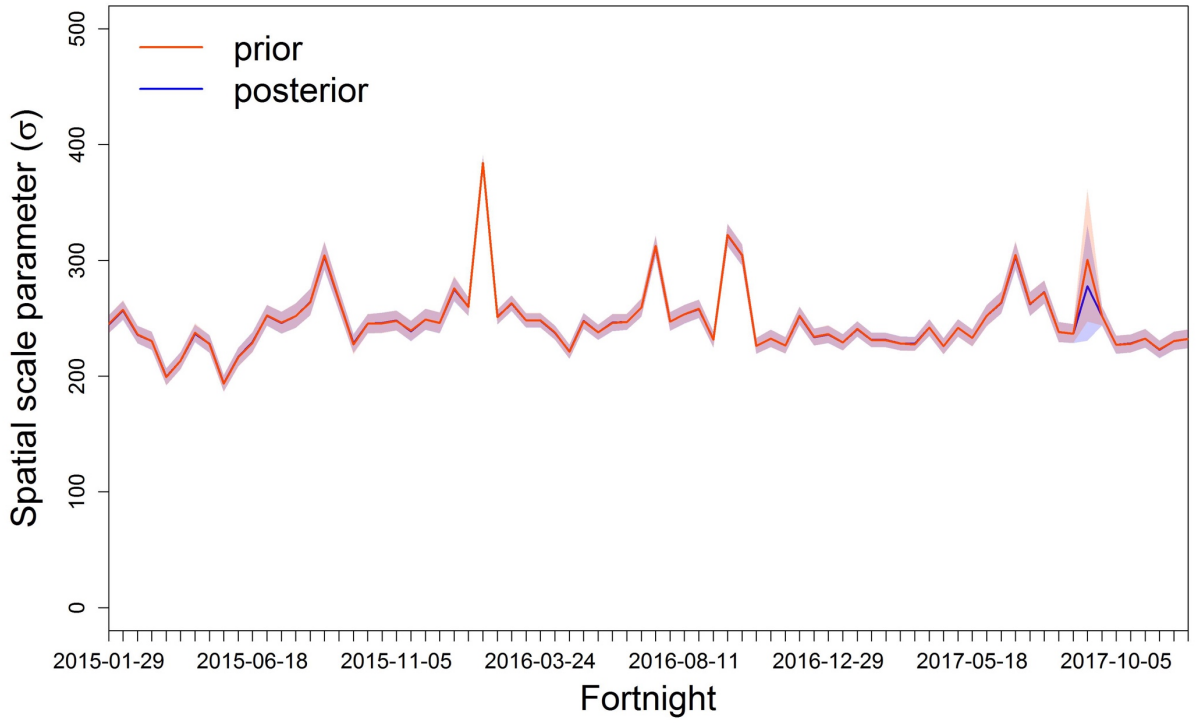

Figure 2.F3. Biweekly estimates and 95% credible intervals of the spatial scale parameter (σ) for the prior and the posterior distribution for the unmarked female white-tailed deer population model in Bear Island. The prior distribution for the unmarked model is defined by the posterior distribution from the marked population model.

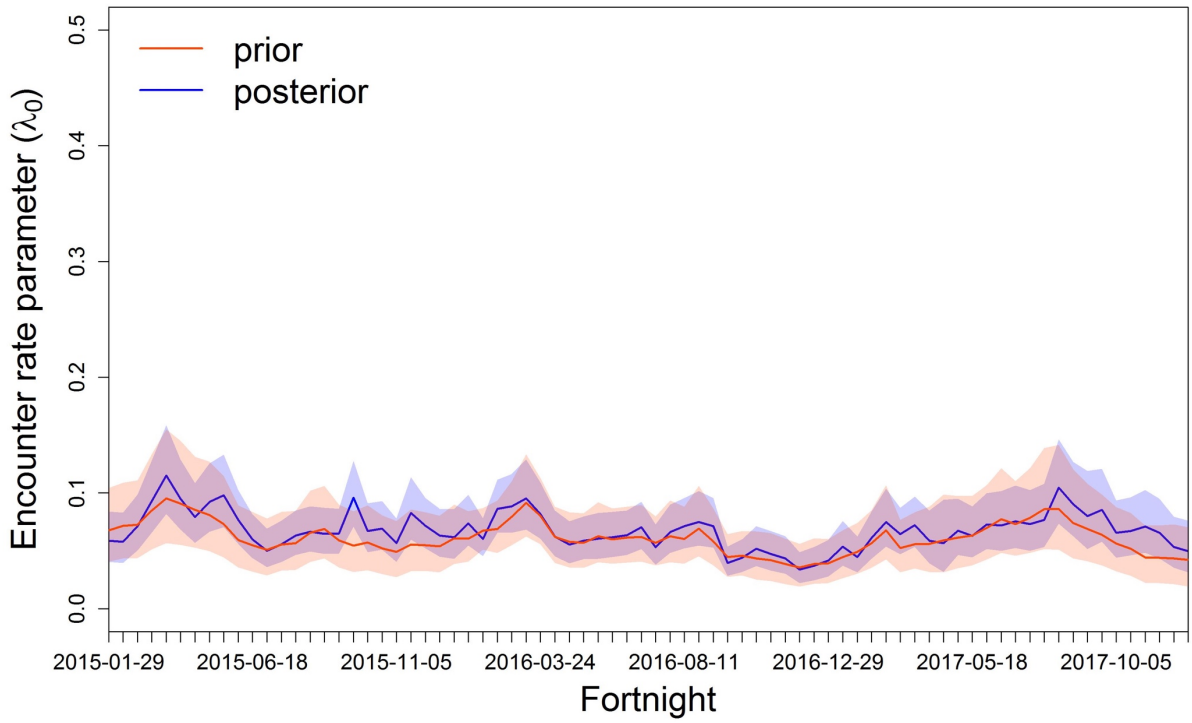

Figure 2.F4. Biweekly estimates and 95% credible intervals of the encounter rate parameter (λ_0) for the prior and the posterior distribution for the unmarked female white-tailed deer population model in Bear Island. The prior distribution for the unmarked model is defined by the posterior distribution from the marked population model.

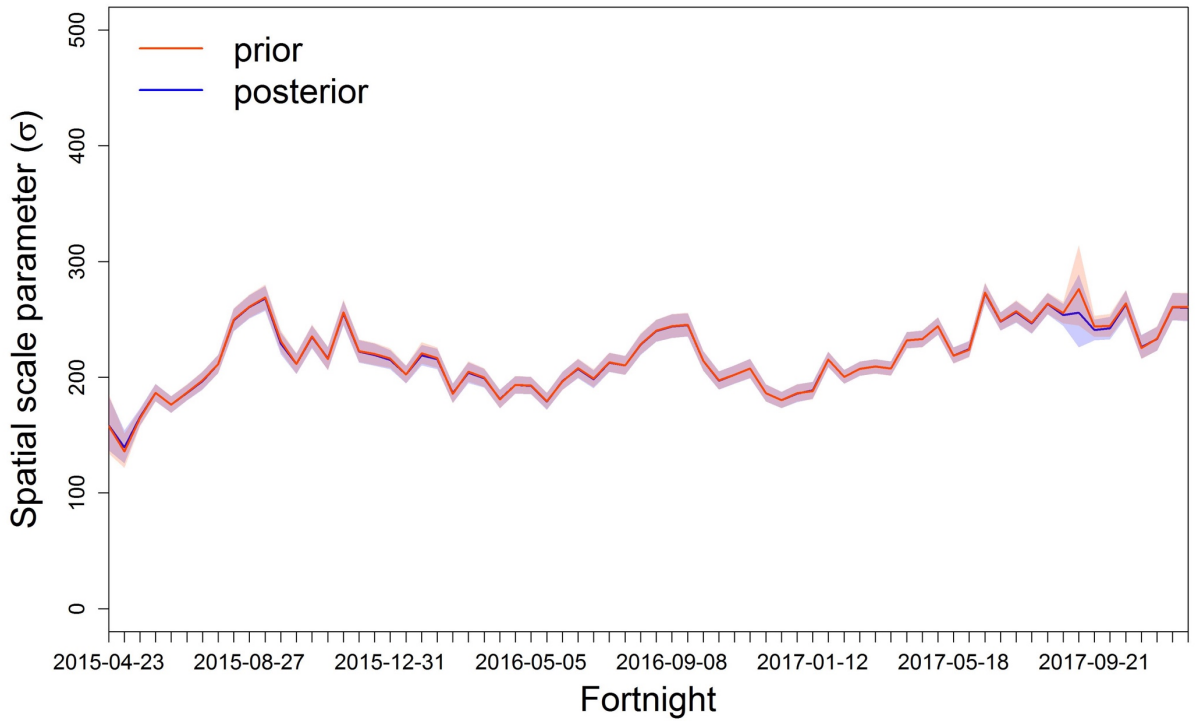

Figure 2.F5. Biweekly estimates and 95% credible intervals of the spatial scale parameter (σ) for the prior and the posterior distribution for the unmarked female white-tailed deer population model in Florida Panther National Wildlife Refuge. The prior distribution for the unmarked model is defined by the posterior distribution from the marked population model.

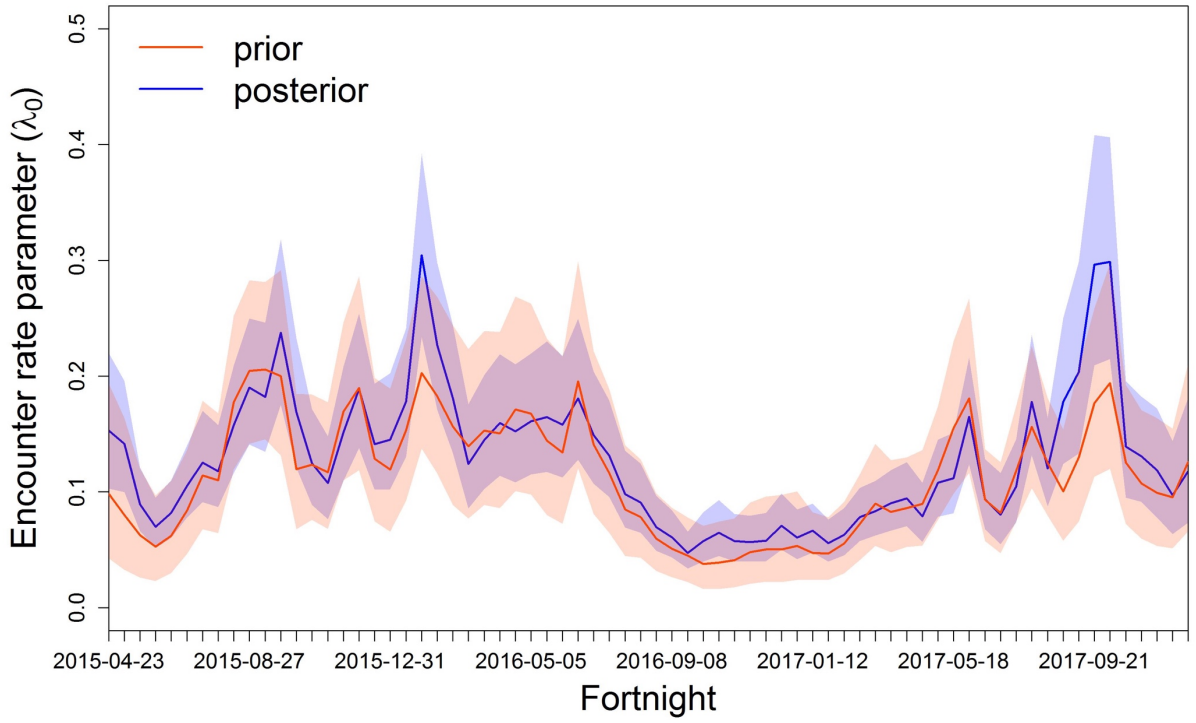

Figure 2.F6. Biweekly estimates and 95% credible intervals of the encounter rate parameter (λ_0) for the prior and the posterior distribution for the unmarked female white-tailed deer population model in Florida Panther National Wildlife Refuge. The prior distribution for the unmarked model is defined by the posterior distribution from the marked population model.

Appendix 2.G. Abundance and density fortnight estimates

Table 2.G1. Posterior density estimates for North Addition Lands. Mean, median, standard deviation (SD), and 95% credible intervals are reported for 76 fortnights.

Parameter	Fortnight	Mean	Median	SD	2.5%	97.5%
D[1]	29 Jan 2015 - 11 Feb 2015	1.458	1.442	0.186	1.117	1.848
D[2]	12 Feb 2015 - 25 Feb 2015	1.326	1.32	0.185	0.975	1.706
D[3]	26 Feb 2015 - 11 Mar 2015	1.429	1.422	0.185	1.077	1.808
D[4]	12 Mar 2015 - 25 Mar 2015	1.441	1.442	0.178	1.097	1.808
D[5]	26 Mar 2015 - 8 Apr 2015	1.393	1.381	0.177	1.077	1.747
D[6]	9 Apr 2015 - 22 Apr 2015	1.297	1.300	0.176	0.975	1.666
D[7]	23 Apr 2015 - 6 May 2015	1.358	1.361	0.173	1.036	1.706
D[8]	7 May 2015 - 20 May 2015	1.300	1.300	0.165	0.995	1.625
D[9]	21 May 2015 - 3 Jun 2015	1.345	1.341	0.165	1.036	1.686
D[10]	4 Jun 2015 - 17 Jun 2015	1.369	1.361	0.167	1.056	1.706
D[11]	18 Jun 2015 - 1 Jul 2015	1.383	1.381	0.173	1.056	1.727
D[12]	2 Jul 2015 - 15 Jul 2015	1.366	1.361	0.170	1.036	1.727
D[13]	16 Jul 2015 - 29 Jul 2015	1.260	1.259	0.168	0.955	1.605
D[14]	30 Jul 2015 - 12 Aug 2015	1.308	1.300	0.171	0.995	1.666
D[15]	13 Aug 2015 - 26 Aug 2015	1.414	1.402	0.172	1.097	1.767
D[16]	27 Aug 2015 - 9 Sep 2015	1.345	1.341	0.174	1.016	1.706
D[17]	10 Sep 2015 - 23 Sep 2015	1.340	1.341	0.170	1.016	1.686
D[18]	24 Sep 2015 - 7 Oct 2015	1.405	1.402	0.172	1.077	1.767
D[19]	8 Oct 2015 - 21 Oct 2015	1.337	1.320	0.175	1.016	1.706
D[20]	22 Oct 2015 - 4 Nov 2015	1.459	1.442	0.175	1.138	1.828
D[21]	5 Nov 2015 - 18 Nov 2015	1.390	1.381	0.175	1.077	1.767
D[22]	19 Nov 2015 - 2 Dec 2015	1.393	1.381	0.171	1.077	1.747
D[23]	3 Dec 2015 - 16 Dec 2015	1.386	1.381	0.173	1.077	1.747
D[24]	17 Dec 2015 - 30 Dec 2015	1.325	1.320	0.168	1.016	1.666
D[25]	31 Dec 2015 - 13 Jan 2016	1.372	1.361	0.169	1.056	1.727
D[26]	14 Jan 2016 - 27 Jan 2016	1.427	1.422	0.167	1.117	1.767
D[27]	28 Jan 2016 - 10 Feb 2016	1.209	1.198	0.159	0.914	1.523
D[28]	11 Feb 2016 - 24 Feb 2016	1.302	1.300	0.162	0.995	1.625
D[29]	25 Feb 2016 - 9 Feb 2016	1.231	1.219	0.157	0.934	1.544
D[30]	10 Mar 2016 - 23 Mar 2016	1.334	1.320	0.158	1.036	1.666
D[31]	24 Mar 2016 - 6 Apr 2016	1.226	1.219	0.154	0.934	1.544
D[32]	7 Apr 2016 - 20 Apr 2016	1.213	1.219	0.158	0.914	1.523
D[33]	21 Apr 2016 - 4 May 2016	1.273	1.280	0.159	0.975	1.605
D[34]	5 May 2016 - 18 May 2016	1.125	1.117	0.157	0.833	1.442
D[35]	19 May 2016 - 1 Jun 2016	1.198	1.198	0.159	0.894	1.523

D[36]	2 Jun 2016 - 15 Jun 2016	1.164	1.158	0.156	0.873	1.483
D[37]	16 Jun 2016 - 29 Jun 2016	1.141	1.138	0.157	0.833	1.463
D[38]	30 Jun 2016 - 13 Jul 2016	1.243	1.239	0.163	0.934	1.564
D[39]	14 Jul 2016 - 27 Jul 2016	1.121	1.117	0.161	0.813	1.442
D[40]	28 Jul 2016 - 10 Aug 2016	1.032	1.036	0.168	0.711	1.361
D[41]	11 Aug 2016 - 24 Aug 2016	1.186	1.178	0.167	0.873	1.523
D[42]	25 Aug 2016 - 7 Sep 2016	1.154	1.158	0.160	0.853	1.483
D[43]	8 Sep 2016 - 21 Sep 2016	1.117	1.117	0.156	0.813	1.422
D[44]	22 Sep 2016 - 5 Oct 2016	1.169	1.158	0.164	0.853	1.503
D[45]	6 Oct 2016 - 19 Oct 2016	1.133	1.138	0.165	0.813	1.463
D[46]	20 Oct 2016 - 2 Nov 2016	1.312	1.300	0.171	0.995	1.666
D[47]	3 Nov 2016 - 16 Nov 2016	1.295	1.280	0.174	0.975	1.666
D[48]	17 Nov 2016 - 30 Nov 2016	1.311	1.300	0.178	0.975	1.686
D[49]	1 Dec 2016 - 14 Dec 2016	1.218	1.219	0.175	0.894	1.584
D[50]	15 Dec 2016 - 28 Dec 2016	1.157	1.158	0.175	0.833	1.523
D[51]	29 Dec 2016 - 11 Jan 2017	1.221	1.219	0.177	0.894	1.584
D[52]	12 Jan 2017 - 25 Jan 2017	1.252	1.239	0.177	0.914	1.625
D[53]	26 Jan 2017 - 8 Feb 2017	1.227	1.219	0.179	0.894	1.605
D[54]	9 Feb 2017 - 22 Feb 2017	1.186	1.178	0.179	0.853	1.564
D[55]	23 Feb 2017 - 8 Mar 2017	1.273	1.259	0.178	0.955	1.645
D[56]	9 Mar 2017 - 22 Mar 2017	1.262	1.259	0.178	0.934	1.625
D[57]	23 Mar 2017 - 5 Apr 2017	1.185	1.178	0.184	0.853	1.584
D[58]	6 Apr 2017 - 19 Apr 2017	1.318	1.300	0.191	0.975	1.727
D[59]	20 Apr 2017 - 3 May 2017	1.299	1.280	0.202	0.934	1.727
D[60]	4 May 2017 - 17 May 2017	1.242	1.219	0.209	0.873	1.686
D[61]	18 May 2017 - 31 May 2017	1.313	1.300	0.196	0.975	1.747
D[62]	1 Jun 2017 - 14 Jun 2017	1.323	1.300	0.201	0.975	1.767
D[63]	15 Jun 2017 - 28 Jun 2017	1.209	1.198	0.203	0.853	1.645

Table 2.G2. Posterior abundance estimates for North Addition Lands. Mean, median, standard deviation (SD), and 95% credible interval are reported for 76 fortnights.

Parameter	Fortnight	Mean	Median	SD	2.5%	97.5%
N[1]	29 Jan 2015 - 11 Feb 2015	71.793	71	9.140	55	91
N[2]	12 Feb 2015 - 25 Feb 2015	65.260	65	9.098	48	84
N[3]	26 Feb 2015 - 11 Mar 2015	70.330	70	9.126	53	89
N[4]	12 Mar 2015 - 25 Mar 2015	70.930	71	8.785	54	89
N[5]	26 Mar 2015 - 8 Apr 2015	68.589	68	8.692	53	86
N[6]	9 Apr 2015 - 22 Apr 2015	63.862	64	8.648	48	82
N[7]	23 Apr 2015 - 6 May 2015	66.868	67	8.513	51	84
N[8]	7 May 2015 - 20 May 2015	64.001	64	8.123	49	80
N[9]	21 May 2015 - 3 Jun 2015	66.236	66	8.119	51	83
N[10]	4 Jun 2015 - 17 Jun 2015	67.400	67	8.225	52	84
N[11]	18 Jun 2015 - 1 Jul 2015	68.064	68	8.495	52	85
N[12]	2 Jul 2015 - 15 Jul 2015	67.272	67	8.376	51	85
N[13]	16 Jul 2015 - 29 Jul 2015	62.038	62	8.278	47	79
N[14]	30 Jul 2015 - 12 Aug 2015	64.381	64	8.403	49	82
N[15]	13 Aug 2015 - 26 Aug 2015	69.616	69	8.446	54	87
N[16]	27 Aug 2015 - 9 Sep 2015	66.226	66	8.542	50	84
N[17]	10 Sep 2015 - 23 Sep 2015	65.974	66	8.386	50	83
N[18]	24 Sep 2015 - 7 Oct 2015	69.191	69	8.479	53	87
N[19]	8 Oct 2015 - 21 Oct 2015	65.808	65	8.637	50	84
N[20]	22 Oct 2015 - 4 Nov 2015	71.831	71	8.63	56	90
N[21]	5 Nov 2015 - 18 Nov 2015	68.426	68	8.613	53	87
N[22]	19 Nov 2015 - 2 Dec 2015	68.595	68	8.434	53	86
N[23]	3 Dec 2015 - 16 Dec 2015	68.222	68	8.52	53	86
N[24]	17 Dec 2015 - 30 Dec 2015	65.254	65	8.283	50	82
N[25]	31 Dec 2015 - 13 Jan 2016	67.561	67	8.299	52	85
N[26]	14 Jan 2016 - 27 Jan 2016	70.249	70	8.234	55	87
N[27]	28 Jan 2016 - 10 Feb 2016	59.521	59	7.836	45	75
N[28]	11 Feb 2016 - 24 Feb 2016	64.074	64	7.995	49	80
N[29]	25 Feb 2016 - 9 Feb 2016	60.594	60	7.73	46	76
N[30]	10 Mar 2016 - 23 Mar 2016	65.676	65	7.784	51	82
N[31]	24 Mar 2016 - 6 Apr 2016	60.377	60	7.558	46	76
N[32]	7 Apr 2016 - 20 Apr 2016	59.701	60	7.756	45	75
N[33]	21 Apr 2016 - 4 May 2016	62.690	63	7.811	48	79
N[34]	5 May 2016 - 18 May 2016	55.399	55	7.747	41	71
N[35]	19 May 2016 - 1 Jun 2016	58.984	59	7.845	44	75
N[36]	2 Jun 2016 - 15 Jun 2016	57.322	57	7.698	43	73
N[37]	16 Jun 2016 - 29 Jun 2016	56.172	56	7.747	41	72
N[38]	30 Jun 2016 - 13 Jul 2016	61.196	61	8.018	46	77

N[39]	14 Jul 2016 - 27 Jul 2016	55.170	55	7.948	40	71
N[40]	28 Jul 2016 - 10 Aug 2016	50.828	51	8.266	35	67
N[41]	11 Aug 2016 - 24 Aug 2016	58.409	58	8.202	43	75
N[42]	25 Aug 2016 - 7 Sep 2016	56.814	57	7.861	42	73
N[43]	8 Sep 2016 - 21 Sep 2016	54.979	55	7.701	40	70
N[44]	22 Sep 2016 - 5 Oct 2016	57.529	57	8.097	42	74
N[45]	6 Oct 2016 - 19 Oct 2016	55.766	56	8.127	40	72
N[46]	20 Oct 2016 - 2 Nov 2016	64.588	64	8.424	49	82
N[47]	3 Nov 2016 - 16 Nov 2016	63.759	63	8.549	48	82
N[48]	17 Nov 2016 - 30 Nov 2016	64.533	64	8.757	48	83
N[49]	1 Dec 2016 - 14 Dec 2016	59.957	60	8.601	44	78
N[50]	15 Dec 2016 - 28 Dec 2016	56.976	57	8.622	41	75
N[51]	29 Dec 2016 - 11 Jan 2017	60.109	60	8.724	44	78
N[52]	12 Jan 2017 - 25 Jan 2017	61.637	61	8.706	45	80
N[53]	26 Jan 2017 - 8 Feb 2017	60.423	60	8.808	44	79
N[54]	9 Feb 2017 - 22 Feb 2017	58.404	58	8.791	42	77
N[55]	23 Feb 2017 - 8 Mar 2017	62.686	62	8.777	47	81
N[56]	9 Mar 2017 - 22 Mar 2017	62.138	62	8.764	46	80
N[57]	23 Mar 2017 - 5 Apr 2017	58.315	58	9.066	42	78
N[58]	6 Apr 2017 - 19 Apr 2017	64.865	64	9.426	48	85
N[59]	20 Apr 2017 - 3 May 2017	63.938	63	9.959	46	85
N[60]	4 May 2017 - 17 May 2017	61.137	60	10.292	43	83
N[61]	18 May 2017 - 31 May 2017	64.663	64	9.665	48	86
N[62]	1 Jun 2017 - 14 Jun 2017	65.125	64	9.896	48	87
N[63]	15 Jun 2017 - 28 Jun 2017	59.527	59	9.975	42	81

Table 2.G3. Posterior density estimates for Bear Island. Mean, median, standard deviation (SD), and 95% credible intervals are reported for 76 fortnights.

Parameter	Fortnight	Mean	Median	SD	2.5%	97.5%
D[1]	29 Jan 2015 - 11 Feb 2015	2.903	2.890	0.513	1.940	3.921
D[2]	12 Feb 2015 - 25 Feb 2015	2.711	2.688	0.500	1.779	3.739
D[3]	26 Feb 2015 - 11 Mar 2015	2.958	2.951	0.459	2.122	3.901
D[4]	12 Mar 2015 - 25 Mar 2015	3.209	3.194	0.469	2.345	4.164
D[5]	26 Mar 2015 - 8 Apr 2015	3.603	3.578	0.483	2.708	4.608
D[6]	9 Apr 2015 - 22 Apr 2015	3.550	3.537	0.478	2.668	4.548
D[7]	23 Apr 2015 - 6 May 2015	3.540	3.537	0.500	2.587	4.548
D[8]	7 May 2015 - 20 May 2015	3.930	3.921	0.511	2.971	4.992
D[9]	21 May 2015 - 3 Jun 2015	4.089	4.063	0.513	3.153	5.174
D[10]	4 Jun 2015 - 17 Jun 2015	4.084	4.063	0.518	3.133	5.174
D[11]	18 Jun 2015 - 1 Jul 2015	4.067	4.063	0.507	3.113	5.114
D[12]	2 Jul 2015 - 15 Jul 2015	3.857	3.840	0.512	2.890	4.871
D[13]	16 Jul 2015 - 29 Jul 2015	3.824	3.820	0.507	2.850	4.831
D[14]	30 Jul 2015 - 12 Aug 2015	3.887	3.861	0.501	2.951	4.912
D[15]	13 Aug 2015 - 26 Aug 2015	3.930	3.921	0.505	2.971	4.932
D[16]	27 Aug 2015 - 9 Sep 2015	3.867	3.840	0.516	2.890	4.932
D[17]	10 Sep 2015 - 23 Sep 2015	4.177	4.164	0.524	3.214	5.275
D[18]	24 Sep 2015 - 7 Oct 2015	4.499	4.467	0.538	3.517	5.619
D[19]	8 Oct 2015 - 21 Oct 2015	4.228	4.204	0.539	3.214	5.336
D[20]	22 Oct 2015 - 4 Nov 2015	4.221	4.204	0.536	3.234	5.336
D[21]	5 Nov 2015 - 18 Nov 2015	4.044	4.022	0.546	3.052	5.195
D[22]	19 Nov 2015 - 2 Dec 2015	3.856	3.840	0.509	2.911	4.891
D[23]	3 Dec 2015 - 16 Dec 2015	3.564	3.537	0.473	2.688	4.548
D[24]	17 Dec 2015 - 30 Dec 2015	3.126	3.113	0.456	2.284	4.083
D[25]	31 Dec 2015 - 13 Jan 2016	2.565	2.567	0.431	1.758	3.436
D[26]	14 Jan 2016 - 27 Jan 2016	2.574	2.547	0.387	1.880	3.375
D[27]	28 Jan 2016 - 10 Feb 2016	1.547	1.536	0.302	1.011	2.183
D[28]	11 Feb 2016 - 24 Feb 2016	2.520	2.506	0.367	1.860	3.295
D[29]	25 Feb 2016 - 9 Feb 2016	2.453	2.425	0.380	1.779	3.254
D[30]	10 Mar 2016 - 23 Mar 2016	2.432	2.425	0.388	1.698	3.234
D[31]	24 Mar 2016 - 6 Apr 2016	2.489	2.466	0.400	1.758	3.315
D[32]	7 Apr 2016 - 20 Apr 2016	2.681	2.668	0.423	1.880	3.557
D[33]	21 Apr 2016 - 4 May 2016	2.899	2.890	0.445	2.082	3.820
D[34]	5 May 2016 - 18 May 2016	3.021	3.012	0.439	2.203	3.921
D[35]	19 May 2016 - 1 Jun 2016	2.810	2.789	0.445	1.981	3.719
D[36]	2 Jun 2016 - 15 Jun 2016	2.969	2.951	0.429	2.183	3.840
D[37]	16 Jun 2016 - 29 Jun 2016	2.964	2.951	0.428	2.183	3.840
D[38]	30 Jun 2016 - 13 Jul 2016	2.875	2.850	0.409	2.122	3.719
D[39]	14 Jul 2016 - 27 Jul 2016	2.528	2.527	0.422	1.718	3.375
D[40]	28 Jul 2016 - 10 Aug 2016	2.916	2.890	0.425	2.143	3.800

D[41]	11 Aug 2016 - 24 Aug 2016	3.082	3.052	0.436	2.284	4.002
D[42]	25 Aug 2016 - 7 Sep 2016	3.079	3.052	0.430	2.284	3.962
D[43]	8 Sep 2016 - 21 Sep 2016	3.113	3.093	0.429	2.324	4.002
D[44]	22 Sep 2016 - 5 Oct 2016	2.796	2.789	0.426	2.001	3.658
D[45]	6 Oct 2016 - 19 Oct 2016	2.854	2.850	0.436	2.041	3.739
D[46]	20 Oct 2016 - 2 Nov 2016	3.126	3.113	0.461	2.264	4.083
D[47]	3 Nov 2016 - 16 Nov 2016	3.060	3.032	0.481	2.183	4.063
D[48]	17 Nov 2016 - 30 Nov 2016	2.908	2.890	0.475	2.021	3.901
D[49]	1 Dec 2016 - 14 Dec 2016	2.639	2.628	0.471	1.758	3.598
D[50]	15 Dec 2016 - 28 Dec 2016	2.588	2.567	0.461	1.718	3.537
D[51]	29 Dec 2016 - 11 Jan 2017	2.540	2.527	0.449	1.718	3.477
D[52]	12 Jan 2017 - 25 Jan 2017	2.630	2.607	0.446	1.799	3.557
D[53]	26 Jan 2017 - 8 Feb 2017	2.579	2.567	0.435	1.779	3.477
D[54]	9 Feb 2017 - 22 Feb 2017	2.834	2.810	0.433	2.041	3.719
D[55]	23 Feb 2017 - 8 Mar 2017	3.027	3.012	0.454	2.183	3.962
D[56]	9 Mar 2017 - 22 Mar 2017	3.352	3.335	0.459	2.506	4.325
D[57]	23 Mar 2017 - 5 Apr 2017	3.416	3.396	0.463	2.567	4.386
D[58]	6 Apr 2017 - 19 Apr 2017	3.233	3.214	0.524	2.244	4.305
D[59]	20 Apr 2017 - 3 May 2017	3.085	3.072	0.579	1.961	4.285
D[60]	4 May 2017 - 17 May 2017	3.094	3.072	0.491	2.183	4.103
D[61]	18 May 2017 - 31 May 2017	2.907	2.890	0.456	2.062	3.861
D[62]	1 Jun 2017 - 14 Jun 2017	2.758	2.749	0.413	2.001	3.618
D[63]	15 Jun 2017 - 28 Jun 2017	2.250	2.244	0.400	1.516	3.093
D[64]	29 Jun 2017 - 12 Jul 2017	2.115	2.102	0.369	1.435	2.87
D[65]	13 Jul 2017 - 26 Jul 2017	2.172	2.163	0.377	1.476	2.951
D[66]	27 Jul 2017 - 9 Aug 2017	2.366	2.345	0.381	1.657	3.173
D[67]	10 Aug 2017 - 23 Aug 2017	2.569	2.547	0.399	1.839	3.396
D[68]	24 Aug 2017 - 6 Sep 2017	2.494	2.486	0.397	1.778	3.315
D[69]	7 Sep 2017 - 20 Sep 2017	2.115	2.102	0.420	1.334	2.971
D[70]	21 Sep 2017 - 4 Oct 2017	2.337	2.324	0.411	1.577	3.194
D[71]	5 Oct 2017 - 18 Oct 2017	2.506	2.486	0.441	1.698	3.416
D[72]	19 Oct 2017 - 1 Nov 2017	2.890	2.870	0.462	2.062	3.861
D[73]	2 Nov 2017 - 15 Nov 2017	3.045	3.022	0.483	2.163	4.042
D[74]	16 Nov 2017 - 29 Nov 2017	3.103	3.072	0.505	2.183	4.144
D[75]	30 Nov 2017 - 13 Nov 2017	3.107	3.093	0.528	2.143	4.204
D[76]	14 Dec 2017 - 27 Dec 2017	2.987	2.951	0.595	1.900	4.245

Table 2.G4. Posterior abundance estimates for Bear Island. Mean, median, standard deviation (SD), and 95% credible intervals are reported for 76 fortnights.

Parameter	Fortnight	Mean	Median	SD	2.5%	97.5%
N[1]	29 Jan 2015 - 11 Feb 2015	143.637	143	25.390	96	194
N[2]	12 Feb 2015 - 25 Feb 2015	134.148	133	24.717	88	185
N[3]	26 Feb 2015 - 11 Mar 2015	146.358	146	22.714	105	193
N[4]	12 Mar 2015 - 25 Mar 2015	158.785	158	23.214	116	206
N[5]	26 Mar 2015 - 8 Apr 2015	178.279	177	23.890	134	228
N[6]	9 Apr 2015 - 22 Apr 2015	175.632	175	23.628	132	225
N[7]	23 Apr 2015 - 6 May 2015	175.147	175	24.717	128	225
N[8]	7 May 2015 - 20 May 2015	194.435	194	25.300	147	247
N[9]	21 May 2015 - 3 Jun 2015	202.315	201	25.359	156	256
N[10]	4 Jun 2015 - 17 Jun 2015	202.076	201	25.629	155	256
N[11]	18 Jun 2015 - 1 Jul 2015	201.221	201	25.101	154	253
N[12]	2 Jul 2015 - 15 Jul 2015	190.823	190	25.341	143	241
N[13]	16 Jul 2015 - 29 Jul 2015	189.200	189	25.060	141	239
N[14]	30 Jul 2015 - 12 Aug 2015	192.296	191	24.791	146	243
N[15]	13 Aug 2015 - 26 Aug 2015	194.432	194	25.008	147	244
N[16]	27 Aug 2015 - 9 Sep 2015	191.307	190	25.543	143	244
N[17]	10 Sep 2015 - 23 Sep 2015	206.659	206	25.917	159	261
N[18]	24 Sep 2015 - 7 Oct 2015	222.561	221	26.640	174	278
N[19]	8 Oct 2015 - 21 Oct 2015	209.175	208	26.691	159	264
N[20]	22 Oct 2015 - 4 Nov 2015	208.832	208	26.519	160	264
N[21]	5 Nov 2015 - 18 Nov 2015	200.090	199	27.015	151	257
N[22]	19 Nov 2015 - 2 Dec 2015	190.750	190	25.191	144	242
N[23]	3 Dec 2015 - 16 Dec 2015	176.333	175	23.407	133	225
N[24]	17 Dec 2015 - 30 Dec 2015	154.641	154	22.569	113	202
N[25]	31 Dec 2015 - 13 Jan 2016	126.879	127	21.325	87	170
N[26]	14 Jan 2016 - 27 Jan 2016	127.329	126	19.137	93	167
N[27]	28 Jan 2016 - 10 Feb 2016	76.5360	76	14.926	50	108
N[28]	11 Feb 2016 - 24 Feb 2016	124.683	124	18.158	92	163
N[29]	25 Feb 2016 - 9 Feb 2016	121.361	120	18.790	88	161
N[30]	10 Mar 2016 - 23 Mar 2016	120.328	120	19.177	84	160
N[31]	24 Mar 2016 - 6 Apr 2016	123.128	122	19.797	87	164
N[32]	7 Apr 2016 - 20 Apr 2016	132.660	132	20.923	93	176
N[33]	21 Apr 2016 - 4 May 2016	143.442	143	22.004	103	189
N[34]	5 May 2016 - 18 May 2016	149.472	149	21.711	109	194
N[35]	19 May 2016 - 1 Jun 2016	139.028	138	22.030	98	184
N[36]	2 Jun 2016 - 15 Jun 2016	146.874	146	21.214	108	190
N[37]	16 Jun 2016 - 29 Jun 2016	146.664	146	21.173	108	190
N[38]	30 Jun 2016 - 13 Jul 2016	142.239	141	20.212	105	184

N[39]	14 Jul 2016 - 27 Jul 2016	125.070	125	20.899	85	167
N[40]	28 Jul 2016 - 10 Aug 2016	144.283	143	21.029	106	188
N[41]	11 Aug 2016 - 24 Aug 2016	152.494	151	21.583	113	198
N[42]	25 Aug 2016 - 7 Sep 2016	152.315	151	21.276	113	196
N[43]	8 Sep 2016 - 21 Sep 2016	153.995	153	21.200	115	198
N[44]	22 Sep 2016 - 5 Oct 2016	138.312	138	21.071	99	181
N[45]	6 Oct 2016 - 19 Oct 2016	141.207	141	21.554	101	185
N[46]	20 Oct 2016 - 2 Nov 2016	154.672	154	22.796	112	202
N[47]	3 Nov 2016 - 16 Nov 2016	151.388	150	23.782	108	201
N[48]	17 Nov 2016 - 30 Nov 2016	143.858	143	23.500	100	193
N[49]	1 Dec 2016 - 14 Dec 2016	130.584	130	23.279	87	178
N[50]	15 Dec 2016 - 28 Dec 2016	128.021	127	22.816	85	175
N[51]	29 Dec 2016 - 11 Jan 2017	125.670	125	22.237	85	172
N[52]	12 Jan 2017 - 25 Jan 2017	130.106	129	22.079	89	176
N[53]	26 Jan 2017 - 8 Feb 2017	127.616	127	21.533	88	172
N[54]	9 Feb 2017 - 22 Feb 2017	140.232	139	21.432	101	184
N[55]	23 Feb 2017 - 8 Mar 2017	149.780	149	22.470	108	196
N[56]	9 Mar 2017 - 22 Mar 2017	165.831	165	22.694	124	214
N[57]	23 Mar 2017 - 5 Apr 2017	169.016	168	22.886	127	217
N[58]	6 Apr 2017 - 19 Apr 2017	159.972	159	25.901	111	213
N[59]	20 Apr 2017 - 3 May 2017	152.622	152	28.647	97	212
N[60]	4 May 2017 - 17 May 2017	153.065	152	24.269	108	203
N[61]	18 May 2017 - 31 May 2017	143.821	143	22.543	102	191
N[62]	1 Jun 2017 - 14 Jun 2017	136.463	136	20.436	99	179
N[63]	15 Jun 2017 - 28 Jun 2017	111.317	111	19.795	75	153
N[64]	29 Jun 2017 - 12 Jul 2017	104.640	104	18.252	71	142
N[65]	13 Jul 2017 - 26 Jul 2017	107.476	107	18.646	73	146
N[66]	27 Jul 2017 - 9 Aug 2017	117.057	116	18.862	82	157
N[67]	10 Aug 2017 - 23 Aug 2017	127.095	126	19.755	91	168
N[68]	24 Aug 2017 - 6 Sep 2017	123.387	123	19.644	88	164
N[69]	7 Sep 2017 - 20 Sep 2017	104.628	104	20.801	66	147
N[70]	21 Sep 2017 - 4 Oct 2017	115.646	115	20.358	78	158
N[71]	5 Oct 2017 - 18 Oct 2017	123.963	123	21.816	84	169
N[72]	19 Oct 2017 - 1 Nov 2017	142.988	142	22.837	102	191
N[73]	2 Nov 2017 - 15 Nov 2017	150.659	149.5	23.882	107	200
N[74]	16 Nov 2017 - 29 Nov 2017	153.510	152	25.006	108	205
N[75]	30 Nov 2017 - 13 Nov 2017	153.708	153	26.127	106	208
N[76]	14 Dec 2017 - 27 Dec 2017	147.778	146	29.444	94	210

Table 2.G5. Posterior density estimates for Florida Panther National Wildlife Refuge. Mean, median, standard deviation (SD), and 95% credible intervals are reported for 70 fortnights.

Parameter	Fortnight	Mean	Median	SD	2.5%	97.5%
D[1]	23 Apr 2015 - 6 May 2015	7.733	7.830	0.977	5.734	9.296
D[2]	7 May 2015 - 20 May 2015	8.033	8.096	0.813	6.325	9.373
D[3]	21 May 2015 - 3 Jun 2015	7.990	8.020	0.768	6.344	9.296
D[4]	4 Jun 2015 - 17 Jun 2015	7.530	7.563	0.763	5.963	9.011
D[5]	18 Jun 2015 - 1 Jul 2015	6.923	6.915	0.727	5.505	8.344
D[6]	2 Jul 2015 - 15 Jul 2015	6.185	6.191	0.688	4.858	7.563
D[7]	16 Jul 2015 - 29 Jul 2015	5.229	5.201	0.663	3.981	6.610
D[8]	30 Jul 2015 - 12 Aug 2015	4.447	4.420	0.580	3.391	5.639
D[9]	13 Aug 2015 - 26 Aug 2015	3.353	3.334	0.483	2.457	4.362
D[10]	27 Aug 2015 - 9 Sep 2015	2.692	2.686	0.403	1.943	3.524
D[11]	10 Sep 2015 - 23 Sep 2015	2.240	2.229	0.372	1.562	3.010
D[12]	24 Sep 2015 - 7 Oct 2015	2.870	2.858	0.413	2.096	3.715
D[13]	8 Oct 2015 - 21 Oct 2015	3.339	3.315	0.487	2.457	4.362
D[14]	22 Oct 2015 - 4 Nov 2015	3.100	3.067	0.494	2.210	4.153
D[15]	5 Nov 2015 - 18 Nov 2015	3.315	3.296	0.494	2.400	4.324
D[16]	19 Nov 2015 - 2 Dec 2015	2.898	2.877	0.460	2.038	3.848
D[17]	3 Dec 2015 - 16 Dec 2015	3.177	3.162	0.459	2.324	4.115
D[18]	17 Dec 2015 - 30 Dec 2015	3.291	3.277	0.482	2.400	4.267
D[19]	31 Dec 2015 - 13 Jan 2016	3.378	3.353	0.519	2.419	4.458
D[20]	14 Jan 2016 - 27 Jan 2016	3.863	3.848	0.525	2.877	4.934
D[21]	28 Jan 2016 - 10 Feb 2016	4.197	4.172	0.500	3.277	5.239
D[22]	11 Feb 2016 - 24 Feb 2016	4.410	4.382	0.538	3.429	5.525
D[23]	25 Feb 2016 - 9 Feb 2016	4.379	4.343	0.560	3.353	5.544
D[24]	10 Mar 2016 - 23 Mar 2016	3.833	3.791	0.583	2.762	5.067
D[25]	24 Mar 2016 - 6 Apr 2016	3.760	3.734	0.568	2.724	4.972
D[26]	7 Apr 2016 - 20 Apr 2016	3.979	3.962	0.546	2.991	5.124
D[27]	21 Apr 2016 - 4 May 2016	3.713	3.677	0.555	2.705	4.877
D[28]	5 May 2016 - 18 May 2016	3.788	3.772	0.542	2.781	4.896
D[29]	19 May 2016 - 1 Jun 2016	3.777	3.753	0.542	2.762	4.896
D[30]	2 Jun 2016 - 15 Jun 2016	3.780	3.753	0.542	2.762	4.896
D[31]	16 Jun 2016 - 29 Jun 2016	3.361	3.334	0.533	2.381	4.458
D[32]	30 Jun 2016 - 13 Jul 2016	3.828	3.810	0.553	2.800	4.953
D[33]	14 Jul 2016 - 27 Jul 2016	4.349	4.343	0.571	3.277	5.505
D[34]	28 Jul 2016 - 10 Aug 2016	4.684	4.667	0.649	3.467	6.058
D[35]	11 Aug 2016 - 24 Aug 2016	4.866	4.858	0.681	3.600	6.248
D[36]	25 Aug 2016 - 7 Sep 2016	5.132	5.105	0.726	3.772	6.629
D[37]	8 Sep 2016 - 21 Sep 2016	5.417	5.391	0.750	4.020	6.915
D[38]	22 Sep 2016 - 5 Oct 2016	5.670	5.639	0.767	4.229	7.220

D[39]	6 Oct 2016 - 19 Oct 2016	5.903	5.886	0.786	4.420	7.487
D[40]	20 Oct 2016 - 2 Nov 2016	6.041	6.001	0.814	4.534	7.696
D[41]	3 Nov 2016 - 16 Nov 2016	6.290	6.248	0.848	4.763	8.077
D[42]	17 Nov 2016 - 30 Nov 2016	6.530	6.496	0.856	4.953	8.382
D[43]	1 Dec 2016 - 14 Dec 2016	6.684	6.648	0.872	5.067	8.553
D[44]	15 Dec 2016 - 28 Dec 2016	6.749	6.725	0.866	5.144	8.611
D[45]	29 Dec 2016 - 11 Jan 2017	6.741	6.706	0.858	5.124	8.496
D[46]	12 Jan 2017 - 25 Jan 2017	6.847	6.820	0.791	5.353	8.439
D[47]	26 Jan 2017 - 8 Feb 2017	6.523	6.477	0.828	4.953	8.230
D[48]	9 Feb 2017 - 22 Feb 2017	6.272	6.229	0.809	4.763	7.963
D[49]	23 Feb 2017 - 8 Mar 2017	6.101	6.077	0.760	4.705	7.715
D[50]	9 Mar 2017 - 22 Mar 2017	5.926	5.906	0.711	4.610	7.430
D[51]	23 Mar 2017 - 5 Apr 2017	5.658	5.620	0.683	4.401	7.068
D[52]	6 Apr 2017 - 19 Apr 2017	5.069	5.048	0.653	3.886	6.439
D[53]	20 Apr 2017 - 3 May 2017	4.394	4.382	0.610	3.258	5.639
D[54]	4 May 2017 - 17 May 2017	3.686	3.677	0.545	2.648	4.763
D[55]	18 May 2017 - 31 May 2017	3.429	3.410	0.514	2.477	4.496
D[56]	1 Jun 2017 - 14 Jun 2017	3.688	3.677	0.476	2.800	4.648
D[57]	15 Jun 2017 - 28 Jun 2017	3.067	3.048	0.481	2.172	4.039
D[58]	29 Jun 2017 - 12 Jul 2017	2.767	2.743	0.483	1.886	3.772
D[59]	13 Jul 2017 - 26 Jul 2017	2.460	2.438	0.429	1.657	3.353
D[60]	27 Jul 2017 - 9 Aug 2017	2.687	2.667	0.402	1.962	3.524
D[61]	10 Aug 2017 - 23 Aug 2017	2.594	2.572	0.409	1.848	3.448
D[62]	24 Aug 2017 - 6 Sep 2017	2.426	2.400	0.403	1.695	3.277
D[63]	7 Sep 2017 - 20 Sep 2017	1.955	1.943	0.357	1.314	2.724
D[64]	21 Sep 2017 - 4 Oct 2017	1.677	1.657	0.306	1.143	2.324
D[65]	5 Oct 2017 - 18 Oct 2017	2.043	2.019	0.333	1.448	2.743
D[66]	19 Oct 2017 - 1 Nov 2017	2.258	2.248	0.395	1.543	3.086
D[67]	2 Nov 2017 - 15 Nov 2017	2.739	2.724	0.449	1.943	3.696
D[68]	16 Nov 2017 - 29 Nov 2017	2.349	2.324	0.459	1.543	3.334
D[69]	30 Nov 2017 - 13 Nov 2017	2.055	2.019	0.428	1.295	2.972
D[70]	14 Dec 2017 - 27 Dec 2017	1.758	1.715	0.420	1.048	2.686

Table 2.G6. Posterior abundance estimates for Florida Panther National Wildlife Refuge. Mean, median, standard deviation (SD), and 95% credible intervals are reported for 70 fortnights.

Parameter	Fortnight	Mean	Median	SD	2.5%	97.5%
N[1]	23 Apr 2015 - 6 May 2015	405.909	411	51.260	301	488
N[2]	7 May 2015 - 20 May 2015	421.654	425	42.653	332	492
N[3]	21 May 2015 - 3 Jun 2015	419.443	421	40.323	333	488
N[4]	4 Jun 2015 - 17 Jun 2015	395.279	397	40.059	313	473
N[5]	18 Jun 2015 - 1 Jul 2015	363.397	363	38.138	289	438
N[6]	2 Jul 2015 - 15 Jul 2015	324.695	325	36.099	255	397
N[7]	16 Jul 2015 - 29 Jul 2015	274.499	273	34.807	209	347
N[8]	30 Jul 2015 - 12 Aug 2015	233.454	232	30.472	178	296
N[9]	13 Aug 2015 - 26 Aug 2015	176.018	175	25.354	129	229
N[10]	27 Aug 2015 - 9 Sep 2015	141.335	141	21.169	102	185
N[11]	10 Sep 2015 - 23 Sep 2015	117.563	117	19.544	82	158
N[12]	24 Sep 2015 - 7 Oct 2015	150.652	150	21.701	110	195
N[13]	8 Oct 2015 - 21 Oct 2015	175.268	174	25.562	129	229
N[14]	22 Oct 2015 - 4 Nov 2015	162.737	161	25.943	116	218
N[15]	5 Nov 2015 - 18 Nov 2015	174.021	173	25.913	126	227
N[16]	19 Nov 2015 - 2 Dec 2015	152.117	151	24.142	107	202
N[17]	3 Dec 2015 - 16 Dec 2015	166.757	166	24.097	122	216
N[18]	17 Dec 2015 - 30 Dec 2015	172.739	172	25.317	126	224
N[19]	31 Dec 2015 - 13 Jan 2016	177.312	176	27.259	127	234
N[20]	14 Jan 2016 - 27 Jan 2016	202.767	202	27.553	151	259
N[21]	28 Jan 2016 - 10 Feb 2016	220.335	219	26.265	172	275
N[22]	11 Feb 2016 - 24 Feb 2016	231.496	230	28.223	180	290
N[23]	25 Feb 2016 - 9 Feb 2016	229.861	228	29.378	176	291
N[24]	10 Mar 2016 - 23 Mar 2016	201.218	199	30.588	145	266
N[25]	24 Mar 2016 - 6 Apr 2016	197.358	196	29.812	143	261
N[26]	7 Apr 2016 - 20 Apr 2016	208.859	208	28.664	157	269
N[27]	21 Apr 2016 - 4 May 2016	194.910	193	29.137	142	256
N[28]	5 May 2016 - 18 May 2016	198.839	198	28.463	146	257
N[29]	19 May 2016 - 1 Jun 2016	198.260	197	28.469	145	257
N[30]	2 Jun 2016 - 15 Jun 2016	198.409	197	28.457	145	257
N[31]	16 Jun 2016 - 29 Jun 2016	176.424	175	27.986	125	234
N[32]	30 Jun 2016 - 13 Jul 2016	200.946	200	29.025	147	260
N[33]	14 Jul 2016 - 27 Jul 2016	228.315	228	29.992	172	289
N[34]	28 Jul 2016 - 10 Aug 2016	245.860	245	34.080	182	318
N[35]	11 Aug 2016 - 24 Aug 2016	255.434	255	35.761	189	328
N[36]	25 Aug 2016 - 7 Sep 2016	269.371	268	38.108	198	348
N[37]	8 Sep 2016 - 21 Sep 2016	284.366	283	39.361	211	363
N[38]	22 Sep 2016 - 5 Oct 2016	297.650	296	40.265	222	379

N[39]	6 Oct 2016 - 19 Oct 2016	309.847	309	41.280	232	393
N[40]	20 Oct 2016 - 2 Nov 2016	317.122	315	42.756	238	404
N[41]	3 Nov 2016 - 16 Nov 2016	330.199	328	44.527	250	424
N[42]	17 Nov 2016 - 30 Nov 2016	342.769	341	44.926	260	440
N[43]	1 Dec 2016 - 14 Dec 2016	350.882	349	45.772	266	449
N[44]	15 Dec 2016 - 28 Dec 2016	354.285	353	45.470	270	452
N[45]	29 Dec 2016 - 11 Jan 2017	353.833	352	45.023	269	446
N[46]	12 Jan 2017 - 25 Jan 2017	359.447	358	41.531	281	443
N[47]	26 Jan 2017 - 8 Feb 2017	342.436	340	43.443	260	432
N[48]	9 Feb 2017 - 22 Feb 2017	329.231	327	42.466	250	418
N[49]	23 Feb 2017 - 8 Mar 2017	320.283	319	39.915	247	405
N[50]	9 Mar 2017 - 22 Mar 2017	311.055	310	37.322	242	390
N[51]	23 Mar 2017 - 5 Apr 2017	297.003	295	35.832	231	371
N[52]	6 Apr 2017 - 19 Apr 2017	266.066	265	34.275	204	338
N[53]	20 Apr 2017 - 3 May 2017	230.647	230	32.042	171	296
N[54]	4 May 2017 - 17 May 2017	193.494	193	28.591	139	250
N[55]	18 May 2017 - 31 May 2017	180.007	179	26.975	130	236
N[56]	1 Jun 2017 - 14 Jun 2017	193.619	193	25.007	147	244
N[57]	15 Jun 2017 - 28 Jun 2017	160.978	160	25.230	114	212
N[58]	29 Jun 2017 - 12 Jul 2017	145.238	144	25.339	99	198
N[59]	13 Jul 2017 - 26 Jul 2017	129.123	128	22.528	87	176
N[60]	27 Jul 2017 - 9 Aug 2017	141.036	140	21.108	103	185
N[61]	10 Aug 2017 - 23 Aug 2017	136.174	135	21.483	97	181
N[62]	24 Aug 2017 - 6 Sep 2017	127.338	126	21.134	89	172
N[63]	7 Sep 2017 - 20 Sep 2017	102.627	102	18.741	69	143
N[64]	21 Sep 2017 - 4 Oct 2017	88.052	87	16.055	60	122
N[65]	5 Oct 2017 - 18 Oct 2017	107.223	106	17.501	76	144
N[66]	19 Oct 2017 - 1 Nov 2017	118.516	118	20.719	81	162
N[67]	2 Nov 2017 - 15 Nov 2017	143.786	143	23.578	102	194
N[68]	16 Nov 2017 - 29 Nov 2017	123.294	122	24.104	81	175
N[69]	30 Nov 2017 - 13 Nov 2017	107.861	106	22.484	68	156
N[70]	14 Dec 2017 - 27 Dec 2017	92.259	90	22.037	55	141

CHAPTER 3

OBJECTIVE WEIGHTING AND OPTIMAL SAMPLING DESIGN FOR CAMERA-BASED STUDIES OF UNMARKED POPULATIONS[2]

[2] Margenau, L. L. S. and R. B. Chandler. To be submitted to the *Biological Conservation*

ABSTRACT

Sampling designs should be cost-effective while allowing for inferences about populations that improve understanding and facilitate conservation decision-making. However, few studies have explicitly evaluated the relationship between the cost of implementing a sampling design and the precision of population estimates. To address this issue, we propose a conceptual and analytical framework that incorporates objective weighting to identify optimal sampling designs when using camera traps and spatial capture-recapture (SCR) methods to monitor unmarked populations. We conducted a simulation study to identify the optimal design for camera-based monitoring of white-tailed deer (*Odocoileus virginianus*) within the Big Cypress Basin, Florida, USA. We assessed 10 potential designs varying in the number (20-60) and spatial configuration of cameras. The designs were based on feasibility constraints provided by managers and prior information about encounter rate parameters from a previous telemetry and camera study conducted in 2015–2017. Our results demonstrated that the camera design from the previous study resulted in relatively low bias and high precision, however, little was gained with the labor-intensive step of deploying a portion of cameras off trails. The best design for estimating abundance and density involved 60 on-trail cameras. However, when balancing the costs of each design with the accuracy of the estimates, the optimal design involved 40 on-trail cameras. The framework we describe for accounting for costs constraints is general, and the analysis could be extended to identify optimal designs in monitoring efforts focused on long-term spatio-temporal dynamics.

INTRODUCTION

Obtaining reliable estimates of abundance and density is often an important component of many wildlife conservation initiatives (Williams et al. 2002). Camera traps have become a valuable tool in monitoring projects because they provide a relatively cost-effective and non-invasive means of collecting data on populations and communities (Nichols et al. 2011, O'Connell et al. 2011, Royle et al. 2018). For species with unique natural markings, camera data can be used with spatial capture-recapture (SCR) models to make inferences about population dynamics using individual encounter histories (Efford 2004, Borchers and Efford 2008, Royle et al. 2013). Spatial capture-recapture models utilize the spatial information in individual encounter histories to describe spatial variation in density and individual heterogeneity in capture probability.

The design of SCR studies has received recent attention as it influences not only the data collected, but also the accuracy, reliability, and robustness of modeling estimates. Because SCR is a model-based, rather than design-based, inference framework, random trap placement is not required (Royle et al. 2013). However, the number of traps deployed and the distribution of traps strongly influence estimator precision. Investigation of SCR design has involved either simulation methods to assess precision of density estimators (Sollmann et al. 2012, Sun et al. 2014) or optimization methods to find trap configurations that maximize specific design criteria (Royle et al. 2013, Kristensen and Kovach 2018, Clark 2019, Efford and Boulanger 2019, Kays et al. 2020, Dupont et al. 2021, Durbach et al. 2021). Both approaches have highlighted the importance of using designs that aim to maximize: (1) the number of unique individuals detected, (2) the number of recaptures, and (3) the number of individuals captured at more than one location (i.e., spatial recapture rate; Royle et al. 2013). The first criterion is important for

achieving thorough coverage of the population of interest. The second criterion impacts the ability to estimate the baseline capture probability. The third criterion affects estimates of the spatial scale parameter that is associated with home range size. Because resources are finite, a trade-off exists among these criteria. Maximizing the number of individuals captured can be achieved by spreading traps over a large area, but at the expense of the spatial recapture rate. Conversely, the spatial recapture rate can be maximized by using dense clusters of traps in a small area, but at the expense of the number of individuals captured. Software now exists for finding optimal designs that balance these criteria to achieve the objective of precise density estimates when studying animals that can be individually identified (Royle et al. 2013, Efford 2016, Sutherland et al. 2018, Efford and Boulanger 2019).

Many species lack natural markings and are difficult to capture, and it is therefore impossible to use standard SCR techniques, which complicates efforts to identify optimal designs. Recent extensions of SCR models have relaxed the requirement of individual recognition, allowing for inferences about abundance and density to be drawn from camera data on unmarked or partially marked populations (Chandler and Royle 2013, Sollmann et al. 2013, Evans and Rittenhouse 2018, Margenau et al. *In Review*). These approaches work best when ancillary information about detection probability is available, such as when a subset of the population has been marked and when telemetry data is available (Chandler and Royle 2013, Sollmann et al. 2013, Whittington et al. 2018, Augustine et al. 2019).

Sampling designs should be cost-effective while allowing for inferences about populations that improve understanding and facilitate conservation decision-making (Elzinga et al. 2001, Runge et al. 2020). However, few studies have evaluated the relationship between the cost of sampling and the design criteria (Giudice et al. 2010, Clare et al. 2015, Davis et al. 2020).

The number of traps deployed and the distribution of traps not only impact the cost of data collection, but also the time spent processing the photographic images and analyzing the data. Objective weighting is a quantitative framework for ranking study designs using weighted, normalized objective scores, which allows for the assessment of the tradeoffs between cost and estimator precision (Gregory et al. 2012, Runge et al. 2020).

We accessed the performance and cost of camera trap surveys and unmarked SCR models for monitoring white-tailed deer (*Odocoileus virginianus*) within the Big Cypress Basin, Florida, USA, where deer are the primary prey of the endangered Florida panther (*Puma concolor coryi*). We used input from managers to constrain the design space to scenarios that were logistically feasible, and compared the logistical costs of camera surveys to aerial line transect distance sampling, which is traditionally employed for surveying deer within the region (Buckland et al. 2001). The explicit selection of design criteria allows for an objective-based assessment towards an optimal survey design that can be later implemented in the field (Williams and Hooten 2016).

METHODS

MOTIVATING CASE STUDY

Managers in South Florida monitor white-tailed deer populations to inform harvest and predator conservation decisions. Aerial line transects distance surveys have been the primary monitoring method. While aerial surveys make it possible to cover large regions that are difficult to access, they are inherently dangerous and expensive, and the precision and accuracy of estimates are often highly variable and dependent on time of day, flying altitude, observer skill, and population density within an area (Graves et al. 1972, Rice and Harder, 1977, Beasom 1979,

Beasom et al. 1986, Caughley 1997, Dunn et al. 2002, DeYoung 2011). Moreover, detection probability can be zero in closed-canopy habitats, such as pine and cypress forests prevalent throughout South Florida, which prevents inferences about population density and trends in these areas (Dunn et al. 2002, Potvin et al. 2004, DeYoung 2011).

We informed our design analysis using prior information from a three-year (2015-2017) study of white-tailed deer in the Big Cypress Basin, Florida that assessed the impacts of hydrology, hunting, and wildfires on the abundance and distribution of deer in the core of the Florida panther's (*Puma concolor coryi*) range (Chandler et al. 2018, Cherry et al. 2018, Abernathy et al. 2019, Crawford et al. 2019). This region consisted of a mosaic of vegetative communities influenced by seasonal fluctuations in hydrology and wildfires (McPherson 1974). Within the Big Cypress Basin, sampling occurred in the Bear Island (BI) and North Addition Lands (AL) management units of the Big Cypress National Preserve (BCNP) and in the adjacent Florida Panther National Wildlife Refuge (FP; Fig. 1). The previous study involved 180 infrared motion-triggered white-flash cameras (HCO Outdoor Products, model SG565FV, Norcross, GA, USA) continuously from 1 January 2015 – 31 December 2017, such that each study site contained 60 cameras within a 29 km^2 rectangular region. Of the 60 cameras within each site, 40 cameras were placed along outdoor recreation vehicle (ORV) trails, with the remaining 20 placed approximately 250 m from the nearest on-trail camera. The on-trail camera trap locations were selected by using ArcGIS 10.2 (Environmental Systems Research Institute [ESRI], Redlands, CA, USA) to overlay a 700 m grid over the study area and placing cameras on the closest trail to each grid point. Cameras were deployed on the most-well defined wildlife trail or habitat edge within 50 m of the selected point location, while maintaining a distance of approximately 250 m

from the closest trail. Cameras were positioned approximately 0.30 m above the ground, oriented north, and adjusted height according to surface water levels to avoid inundation.

CAMERA TRAP DESIGNS

We assessed 10 potential designs for future monitoring at each of the study sites described above. Designs were developed using results from the camera study and input from agency biologists about the feasibility of operating cameras in the region (Table 3.1, Appendix 3.A). We evaluated four types of designs: status quo, paired, random, and on-trail. The status quo (SQ) corresponded to the design used during the previous study, with 60 cameras (40 on-trail, 20 off-trail) at each of the sites. The paired design (P) consisted of all pairs of on- and off-trail camera locations within the status quo design resulting in the assessment of 40 cameras (20 on-trail and 20 off-trial cameras) at each of the sites. We assessed three random camera designs (R20, R30, and R40) consisting of 20, 30, or 40 cameras per site that were randomly sampled from the status quo design allowing for both on- and off-trail. We assessed five on-trail camera designs (T20, T30, T40, T50, and T60) consisting of 20, 30, 40, 50, or 60 cameras per site positioned on trails. For on-trail designs with 20, 30, or 40 cameras, we randomly sampled existing on-trail locations from the status quo design. For on-trail designs with 50 or 60 cameras, we used all 40 on-trail camera locations from the status quo design and supplemented the remaining camera locations by randomly selecting locations on the trail systems with a minimum 250 m buffer from existing cameras.

DATA SIMULATION

For each combination of study site and design, we simulated 500 datasets using an extension of the model of Chandler and Royle (2013). We assigned a population size of 75 adult female deer in AL, 200 adult female deer in BI, and 250 adult female deer in FL to reflect naturally occurring variation in the population (Margenau et al. *In Review*). We used a 14-day sampling window with each day treated as a sampling occasion. We used prior information about site-specific detection from a marked SCR analysis of camera and telemetry data for a subset of ear-tagged and GPS-collared female white-tailed deer from 2015–2017.

The model assumes each deer has an activity center that is uniformly distributed within the spatial region of interest, $s_i \sim \text{Uniform}(S)$. The expected number of detections (λ_{ijk}) of individual i ($i = 1, \dots, N$) at camera j ($j = 1, \dots, J$) on sampling occasion $k (k = 1, \dots, K)$ is assumed to decrease with Euclidean distance (d_{ij}) between the activity center and the traps, whose locations are denoted by $x_1, \dots, x_J$. We allowed the baseline detection rate to differ between on-trail (λ_0^{on}) and off-trail (λ_0^{off}) cameras, such that the expected number of detections on a single occasion for an individual when the distance between its activity center and a trap is zero varied based on camera placement. We used the encounter rate function $\lambda_{ijk} = \lambda_0 e^{-d_{ij}^2/2\sigma}$, where the spatial scale parameter σ determines the rate at which detection probability decreases with distance. The prior distributions for the detection parameters were informed using site-specific logarithmic means representing the posterior distribution trend of 14-day sampling occasions for three years of data from a marked SCR model.

DESIGN EVALUATION

Female white-tailed deer cannot be uniquely identified using natural markings and thus we needed to convert individual detection histories (y_{ijk}) to trap-specific detection histories (n_{jk}) such that the data reflected counts of individuals, or binary values indicating if at least one adult female deer was detected at a camera during a 24-h sampling occasion (i.e., deer detection event). Using a data augmentation approach in which, rather than putting a prior directly on abundance (N), we specify an implied binomial prior on N with a fixed upper bound (M), with $M \gg N$ (Royle et al. 2007). Under the assumption that the number of independent detections of each deer is Poisson distributed, the model for the binary data becomes $n_{jk} \sim \text{Bernoulli}(1 - e^{-\Lambda_{jk}})$ where $\Lambda_{jk} = \sum_{i=1}^{M} \lambda_{ijk} z_i$. When using data augmentation, abundance is estimated as $N = \sum_{i=1}^{M} z_i$, where $z_i \sim \text{Bernoulli}(\psi)$ and $\psi = E(N)/M$. Density is estimated as N/A, where A is the area of the spatial region within which the N individuals occur. We fitted the unmarked model to each simulated dataset using the package *rjags* (Plummer et al. 2018) in program R (R Core Team 2019) and made inferences using 10,000 posterior samples with an initial burn-in of 1,000 iterations.

For each design, we computed the bias, precision, and root-mean-squared-error (RMSE) of the point estimate of abundance for the 500 posterior distributions (Walther and Moore 2005, Chai and Draxler 2014). We used the posterior median as the point estimator. Bias is defined as the expected differences between the estimates of abundances and the actual abundance: $Bias = \frac{1}{s}\sum_{i=1}^{s}(\widehat{N}_i - N)$, where s is the number of simulated datasets, $\widehat{N}_i$ is the abundance estimate from the i^{th} dataset, and N is the known abundance. Precision is defined as the inverse of the variance. Together, bias and precision combined can be used to assess the performance, or

"accuracy", of an estimator. A composite measure of accuracy is RMSE: $RMSE = \sqrt{\frac{1}{s}\sum_{i=1}^{s}(\widehat{N}_i - N)^2}$.

COST ANALYSIS

The Florida Fish and Wildlife Conservation Commission conducts annual helicopter surveys for white-tailed deer in BCNP to determine fawn:doe ratios and generate an index of abundance. To compare costs of camera and helicopter surveys, we used the Bear Island unit as an example survey unit for both monitoring techniques. We estimated an annual and 5-year long-term monitoring program cost for each camera monitoring design under the assumption of 14 camera days. We assessed three main components to population surveying costs: field equipment, field labor, and data processing. Field equipment costs included the initial purchasing/renting of implements used during surveying. For trail camera monitoring this included the initial cost of purchasing of trail cameras ($160/camera), camera boxes ($25/box), memory cards ($15/camera), batteries ($30/camera), and GPS units ($575). For aerial surveying, this included the helicopter flight cost (renting of helicopter and pilot services; $5,753) and the purchase of GPS units ($575) (E. Garrison, personal communication). We generated field labor costs based on survey duration and hourly wages ($20/hour) for two surveyors. Field labor costs for camera surveying included estimated labor for deploying and retrieving trail cameras, with off-trail cameras being more labor intensive than on-trail. The estimated time to deploy and retrieve cameras for each design was: 44 hrs for SQ, 28 hrs for P, 16 hrs for R20, 24 hrs for R30, 28 hrs for R40, 12 hrs for T20, 16 hrs for T30, 20 hrs for T40, 28 hrs for T50, 32 hrs for T60. Aerial surveying labor costs reflected the wages of two surveyors earned for two 8-hour workdays of helicopter transect surveying. Data processing costs for camera monitoring reflected

estimated labor for camera photo processing and data analysis, while aerial surveying consisted of data analysis labor, which incorporated data digitalization costs. We calculated the annual cost of conducting trail camera monitoring and aerial surveying by totaling field equipment, field labor, and data processing costs. We calculated the costs of a 5-year monitoring program as the sum of the initial annual cost of implementing surveying and the costs of subsequent years of surveying, which excluded the initial purchasing of equipment but included renting of equipment. We assumed no replacement of cameras would be necessary given the short sampling period of 14 days/year. All costs reflect general approximations or average costs, which could be adjusted based on specific equipment brand costs and employee wages.

OBJECTIVE WEIGHTING

We defined the optimal survey design as the design maximizing the accuracy of density estimation from the unmarked SCR model and minimizing logistical costs. We used RMSE of the point estimates as the performance metric for maximizing model performance. We used cost (in US dollars) as the performance metric for minimizing logistical costs.

To evaluate the tradeoffs between cost, performance, and objectives, we assessed three objective weighting scenarios. Scenario 1 used 100% weighting on the objective of maximizing model accuracy of population parameters with 0% weight on cost. Scenario 2 implemented 100% weighting for the objective of minimizing costs and 0% weight for model performance. Finally, Scenario 3 used equal weightings of 50% for both objectives. For each scenario, we normalized and weighted the performance metric for each objective. Normalizing recalculates performance scores into a unitless utility value between 0 and 1, where a utility of 1 indicates high performance, while a utility of 0 indicates poor performance relative to the camera designs

implemented. We calculated the overall performance score of each study design by calculating the weighted sum of its performance metrics:

$$Q_D = W_A X_A + W_c X_c,$$

where Q_D is the overall score of each design, X_A is the utility value assigned to RMSE, W_A is the weight assigned to maximizing model accuracy, X_c is the utility value assigned to cost, and W_c is the weight assigned to minimizing logistical costs. The highest overall score determined the optimal survey design for each objective weighting.

RESULTS

Results of the simulation study indicated that increasing the number of cameras increased the average number of deer detection events for the 14-day period (n_{jk}, Fig. 3.2). In general, all camera designs performed well in estimating abundances, reflecting the assigned abundance value with minimal bias and nominal coverage of 95% CI (Appendix 3.B). As abundance increased between sites, bias and precision decreased (Table 3.2, Fig. 3.3). Additionally, within sites, precision increased with the number of camera traps, but precision was not influenced by the placement of cameras on vs. off trails. Although the spatial configuration of the design that best reduced bias varied across study sites, the designs each consisted of 40 cameras. However, the T60 design, which involved 60 on-trail cameras, maximized precision across sites. For all three sites, the optimal design for estimating abundance (i.e., the design with the lowest RMSE), without considering costs was the design with 60 on-trail cameras. Camera designs involving only 20 camera traps performed worst overall in terms of model performance.

The camera design with 20 on-trail cameras and no off-trail cameras was the most cost-efficient approach to monitoring deer in South Florida (Table 3.3). When comparing a single

year of surveying, only two camera designs produced costs less than costs of aerial surveying. Both designs used the minimum number of trail cameras proposed. The majority of costs for each camera design survey was incurred during the initial purchase of equipment. Labor required for surveying was higher for trail camera monitoring than aerial surveying. Aerial surveying required a two-person survey team for two half-day flights. In contrast, trail camera surveying required both the deployment and retrieval of cameras following the survey period. Camera designs that implemented both on- and off-trail cameras resulted in higher field labor due to the extended time needed to travel to off-trail locations. Data management and analysis costs were comparable between camera monitoring and aerial surveying.

When evaluating the costs of surveying on a recurring yearly basis, aerial surveys were three times more expensive to implement than trail camera monitoring (Table 3.3). Aerial surveying required the continued rental of helicopter services for two flight paths, resulting in an estimated annual cost of $5,753. In contrast, trail camera monitoring only required labor since all equipment was purchased during the first year. Variation in recurring yearly costs became noticeable when investigating the potential for implementing a 5-year study program. Trail camera monitoring became more cost efficient than aerial surveying with a minimum estimated savings of $7,765 using the most expensive camera design.

An inverse relationship existed between the two objectives with regards to camera designs, such that designs with fewer cameras had relatively poorer model performance but lower costs (Fig. 3.3). When comparing the camera designs across all sites, T60 performed best at maximizing model performance, while T20 best minimized the costs of surveying with utility values of 1. However, T40 performed best overall (Q_D = 0.61) at meeting both objectives when equally weighting each objective. Only designs implementing 40 cameras received overall utility

scores of $Q_D \geq 0.50$ for the scenarios weighting 100% for maximizing model performance and 100% for minimizing costs.

DISCUSSION

Understanding how to best allocate limited resources for monitoring remains a critical area of conservation need (Nichols and Williams 2006). Monitoring may be ineffective at best, and wasteful of precious resources at worst, if sampling designs are not aligned with specific objectives and are not implemented at appropriate spatio-temporal scales (Yoccoz et al. 2001, Elzinga et al. 2001, Vesely et al. 2006). We presented a conceptual and analytical framework for evaluating camera-based survey designs that allows managers to weight objectives in terms of accuracy and costs.

In our case study, the optimal monitoring design was defined as the design that maximized a utility function with equal weights on accuracy of abundance estimates and minimizing costs of monitoring. However, inherent tradeoffs exist between the chosen design criteria. In order to improve abundance estimation, SCR designs rely on maximizing the number of unique individuals detected, the number of recaptures, and the number of spatial recaptures (Royle et al. 2013). This is often achieved by increasing the number of cameras within a trapping array, which inherently increases costs. The use of objective weighting provided a means to evaluate tradeoffs in design criteria using scaled performance metrics, such that 40 on-trail cameras was deemed the optimal choice among the proposed designs. However, objective weighting is a decision-aiding process used to provide conservation agencies with information and insight about aspects of study designs. Ultimately, conservation agencies must determine

how the uncertainties inherent at the different spatio-temporal scales could affect performance metrics and tradeoffs and potentially change the decision.

We used RMSE as a performance metric for assessing SCR model performance as it provides a measure of the uncertainty surrounding the expected deer abundance. Despite differences in camera counts and spatial configuration, differences in design estimation performance were mostly negligible. This may be due in part to the use of informative prior distributions for the detection parameters (σ, λ_0^{on}, and λ_0^{off}) in the unmarked SCR model. In Bayesian analyses, the prior information and the data combine to produce posterior distributions for parameter estimates. The contribution of the prior and the data to the posterior distribution depends on their relative precision, with the more precise of the two having the greater influence. Commonly, vague, relatively uninformative priors are used to ensure the posterior distributions are driven by the data alone. However, this disregards the inherent benefit of Bayesian inference of using informative priors to improve parameter estimation (McCarthy and Masters 2005, Morris et al. 2013, Morris et al. 2014). Additionally, we found no difference in model performance between designs implementing only on-trail cameras versus designs implementing a mix of on- and off-trail cameras. This may be related to similarities in encounter probability between on-trail (λ_0^{on}) and off-trial (λ_0^{off}) cameras.

Although our analysis focused on developing an optimal spatial design for monitoring an unmarked white-tailed deer population, the analysis could be extended to include explicit spatio-temporal assessments through the use of recursive Bayesian inference (Hooten et al. 2019). Dynamic survey designs provide a succinct framework for understanding the current dynamics and associated uncertainty within a population in order to inform future monitoring (Williams et al. 2018). Using the SCR statistical framework along with historical or baseline data, posterior

density estimates could be used to examine potential survey designs for future monitoring. Incorporating temporally-variant SCR parameter estimates would allow for changes in the performance of camera sampling designs in response to shifting environmental or biological conditions. Dynamic survey designs behave similarly to adaptive resource management in that it encompasses an iterative process of model assessment and objective reevaluation in order to reduce uncertainty in parameter and density estimates (Williams et al. 2018, Dupont et al. 2021, Runge et al. 2020). Additionally, the optimal spatial design selected from our analysis was based on the primary objective of monitoring a single species. Transitioning towards multi-species or community-based monitoring program would alter each step of the sampling design process from selection of monitoring objectives to potential spatial camera designs and statistical model development (Tober et al. 2008, Kays et al. 2011, Ahumada et al. 2013, Tobler et al. 2015, Rich et al. 2019). Ultimately, the best use of available resources for ecological monitoring and management should be objective-driven to produce sampling designs resulting in accurate and unbiased estimates of population parameters.

LITERATURE CITED

Abernathy, H., D. A. Crawford, E. P. Garrison, R. B. Chandler, L. M. Conner, K. V. Miller, and M. J. Cherry. 2019. Deer movement and resource selection during Hurricane Irma: implications for extreme climatic events and wildlife. Proceedings of the Royal Society B 286: 20192230.

Ahumada, J.A., J. Hurtado, and D. Lizcano. 2013. Monitoring the status and trends of tropical forest terrestrial vertebrate communities from camera trap data: a tool for conservation. PLoS ONE 8: e73707.

Augustine, B. C., J. A. Royle, S. M. Murphy, R. B. Chandler, J. J. Cox, and M. J. Kelly. 2019. Spatial capture-recapture for categorically marked populations with an application to genetic capture-recapture. Ecosphere 10: e02627.

Beasom, S. L. 1979. Precision in helicopter censusing of white-tailed deer. Journal of Wildlife Management 43: 777–780.

Beasom, S. L., F. G. Leon III, and D. R. Synatzske. 1986. Accuracy and precision of counting white-tailed deer with helicopters at different sampling intensities. Wildlife Society Bulletin 14: 364–368.

Borchers, D. L. and M. G. Efford. 2008. Spatially explicit maximum likelihood methods for capture-recapture studies. Biometrics 64:377–385.

Buckland, S. T., E. A. Rexstad, T. A. Marques, and C. S. Oedekoven. 2001. Introduction to distance sampling: estimating abundance of biological populations. Oxford University Press, New York, New York, USA.

Caughley, G. 1977. Sampling in aerial survey. Journal of Wildlife Management 41: 605–615.

Chai, T. and R. R. Draxler. 2014. Root mean square error (RMSE) or mean absolute error (MAE)? Geoscientific Model Development Discussions 7: 1525–2534.

Chandler, R. B., K. Engebretsen, M. J. Cherry, E. P. Garrison, K. V. Miller. 2018. Estimating recruitment from capture–recapture data by modeling spatio-temporal variation in birth and age-specific survival rates. Methods in Ecology and Evolution 9: 2115–2130.

Chandler, R. B. and J. A. Royle. 2013. Spatially explicit models for inference about density in unmarked or partially marked populations. Annuals of Applied Statistics 7: 936–954.

Cherry, M. J., R. B. Chandler, E. P. Garrison, D. A. Crawford, B. D. Kelly, D. B. Shindle, K. G. Godsea, K. V. Miller, and L. M. Conner. 2018. Wildfire affects space use and movement

of white-tailed deer in a tropical pyric landscape. Forest Ecology and Management 409: 161–169.

Clare, J. D. J., E. M. Anderson, D. M. MacFarland, and B. L. Sloss. 2015. Comparing the costs and detectability of bobcats using scat-detecting dog and remote camera surveys in central Wisconsin. Wildlife Society Bulletin 39: 210–217.

Clark, J. D. 2019. Comparing clustered sampling designs for spatially explicit estimation of population density. Population Ecology 61: 93–101.

Crawford, D. A. 2017. Behavioral and spatial ecology of white-tailed deer in the Big Cypress Basin of Florida. Thesis, University of Georgia, Athens, Georgia, USA.

Crawford, D. A., M. J. Cherry, B. D. Kelly, E. P. Garrison, D. B. Shindle, L. M. Conner, R. B. Chandler, and K. V. Miller. 2019. Chronology of reproductive investment determines predation risk aversion in a felid-ungulate system. Ecology and Evolution 9: 3264–3275.

Davis, A. J., D. A. Keiter, E. M. Kierepka, C. Slootmaker, A. J. Piaggio, J. C. Beasley, and K. M. Pepin. 2020. A comparison of cost and quality of three methods for estimating density for wild pig (*Sus scrofa*). Scientific Reports 10: 2047. DOI: 10.1038/s41598-020-58937-0.

DeYoung, C. A. 2011. Population dynamics. Pages 147–180 *in* D. G. Hewitt (ed.). Biology and management of white-tailed deer. CRC Press, Boca Raton, Florida, USA.

Dupont, G., J. A. Royle, M. A. Nawaz, and C. Sutherland. 2021. Optimal sampling design for spatial capture-recapture. Ecology 102, e03262. DOI: 10.1002/ecy.3262.

Durbach, I., D. Borchers, C. Sutherland, and K. Sharma. 2021. Fast, flexible alternatives to regular grid designs for spatial capture-recapture. Methods in Ecology and Evolution 12: 298–310. DOI: 10.1111/2041-210X.13517.

Dunn, W. C., J. P. Donnelly, and W. K. Krausmann. 2002. Using thermal infrared sensing to count elk in the southwestern United States. Wildlife Society Bulletin 30: 963–967.

Efford, M. 2004. Density estimation in live-trapping studies. Oikos 106:598–610.

Efford, M. G. 2016. secr: Spatially explicit capture-recapture models. R package version 4.3.3. https://CRAN.R-project.org/package=secr.

Efford, M. G. and J. Boulanger. 2019. Fast evaluation of study designs for spatially explicit capture-recapture. Methods in Ecology and Evolution 10: 1529–1535.

Elzinga, C. L., D. W. Salzer, J. W. Willoughby, and J. P. Gibbs. 2001. Monitoring plant and animal populations: a handbook for field biologists. Blackwell: Malden, Massachusetts, USA.

Evans, M. J. and T. A. G. Rittenhouse. 2018. Evaluating spatially explicit density estimates of unmarked wildlife detected by remote cameras. Journal of Applied Ecology 55: 2565–2574.

Giudice, J. H., J. R. Fieberg, M. C. Zicus, D. P. Rave, and R. G. Wright. 2010. Cost and precision functions for aerial quadrat surveys: a case study of ring-necked ducks in Minnesota. Journal of Wildlife Management 74: 342–349.

Graves, H. B., E. D. Bellis, and W. M. Knuth. 1972. Censusing white-tailed deer by airborne thermal infrared imagery. Journal of Wildlife Management 36: 875–884.

Gregory, R., L. Failing, M. Harstone, G. Long, T. McDaniels, and D. Ohlson. 2012. Structured decision making: A practical guide to environmental management choices. Wiley-Blackwell: Hoboken, New Jersey, USA.

Hooten, M. B., D. S. Johnson, and B. M. B. 2019. Making recursive Bayesian inference accessible. American Statistician 00: 1–10. DOI: 10.1080/00031305.2019.1665584.

Kays, R., B. S. Arbogast, M. Baker-Whatton, C. Beirne, H. M. Boone, M. Bowler, S. F. Burneo, M. V. Cove, P. Ding, S. Espinosa, A. L. S. Gonçalves, C. P. Hansen, P. A. Jansen, J. M. Kolowski, T. W. Knowles, M. G. M. Lima, J. Millspaugh, W. J. McShea, K. Pacifici, A. W. Parsons, B. S. Pease, F. Rovero, F. Santos, S. G. Schuttler, D. Sheil, X. Si, M. Snider, W. R. Spironello. 2020. An empirical evaluation of camera trap study design: How many, how long and when? Methods in Ecology and Evolution 11: 700–713.

Kays, R., S. Tilak, B. Kranstauber, P. Jansen, C. Carbone, M. Rowcliffe, T. Fountain, J. Eggert, and Z. He. 2011. Camera traps as sensor networks for monitoring animal communities. International Journal of Research and Reviews in Wireless Sensor Networks 1: 19–29.

Kristensen, T. V. and A. I. Kovach. 2018. Spatially explicit abundance estimation of a rare habitat specialist: Implications for SECR study design. Ecosphere 9: e02217.

Margenau, L. L. S., M. J. Cherry, K. V. Miller, E. P. Garrison, and R. B. Chandler. 2021. Monitoring partially-marked populations using camera and telemetry data. Manuscript in review.

McCarthy, M. A. and P. Masters, 2005. Profiting from prior information in Bayesian analyses of ecological data. Journal of Applied Ecology 42: 1012–1019.

McPherson, B. F. 1974. The Big Cypress Swamp. Environments of South Florida: present and past. Miami Geological Society, Miami, Florida, USA.

Morris, W. K., P. A. Vesk, and M. A. McCarthy. 2013. Profiting from pilot studies: analysiing mortality using Bayesian models with informative priors. Basic and Applied Ecology 14: 81–89.

Morris, W. K., P. A. Vesk, M. A. McCarthy, S. Bunyavejchewin, P. J. Baker. 2014. The neglected tool in the Bayesian ecologist's shed: a case study testing informative priors' effect on model accuracy. Ecology and Evolution 5: 102–108.

Nichols, J. D. and B. K. Williams. 2006. Monitoring for conservation. Trends in Ecology and Evolution 21: 668–673.

O'Connell, A. F., J. D. Nichols, and K. U. Karanth. 2011. Camera traps in animal ecology: Methods and analyses. Springer, New York, New York, USA.

Potvin, F., L. Breton, and L.-P. Rivest. 2004. Aerial surveys for white-tailed deer with the double-count technique in Québec: two 5-year plans completed. Wildlife Society Bulletin 32: 1099–1107.

Plummer, M. 2018. rjags: Bayesian Graphical Models using MCMC. R package version 4-8. https://CRAN.R-project.org/package=rjags.

R Core Team. 2019. R: A language and environment for statistical computing. R Foundation for Statistical Computing, Vienna, Austria. URL: https://www.R-project.org.

Rice, W. R. and J. D. Harder. 1977. Application of multiple aerial sampling to a mark-recapture census of white-tailed deer. Journal of Wildlife Management 41: 197–206.

Rich, L. N., D. A. Miller, D. J. Muñoz, H. S. Robinson, J. W. McNutt, and M. J. Kelly. 2019. Sampling design and analytical advances allow for simultaneous density estimation of seven sympatric carnivore species from camera trap data. Biological Conservation 233: 12–20.

Royle, J. A., R. M. Dorazio, and W. A. Link. 2007. Analysis of multinomial models with unknown index using data augmentation. Journal of Computation and Graphical Statistics 16: 67–85.

Royle, J. A., R. B. Chandler, R. Sollmann, and B. Gardner. 2013. Spatial Capture-Recapture. Academic Press, Boston, Massachusetts, USA.

Royle, J. A., A. K. Fuller, and C. Sutherland. 2018. Unifying population and landscape ecology with spatial capture-recapture. 41: 444–456.

Runge, M. C., S. J. Converse, J. E. Lyons, and D. R. Smith. 2020. Structured decision making: Case studies in natural resource management. Johns Hopkins University Press, Baltimore, Maryland, USA.

Sollmann, R., B. Gardner, and J. L. Belant. 2012. How does spatial study design influence density estimates from spatial capture-recapture models? PLoS ONE 7: e34575.

Sun, C. C., Fuller, A. K., & Royle, J. A. 2014. Trap configuration and spacing influences parameter estimates in spatial capture–recapture models. PLoS ONE 9: e88025.

Sutherland, C., J. A. Royle, D. Linden. 2018. oSCR: Multi-Session Sex-Structured Spatial Capture-Recapture Models. R package version 0.42.0. https://rdrr.io/github/jaroyle/oSCR/.

Tobler, M. W., S. E. Carrillo-Percastegui, R. L. Pitman, R. Mares, and G. Powell. 2008. An evaluation of camera traps for inventorying large- and medium-sized terrestrial rainforest mammals. Animal Conservation 11: 169–178.

Tobler, M. W., A. Z. Hartley, S. E. Carrillo-Percastegui, and G. V. N. Powell. 2015. Spatio-temporal hierarchical modelling of species richness and occupancy using camera trap data. Journal of Applied Ecology 52: 413–421.

Vesely, D., B. C. McComb, C. D. Vojta, L. H. Suring, J. Halaj, R. S. Holthausen, B. Zuckerberg, and P. M. Manley. 2006. Development of protocols to inventory or monitor wildlife, fish, or rare plants. U.S. Department of Agriculture, Forest Service.

Walther, B. A. and J. L. Moore. 2005. The concepts of bias, precision, and accuracy, and their use in testing the performance of species richness estimators, with a literature review of estimator performance. Ecography 28: 815–829.

Whittington, J., M. Hebblewhite, and R. B. Chandler. 2018. Generalized spatial mark-resight models with an application to grizzly bears. Journal of Applied Ecology 55: 157–168.

Williams, P. J. and M. B. Hooten. 2016. Combining statistical inference and decisions in ecology. Ecological Applications 26: 1930–1942.

Williams, P. J., M. B. Hooten, J. N. Womble, G. G. Esslinger, and M. R. Bower. 2018. Monitoring dynamic spatio-temporal ecological processes optimally. Ecology 99: 524–535.

Williams, B. K., J. D. Nichols, and M. J. Conroy. 2002. Analysis and management of animal populations. Academic Press, San Diego, California, USA.

Yoccoz, N. G., J. D. Nichols, and T. Boulinier. 2001. Monitoring of biological diversity in space and time. Trends in Ecology and Evolution 16: 446–453.

Table 3.1. Camera trap placements for each study design. The Status Quo design used camera locations from a previous study conducted at each of the three sites: North Addition Lands (FP), Bear Island (BI), and Florida Panther National Wildlife Refuge (FP). The Paired design consisted of all locations used in the Status Quo that had paired on- and off-trail cameras. Random designs consisted of randomly sampled camera locations from the Status Quo, allowing for both on- and off-trail placements. On-trail designs were restricted to only on-trail camera locations.

Abbreviation	Description	Site(s)	On-trail Cameras	Off-trail Cameras
SQ	Status Quo	All	40	20
P	Paired	All	20	20
R20	Random	AD	10	10
		BI	12	8
		FP	14	6
R30	Random	AD	19	11
		BI	22	8
		FP	17	13
R40	Random	AD	23	17
		BI	29	11
		FP	28	12
T20	On-trail	All	20	0
T30	On-trail	All	30	0
T40	On-trail	All	40	0
T50	On-trail	All	50	0
T60	On-trail	All	60	0

Table 3.2. Average median posterior abundance estimates, bias, precision, and root mean squared error (RMSE) for 500 simulated data sets for each trail camera design. Data were simulated using assigned values of abundance (N) and detection parameters estimated from the three years of camera and telemetry data from each of the three study sites in South Florida (AL - North Addition Lands, BI - Bear Island, and FP - Florida Panther National Wildlife Refuge). The design with the lowest RMSE was considered to be optimal in terms of bias and precision.

Site	Design	Assigned N	Average estimate of $\bar{N}$	Bias	Precision	RMSE
AL	SQ	75	75.40	0.40	0.0049	14.28
AL	P	75	74.86	-0.14	0.0036	16.65
AL	R20	75	74.46	-0.54	0.0017	24.43
AL	R30	75	74.74	-0.26	0.0027	19.22
AL	R40	75	74.44	-0.56	0.0036	16.73
AL	T20	75	75.55	0.55	0.0019	22.80
AL	T30	75	75.92	0.92	0.0029	18.67
AL	T40	75	75.53	0.53	0.0037	16.38
AL	T50	75	74.78	-0.22	0.0044	15.12
AL	T60	75	75.41	0.41	0.0051	14.02
BI	SQ	200	200.83	0.83	0.0010	31.52
BI	P	200	203.70	3.70	0.0007	38.45
BI	R20	200	196.88	-3.21	0.0004	47.77
BI	R30	200	199.61	-0.39	0.0005	44.41
BI	R40	200	200.02	0.02	0.0007	37.04
BI	T20	200	200.95	0.95	0.0004	50.09
BI	T30	200	198.56	-1.44	0.0005	45.14
BI	T40	200	198.96	-1.04	0.0007	37.69
BI	T50	200	199.69	-0.31	0.0009	33.66
BI	T60	200	200.65	0.65	0.0010	31.37
FP	SQ	250	250.94	0.94	0.0008	35.72
FP	P	250	248.27	-1.73	0.0005	43.63
FP	R20	250	249.25	-0.75	0.0003	57.65
FP	R30	250	252.02	2.02	0.0005	46.35
FP	R40	250	249.08	-0.92	0.0006	41.74
FP	T20	250	248.11	-1.89	0.0004	51.20
FP	T30	250	247.08	-2.92	0.0005	44.26
FP	T40	250	249.96	-0.04	0.0006	40.22
FP	T50	250	249.11	-0.89	0.0008	36.46
FP	T60	250	251.17	1.17	0.0009	32.83

Table 3.3. Cost analysis of aerial surveying and trail camera surveying designs for a 14-day sampling period. The camera design options are described in the Methods. Field equipment costs for camera surveying includes costs of trail cameras, camera boxes, memory cards, batteries, and GPS units. Field equipment costs for aerial surveying includes flight cost and purchase of GPS units. Field labor costs for camera surveying includes estimated labor for deploying and retrieving trail cameras. Annual Cost in Year 1 is defined as the initial purchase of equipment and labor. Annual Cost in Subsequent Years does not include the initial costs of purchasing equipment and labor. The 5 Year Total is the estimated cost to implement a 5-year monitoring program.

Survey Method	Field Surveying	Field Labor	Data Processing	Annual Cost in Year 1	Annual Cost in Subsequent Years	5 Year Total
SQ	$14,375	$1,760	$480	$16,615	$2,240	$25,575
P	$9,775	$1,120	$440	$11,335	$1,560	$17,575
R20	$5,175	$640	$400	$6,215	$1,040	$10,375
R30	$7,475	$960	$400	$8,835	$1,360	$14,275
R40	$9,775	$1,120	$440	$11,335	$1,560	$17,575
T20	$5,175	$480	$400	$6,055	$880	$9,575
T30	$7,475	$640	$400	$8,515	$1,040	$12,675
T40	$9,775	$800	$440	$11,015	$1,240	$15,975
T50	$12,075	$1,120	$440	$13,635	$1,560	$19,875
T60	$14,375	$1,280	$480	$16,135	$1,760	$23,175
Aerial	$6,328	$320	$480	$7,128	$6,553	$33,340

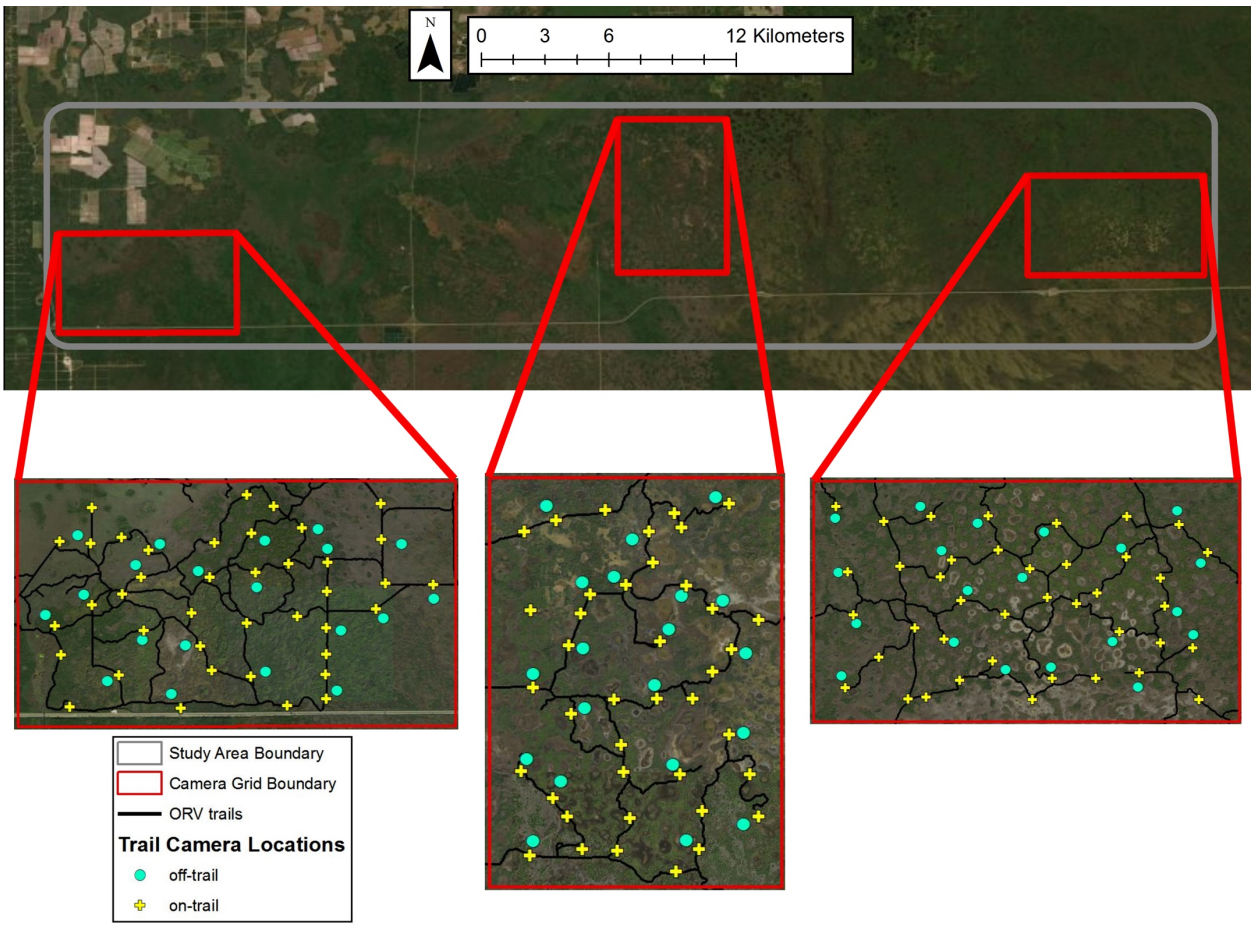

Figure 3.1. South Florida white-tailed deer study area and camera trapping arrays. The central (Bear Island) and eastern (North Addition Lands) grids were located in Big Cypress National Preserve. The western grid was located in the Florida Panther National Wildlife Refuge.

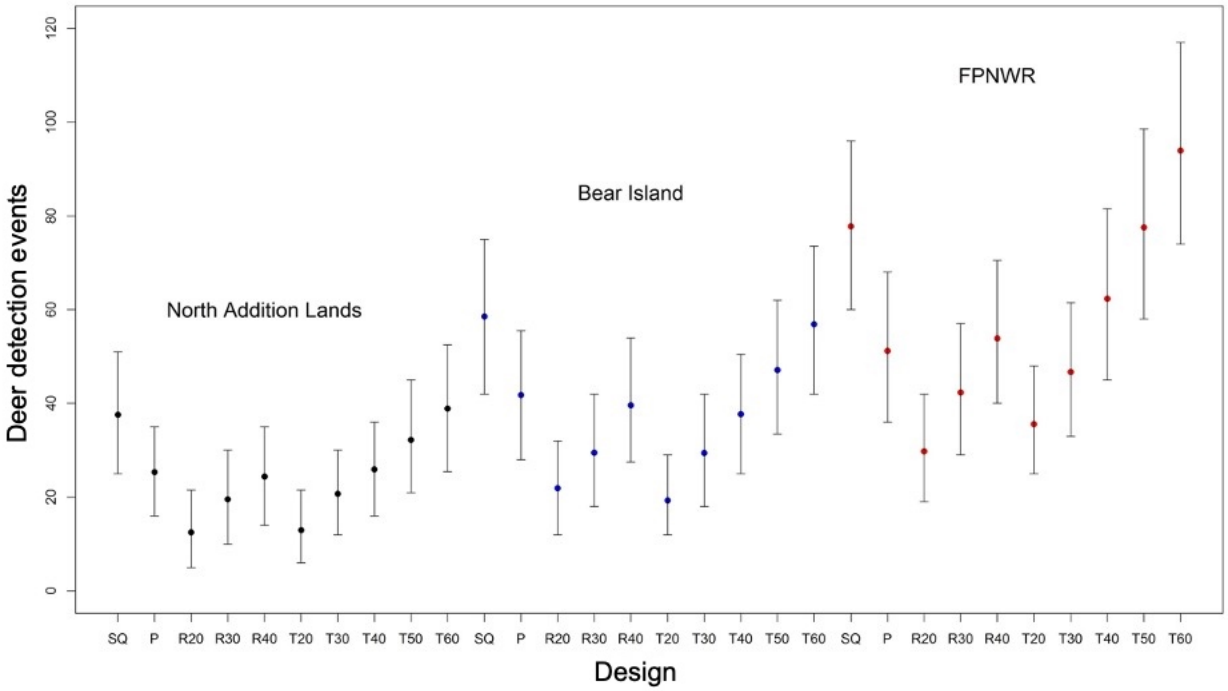

Figure 3.2. Mean and 95% intervals of white-tailed deer detections from 500 simulated datasets for each camera design during a 14-day sampling period in North Addition Lands, Bear Island, and Florida Panther National Wildlife Refuge (FPNWR). A deer detection event is defined as the detection of at least one adult female deer at a camera during a 24-h sampling occasion.

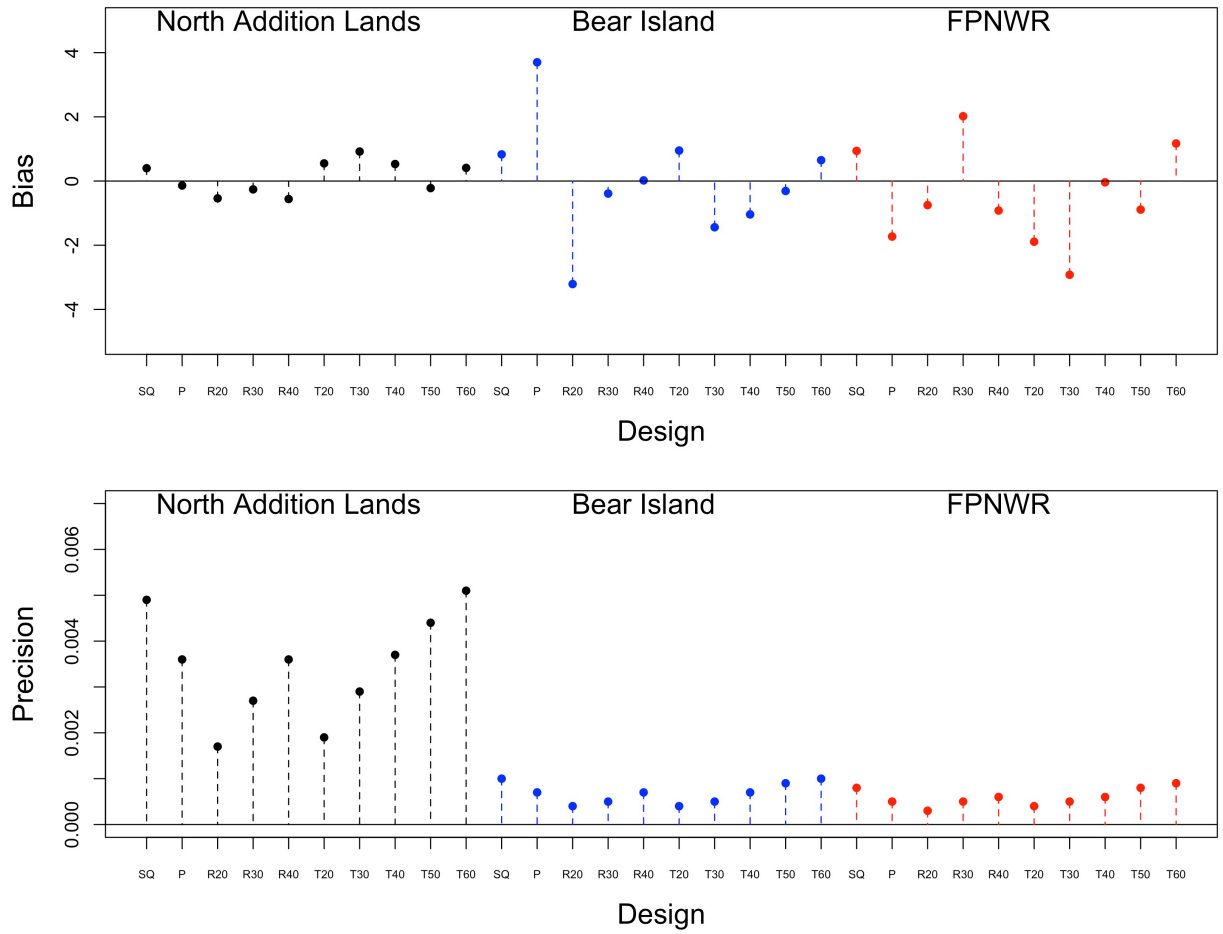

Figure 3.3 Bias and precision of median posterior abundance estimates from 500 simulated datasets for each camera design during a 14-day sampling period in North Addition Lands, Bear Island, and Florida Panther National Wildlife Refuge (FPNWR).

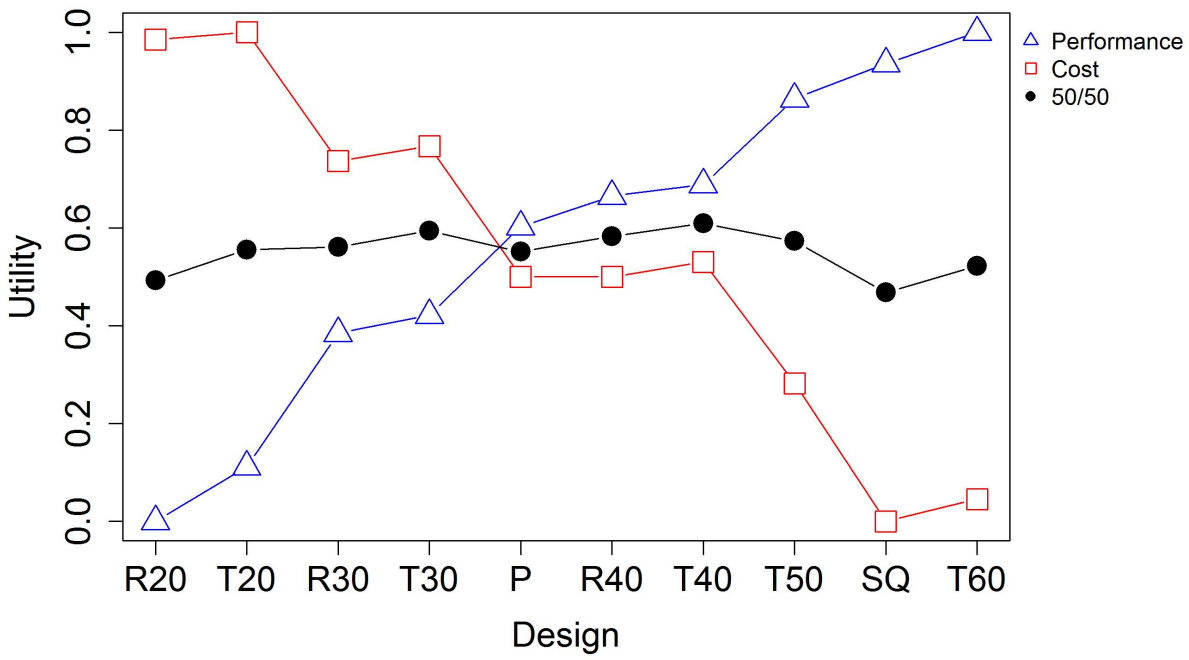

Figure 3.4. Camera design performance for achieving the objectives of maximizing model performance and minimizing logistical costs. Three objective weightings were assessed to evaluate tradeoffs. The ‘performance’ objective uses 100% weighting for minimizing root mean squared error (RMSE), while the ‘cost’ objective uses 100% weighting for minimizing costs. The ‘50/50’ objective gives equal weight to minimizing RMSE and cost. A utility of 1 indicates high performance, while a utility of 0 indicates poor performance relative to the camera designs implemented. Using the 50/50 objective, the optimal design was T40, which involves 40 on-trail cameras and no off-trail cameras.

APPENDICES

Appendix 3.A. Camera trapping array designs

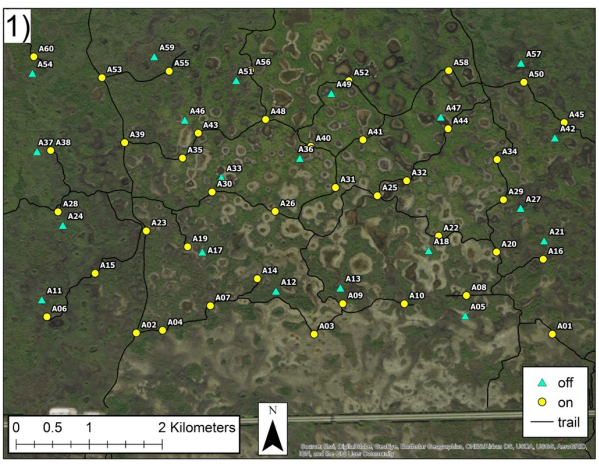

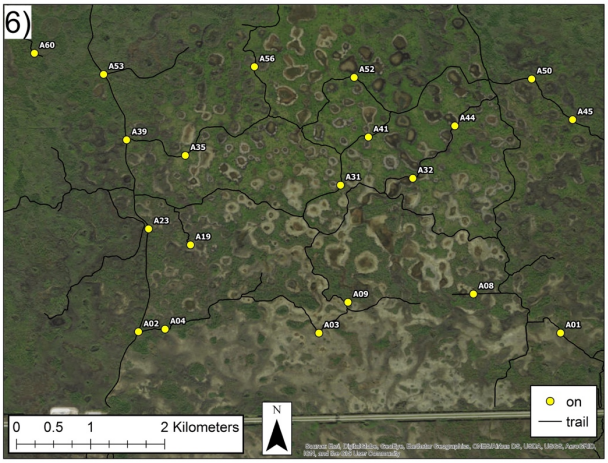

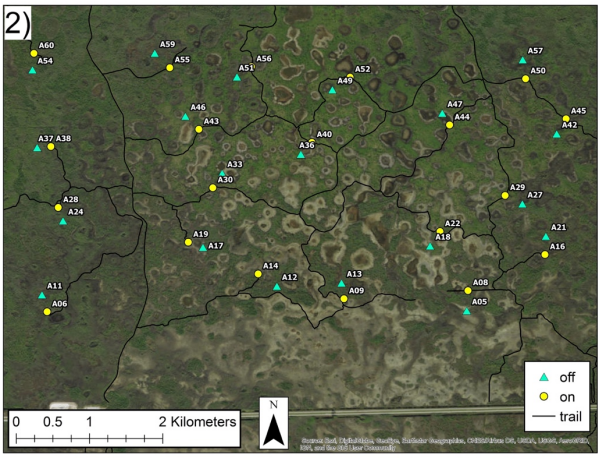

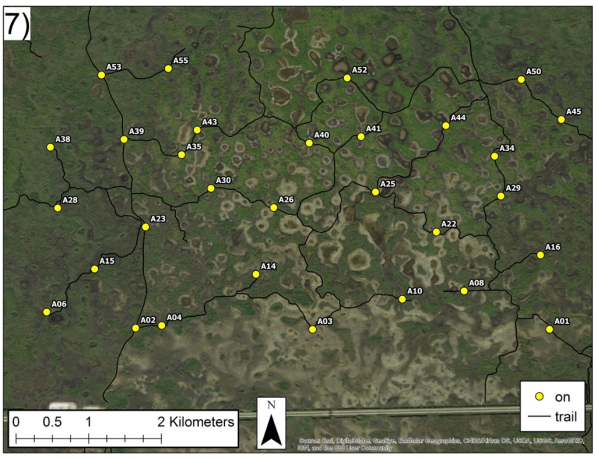

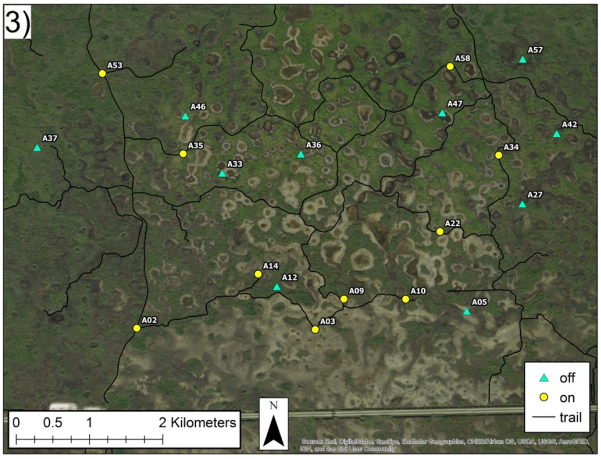

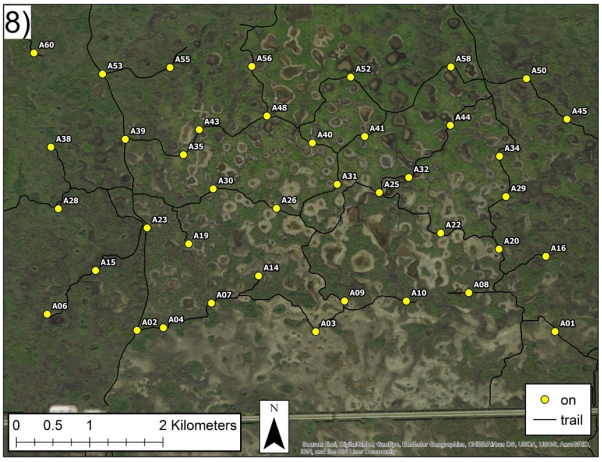

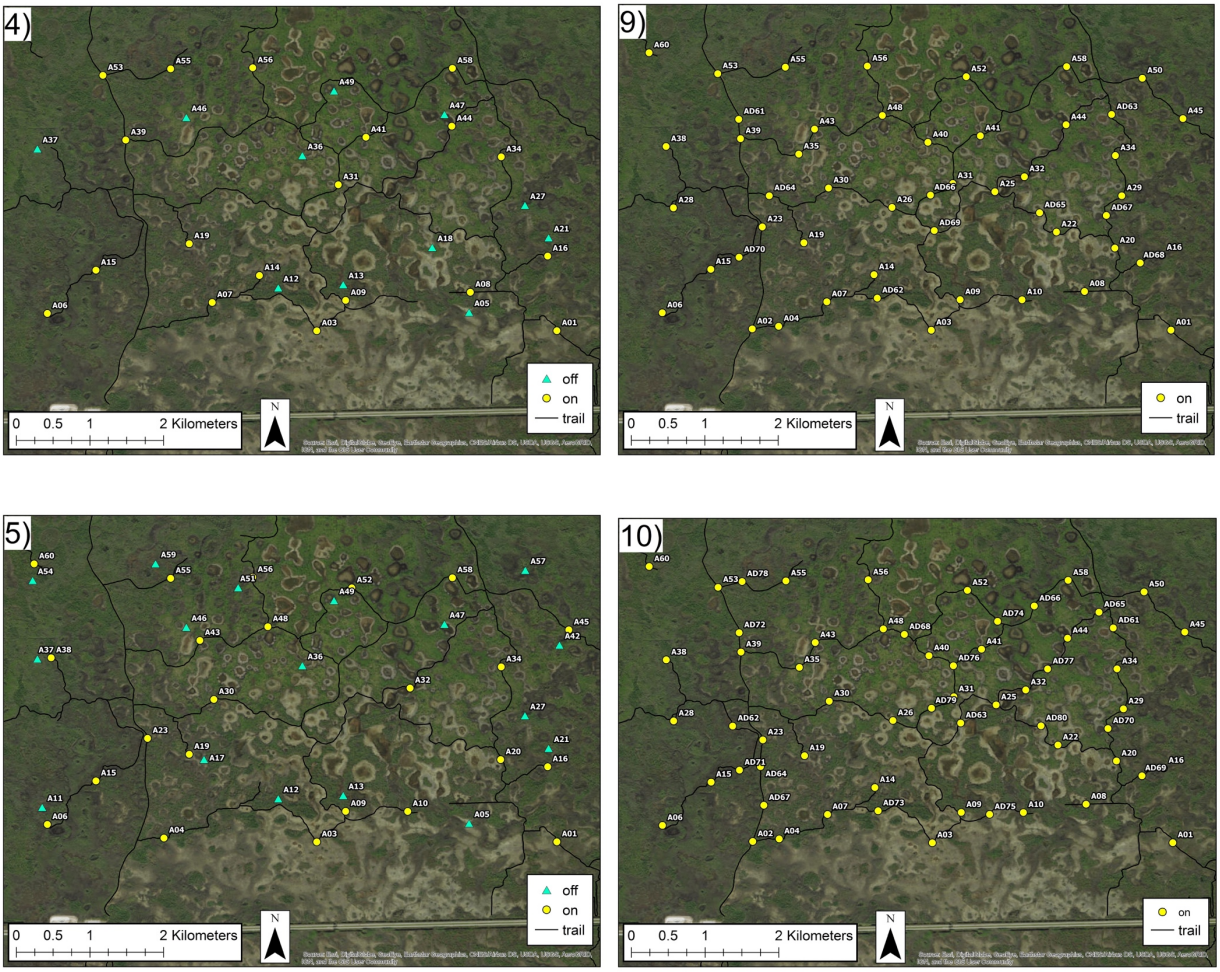

Figure 3.A1. Location of the cameras on North Addition Lands for the camera design simulation study. Left column - 1) Status quo: 40 on-trail and 20 off-trail cameras, 2) 40 paired on- and off-trail cameras, 3) 20 random cameras, 4) 30 random cameras, 5) 40 random cameras. Right column - 6) 20 on-trail cameras, 7) 30 on-trail cameras, 8) 40 on-trail cameras, 9) 50 on-trail cameras, 10) 60 on-trail cameras.

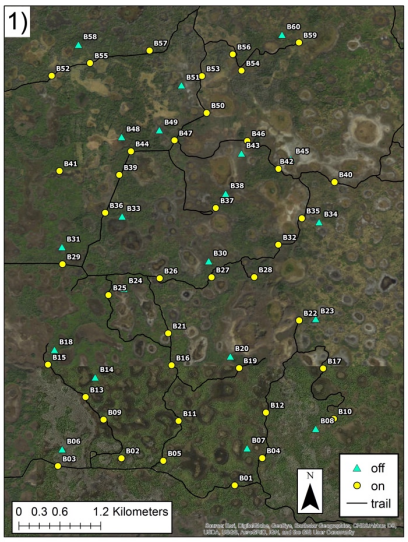
1)
off
on
trail
0 0.3 0.6 1.2 Kilometers

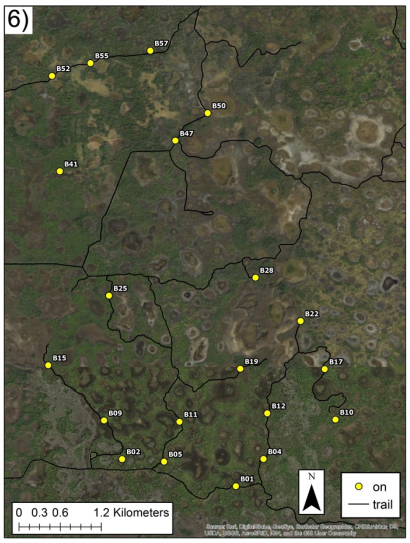
6)
on
trail
0 0.3 0.6 1.2 Kilometers

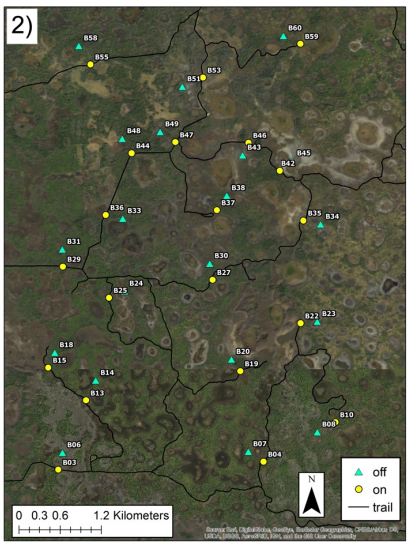
2)
off
on
trail
0 0.3 0.6 1.2 Kilometers

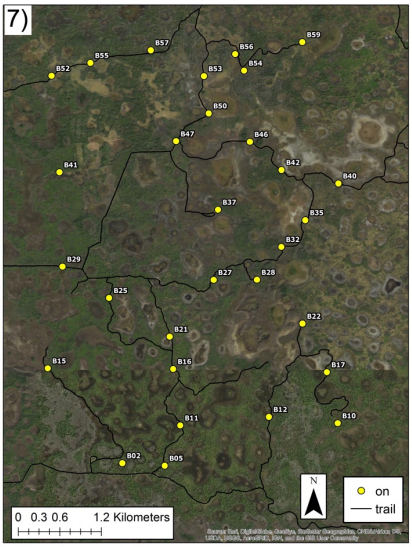
7)
on
trail
0 0.3 0.6 1.2 Kilometers

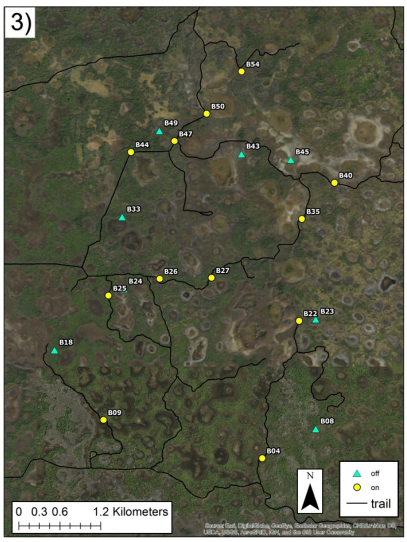
3)
off
on
trail
0 0.3 0.6 1.2 Kilometers

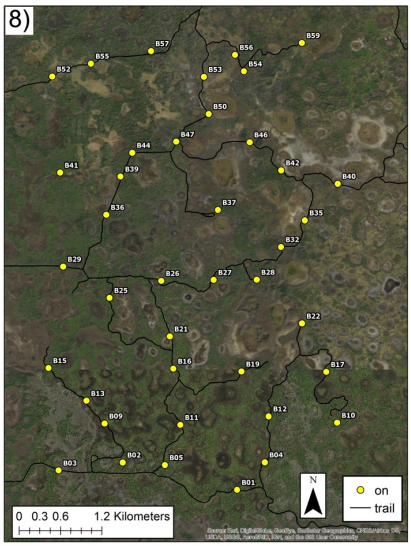
8)
on
trail
0 0.3 0.6 1.2 Kilometers

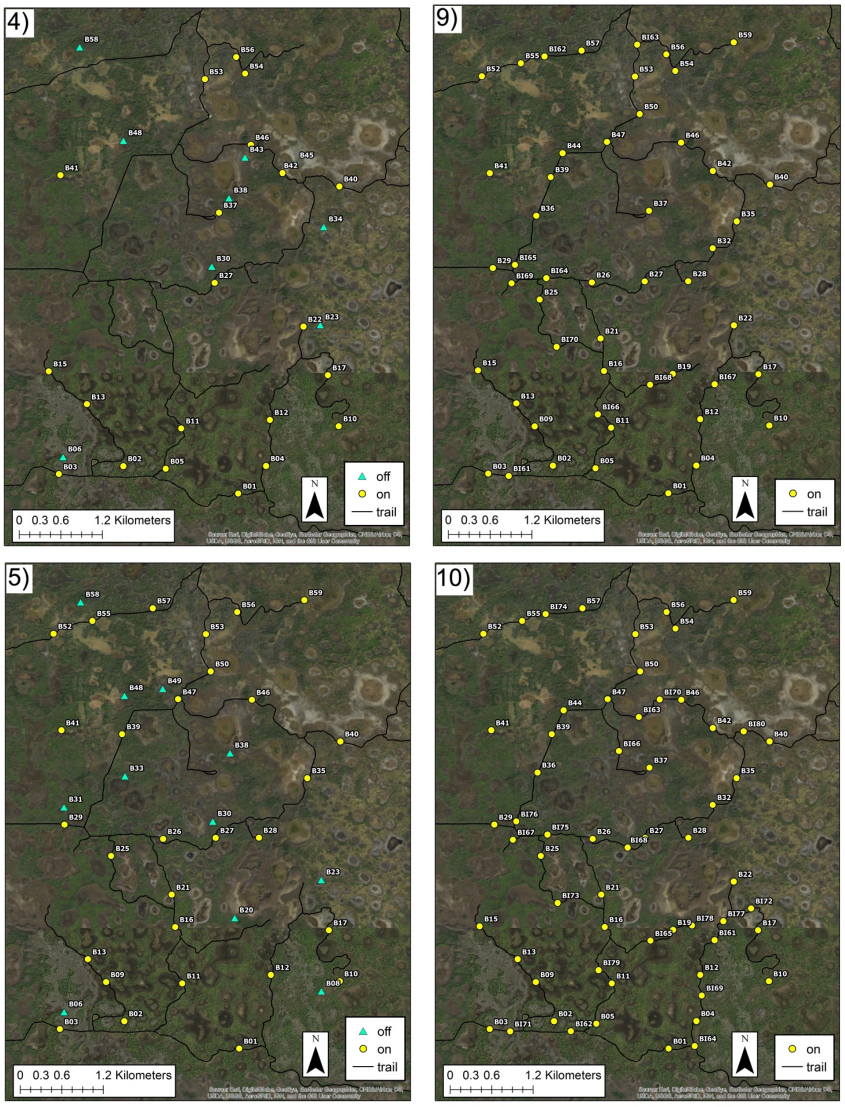

Figure 3.A2. Location of the cameras on Bear Island for the camera design simulation study. Left column - 1) Status quo: 40 on-trail and 20 off-trail cameras, 2) 40 paired on- and off-trail cameras, 3) 20 random cameras, 4) 30 random cameras, 5) 40 random cameras. Right column - 6) 20 on-trail cameras, 7) 30 on-trail cameras, 8) 40 on-trail cameras, 9) 50 on-trail cameras, 10) 60 on-trail cameras.

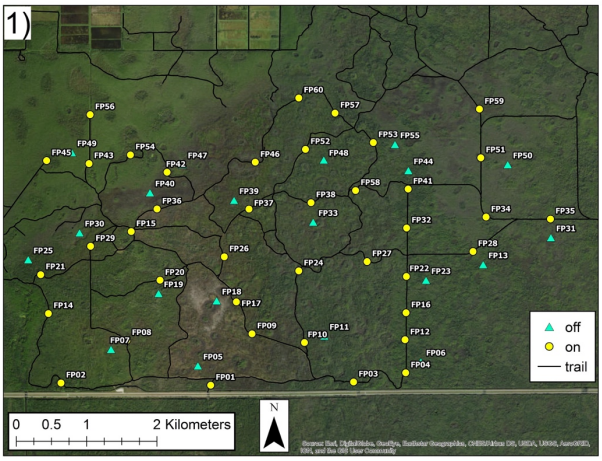
1)
FP60
FP56
FP57
FP59
FP49
FP45
FP43
FP54
FP47
FP42
FP46
FP52
FP48
FP53
FP55
FP51
FP50
FP44
FP40
FP39
FP37
FP38
FP58
FP41
FP36
FP33
FP34
FP35
FP30
FP15
FP32
FP31
FP29
FP25
FP26
FP24
FP27
FP28
FP13
FP21
FP20
FP22
FP23
FP19
FP18
FP17
FP16
FP14
FP09
FP11
FP08
FP07
FP10
FP12
FP05
FP06
FP04
FP02
FP01
FP03
off
on
trail
0 0.5 1 2 Kilometers
N

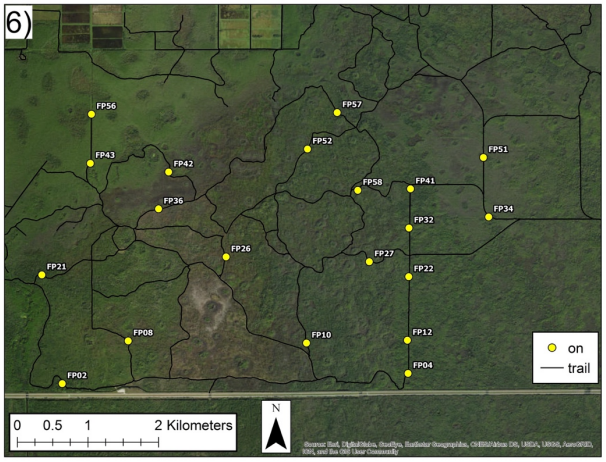
6)
FP56
FP57
FP52
FP43
FP51
FP42
FP58
FP41
FP36
FP34
FP32
FP26
FP27
FP21
FP22
FP08
FP10
FP12
FP02
FP04
on
trail
0 0.5 1 2 Kilometers
N

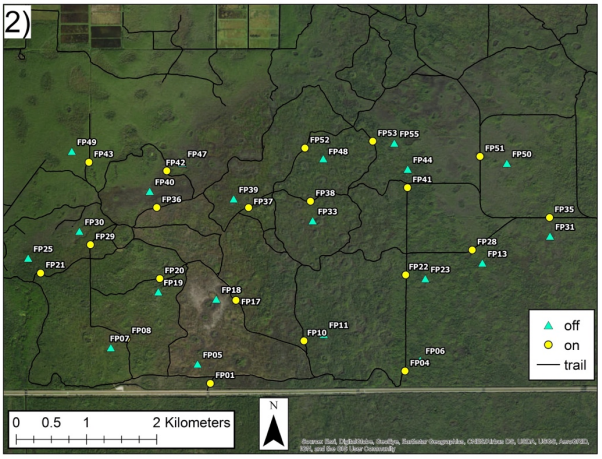
2)
FP49
FP43
FP47
FP42
FP52
FP53
FP55
FP48
FP51
FP50
FP44
FP40
FP39
FP37
FP38
FP41
FP36
FP33
FP35
FP30
FP31
FP29
FP28
FP25
FP13
FP21
FP22
FP23
FP20
FP19
FP18
FP17
FP08
FP11
FP07
FP10
FP06
FP05
FP04
FP01
off
on
trail
0 0.5 1 2 Kilometers
N

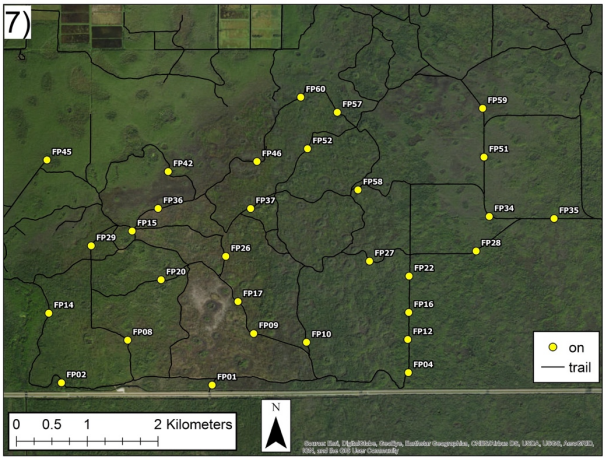
7)
FP60
FP57
FP59
FP52
FP45
FP42
FP46
FP51
FP58
FP36
FP37
FP34
FP35
FP15
FP29
FP26
FP27
FP28
FP20
FP22
FP17
FP16
FP14
FP09
FP08
FP10
FP12
FP02
FP01
FP04
on
trail
0 0.5 1 2 Kilometers
N

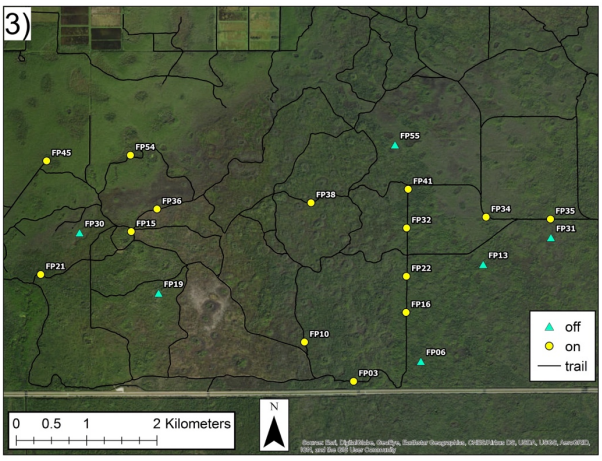
3)
FP45
FP54
FP55
FP41
FP38
FP36
FP34
FP35
FP30
FP15
FP32
FP31
FP13
FP21
FP22
FP19
FP16
FP10
FP06
FP03
off
on
trail
0 0.5 1 2 Kilometers
N

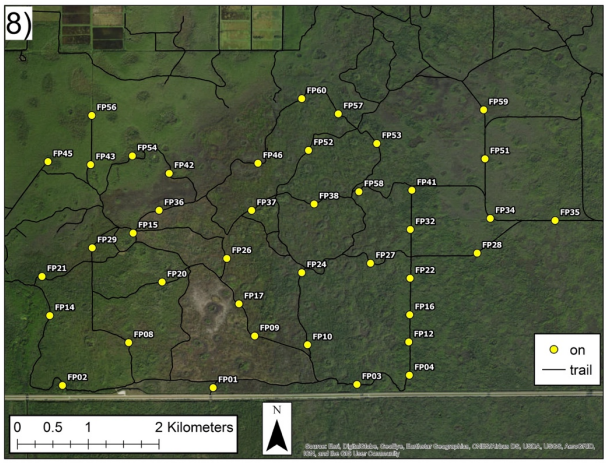
8)
FP60
FP56
FP57
FP59
FP53
FP52
FP45
FP43
FP54
FP51
FP46
FP42
FP58
FP41
FP36
FP37
FP38
FP34
FP35
FP15
FP32
FP29
FP28
FP26
FP27
FP24
FP21
FP20
FP22
FP17
FP16
FP14
FP09
FP08
FP10
FP12
FP02
FP01
FP03
FP04
on
trail
0 0.5 1 2 Kilometers
N

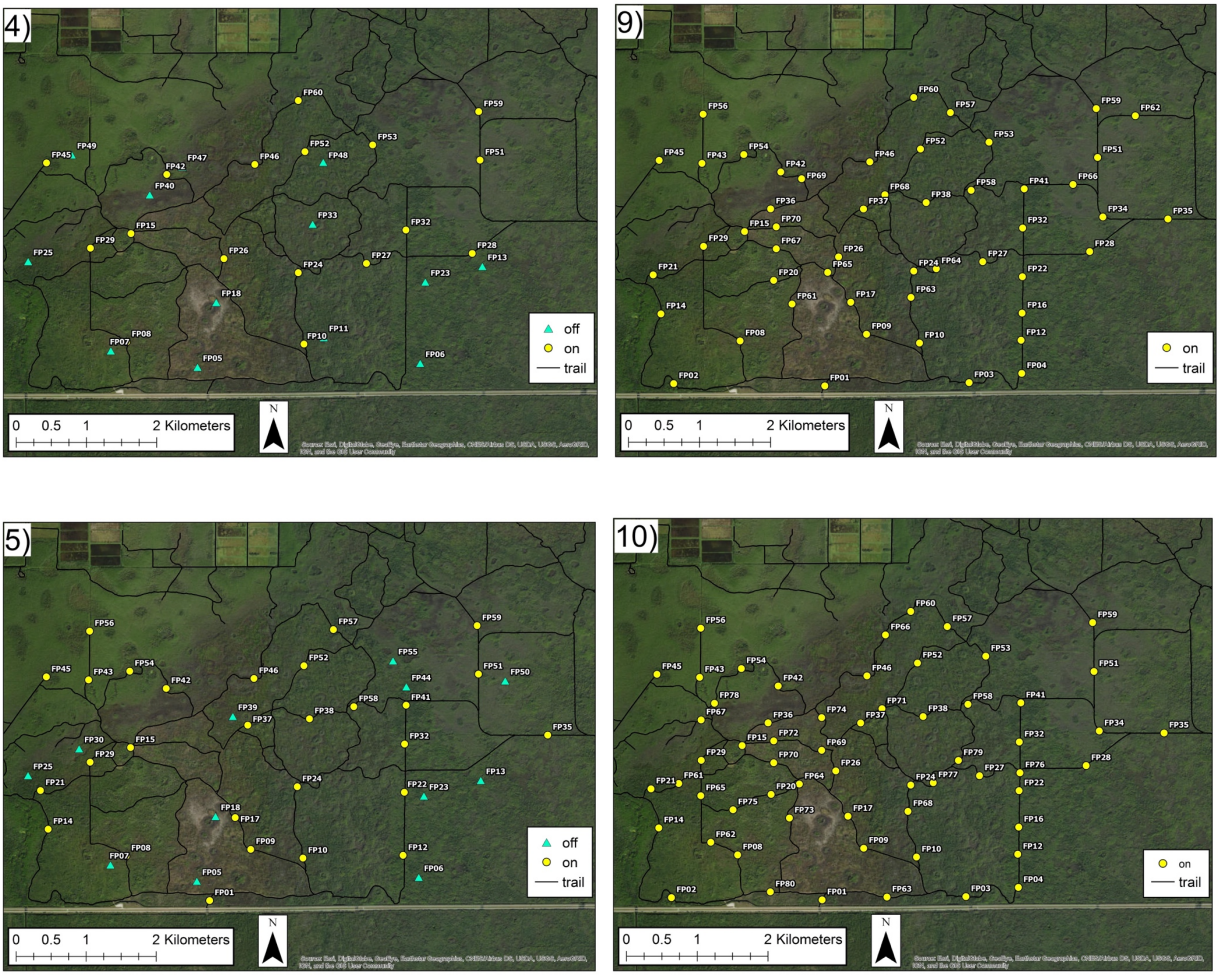

Figure 3.A3. Location of the cameras on Florida Panther National Wildlife Refuge for the camera design simulation study. Left column - 1) Status quo: 40 on-trail and 20 off-trail cameras, 2) 40 paired on- and off-trail cameras, 3) 20 random cameras, 4) 30 random cameras, 5) 40 random cameras. Right column - 6) 20 on-trail cameras, 7) 30 on-trail cameras, 8) 40 on-trail cameras, 9) 50 on-trail cameras, 10) 60 on-trail cameras.

Appendix 3.B. Abundance simulation results

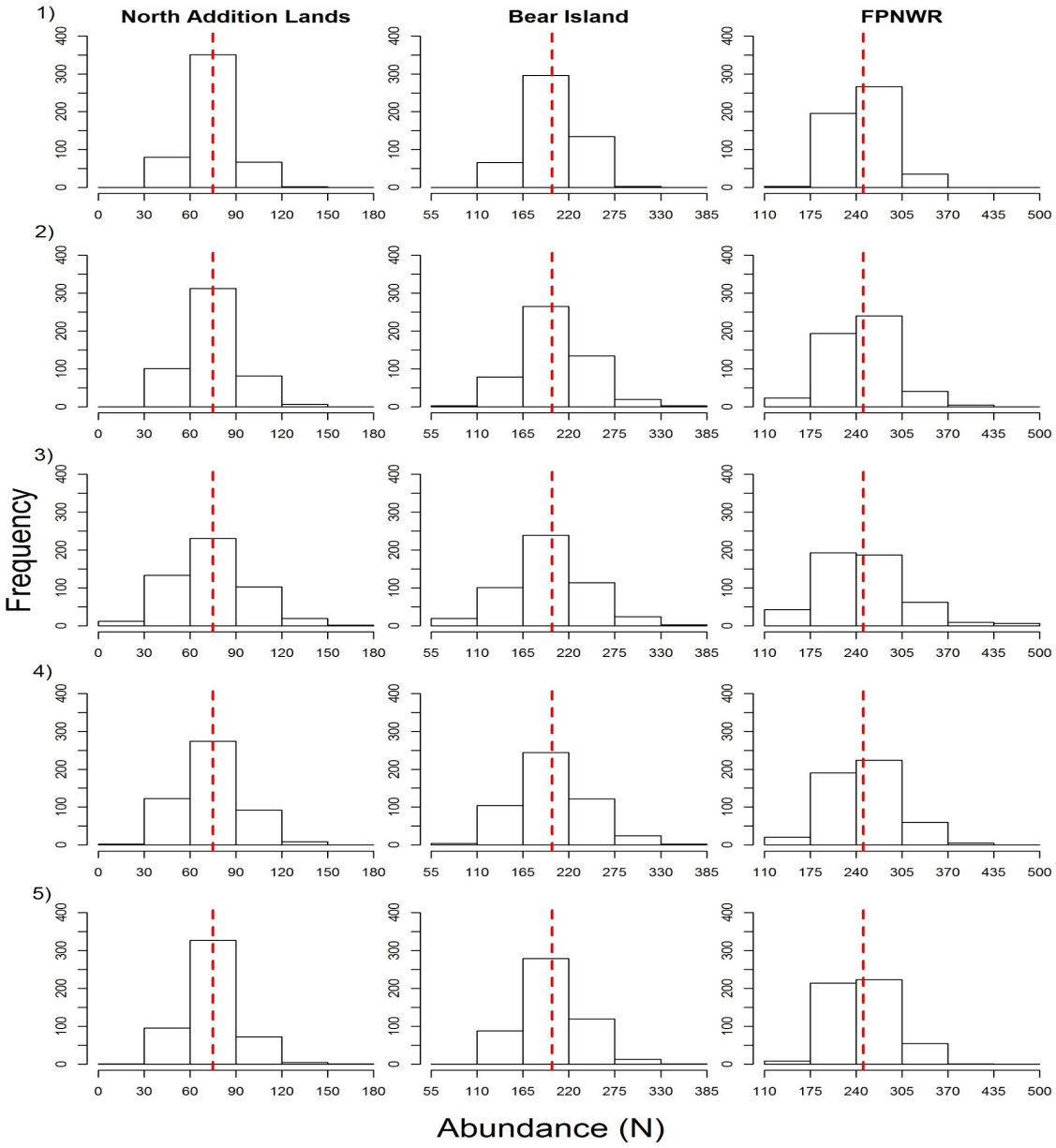

Figure 3.B1. Abundance estimates from 500 simulated datasets for camera designs for North Addition Lands, Bear Island, and Florida Panther National Wildlife Refuge (FPNWR): 1) status quo, 2) 40 paired on- and off-trail cameras, 3) 20 random cameras, 4) 30 random cameras, and 5) 40 random cameras. The dashed line indicates the value of abundance used to simulate the data.

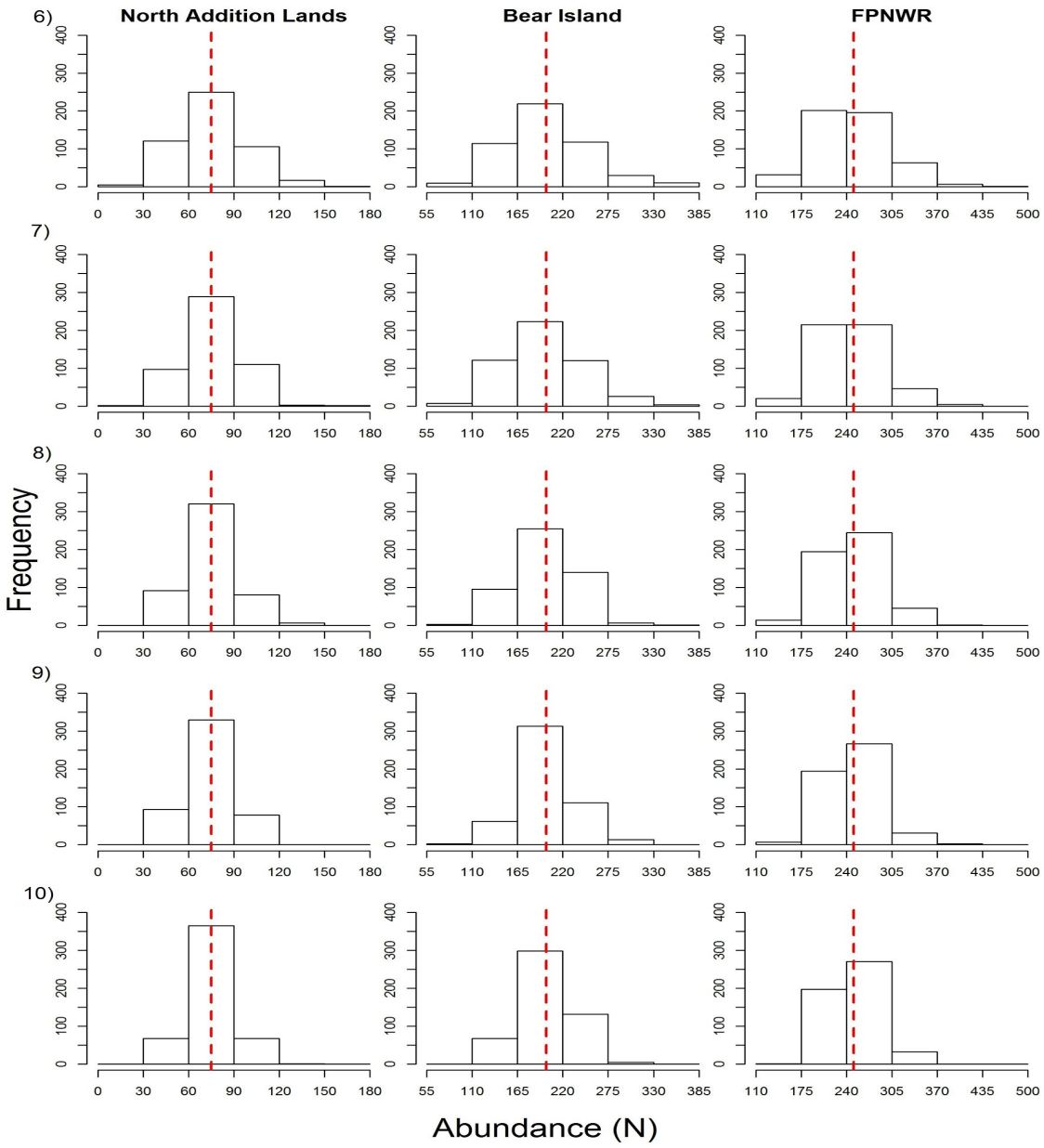

Figure 3.B2. Abundance estimates from 500 simulated datasets for camera designs for North Addition Lands, Bear Island, and Florida Panther National Wildlife Refuge (FPNWR): 6) 20 on-trail cameras, 7) 30 on-trail cameras, 8) 40 on-trail cameras, 9) 50 on-trail cameras, 10) 60 on-trail cameras. The dashed line indicates the value of abundance used to simulate the data.

CHAPTER 4

WHITE-TAILED DEER POPULATION VIABILITY FOLLOWING FLORIDA PANTHER RESTORATION IN THE BIG CYPRESS NATIONAL PRESERVE[3]

[3] Margenau, L. L. S., M. J. Cherry, K. V. Miller, E. P. Garrison, and R. B. Chandler. To be submitted to *Journal of Wildlife Management*

ABSTRACT

Successful large carnivore restoration depends on a viable prey base. South Florida, USA is home to the endangered Florida panther (*Puma concolor coryi*), whose population has been increasing since genetic reintroduction efforts began in 1995. The larger panther population coupled with changes in the predator community and disturbance regime have raised concerns over the population viability of the primary prey species, white-tailed deer (*Odocoileus virginianus*). We assessed deer population growth (λ) and sensitivity of λ in the northern management units of the Big Cypress National Preserve (BCNP) using vital rates and density estimates from pre- and post-panther genetic. Although we found that the deer population has declined since the panther restoration ($\lambda = 0.845$), our analysis indicates that the population was declining prior to the panther genetic restoration ($\lambda = 0.957$). For all scenarios, population growth was most sensitive to changes in adult female survival. Large increases in adult female survival are needed to stabilize population growth. Habitat and water management directed at improving adult survival should be considered to ward off future deer population declines. Formally accounting for the effects of increasing predator populations on prey dynamics should be incorporated in large carnivore restoration plans.

INTRODUCTION

The success of large carnivore restoration efforts depends on viable prey populations (Carbone and Gittleman 2002, Ripple et al. 2014, Wolf and Ripple 2016). Although it is generally assumed that the dynamics of native predator-prey populations are stable, novel environmental conditions resulting from anthropogenic disturbances can destabilize systems that persisted for thousands of years before human encroachment (Hebblewhite et al. 2005, Lovari et

al. 2009, Whittington et al. 2011). The effect of predation on prey population dynamics depends on predator and prey behaviors and demographic responses (Holling 1959, Brown et al. 1999, Preisser et al. 2005, Gaynor et al. 2019). In a highly dynamic ecosystem, predators may increase the probability of prey extinction resulting from disturbances by reducing prey population size and by inducing antipredator behaviors such as increased vigilance, increased grouping, decreased foraging, and altered movement patterns (Schoener et al. 2001, Gaynor et al. 2019, Commander et al. 2019).

The Big Cypress Basin in South Florida, USA is home to the last remaining population of the endangered Florida panther (*Puma concolor coryi*). By the 1920's panthers only existed in Central and South Florida. In 1967, they were listed as endangered under the US Endangered Species Act, yet the population continued to decline as their range contracted to a few areas in South Florida (Onorato et al. 2010). To restore genetic diversity and avoid inbreeding depression, a genetic reintroduction effort began in 1995, in which eight female Texas pumas (*P. c. stanleyana*) were released in Florida (Johnson et al. 2010). Following legal protection, and habitat and prey conservation, the Florida panther population has steadily increased to at least 200 individuals (USFWS 2008).

Prior to genetic reintroduction efforts, the small size of the panther population and an abundance of invasive wild pigs (*Sus scrofa*) resulted in a low panther predation rate on white-tailed deer (*Odocoileus virginianus*). During this time, wild pigs were the dominant prey of panthers (Maehr et al. 1990) and bobcats (*Lynx rufus*) were the primary predators of fawns and adult deer (Boulay 1992, Labisky and Boulay 1998). However, following panther restoration, and concomitant changes in the hydrology and hunting regulations, bobcat and wild pig abundances declined (Roberts and Crimmins 2010, Dorcas et al. 2012, Caudill et al. 2019) and

panther predation on deer increased (Maehr et al. 1990, McBride et al. 2008, McClintock et al. 2015, Caudill et al. 2019, van de Kerk et al. 2019, Bled et al. *In Review*). Additionally, black bear (*Ursus americanus*) populations increased, coyotes (*Canis latrans*) colonized the region, and invasive Burmese pythons (*Python bivittatus*) became established. All of these changes have reduced the abundance of alternative prey (Wilson et al. 2010, Dorcas et al. 2012, Telesco 2012, Humm et al. 2017, McCleery et al. 2015, Bragina et al. 2019).

Since the early 2000's, the deer population has declined in the southernmost units of the Big Cypress National Preserve (BCNP), while other units have experienced fluctuating densities (Garrison et al. 2011). These declines have coincided with shifts in the predator community and disturbance regime. Recently, South Florida has undergone major hydrological restoration efforts following the authorization of the Comprehensive Everglades Restoration Plan (Sklar et al. 2005, Wiederholt et al. 2020). With the predicted increase in water levels, the deer population may experience negative effects through reduced survival and recruitment and alterations in habitat use (Loveless 1959, Labisky et al. 1999, MacDonald-Beyers and Labisky 2005, Abernathy et al. 2019, Paudel et al. 2020). These effects may be compounded by the low population density, low productivity, high fawn mortality, and small body size in the South Florida deer population (Harlow and Jones 1965, Richter and Labisky 1985, Labisky et al. 1991, Boulay 1992, Heffelfinger 2011). Low productivity and high fawn mortality (Labisky et al. 1991) raise concerns about the capacity of the South Florida deer population to sustain the increased predation rate resulting from the panther recovery.

Demographic models are the most widely used tool for predicting how populations will respond to management actions and uncertain environmental conditions (Caswell 2001). These models are critical components of population viability analysis (PVA) in which estimates of

survival and reproduction combined with information about environmental and demographic stochasticity are used to forecast population growth rates and extinction risk (Boyce 1992, Pascual et al. 1997, Bessinger and McCullough 2002, Morris and Doak 2002).

Our goal was to assess how white-tailed deer population viability in the northern management units of the BCNP. Our first objective was to compare predictions of population growth using vital rates and density estimates from pre- and post-panther genetic restoration. Our second objective was to evaluate the sensitivity and elasticity of population growth rate to changes in vital rates. Finally, we determined the vital rate thresholds required to achieve population stability.

STUDY AREA

We focused our analysis on the deer population in a 460-km^2 region of BCNP, north of I-75, which contained the Bear Island management unit and the northern portion of the Addition Unit. The interactive effects of hydrologic, pyrogenic, and anthropogenic disturbance regimes largely defined the area. The area was characterized by distinct wet and dry hydrological seasons with high variation in annual precipitation varying across the landscape (Duever et al. 1986, Obeysekera et al. 1999). The topography consisted of minimal relief with slight ridges delineating relatively flat basins interspersed with depressions that can retain standing water throughout the dry season (Obeysekera et al. 1999, Duever et al. 1986). Seasonal fluctuations in hydrology and fire coupled with low soil fertility influence the distribution and succession of plant communities thereby altering resource availability for wildlife communities (Klein et al. 1970, Duever 1984, Duever 2005). This area contained a mosaic of vegetation communities ranging from upland pine and cypress forests to freshwater marshes intermixed with hammock

forests and wet prairies (McPherson 1974, Duever et al. 1986). Year-round public access was permitted, although off-road vehicle access was limited in Bear Island and restricted in Addition Lands. Antlerless harvest has been prohibited within BCNP since its creation in 1974, with additional antler point restrictions implemented to further protect the fawn age class and females (Schortemeyer et al. 1991, Garrison et al. 2011).

METHODS

Model Structure and Development

Deterministic Stage-structured Population Model

To examine how deer population dynamics have changed over the last 25 years, we used a post-reproductive female-based Lefkovitch matrix model (Lefkovitch 1965, Caswell 2001) with a 1-year time step:

$$\mathbf{A} = \begin{bmatrix} f_1 & f_2 & f_3 \\ s_1 & 0 & 0 \\ 0 & s_2 & s_3 \end{bmatrix} = \begin{bmatrix} f_{\text{fawn}} & f_{\text{yearling}} & f_{\text{adult}} \\ s_{\text{fawn}} & 0 & 0 \\ 0 & s_{\text{yearling}} & s_{\text{adult}} \end{bmatrix}$$

The model was composed of 3 stages, which corresponded to fawns (0 – 1 yr old), yearlings (1 – 2 yrs old), and adults (>2 yrs old) and included elements of fecundity (*f*) and survival (*s*) for each stage. We defined s_1 and s_2 as the probability of surviving and transitioning to the next stage during time *t*, while s_3 was the probability of surviving and remaining in the adult stage. We defined fecundity (*f*) as the expected number of female offspring born at time *t* to each female alive at time *t* – 1. Fecundity therefore depended on stage-specific survival probabilities (*s*), pregnancy probabilities (p, i.e., the probability a female become pregnant after mating), conditional birth rates (b, i.e., productivity conditional on being pregnant), and the fetal sex ratio

(r, i.e., the proportion of offspring that are female). For example, for the adult stage class, the number of offspring born to each individual is

$$f_3 = s_3 \times p_3 \times b_3 \times r.$$

Using the matrix (**A**), we projected the deterministic change in population size using the linear time-invariant equation: $\mathbf{n}_{t+1} = \mathbf{A} \times \mathbf{n}_t$, where the vector $\mathbf{n}_t$ is the number of individuals in each stage at time *t*.

$$\begin{bmatrix} n_1 \\ n_2 \\ n_3 \end{bmatrix}_{(t+1)} = \begin{bmatrix} f_1 & f_2 & f_3 \\ s_1 & 0 & 0 \\ 0 & s_2 & s_3 \end{bmatrix} \times \begin{bmatrix} n_1 \\ n_2 \\ n_3 \end{bmatrix}_{(t)}$$

Total abundance is given by: $N_t = n_{1,t} + n_{2,t} + n_{3,t}$. We referenced each vital rate (a_{ij}) by its i^{th} row location and j^{th} column in **A**. Using **A**, we calculated three significant population demographics. The dominant eigenvalue of **A** provided the population growth rate (λ), the right eigenvector of **A** described the stable stage distribution (SSD, proportion of the population in each stage), and the left eigenvector of **A** reported the reproductive value (RV, expected relative contribution of a female in a given stage to future population growth).

Using the projection matrix, we calculated the sensitivity and elasticity of λ to changes in vital rates. Sensitivity analysis describes the rate of change in λ when altering one vital rate while holding all other rates constant (Caswell 1978). By simulating the same perturbation for each stage successively, we can compare the relative effect on the different stages. The sensitivity of λ to changes in a vital rate (a_{ij}) is proportional to the product of the i^{th} reproductive value and the j^{th} stable stage distribution. Because survival probabilities, which are bounded [0,1], and fecundities, which are bounded [0, 2], are measured on different scales, we also explored the elasticity of λ to changes in a vital rate (a_{ij}) as it considers proportional, rather than absolute, responses on the logarithmic scale (de Kroon 1986). For comparison to previous

research (Chitwood et al. 2015, Peters et al. 2020), we made 5 simplifying assumptions: density independence, geographic closure, homogeneity of parameters among individuals within each stage, and no reproductive senescence. The northern units of BCNP comprise a small portion of an extensive network of public lands expanding over 12,500 km^2 in South Florida. These protected areas abut vast urbanized and agricultural areas leading to the use of high fencing along southern, eastern, and western boundaries to maintain the human-wildlife interface, thereby justifying our assumption of geographic closure. Additionally, our models assumed no senescence relative to fecundity, which is consistent with free-ranging white-tailed deer (DelGiudice et al. 2007).

Stochastic Stage-structured Population Model

To investigate how stochastic environmental and demographic variability in vital rates affect population growth, we adjusted the stage-structured model such that $n_{1,t+1}$ was a stochastic outcome of a multinomial process describing the probabilities each stage gave birth to 0, 1, or 2 female offspring. We allowed all vital rates (survival, pregnancy rate, conditional productivity, and fetal sex ratio) to vary over time according to $Normal(\mu, \sigma)$, where μ is the mean vital rate and σ is the standard deviation of the vital rate. The number of fawns born into the population ($n_{1,t+1}$) is the sum of singletons and twins born to individuals in each of the three stages:

$$n_{1,t+1} \sim \sum_{k=2}^{3} Multinomial\left(n_{1,t}, \left\{\pi_{1,1,t},\ \pi_{1,2,t}, \pi_{1,3,t}\right\}\right)$$

$$+ \sum_{k=2}^{3} Multinomial(n_{2,t}, \{\pi_{2,1,t},\ \pi_{2,2,t}, \pi_{2,3,t}\})$$

$$+ \sum_{k=2}^{3} Multinomial(n_{3,t}, \{\pi_{3,1}, t,\ \pi_{3,2,t}, \pi_{3,3,t}\})$$

The multinomial probabilities, which must sum to 1, depend on litter size (l) and stage-specific survival and fecundity. For example, for the fawn stage class, the probability of one female offspring is

$$\pi_{1,2,t} = s_{1,\mathrm{t},} \times l_1 \times p_{1,\mathrm{t}} \times r_t$$

and the probability of two female offspring is

$$\pi_{1,3,t} = s_{1,\mathrm{t}} \times l_2 \times p_{1,\mathrm{t}} \times r_t,$$

where l_1 and l_2 are the probabilities of having a litter size of one and two respectively. Consequently, the probability of having no female offspring is

$$\pi_{1,1,t} = 1 - \pi_{1,2,t} - \pi_{1,3,t}.$$

The relationship between litter size (L) and productivity at parturition (f) from the deterministic model is

$$f = (1 \times l_1) + (2 \times l_2).$$

The abundance of yearlings ($n_{2,t+1}$) is a binomial outcome dependent on the survival of fawns from the previous time period:

$$n_{2,t+1} \sim \mathrm{Binomial}(n_{1,t},\ s_{1,\mathrm{t}})$$

The abundance of adults ($n_{3,t+1}$) is the sum of two binomials:

$$n_{3,t+1} \sim \mathrm{Binomial}\left(n_{2,t},\ s_{2,\mathrm{t}}\right) + \mathrm{Binomial}(n_{3,t},\ s_{3,\mathrm{t}}).$$

For the stochastic model, we additionally assumed that 1) environmental conditions in successive years were uncorrelated; 2) productivity and survival rates were uncorrelated; and 3) no catastrophic events occurred.

Model Parameterization

Pre-panther Restoration Model Parameterization

We distinguished pre-panther restoration as the time leading up to the panther genetic restoration program initiation in 1995 and post-panther restoration as years following. We parameterized the pre-panther genetic restoration population matrix using vital rates derived from literature on white-tailed deer populations in South Florida, and specifically the BCNP and the ENP when available (Table 4.1, Figure 4.1, Appendix 4.A). We used weighted averages for each survival probability to account for the sample size associated with each parameter estimate within the literature. We used a fawn survival probability of 26% (Boulay 1992, Labisky et al. 1995, Smith et. al 1996), a yearling female survival of 88% (Labisky et al. 1995, Smith et al. 1996), and an adult female survival of 81% (Labisky et al. 1995, Smith et al. 1996). We averaged estimates of stage-specific conditional productivity rates from several ecoregions in Florida to arrive at values of 1.0 fetuses/pregnant fawn (Garrison et al. 2021), 1.23 fetuses/pregnant yearling (Ritcher and Labisky 1985, Garrison et al. 2021), and 1.32 fetuses/pregnant adult (Harlow 1972, Ritcher and Labisky 1985, McCown et al. 1991, Fleming et al. 1994, Garrison et al. 2021). We used pregnancy probabilities of 14% for fawns, 93% for yearlings, and 92% for adults (Ritcher and Labisky 1985). We set the fetal sex ratio to 1:1 (Labisky et al. 1995). We estimated initial population size ($N_0 = 1{,}293$) for fawns ($n_{1,0} = 155$), yearlings ($n_{2,0} = 168$), and adults ($n_{3,0} = 970$) for the pre-panther restoration model using historical deer density (3.65

deer/km^2) and sex ratio (77% female) estimates (Labisky et al. 1995) and an estimated female stage structure based on vital rates extrapolated to the 460 km^2 study area.

Post-panther Restoration Model Parameterization

We parameterized the post-panther genetic restoration population matrix using a combination of vital rates from previous literature and more recent survival rates derived from camera and radio-telemetry data collected in BCNP in 2015–2018 (Table 4.1, Figure 4.1, Appendix 4.A). For fecundity, we used vital rates similar to the pre-panther restoration model, with the exception of pregnancy probabilities. We used updated pregnancy probabilities of 12% for fawns, 95% for yearlings, and 94% for adults (Garrison et al. 2021). We used a fawn survival probability of 28% by averaging survival estimates from 2015 (42.5%) and 2016 (13.2%) derived from capture-recapture data (Chandler et al. 2018). We used the mean annual survival (70%) of GPS-collared female deer in BCNP from 2015–2018 to describe both yearling and adult survival (Bled et al. *In Review*). We estimated initial population size ($N_0 = 1{,}426$) for fawns ($n_{1,0} = 171$), yearlings ($n_{2,0}$ = 185), and adults ($n_{3,0}$ = 1070) for the post-panther restoration model using female density estimates for Bear Island (Margenau et al. *In Review*) and estimated female age structure based on fecundity and survival rates extrapolated to a 460 km^2 study area.

Population Modeling

We parameterized the deterministic stage-based population models using both pre-panther genetic restoration and post-panther genetic restoration vital rates. To compare how deer population dynamics have changed over the last 25 years, we assessed the population growth rate

(λ) and sensitivity and elasticity of λ to changes in vital rates for each population matrix. We parameterized the stochastic stage-based population model using the pre- and post-panther genetic restoration vital rates. For the stochastic model, we conducted 10,000 simulations in which we projected annual population growth for 10 years. For the time-varying vital rates, we used $\sigma = 0.05$ for all stage-specific survival probabilities and productivities for the yearling and survival stages and used $\sigma = 0.02$ for the fetal sex ratio, fawn productivity, and stage-specific pregnancy probabilities.

Using the post-panther restoration deterministic model, we examined λ across a range of fetal sex ratios and stage-specific fecundities, survivals, and pregnancy probabilities to determine the threshold at which $\lambda \geq 1$, while keeping all other vital rates constant. Finally, we expanded on the previous analysis by examining the response of λ to a range fawn survival, adult survival, and adult productivity to current and potential future population growth under various management goals. All reported abundance intervals represent 2.5 and 97.5 percentiles of the forecast distributions.

RESULTS

The deterministic population model for the pre-panther restoration scenario yielded a population growth rate of $\lambda = 0.957$, with reproductive values of 1.000, 3.61, and 3.35 for the fawn, yearling, and adult stages respectively. The stable stage distribution was 34% fawns, 9% yearlings, and 56% adults. Incorporating environmental and demographic stochasticity into the population model resulted in a mean population growth rate of $\lambda = 0.967$ (95% CI: 0.864-1.068). Abundance was projected to be N_5 = 1081 (830-1369) females and N_{10} = 771 (529-1070) females (Figure 2). Using updated estimates of survival, pregnancy probability, and density

following 25 years of Florida panther recovery, the deterministic model projected the population to decline with a growth rate of $\lambda = 0.845$ and associated reproductive values of 1.000, 2.959, and 2.989 for the fawn, yearling, and adult stages, respectively. The stable stage distribution was similar to the pre-panther restoration model with 33% fawns, 11% yearlings, and 55% adults. Incorporating environmental and demographic stochasticity into this population model resulted in a mean population growth rate of $\lambda = 0.853$ (95% CI: 0.756-0.950). Abundance was forecasted to be N_5 = 749 (574-946) females and N_{10} = 281 (185-402) females (Figure 4.2).

The sensitivity of λ to vital rates was similar between the pre- and post-panther genetic restoration model (Table 4.2). Adult survival had the strongest influence on λ, followed by fawn survival and adult fecundity. Fawn fecundity had the weakest influence on λ. Elasticity was similar to sensitivity.

Only two vital rates in the evaluated ranges resulted in stable and/or increasing population growth rates (Figures 4.3–4.4). Increasing fawn survival to 68% or increasing adult survival to 88% would yield a stable population when maintaining all other vital rates constant. However, the three-way interaction between adult survival, fawn survival, and adult productivity indicated that there are several options for achieving $\lambda \geq 1$ (Figure 4.5). A stable population growth rate could be achieved while maintaining an adult survival to 70% by increasing fawn survival to at least 60% and an adult productivity to 1.55. Alternatively, stability could be met with adult survival at 70%, adult productivity at 1.30, and fawn survival at 68%. Maintaining the current fawn survival of 28% resulted in $\lambda \geq 1$ only when adult survival was at least 86% and adult productivity was 1.55. Alternatively, stability could be met with fawn survival at 28%, adult survival at 88%, and adult productivity at 1.30.

DISCUSSION

Our study suggest that large predator restoration can reduce the viability of prey populations. Although predator restoration plans often list prey viability as a key objective, quantitative assessments of the effects of increasing predator populations on the prey growth is rare (US Seal and Lacy 1994, USFWS 2008, Marshall et al. 2016). Theory suggests that predator restoration should not result in extinction of prey populations because of cyclic dynamics arising from reduced predator growth following periods of low prey densities (Lotka 1920, Volterra 1926, Rosenzweig and Macarthur 1963). Additionally, when two or more prey species exist within a system, predators may exhibit prey switching thereby preventing either prey species from being drastically reduced or overabundant (Murdoch 1969). However, large-scale environmental change resulting from anthropogenic disturbances may alter predictions of theoretical models (Hunter 1998, Novaro et al. 2000, Boulanger et al. 2011, Latham et al. 2011).

Although we found white-tailed deer population growth rates have declined since the panther restoration, our estimates of λ suggest the deer population was already declining prior to the initiation of the restoration efforts in 1995. The recent decrease in deer population growth rates appears to be the result of increased adult mortality rates (Bled et al. *In Review*). Nonetheless, the fact that the deer population was predicted to decline before the panther restoration suggests that other factors such as hydrology, bobcat predation, poor soil fertility, and hunting regulations were limiting the population. While our results do not support the conclusion that panthers have caused the deer population declines, it does appear that the shifting predator community has sped up the declines, which could threaten the long-term viability of the panther population unless management can intervene to bolster the prey population.

Population growth rate was the most sensitive to changes in adult female survival, which is consistent with other studies of large ungulates (Gaillard et al. 1998, Chitwood et al. 2015, Peters et al. 2020). In general, adult survival is a better fitness surrogate than reproduction for slow reproducing species (Crone 2001, van de Kerk et al. 2013). Although sensitivity analysis is a valuable analytical tool, it is important to note the limitations when assessing implications of management decisions. First, while these analyses indicate which vital rate to manipulate to produce the quickest population recovery, they do not necessarily indicate which vital rate is causing the decline (Bessinger and Westphal 1998). Second, change in one demographic rate or the variability surrounding the rate can alter the values and qualitative ranking of a sensitivity analysis (Mills et al. 1999). Thus, uncertainty surrounding vital rates can alter the projected performance of a management decision. Third, rarely do management actions alter vital rates by the amounts determined by these analyses (Mills et al. 1999). Lastly, negative correlation exists between vital rate variances and elasticity, such that vital rates with higher variances typically have low elasticity (Pfister 1998). This suggests that rates with low elasticity changing over wide ranges could potentially alter growth rate as much as the vital rate ranked as most influential based on elasticity alone (Gaillard et al. 1998). These limitations emphasize the need to account for all vital rates when assessing management decisions and to select management actions that have the potential to impact both survival and fecundity. We addressed the issues of parameter uncertainty by evaluating a range of simultaneous proportional changes in vital rates.

Using results from our PVA and previous studies of deer survival and fecundity in South Florida, we can predict the effects of management actions on population growth rate and abundance. Restoration of the historical hydrological regime within the Greater Everglades Ecosystem will likely lead to increasing water levels, which is expected to negatively impact

deer mobility, survival, foraging, and productivity at multiple life-stages by altering resource availability and selection and increasing predator-prey interactions on upland refugia (Fleming et al. 1994, MacDonald-Beyers & Labisky 2005, Chandler et al. 2018, Bled et al. *In Review*). In addition to hydrological restoration, managers are attempting to restore the pyrogenic regime with shifts in the intensity and frequency of prescribed fire and the spatial extent of wildfire burns thereby reversing decades of fire suppression (Cherry et al. 2018, Noss 2018). Habitat management through the use of prescribed fire improves forage availability and nutrient quality, positively affecting productivity (Lewis et al. 1982, Carlson et al. 1993). Additionally, recently burned areas decrease the available cover, hindering the stalk-and-ambush panther, which may reduce perceived predation risk and increase survival in deer (Cherry et al. 2018). The shifting predator community with increases in panther, black bear, coyote, and python abundances have decreased the mammalian prey community during the past 25 years through increases in mortality and altering of foraging behaviors which may lead to decreases in productivity (Beason 1974, Dorcas et al. 2012, McCleery et al. 2015, Bragina et al. 2019, Caudill et al. 2019).

Several limitations of the data available to us should be considered when interpreting our results. First, our models used local and regional estimates of vital rates from a variety of sampling methods, each with intrinsic sources of error. The survival estimates used to parameterize the pre-panther restoration model came from studies conducted in the southern units of BCNP and Everglades National Park, which have seen dramatic declines in estimated deer abundances from harvested and aerial surveys in recent years (Garrison et al. 2011). These regions are dominated by wet prairies with extended hydroperiods that are further exacerbated by the increasing number and duration of high-water events known to decrease survival (MacDonald-Beyers and Labisky 2005, Garrison et al. 2011, Bled et al. *In Review*). However,

the northern units of BCNP are comprised on larger extents of upland forests and shrub areas, which may alter predator-prey interactions and the resulting deer survival probabilities. Second, we parameterized the post-panther restoration model using a mean annual adult female survival estimate of 0.70 across four years (Bled et al. *In Review*). However, yearly female survival probabilities were shown to increase from 0.60 (0.51-0.69) in 2015 to 0.84 (0.76-0.90) by 2018, showcasing the high interannual variability in adult survival within the system. Lastly, the post-panther restoration model would benefit from updated fecundity estimates from South Florida to accompany the recently updated survival and pregnancy rate estimates. In Florida, current breeding chronology estimates are generated using hunter harvested females, which excludes BCNP where female harvest is prohibited (Garrison et al. 2021).

Our modeling results should be interpreted with caution and extrapolated to other deer populations carefully because they are based on several assumptions we were unable to test. First, we projected population growth assuming density independence. Theory predicts that density-dependence should help regulate predator-prey dynamics because predators should decline in response to decreasing prey, thereby providing an opportunity for prey to recover (Ballard and Van Ballenberghe 1997, Rosenzweig and Macarthur 1963). However, in South Florida, theoretical models may not describe the complexity of predation patterns, prey population dynamics, and abiotic factors impacting both predator and prey. Deer-panther dynamics are a singular interaction within the larger, complex ecological web. With predicted declines in deer availability, panthers may sustain population numbers by implementing prey switching and may be further subsidized by domesticate livestock (Jacobs and Main 2015, Caudill et al. 2019). Additionally, abiotic factors, such as intermittent and extensive floods and droughts, alter spatio-temporal patterns of predator-prey interactions potentially increasing

predation pressure (MacDonald-Beyers and Labisky 2005, Crawford 2017). The stochastic environment of South Florida coupled with poor soil fertility and low forage quality may ultimately be limiting the deer herd (Shea et. al 1992, DeYoung et al. 2019). Further exploration into the degree to which density-dependent and density-independent factors affect the deer population in this system is warranted (Bowyer et al. 2005, Pierce et al. 2012, Sora-Díaz et al. 2017).

Within the stochastic population model, we assumed environmental conditions in successive years were uncorrelated. However, climate change is expected to accelerate the rate of increase of spatial and temporal autocorrelation, having strong implications for community structure and persistence within dynamic ecosystems (van der Valk 2015, Cherry and Barton 2017, Di Cecco and Gouhier 2018). Additionally, ours models do not account for deer demographic responses to changes in interannual water-level fluctuations and catastrophic events, such as hurricanes (Emanuel 2005, Elsner 2006, van der Valk et al. 2015, Abernathy et. al 2019). These environmental conditions, especially during the early developmental stages, can have long-term consequences for life-history traits (Beckerman et al. 2002, Douhard et al. 2014). Finally, we assumed fecundity and survival rates were uncorrelated. Understanding the effects of this correlation on population growth can be explored through theoretical simulations. However, evaluating the strength of this correlation within the BCNP deer population would be logistically challenging since it would require a large sample size of individuals with known fates and birth rates.

As a final consideration, stochastic stage-structured population models do not consider spatial factors affecting population growth rates. Spatially explicit approaches to the study of demography may be especially important within dynamic ecosystems, such as South Florida, in

which vital rates and habitat selection decisions can depend strongly on where an individual occurs in the landscape. Linking population dynamics with landscape structure provides a more sensitive approach to demographic modeling for population viability (Dunning et al. 1995, Gurevitch et al. 2016, Royle et al. 2017). However, spatially explicit models have immense data requirements, which can make development challenging (Dunning et al. 1995). Future endeavors should explore the use of spatially explicit agent-based models (DeAngelis and Gross 1992, Grimm 1999) or integrated population models (Chandler and Clark 2014) to assess trends and drivers of white-tailed deer population dynamics in BCNP through the joint analysis of data on population size and data on demographic parameters.

The current panther recovery goal is to achieve long-term viability through a strategy that maintains the viability of the current population in South Florida and expands the breeding portion of the population to areas north of the Caloosahatchee River. Our results suggest that future research should assess prey population viability in areas north of the Caloosahatchee River prior to the expansion of the Florida panther range. The analysis of prey population viability prior to large carnivore restoration efforts would indicate if prey management is likely to be necessary and would allow ample time to plan and implement management actions if deemed necessary.

MANAGEMENT IMPLICATIONS

Our results suggest the deer population is likely to decline in the northern management units of BCNP, similar to the declines observed in the southern units. Habitat and water management directed at improving adult survival should be considered to ward off these declines. The use of prescribed fire and invasive vegetation management could reduce

concealment cover, increase predator detection, and potentially improve deer survival. In the event that habitat management is not effective at increasing survival, managers should consider more drastic actions such as prey supplementation to alleviate predation pressure. Supplementation of the prey community through stocking programs could enhance prey abundances, potentially alleviating predation pressure on deer; however, reintroducing non-native species such as wild hogs would be highly controversial as it could negatively affect plant communities and possibly increase disease transmission. Additionally, although wildlife populations are only one consideration influencing decisions about water management in South Florida, adding more water to the northern units of BCNP, especially during the fawning season, would likely negatively affect the deer population and the predators it supports.

LITERATURE CITED

Abernathy, H. N., D. A. Crawford, E. P. Garrison, R. B. Chandler, M. L. Conner, K. V. Miller, and M. J. Cherry. 2019. Deer movement and resource selection during Hurricane Irma: implications for extreme climatic events and wildlife. Proceedings of the Royal Society B 286: 20192230. DOI: 10.1098/rspb.2019.2230.

Ballard, W. B., and V. Van Ballenberghe. 1997. Predator-prey relationships. Pages 247–273 *in* A. W. Frazmann and C. C. Schwartz, editors. Ecology and management of the North American moose. Smithsonian Institution, Washington, D.C., USA.

Beasom, S. L. 1974. Relationship between predator removal and white-tailed deer net productivity. Journal of Wildlife Management. 38:854–859.

Beckerman, A. T. G. Benton, E. Ranta, V. Kaitala, and P. Lunderberg. 2002. Population dynamics consequences of delayed life-history effects. Trends in Ecology and Evolution 17:263–269.

Bessinger, S. R., and D. R. McCullough. 2002. Population viability analysis. University of Chicago Press, Chicago, Illinois, USA.

Bessinger, S. R., and M. I. Westphal. 1998. On the use of demographic models of population viability in endangered species management. Journal of Wildlife Management 62:821–841.

Bled, F., M. J. Cherry, E. P. Garrison, K. V. Miller, L. M. Conner, H. N. Abernathy, W. H. Ellsworth, L. L. S. Margenau, D. A. Crawford, K. N. Engebretsen, B. D. Kelly, D. B. Shindle, and R. B. Chandler. 2021. Impacts of large carnivore restoration on prey species with high economic and cultural value: A case study of Florida panther and white-tailed deer. Manuscript in review.

Boulanger, J., A. Gunn, J. Adamczewski, and B. Croft. 2011. A data-driven demographic model to explore the decline of the Bathurst caribou herd. Journal of Wildlife Management 75: 883–896.

Boulay, M.C. 1992. Mortality and recruitment of white-tailed deer fawns in the wet prairie/tree island habitat of the Everglades. Thesis, University of Florida, Gainesville, Florida, USA.

Bowyer, R. T., D. K. Person, and B. M. Pierce. 2005. Detecting top-down versus bottom-up regulation by large carnivores: Implications for conservation of biodiversity. Pages 342–361 *in* J.C. Ray, K. H. Redford, R. S. Steneck, and J. Berger, editors. Large carnivores and the conservation of biodiversity. Island Press, Washington, D.C, USA.

Boyce, M. S. 1992. Population viability analysis. Annual Review of Ecology and Systematics 23:481–506.

Bragina, E. V., R. Kays, A. Hody, C. E. Moorman, C. S. Deperno, and L. S. Mills. 2019. Effects on white-tailed deer following eastern coyote colonization. Journal of Wildlife Management 83:916–924.

Brown, J. S., J. W. Laundre, and M. Gurung. 1999. The ecology of fear: Optimal foraging, game theory, and trophic interactions. Journal of Mammalogy 80:385–399.

Carbone, C., and J. L. Gittleman. 2002. A common rule for the scaling of carnivore density. Science 295:2273–2276.

Carlson, P. C., G. W. Tanner, J. M. Wood, and S. R. Humphrey. 1993. Fire in Key deer habitat improves browse, prevents succession, and preserves endemic herbs. Journal of Wildlife Management 57:914–928.

Caswell, H. 1978. A general formula for the sensitivity of population growth rate to changes in life history parameters. Theoretical Population Biology 14:215–230.

Caswell, H. 2001. Matrix population models: Construction, analysis, and interpretation (2nd ed.). Sinauer Associates Inc, Sunderland, Massachusetts, USA.

Caudill, G., D. P. Onorato, M. W. Cunningham, D. Caudill, E. H. Leone, L. M. Smith, and D. Jansen. 2019. Temporal trends in Florida panther food habits. Human-Wildlife Interactions 13:87–97.

Chandler, R. B., and J. D. Clark. 2014. Spatially explicit integrated population models. Methods in Ecology and Evolution 5:1351–1360.

Chandler, R. B, K. Engebretsen, M. J. Cherry, E. P. Garrison, and K. V. Miller. 2017. Estimating recruitment from capture-recapture data by modeling spatio-temporal variation in birth and age-specific survival rates. Methods in Ecology and Evolution 9:2115–2130.

Cherry, M. J., and B. T. Barton. 2017. Effects of wind on predator-prey interactions. Food Webs 13:92–97.

Cherry, M. J., R. B. Chandler, E. P. Garrison, D. A. Crawford, B. D. Kelly, D. B. Shindle, K. G. Godsea, K. V. Miller, and L. M. Conner. 2018. Wildfire affects space use and movement of white-tailed deer in a tropical pyric landscape. Forest Ecology and Management 409:161–169.

Chitwood, M. C., M. A. Lashley, J. C. Kilgo, C. E. Moorman, and C. S. DePerno. 2015. White-tailed deer population dynamics and adult female survival in the presence of a novel predator. Journal of Wildlife Management 79:211–219.

Commander, C. J. C., and J. W. Wilson. 2019. Not all disturbances are created equal: Disturbance magnitude affects predator-prey populations more than disturbance frequency. Oikos 129:1–12.

Crawford, D. A. 2017. Behavioral and spatial ecology of white-tailed deer in the Big Cypress Basin of Florida. Thesis, University of Georgia, Athens, Georgia, USA.

Crone, E. E. 2001. Is survivorship a better fitness surrogate than fecundity? Evolution 55:2611–2614.

de Kroon, H., A. Plaisier, J. van Goenendael, and H. Caswell. 1986. Elasticity: the relative contribution of demographic parameters to population growth rate. Ecology 67:1427–1431.

DeAngelis, D. L., and L. J. Gross (eds.). 1992. Individual-based models and approaches in

ecology: populations, communities, and ecosystems. Chapman and Hall, New York, New York, USA.

DelGiudice, G. D., M. S. Lenarz, and M. C. Powell. 2007. Age-specific fertility and fecundity in northern free-ranging white-tailed deer: Evidence for reproductive senescence? Journal of Mammalogy 88:427–437.

DeYoung, C. A., T. E. Fulbright, D. G. Hewitt, D. B. Webster, and D. A. Draeger. 2019. Linking white-tailed deer density, nutrition, and vegetation in a stochastic environment. Wildlife Monographs 202:1–63.

Di Cecco, G. J., and T. C. Gouhier. 2018. Increased spatial and temporal autocorrelation of temperature under climate change. Scientific Reports 8:14850. DOI: 10.1038/s41598-018-33217-0.

Dorcas, M. E., J. D. Wilson, R. N. Reed, R. W. Snow, M. R. Rochford, M. A. Miller, W. E. Meshaka Jr., P. T. Andreadis, F. J. Mazzotti, C. M. Romagosa, and K. M. Hart. 2012. Severe mammal declines coincide with proliferation of invasive Burmese pythons in Everglades National Park. Proceedings of the National Academy of Science of the United States of America 109:2418–2422.

Douhard, M. F. Plard, J.-M. Gaillard, G. Capron, D. Delorme, F. Klein, P. Duncan, L. E. Loe, and C. Bonenfant. 2014. Fitness consequences of environmental conditions at different life stages in a long-lived vertebrate. Proceedings of the Royal Society B 281:20140276. DOI: 10.1098/rspb.2014.0276.

Duever, M. J. 1986. Environmental factors controlling plant communities of the Big Cypress Swamp. Pages 127–137 *in* P. J. Gleason, editor. Environments of South Florida: Past and present II. Miami Geological Society, Miami, Florida, USA.

Duever, M. J. 2005. Big Cypress regional ecosystem conceptual ecological model. Wetlands 25: 843–853.

Dunning, J. B. Jr., D. J. Stewart, B. J. Danielson, B. R. Noon, T. L. Root, R. H. Lamberson, and E. E. Stevens. Spatially explicit population models: current forms and future uses. Ecological Applications 5:3–11.

Elsner, J. B. 2006. Evidence in support of the climate change-Atlantic hurricane hypothesis. Geophysical Research Letters 33: L16705. DOI: 10.1029/2006GL026869.

Emanuel, K. 2005. Increasing destructiveness of tropical cyclones over the past 30 years. Nature 436:686–688.

Fleming, D. M., J. Schortemeyer, and J. Ault. 1994. Distribution, abundance and demography of white-tailed deer in the Everglades. Pages 494–503 *in* D. Jordan, editor. Proceedings of the Florida Panther Conference. U.S. Fish and Wildlife Service, Fort Myers, Florida, USA.

Gaillard, J.-M., M. Festa-Bianchet, and N. G. Yoccoz. 1998. Population dynamics of large herbivores: variable recruitment with constant adult survival. Trends in Ecology and Evolution 13:58–63.

Garrison, E., E. Leone, K. Smith, T. Bartareau, J. Bozzo, R. Sobczak, and D. Jansen. 2011. Analysis of hydrological impacts on white-tailed deer in the Stairsteps Unit, Big Cypress National Preserve. Fish and Wildlife Research Institute Technical Report US National Park Service, Gainesville, Florida, USA.

Garrison, E. P., E. H. Leone, L. S. Perrin, R. M. Peters, C. R. Morea, and F. Bled. 2021. White-tailed deer breeding chronology and productivity in Florida. Unpublished manuscript.

Gaynor, K. M., J. S. Brown, A. D. Middleton, M. E. Power, and J. S. Brashares. 2019. Landscape of fear: Spatial patterns of risk perception and response. Trends in Ecology and Evolution 34:355–368.

Grimm, V. 1999. Ten years of individual-based modelling in ecology: what have we learned and what could we learn in the future? Ecological Modelling 115:129–148.

Gurevitch, J., G. A. Fox, N. L. Fowler, and C. H. Graham. 2016. Landscape demography: population change and its drivers across spatial scales. Quarterly Review of Biology 91:459-485.

Harlow, R. F. 1972. Reproductive rates in white-tailed deer of Florida. Quarterly Journal of the Florida Academy of Sciences 35: 165–170.

Harlow, R. F., and F. K. Jones, editors. 1965. The white-tailed deer in Florida. Florida Game and Fresh Water Fish Commission Technical Bulletin No. 9, Tallahassee, Florida, USA.

Hebblewhite, M., C. A. White, C. G. Nietvelt, J. A. Mckenzie, T. E. Hurd, J. M. Fryxell, S. E. Bayley, and P. C. Paquet. 2005. Human activity mediates a trophic cascade caused by wolves. Ecology 86:2135–2144.

Heffelfinger, J. R. 2011. Taxonomy, evolutionary history, and distribution. Pages 3–39 *in* D. G. Hewitt, editor. Biology and management of white-tailed deer. CRC Press, Boca Raton, Florida, USA.

Holling, C. S. 1959. The components of predation as revealed by a study of small-mammal predation of the European pine sawfly. Canadian Entomologist 91:293–320.

Humm, J. M., J. W. McCown, B. K. Scheick, and J. D. Clark. 2017. Spatially explicit population estimates for black bears based on cluster sampling. Journal of Wildlife Management 81:1187–1201.

Hunter, L. T. B. 1998. The behavioural ecology of reintroduced lions and cheetahs in the Phinda Resource Preserve, KwaZulu-Natal, South Africa. Ph.D. Dissertation, University of Pretoria, South Africa.

Jacobs, C. E., and M. B. Main. 2015. A conservation-based approach to compensation for livestock depredation: The Florida panther case study. PLoS ONE 10:e0139203. DOI:10.1371/ journal.pone.0139203.

Johnson, H. E., L. S. Mills, T. R. Stephenson, and J. D. Wehausen. 2010. Population-specific vital rate contributions influence management of an endangered ungulate. Ecological Applications 20:1753–1765.

Johnson, W. E., D. P. Onorato, M. E. Roelke, E. D. Land, M. Cunningham, R. C. Belden, R. McBride, D. Jansen, M. Lotz, D. Shindle, and J. Howard. 2010. Genetic restoration of the Florida panther. Science 329:1641–1645.

Klein, H., W. J. Schneider, B. F. McPherson, and T. J. Buchanan. 1970. Some hydrologic and biologic aspects of the Big Cypress Swamp drainage area. United States Geological Survey, Washington, DC, USA.

Labisky, R. F., and M. C. Boulay. 1998. Behaviors of bobcats preying on white-tailed deer in the Everglades. American Midland Naturalist 139:275–281.

Labisky, R. F., M. C. Boulay, K. E. Miller, R. A. Sargent, Jr., and J. M. Zultowsky. 1995. Population ecology of white-tailed deer in Big Cypress National Preserve and Everglades National Park. Final Report to United States Department of Interior – National Park Service, Department of Wildlife Ecology and Conservation, University of Florida, Gainesville, Florida, USA.

Labisky, R. F., D. E. Fritzen, and J. C. Kilgo. 1991. Population ecology and management of white-tailed deer in the Osceola National Forest, Florida. Final Report to Florida Game and Fresh Water Fish Commission, Department of Wildlife and Range Sciences, University of Florida, Gainesville, Florida, USA.

Labisky, R. F., K. E. Miller, and C. S. Hartless. 1999. Effect of Hurricane Andrew on survival and movements of white-tailed deer in the Everglades. Journal of Wildlife Management 83:872–879.

Land, E. D. 1991. Big Cypress deer/panther relationships: deer mortality. Final Report to Florida Game and Fresh Water Fish Commission, Tallahassee, Florida, USA.

Latham, A. D. M., M. C. Latham, N. A. McCuthchen, and S. Boutin. 2011. Invading white-tailed deer change wolf-caribou dynamics in northeastern Alberta. Journal of Wildlife Management 75:204–212.

Lefkovitch, L. P. 1965. The study of population growth in organisms grouped by stages. Biometrics 21:1–18.

Lewis, C. E., H. E. Grelen, and G. E. Probasco. 1982. Prescribed burning in southern forest and rangeland improves forage and its use. Southern Journal of Applied Forestry 6:19–25.

Lotka, A. J. 1920. Evolution and irreversibility. Science Progress in the Twentieth Century 14:406–417.

Lovari, S., R. Boesi, I. Minder, N. Mucci, E. Randi, A. Dematteis, and S. B. Ale. 2009. Restoring a keystone predator may endanger a prey species in a human-altered ecosystem: the return of the snow leopard to Sagarmatha National Park. Animal Conservation 12:559–570.

Loveless, C. M. 1959. The Everglades deer herd life history and management. Florida Game and Fresh Water Fish Commission Technical Bulletin No. 6, Tallahassee, Florida, USA.

MacDonald-Beyers, K., and R. F. Labisky. 2005. Influence of flood waters on survival, reproduction, and habitat use of white-tailed deer in the Florida Everglades. Wetlands 25:659-666.

Maehr, D. S., R. C. Belden, E. D. Land, and L. Wilkins. 1990. Food habits of panthers in southwest Florida. Journal of Wildlife Management 54:420–423.

Margenau, L. L. S., M. J. Cherry, K. V. Miller, E. P. Garrison, and R. B. Chandler. 2021. Monitoring partially-marked populations using camera and telemetry data. Manuscript in review.

Marshall, K. N., A. C. Stier, J. F. Samhouri, R. P. Kelly, and E. J. Ward. 2016. Conservation challenges of predator recovery. Conservation Letters 9:70–78.

McBride, R. T., R. T. McBride, R. M. McBride, and C. E. McBride. 2008. Counting pumas by categorizing physical evidence. Southeastern Naturalist 7:381–400.

McCleery, R. A., A. Sovie, R. N. Reed, M. W. Cunningham, M. E. Hunter, and K. M. Hart. 2015. Marsh rabbit mortalities tie pythons to the precipitous decline of mammals in the Everglades. Proceedings of the Royal Society B 282:20150120.

McClintock, B. T., D. P. Onorato, and J. Martin. 2015. Endangered Florida panther population size determined from public reports of motor vehicle collision mortalities. Journal of Applied Ecology 52:893–901.

McCown, J. W., M. E. Roelke, D. J. Forrester, C. T. Moore, J. C. Roboski. 1991. Physiological evaluation of 2 white-tailed deer herds in southern Florida. Proceedings of the Annual Conference Southeastern Association of Fish and Wildlife Agencies 45:81–90.

McPherson, B. F. 1974. The Big Cypress Swamp. Environments of South Florida: present and past. Miami Geological Society, Miami, Florida, USA.

Mills, L. S., D. F. Doak, and M. J. Wisdom. 1999. Reliability of conservation actions based on elasticity analysis of matrix models. Conservation Biology 13:815–829.

Morris, W. F., and D. F. Doak. 2002. Quantitative conservation biology: Theory and practice of population viability analysis. Oxford University Press, Oxford, England.

Murdoch, W. W. 1969. Switching in general predators: experiments on predator specificity and stability of prey populations. Ecological Monographs 39:335–354.

Noss, R. F. 2018. Fire ecology of Florida and the Southeastern Coastal Plain. University Press of Florida, Gainesville, Florida, USA.

Novaro, A. J., M. C. Funes, and R. S. Walker. 2000. Ecological extinction of native prey of a carnivore assemblage in Argentine Patagonia. Biological Conservation 92:25–33.

Obeysekera, J., J. Browder, L. Hornung, and M. A. Harwell. 1999. The natural South Florida system I: Climate, geology, and hydrology. Urban Ecosystems 3:223–244.

Onorato, D. P., R. Belden, M. Cunningham, D. Land, R. McBride, and M. E. Roelke. 2010. Long-term research on the Florida panther (*Puma concolor coryi*): historical findings and future obstacles to population persistence. Pages 453–469 *in* D. Macdonald and A. Loveridge, editors. Biology and conservation of wild felids. Oxford University Press, Oxford, United Kingdom.

Pascual, M. A., P. Kareiva, and R. Hilborn. 1997. The influence of model structure on conclusions about the viability and harvesting of Serengeti Wildebeest. Conservation Biology 11:966–976.

Paudel, R. T. Van Lent, G. M. Naja, Y. Khare, R. Wiederholt, and S. E. Davis III. 2020. Assessing the hydrologic response of key restoration components to Everglades ecosystem. Journal of Water Resource Planning and Management 146:04020084. DOI: 10.1061/(ASCE)WR.1943-5452.0001283.

Peters, R. M., M. J. Cherry, J. C. Kilgo, M. J. Chamberlain, and K. V. Miller. 2020. White-tailed deer population dynamics following Louisiana black bear recovery. Journal of Wildlife Management 84:1473–1482.

Pfister, C. A. 1998. Patterns of variance in stage-structured populations: evolutionary predictions and ecological implications. Proceedings of the National Academy of Sciences 95:213–218.

Pierce, B. M., V. C. Bleich, K. L. Monteith, and R. T. Bowyer. 2012. Top-down versus bottom-up forcing: evidence from mountain lions and mule deer. Journal of Mammalogy 93:977–988.

Preisser, E. L., D. I. Bolnick, and M. F. Benard. 2005. Scared to death? The effects of intimidation and consumption in predator-prey interactions. Ecology 86:501–509.

Ripple, W. J., J. A. Estes, R. L. Beschta, C. C. Wilmers, E. G. Ritchie, M. Hebblewhite, J. Berger, B. Elmhagen, M. Letnic, M. P. Nelson, O. J. Schmitz, D. W. Smith, A. D. Wallach, A. J. Wirsing. 2014. Status and ecological effects of the world's largest carnivores. Science 343:1241484. DOI: 10.1126/science.1241484

Ritcher, A. R., and R. F. Labisky. 1985. Reproductive dynamics among disjunct white-tailed deer herds in Florida. Journal of Wildlife Management 49:964–971.

Roberts, N. M., and S. M. Crimmins. 2010. Bobcat population status and management in North America: Evidence of large-scale population increase. Journal of Fish and Wildlife Management 1:169–174.

Rosenzweig, M. L., and R. H. MacArthur. 1963. Graphical representation and stability conditions of predator-prey interactions. American Naturalist 97:209–223.

Royle, J. A., A. K. Fuller, and C. Sutherland. 2017. Unifying population and landscape ecology with spatial capture-recapture. Ecography 40:1–12.

Schoener, T. W., D. A. Spiller, and J. B. Losos. 2001. Predators increase the risk of catastrophic extinction of prey populations. Nature 412:183-186.

Schortemeyer, J. L. D. S. Maehr, J. W. McCown, E. D. Land, and P. D. Manor. 1991. Prey management for the Florida panther: a unique role for wildlife managers. Transactions of the North American Wildlife and Natural Resources Conference 56:512–526.

Shea, S. M., T. A. Breault, and M. L. Richardson. 1992. Herd density and physical condition of white-tailed deer in Florida Flatwoods. Journal of Wildlife Management 56:262–267.

Sklar, F. H., M. J. Chimney, S. Newman, P. McCormick, D. Gawlik, S. Miao, C. McVoy, W. Said, J. Newman, C. Coronado, and G. Crozier. 2005. The ecological–societal underpinnings of Everglades restoration. Frontiers in Ecology and the Environment 3:161–169.

Smith, T. R., C. G. Hunter, J. F. Eisenberg, and M. E. Sunquist. 1996. Ecology of white-tailed deer in eastern Everglades National Park: an overview. Bulletin of the Florida Museum of Natural History 39:141–172.

Soría-DÍaz, L., M. S. Fowler, and O. Monroy-Vilchis. 2017. Top-down and bottom-up control on cougar and its prey in a central Mexican natural reserve. European Journal of Wildlife Research 63:73. DOI: 10.1007/s10344-017-1129-y.

Telesco, D. 2012. Florida black bear removed from list of state threatened species. International Bear News 27:10–11.

U.S. Fish and Wildlife Service [USFWS]. 2008. Florida panther recovery plan (*Puma concolor coryi*), third revision. U.S. Fish and Wildlife Service, Atlanta, Georgia, USA.

U.S. Seal, R. C. Lacy, editors. A plan for genetic restoration and management of the Florida panther (*Felis concolor coryi).* 1994.Report to the Florida Game and Fresh Water Fish Commission, Conservation Breeding Specialist Group, Apple Valley, MN, USA.

van de Kerk, M., H. de Kroon, D. A. Conde, and E. Jongejans. 2013. Carnivora population dynamics are as slows and as fast as those of other mammals: implications for their conservation. PLoS One 8:e70354. DOI: 10.1371/journal.pone.0070354.

van de Kerk, M. D. P. Onorato, J. A. Hostetler, B. M. Bolker, and M. K. Oli. 2019. Dynamics, persistence, and genetic management of the endangered Florida Panther Population. Wildlife Monographs 203:3–35.

van der Valk, A. G., J. C. Volin, and P. R. Wetzel. 2015. Predicted changes in interannual water-level fluctuations due to climate change and its implications for the vegetation of the Florida Everglades. Environmental Management 55:799–806.

Volterra, V. 1926. Fluctuations in the abundance of a species considered mathematically. Nature 118:558–560.

Wiederholt, R., G. A. Stainbeck, R. Paudel, Y. Khare, M. Naja, S. E. Davis III, and T. Van Lent. 2020. Economic valuation of the ecological response to hydrologic restoration in the

Greater Everglades ecosystem. Ecological Indicators 117:106678. DOI: 10.1016/j.ecolind.2020.106678

Wilson, J. D., M. E. Dorcas, and R. W. Snow. 2011. Identifying plausible scenarios for the establishment of invasive Burmnese pythons (*Python molurus*) in Southern Florida. Biological Invasions 13:1492–1504.

Wolf, C., and W. J. Ripple. 2016. Prey depletion as a threat to the world's large carnivores. Royal Society Open Science 3:160252. DOI: 10.1098/rsos.160252.

Whittington, J., M. Hebblewhite, N. J. DeCesare, L. Neufeld, M. Bradley, J. Wilmshurst, and M. Musiani. 2011. Caribou encounters with wolves increase near roads and trails: a time-to-event approach. Journal of Applied Ecology 48:1535–1542.

Table 4.1. Values for parameters used in the population matrices derived from previous literature and observed vital rates from 2015–2017 for white-tailed deer in Big Cypress National Preserve, Florida, USA.

	Stage	Pre-panther restoration	Post-panther restoration
Survival probability (*s*)	Fawn	0.26	0.28
	Yearling	0.88	0.70
	Adult	0.81	0.70
Productivity rate (*b*)	Fawn	1.00	1.00
	Yearling	1.23	1.23
	Adult	1.32	1.32
Pregnancy probability (*p*)	Fawn	0.14	0.12
	Yearling	0.93	0.95
	Adult	0.92	0.94
Female fetal sex ratio (*r*)		0.5	0.5

Table 4.2. Sensitivity and elasticity of λ to vital rates for two post-reproductive stage-structured white-tailed deer population projection models derived from vital rates pre- and post-panther genetic restoration.

Model	Vital rate	Sensitivity	Elasticity
Pre-panther restoration	Fawn fecundity	0.134	0.003
	Yearling fecundity	0.036	0.019
	Adult fecundity	0.219	0.113
	Fawn survival	0.485	0.132
	Yearling survival	0.122	0.113
	Adult survival	0.734	0.621
Post-panther restoration	Fawn fecundity	0.148	0.003
	Yearling fecundity	0.049	0.024
	Adult fecundity	0.236	0.121
	Fawn survival	0.438	0.145
	Yearling survival	0.147	0.121
	Adult survival	0.707	0.585

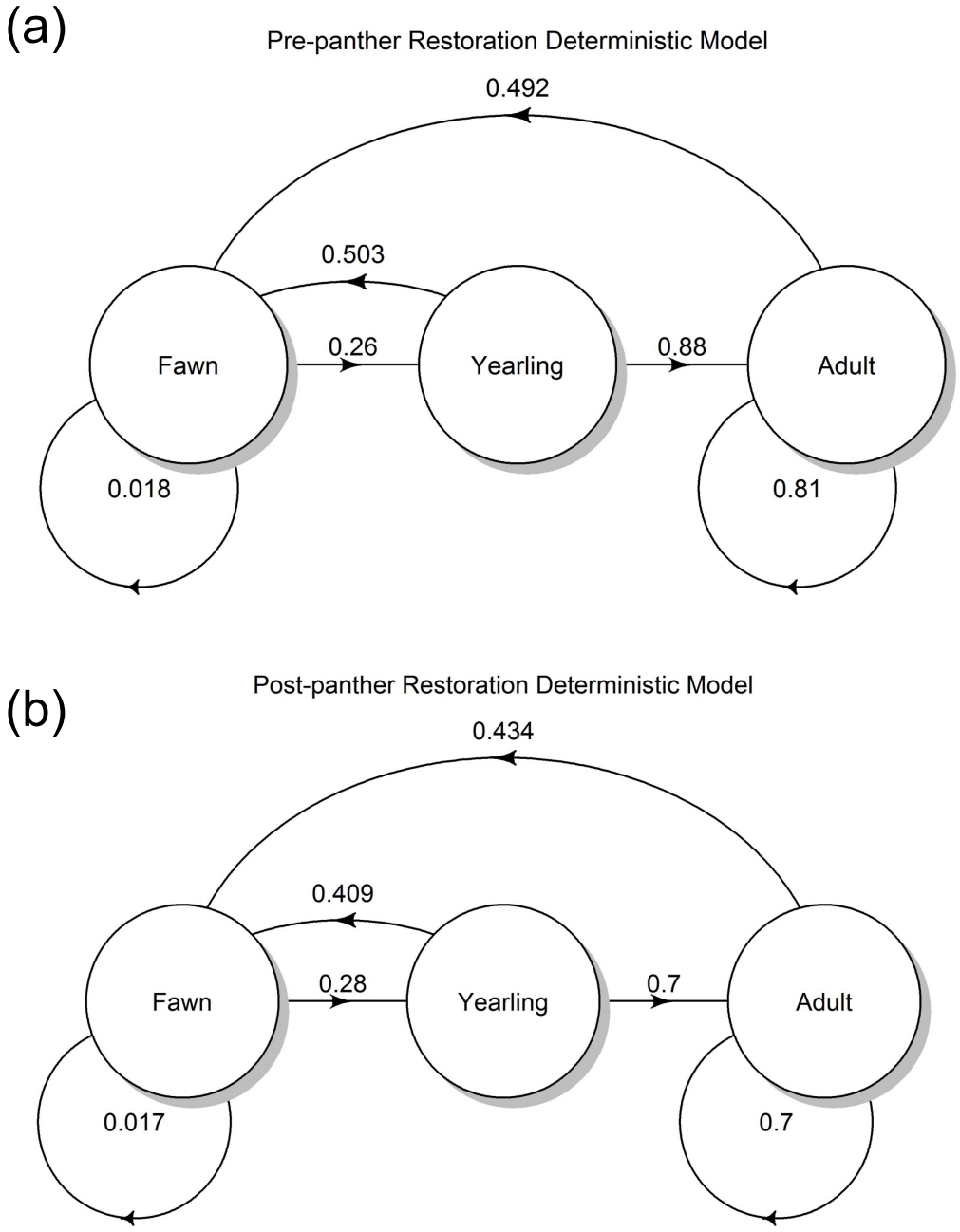

Figure 4.1. Two versions of a life cycle graph for the Big Cypress National Preserve white-tailed deer population with post-reproductive stages. (a) Derived from vital rates estimated prior to panther restoration efforts (b) Derived from vital rates estimated following panther restoration efforts.

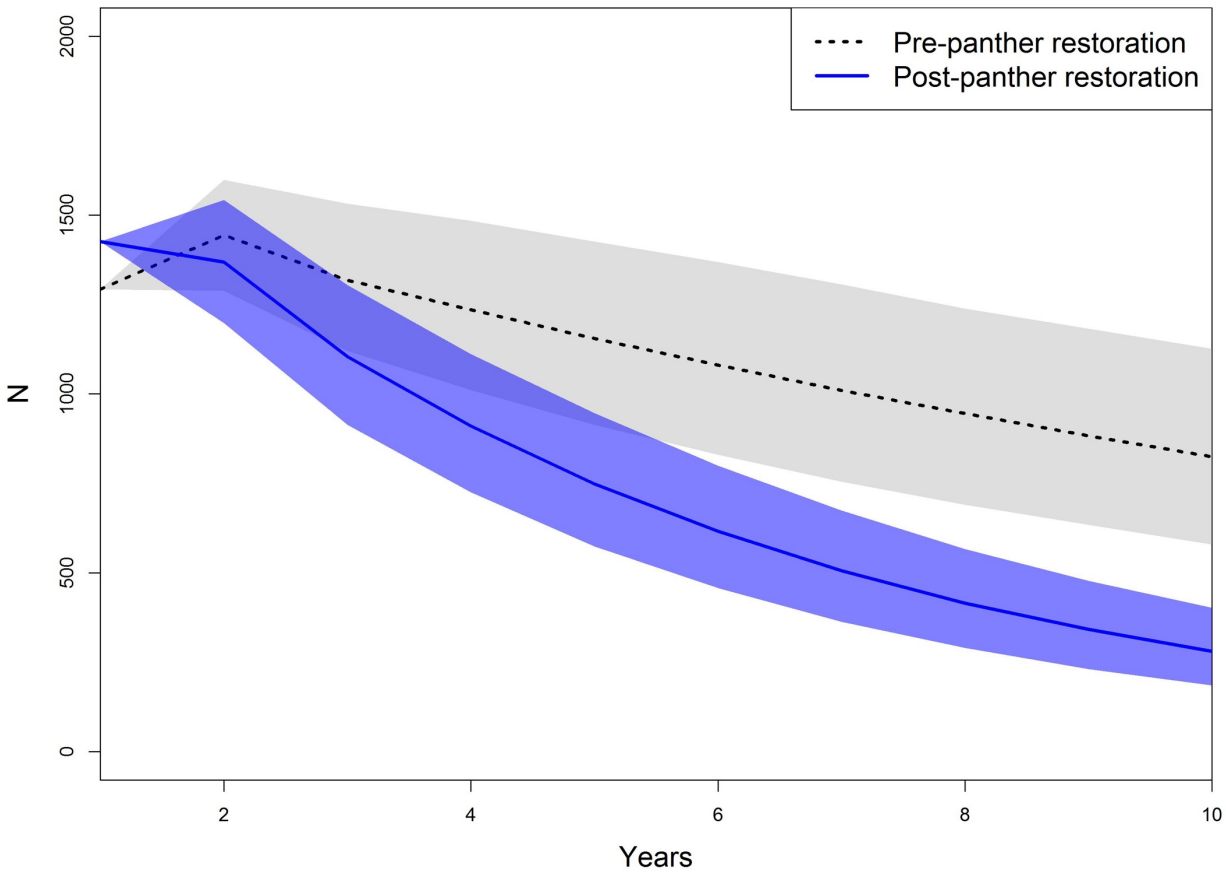

Figure 4.2. A 10-year population projection for a white-tailed deer population in the Bear Island and North Addition Lands units of the Big Cypress National Preserve. The pre-panther restoration model used density and vital rates estimates prior to the genetic rescue of the Florida Panther in 1995, while the post-panther restoration model used updated estimates after 1995.

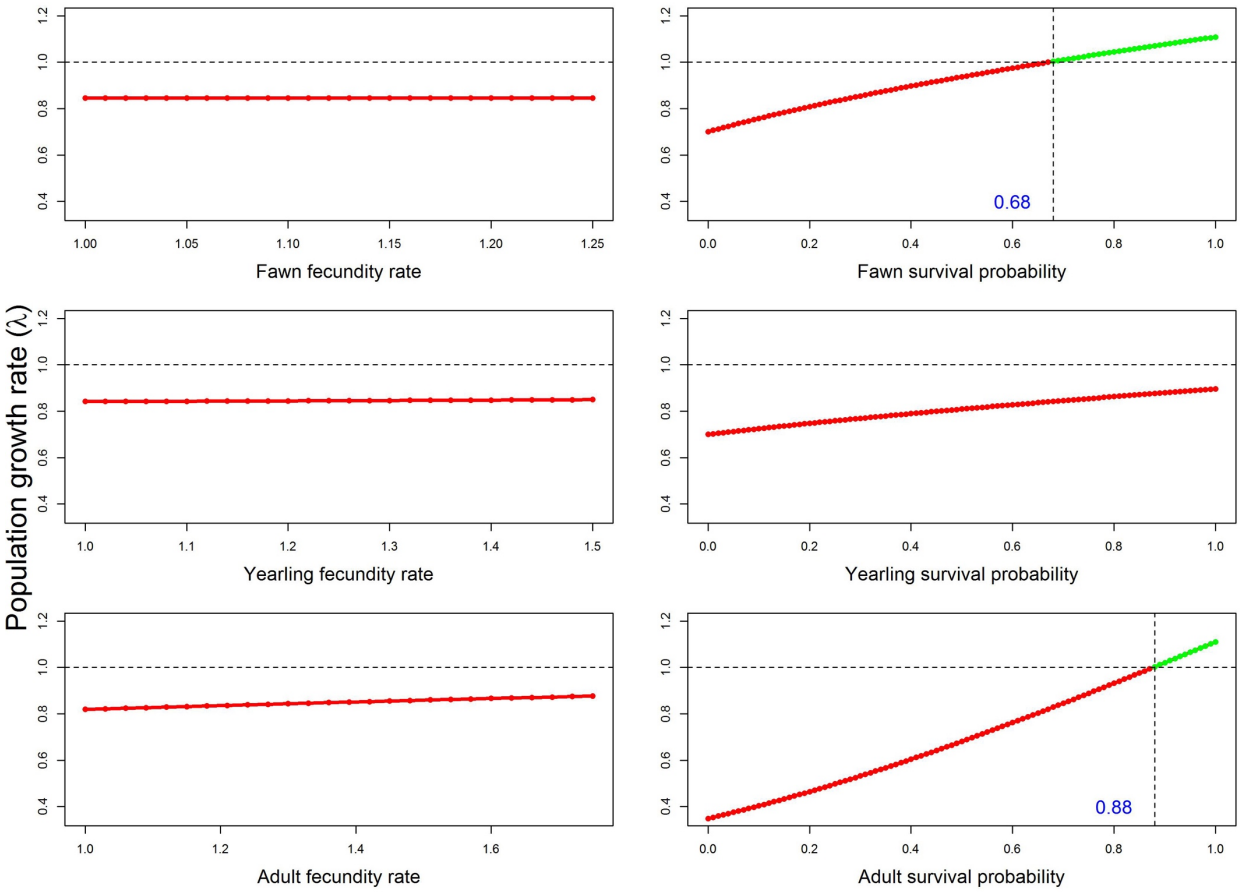

Figure 4.3. The relationship the population growth rate (λ) and vital rates for the South Florida white-tailed deer population. The focal vital rate was varied, while all other rates within the population projection matrix remained constant. The horizontal dashed line at $\lambda = 1$ represented the threshold for a stable population, with a $\lambda < 1$ indicating a declining population and a $\lambda > 1$ a growing population. The vertical dashed represented the minimum value of the vital rate required to achieve $\lambda = 1$.

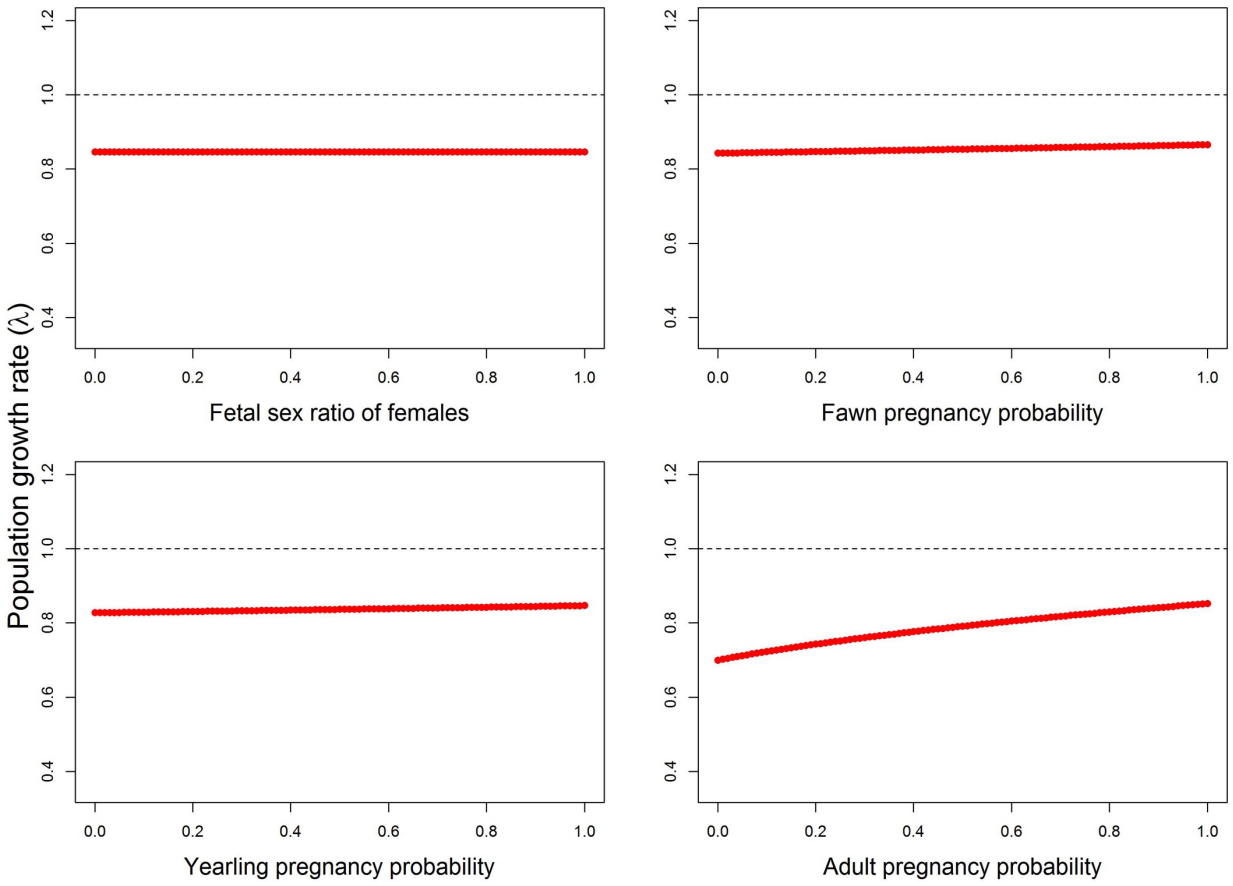

Figure 4.4. The relationship the population growth rate (λ) and vital rates for the South Florida white-tailed deer population. The focal vital rate was varied, while all other rates within the population projection matrix remained constant. The horizontal dashed line at $\lambda = 1$ represented the threshold for a stable population, with a $\lambda < 1$ indicating a declining population and a $\lambda > 1$ a growing population.

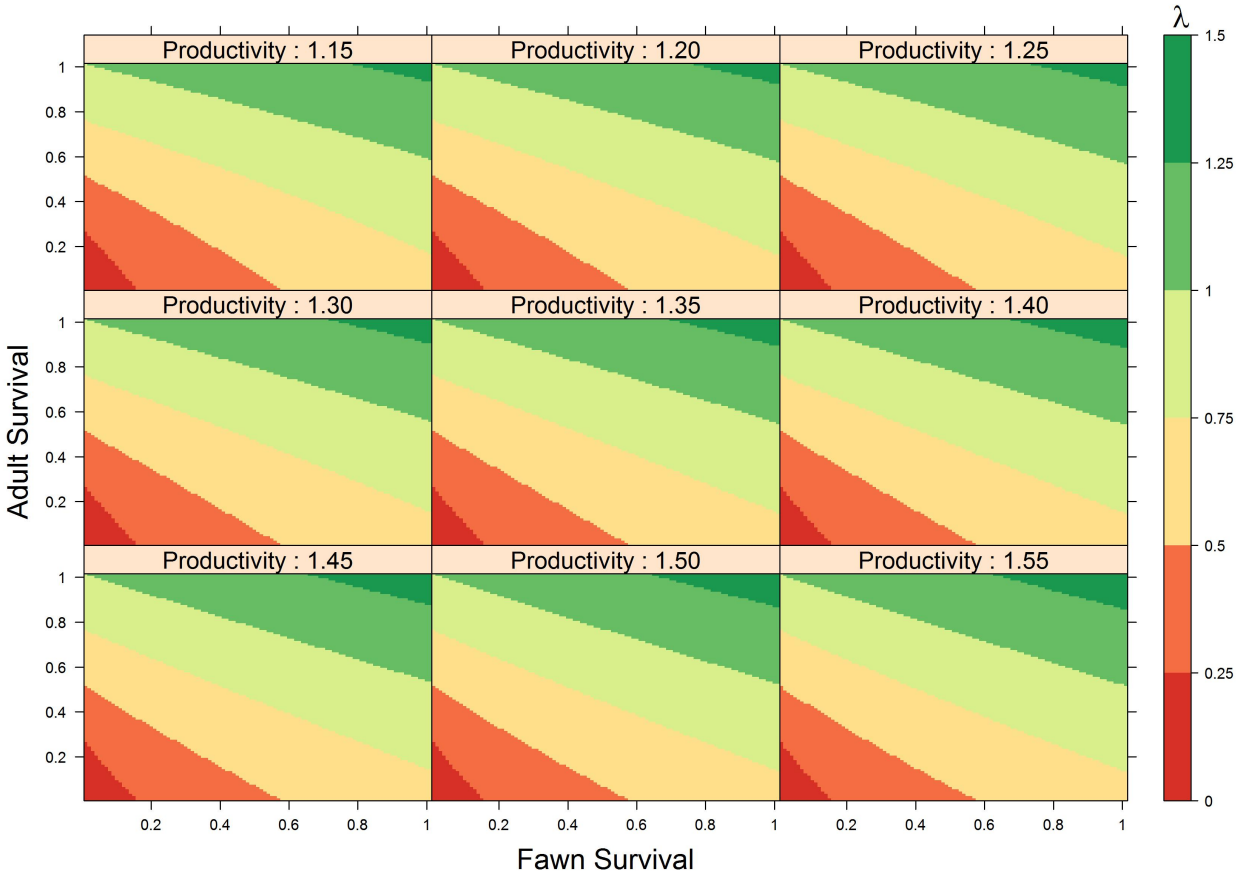

Figure 4.5. A heat map describing the relationship between population growth rate (λ) and vital rates for a Big Cypress National Preserve white-tailed deer population. Fawn and adult survival probability were varied between 0-1, while adult fecundity rates varied between 1.15-1.55. The color of each plot represents λ, with all regions in green ($\lambda > 1$) indicating a growing population.

APPENDICES

Appendix 4.A: Synthesis of population dynamics of white-tailed deer in the southeastern United States.

Table 4.A1. Mean fawn white-tailed deer survival estimates in the southeastern United States.

Location (Citation)	Years	Study method[a]	*n*[b]	Days[c]	Mean estimate	Primary cause of death
Alabama – Auburn (Saalfeld & Ditchkoff 2007)	2004-05	(1)	36	60	0.333	Coyote predation
Alabama – Fort Rucker (Jackson & Ditchkoff 2013)	2009-10	(1)	14	180	0.260	Coyote predation
Florida - Everglades National Park (Smith et al. 1996)	1987-90	(1)	10	365	0.460	Unknown
Florida – Big Cypress National Preserve and Everglades National Park (Boulay 1992)	1989-91	(1)	83	365	0.260	Bobcat predation
Florida – Big Cypress National Preserve and Everglades National Park (Labisky et al. 1995)	1989-92	(1)	80	365	0.233	Bobcat predation
Florida – Big Cypress National Preserve (Chandler et al. 2018)	2015-16	(2)	28	180	0.279	Unknown
Georgia – Joesph J. Jones Ecological Research Center (Nelson et al. 2015)	2007-12	(1)	47	140	0.290	Coyote predation
Louisiana – Tensas River National Wildlife Refuge (Shuman et al. 2017)	2013-15	(1)	70	90	0.271	Black bear predation
North Carolina – Fort Bragg Military Installation (Chitwood et al. 2015)	2011-12	(1)	65	112	0.141	Coyote predation
South Carolina – Tom Yawkey Wildlife Center (Epstein et al. 1985)	1981-82	(1)	48	<90	0.156	Bobcat predation
South Carolina – Savannah River Site (Kilgo et al. 2012)	2006-09	(1)	91	112	0.220	Coyote predation
South Carolina – Brosnan Forest (McCoy et al. 2013)	2006-10	(1)	210	180	0.490	Coyote predation

[a]Method of estimating mortality rates: (1) radio-collared fawns (2) uniquely identified fawns from camera photos
[b]Sample size used in analysis
[c]Number of days monitored/used in analysis

Table 4.A2. Mean female yearling white-tailed deer survival estimates in the southeastern United States.

Location (Citation)	Years	*n*	Mean estimate
Florida – Big Cypress National Preserve and Everglades National Park (Labisky et al. 1995)	1989-92	14	1.000
Florida – Everglades National Park (Smith et al. 1996)	1987-90	10	0.720
Louisiana - Tensas River National Wildlife Refuge (Peters et al. 2020)	2013-15	21	0.857
North Carolina – Fort Bragg Military Installation (Chitwood et al. 2015)	2011-12	4	0.775

Table 4.A3. Mean female adult white-tailed deer survival estimates in the southeastern United States.

State	Years	*n*	Mean estimate
Florida – Big Cypress National Preserve and Everglades National Park (Labisky et al. 1995)	1989-92	45	0.812
Florida - Everglades National Park (Smith et al. 1996)	1987-90	34	0.810
Florida (MacDonald-Beyers & Labisky 2005)	1994-95	51	0.487
Florida – Big Cypress National Preserve (Bled et al. *In Review*)	2015-18	156	0.700
Louisiana - Tensas River National Wildlife Refuge (Peters et al. 2020)	2013-15	70	0.815
North Carolina – Fort Bragg Military Installation (Chitwood et al. 2015)	2011-12	58	0.801

Table 4.A4. Stage-specific mean productivity estimates (fetuses/ pregnant female) for white-tailed deer in the southeastern United States.

Location (Citation)	Years	*n*	Fawn estimate	Yearling estimate	Adult estimate
Florida – North and Central (Harlow 1972)	1972	99			1.24
Florida (Richter & Labisky 1985)	1978-81	380	1.25	1.14	1.32
Florida – Big Cypress National Preserve (McCown et al. 1991)	1984-86	22			1.25
Florida – Everglades National Park (Fleming et al. 1994)	1985-89	32			1.18
Florida (Garrison et al. 2021)	2009-16	489	1.00	1.32	1.57
Louisiana - Tensas River National Wildlife Refuge (Peters et al. 2020)	2013-15	33		1.20	1.82
Mississippi (Jacobson et al. 1979)	1976-79	774	1.00	1.40	1.66
Mississippi (Jones et al. 2010)	1978-2007	5,210		1.30	1.77
North Carolina (Chitwood et al. 2015)	2011-12	30			1.75
South Carolina – Savannah River Site (Rhodes et al. 1985)	1965-85	1,103	1.06	1.56	1.75
South Carolina – Coastal Plain (Stone 2012)	2010-11	219		1.29	1.51

Table 4.A5. Stage-specific mean pregnancy probabilities for white-tailed deer in the southeastern United States.

Location (Citation)	Years	*n*	Fawn estimate	Yearling estimate	Adult estimate
Florida (Richter & Labisky 1985)	1978-81	380	0.14	0.93	0.92
Florida (Smith et al. 1996)	1987-90	30			0.89
Florida (Garrison et al. 2021)	2009-16	580	0.12	0.95	0.94
Mississippi - Mississippi State University Rusty Dawkins Memorial Deer Unit (Dye 2007)	2007	65	0.02		

Table 4.A6. Stage-specific mean twinning probabilities for white-tailed deer in the southeastern United States.

Location (Citation)	Years	*n*	Fawn estimate	Yearling estimate	Adult estimate
Florida (Richter & Labisky 1985)	1978-81	380	0.25	0.14	0.32
Florida – Everglades National Park (Fleming et al. 1994)	1985-89	32			0.25
Florida – (Garrison et al. 2021)	2009-16	580	0	0.30	0.53

Literature Cited

Bled, F., M. J. Cherry, E. P. Garrison, K. V. Miller, L. M. Conner, H. N. Abernathy, W. H. Ellsworth, L. L. S. Margenau, D. A. Crawford, K. N. Engebretsen, B. D. Kelly, D. B. Shindle, and R. B. Chandler. 2021. Impacts of large carnivore restoration on prey species with high economic and cultural value: A case study of Florida panther and white-tailed deer. Manuscript in review.

Boulay, M. C. 1992. Mortality and recruitment of white-tailed deer fawns in the wet prairie/tree island habitat of the Everglades. M. S. Thesis, University of Florida, Gainesville, Florida.

Chandler, R. B., K. Engebretsen, M. J. Cherry, E. P. Garrison, and K. V. Miller. 2017. Estimating recruitment from capture-recapture data by modeling spatio-temporal variation in birth and age-specific survival rates. Methods in Ecology and Evolution 9:2115–2130.

Chitwood, M. C., M. A. Lashley, J. C. Kilgo, C. E. Moorman, and C. S. DePerno. 2015. White-tailed deer population dynamics and adult female survival in the presence of a novel predator. Journal of Wildlife Management 79:211–219.

Dye, M. P. 2007. Effects of body mass, physiographic region, and environmental cues on reproductive timing in deer. M.S. Thesis. Mississippi State University, Starkville, Mississippi.

Epstein, M. B., G. A. Feldhamer, R. L. Joyner, R. J. Hamilton, and W. G. Moore. 1985. Home range and mortality of white-tailed deer fawns in coastal South Carolina. Proceedings of the Annual Conference Southeastern Association of Fish and Wildlife Agencies 39:373–379.

Fleming, D. M., J. Schortemeyer, and J. Ault. 1994. Distribution, abundance and demography of white-tailed deer in the Everglades. Pages 494–503 *in* D. Jordan, editor. The Proceedings of the Florida Panther Conference, Fort Myers, Florida. U.S. Fish and Wildlife Service.

Garrison, E. P., E. H. Leone, L. S. Perrin, R. M. Peters, C. R. Morea, and F. Bled. 2021. White-tailed deer breeding chronology and productivity in Florida. Unpublished manuscript.

Harlow, R. F. 1972. Reproductive rates in white-tailed deer of Florida. Quarterly Journal of the Florida Academy of Sciences 35:165–170.

Jackson, A. M. and S. S. Ditchkoff. 2013. Survival estimates of white-tailed deer fawns at Fort Rucker, Alabama. American Midland Naturalist 170:184–190.

Jacobson, H. A., D. C. Guynn, Jr., R. N. Griffin, and D. Lewis. 1979. Fecundity of white-tailed deer in Mississippi and periodicity of corpora lutea and lactation. Proceedings of the Annual Conference of the Southeastern Association of Fish and Wildlife Agencies 33:30–35.

Jones, P. D., B. K. Strickland, S. Demarais, and A. C. Blaylock. 2010. Reproductive characteristics of white-tailed deer in Mississippi. Southeastern Naturalist 9:803–812.

Kilgo, J. C., H. S. Ray, M. Vukovich, M. J. Goode, and C. Ruth. 2012. Predation by coyotes on white-tailed deer neonates in South Carolina. Journal of Wildlife Management 76:1420–1430.

Labisky, R. F., M. C. Boulay, K. E. Miller, R. A. Sargent, Jr., and J. M. Zultowsky. 1995. Population ecology of white-tailed deer in Big Cypress National Preserve and Everglades National Park. Final Report to United States Department of Interior – National Park Service, Department of Wildlife Ecology and Conservation, University of Florida, Gainesville, Florida.

MacDonald-Beyers, K., and R. F. Labisky. 2005. Influence of flood waters on survival, reproduction, and habitat use of white-tailed deer in the Florida Everglades. Wetlands 25: 659-666.

McCown, J. W., M. E. Roelke, D. J. Forrester, C. T. Moore, J. C. Roboski. 1991. Physiological evaluation of 2 white-tailed deer herds in southern Florida. Proceedings of the Annual Conference of the Southeastern Association of Fish and Wildlife Agencies 45:81–90.

McCoy, J. C., S. S. Ditchkoff, S. B. Raglin, B. A. Collier, and C. Ruth. 2013. Factors influencing survival of white-tailed deer fawns in coastal South Carolina. Journal of Fish and Wildlife Management 4:280–289.

Nelson, M. A., M. J. Cherry, M. B. Howze, R. J. Warren, and L. M. Conner. 2015. Coyote and bobcat predation on white-tailed deer fawns in a longleaf pine ecosystem in southwestern Georgia. Journal of the Southeastern Association of Fish and Wildlife Agencies 2:208–213.

Peters, R. M., M. J. Cherry, J. C. Kilgo, M. J. Chamberlain, and K. V. Miller. 2020. White-tailed deer population dynamics following Louisiana black bear recovery. Journal of Wildlife Management 84:1473–1482.

Rhodes, O. E. Jr., K. T. Scribner, M. H. Smith, P. E. Johns. 1985. Proceedings of the Annual Conference Southeastern Association of Fish and Wildlife Agencies 39: 390–388.

Ritcher, A. R. and R. F. Labisky. 1985. Reproductive dynamics among disjunct white-tailed deer herds in Florida. Journal of Wildlife Management 49:964–971.

Saalfeld, S. T. and S. S. Ditchkoff. 2007. Survival of neonatal white-tailed deer in an exurban population. Journal of Wildlife Management 71:940–944.

Shuman, R. M., M. J. Cherry, T. N. Simoneaux, E. A. Dutoit, J. C. Kilgo, M. J. Chamberlain, K. V. Miller. 2017. Survival of white-tailed deer neonates in Louisiana. Journal of Wildlife Management 81:834–845.

Smith, T. R., C. G. Hunter, J. F. Eisenberg, and M. E. Sunquist. 1996. Ecology of white-tailed deer in eastern Everglades National Park: an overview. Bulletin of the Florida Museum of Natural History 39:141–172.

Stone, D. 2012. Novel data as a source for assessing breeding phenology of white-tailed deer (*Odocoileus virginianus*) in South Carolina. M.S. Thesis. Clemson University, Clemson, South Carolina.

Appendix 4.B. Demographic analysis for Florida Panther National Wildlife Refuge.

The Florida Panther National Wildlife Refuge (FPNWR) is a ~107 km^2 area adjacent to the Big Cypress National Preserve (BCNP) managed by the U.S. Fish and Wildlife Service. We extended our population viability analysis to project female white-tailed deer population growth for the FPNWR under various demographic scenarios. We compared predictions of population growth and extinction risk using vital rates and density estimates from pre- and post-panther genetic restoration. Additionally, we evaluated the sensitivity and elasticity of population growth rate to vital rates.

We parameterized the pre-panther genetic restoration population matrix similar to the analysis for BCNP and estimated initial population size ($N_0 = 301$) for fawns ($n_{1,0} = 36$), yearlings ($n_{2,0}$ = 39), and adults ($n_{3,0}$ = 226). We parameterized the post-panther genetic restoration population matrix using a combination of vital rates from previous literature and more recent survival rates derived from camera and radio-telemetry data collected in Florida Panther National Wildlife Refuge (FPNWR) in 2015–2018 (Table B1, Figure B1). For fecundity, we used vital rates similar to the pre- and post- panther restoration model for BCNP. We used a fawn survival probability of 28% by averaging survival estimates from 2015 (42.5%) and 2016 (13.2%) derived from capture-recapture data (Chandler et al. 2018). We used the average annual survival (78%) of GPS-collared female deer in FPNWR from 2015–2017 to describe both yearling and adult survival (Bled et al. *In Review*, Cherry et al. 2019). We estimated initial population size ($N_0 = 460$) for fawns ($n_{1,0} = 55$), yearlings ($n_{2,0}$ = 60), and adults ($n_{3,0}$ = 345) for the model using a mean female density estimate (4.3 females/ km^2) for FPNWR (Margenau et al. *In Review*) and an estimated female age structure of 12% fawns, 13% yearlings, and 75% adults (Garrison et al. 2021) extrapolated to the ~107 km^2 area of the FPNWR.

The deterministic model for the post-panther restoration scenario on FPNWR yielded a population growth rate of $\lambda = 0.927$, with reproductive values of 1.000, 3.252, and 3.283 for the fawn, yearling, and adult stages, respectively. The stable stage distribution was similar to the pre-panther restoration model with 35% fawns, 10% yearlings, and 55% adults. Incorporating environmental and demographic stochasticity into this population model resulted in a mean population growth rate of $\lambda = 0.936$ (95% CI: 0.837–1.04). Abundance on FPNWR was forecasted to be N_5 = 260 (198-328) females, N_{10} = 174 (113-247) females, N_{15} = 117 (66-182) females, N_{20} = 78 (38-132) females, and N_{25} = 52 (20-97) females (Figure B2). The sensitivity of λ to vital rates was similar between the pre- and post-panther genetic restoration model (Table B2). Adult survival had the strongest influence on λ, followed by fawn survival and adult fecundity. Yearling fecundity had the weakest influence on λ. Elasticity was similar to sensitivity. Only two vital rates resulted in stable and/or increasing population growth rates (Figures B3–B4). Increasing fawn survival to 45% or increasing adult survival to 87% would yield a stable population with the FPNWR.

Table 4.B1. Values for parameters used in the population matrices derived from previous literature and observed vital rates from 2015– 2017 for white-tailed deer in the Florida Panther National Wildlife Refuge, Florida, USA.

	Stage	Pre-panther restoration	Post-panther restoration
Survival probability	Fawn	0.26	0.28
	Yearling	0.88	0.78
	Adult	0.81	0.78
Productivity rate	Fawn	1.0	1.0
	Yearling	1.23	1.23
	Adult	1.32	1.32
Pregnancy probability	Fawn	0.14	0.12
	Yearling	0.93	0.95
	Adult	0.92	0.94
Female fetal sex ratio		0.5	0.5

Table 4.B2. Sensitivity and elasticity of λ to vital rates for a post-reproductive stage-structured white-tailed deer population projection models derived from vital rates pre- and post-panther genetic restoration.

Model	Vital rate	Sensitivity	Elasticity
Pre-panther restoration	Fawn fecundity	0.134	0.003
	Yearling fecundity	0.036	0.019
	Adult fecundity	0.219	0.113
	Fawn survival	0.485	0.132
	Yearling survival	0.122	0.113
	Adult survival	0.734	0.621
Post-panther restoration	Fawn fecundity	0.138	0.003
	Yearling fecundity	0.042	0.024
	Adult fecundity	0.221	0.115
	Fawn survival	0.450	0.136
	Yearling survival	0.137	0.115
	Adult survival	0.726	0.610

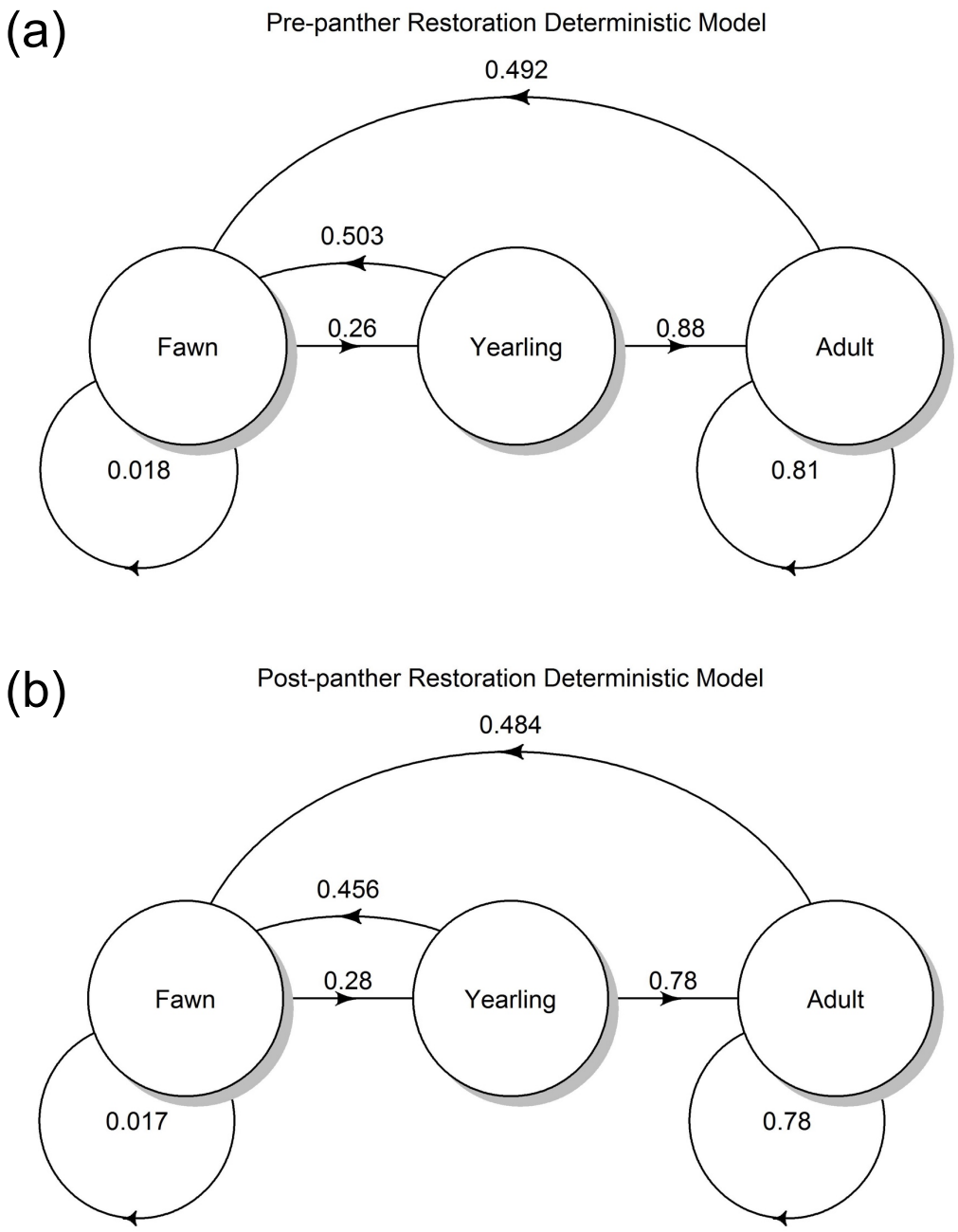

Figure 4.B1. Two versions of a life cycle graph for the Florida Panther National Wildlife Refuge white-tailed deer population with post-reproductive stages. (a) Derived from vital rates estimated prior to panther restoration efforts (b) Derived from vital rates estimated following panther restoration efforts.

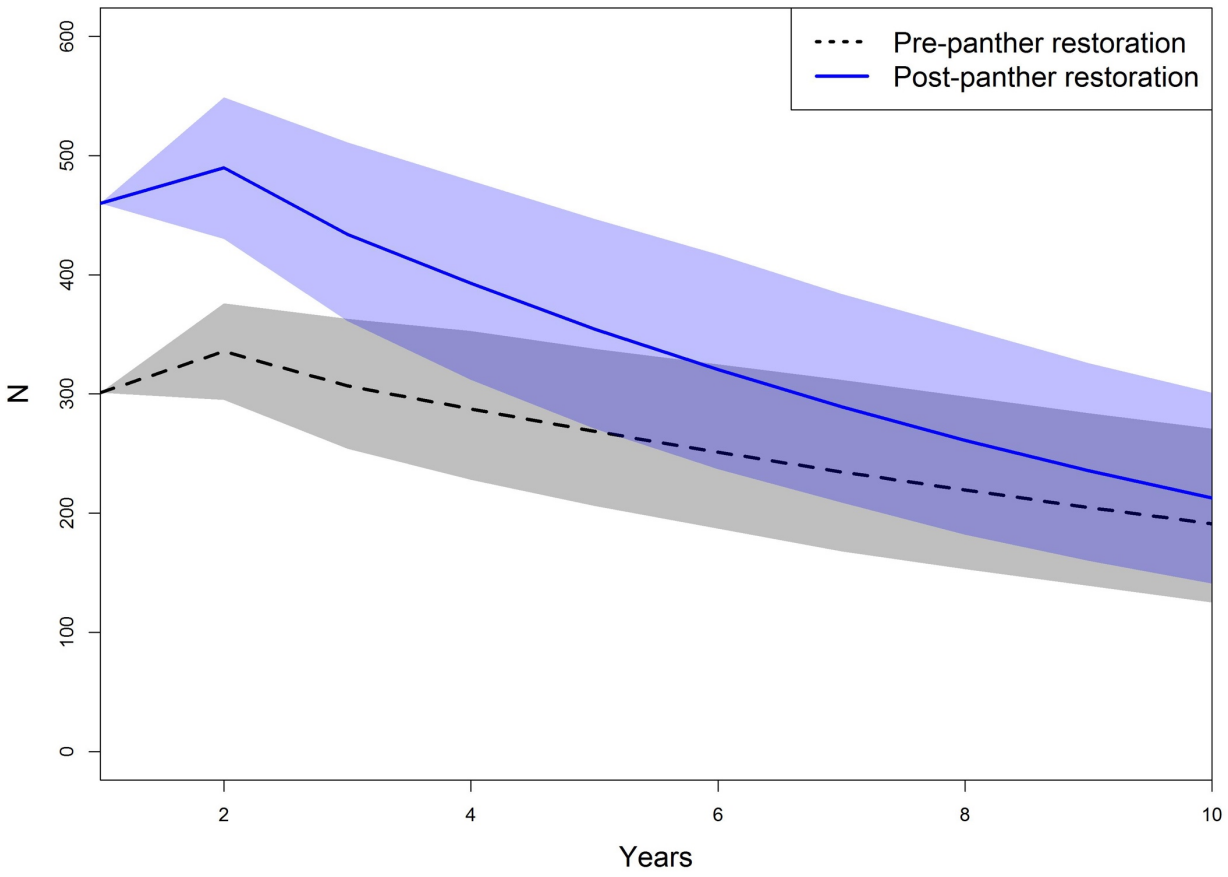

Figure 4.B2. A 10-year population projection for a white-tailed deer population in the Florida Panther National Wildlife Refuge. The pre-panther restoration model used density and vital rates estimates prior to the genetic rescue of the Florida Panther in 1995, while the post-panther restoration model used updated estimates after 1995.

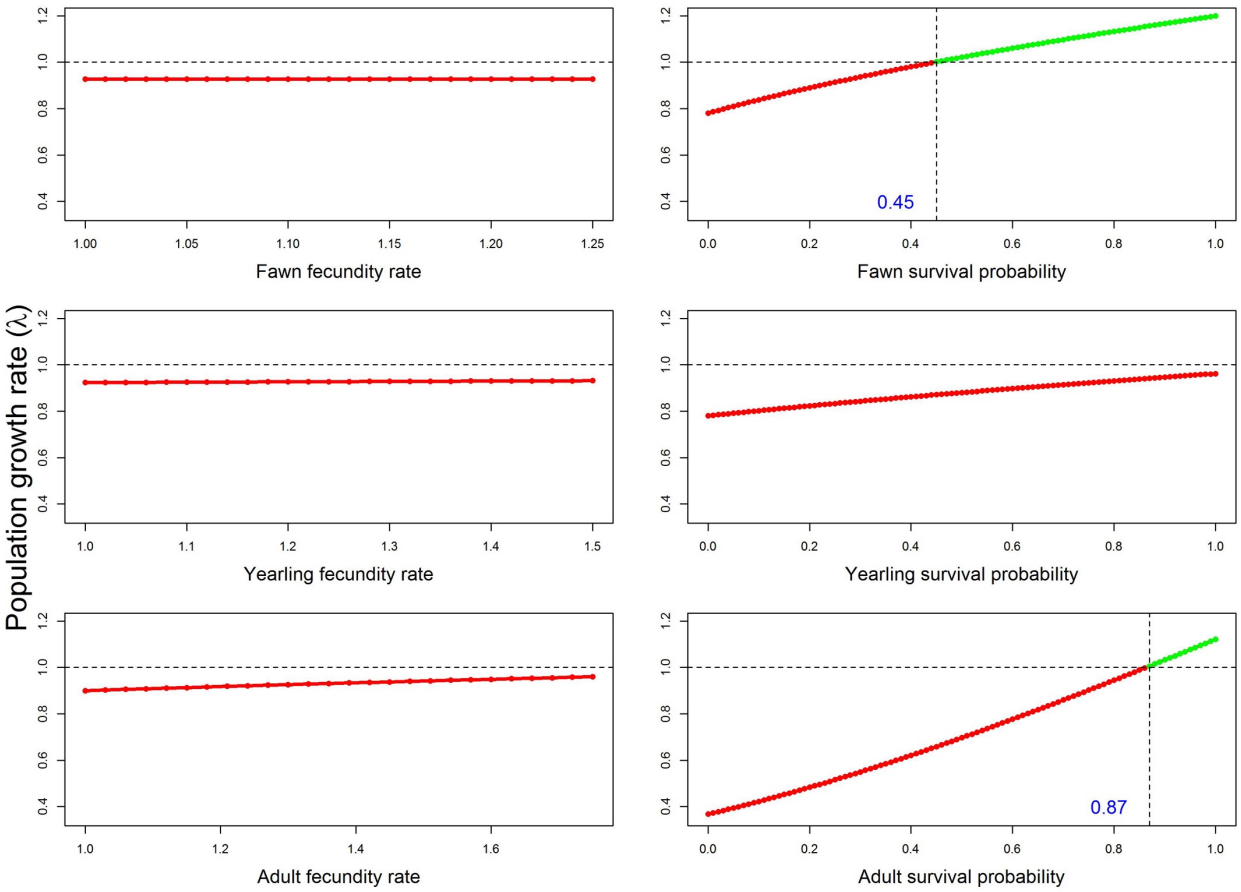

Figure 4.B3. The relationship the population growth rate (λ) and vital rates for the South Florida white-tailed deer population. The response vital rate was varied, while all other rates within the population projection matrix remained constant. The horizontal dashed line at $\lambda = 1$ represented the threshold for a stable population, with a $\lambda < 1$ indicating a declining population and a $\lambda > 1$ a growing population. The vertical dashed represented the value at which the vital rate reached $\lambda = 1$.

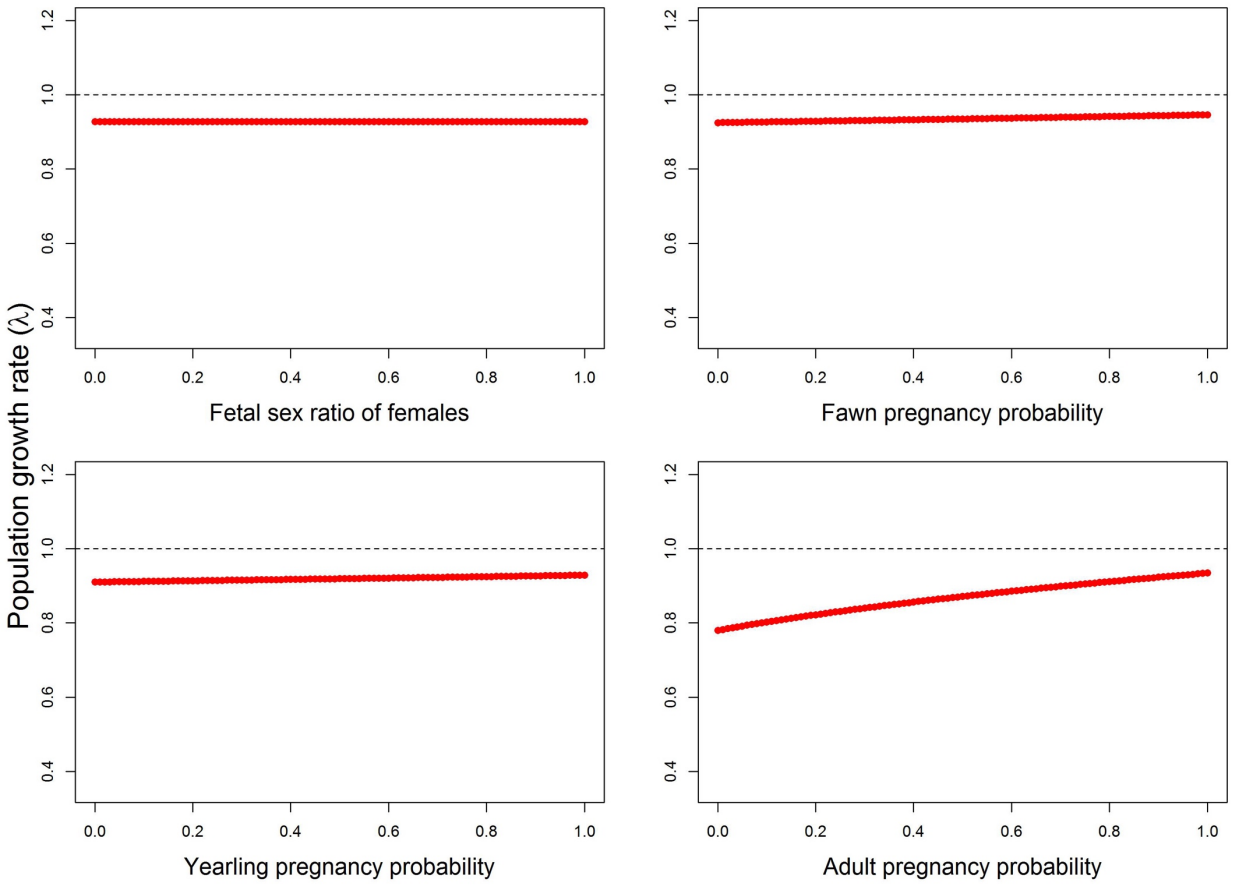

Figure 4.B4. The relationship the population growth rate (λ) and vital rates for the South Florida white-tailed deer population. The response vital rate was varied, while all other rates within the population projection matrix remained constant. The horizontal dashed line at $\lambda = 1$ represented the threshold for a stable population, with a $\lambda < 1$ indicating a declining population and a $\lambda > 1$ a growing population.

CHAPTER 5

CONCLUSIONS, MANAGEMENT RECOMENDATIONS, AND FUTURE RESEARCH

Highly dynamic systems often require long-term data to understand population dynamics and make informed management decisions. I developed a generalized SMR model that can accommodate long-term camera data and auxiliary telemetry data for improved spatio-temporal inference in monitoring efforts. The model can be applied in two-stages, with detection parameters estimated in the first stage using telemetry data and camera detections of instrumented individuals. Density is estimated in the second stage using camera data, with all individuals treated as unmarked. Serial correlation in detection and density parameters is accounted for using time-series models. The two-stage approach reduces computational demands and facilitates the application to large datasets from long-term monitoring initiatives. Density estimates were higher in the western portion of the study area and lower in the eastern region. Temporal variation in density was driven primarily by seasonal environmental conditions, but one study site exhibited a potential long-term population decline. Transitioning the spatial-mark-resight model from the closed population model using fortnights to a three-year open population model or integrated population model would allow for the incorporation of demographic processes (Gardner et al. 2010, Chandler and Clark 2014, Gardner et al. 2018). Incorporating survival (Bled et al. *In Review*) and recruitment processes (Chandler et al. 2018) would provide more precise estimates of population abundance and aid in understanding the mechanisms underlying density trends.

I conducted a simulation study to identify the optimal design for camera-based monitoring of white-tailed deer populations in the study area. I assessed 10 potential designs for each of the three study sites using simulated data based on the camera study. The results demonstrated that the current design resulted in relatively low bias and high precision, however, little is gained with the labor-intensive step of deploying a portion of cameras off trails. The best design for estimating abundance and density involved 60 on-trail cameras at each of the three study sites. However, when balancing the costs of each design with the accuracy of the estimates, the optimal design involved 40 on-trail cameras at each of the three sites.

I conducted a series of population viability analyses which suggested the deer population is likely to decline in the northern management units of BCNP, similar to the declines observed in the southern management units. Although I found white-tailed deer population growth rates have decline since the panther restoration, our estimates of population growth suggest the deer population was already declining prior to the initiation of the restoration efforts in 1995. The recent decrease in deer population growth rates appears to be the result of increased adult mortality rates (Bled et al. *In Review*). Nonetheless, the fact that the deer population was declining before the panther restoration suggests that other factors such as the hydrology, predator community, poor soil fertility, and hunting regulations were limiting the populations. Spatially explicit approaches to the study of demography may be especially important within dynamic ecosystems, such as South Florida, in which vital rates and habitat selection decisions can depend strongly on where an individual occurs in the landscape. Linking population dynamics with landscape structure provides a more sensitive approach to demographic modeling for population viability (Dunning et al. 1995, Gurevitch et al. 2016, Royle et al. 2017). While the results do not support the conclusion that panthers have caused the deer population declines, it

does appear that predator restoration has sped up the declines, which could threaten the long-term viability of the panther population unless management can intervene to bolster the prey population. The study demonstrates that large predator restoration can reduce the viability of prey populations, suggesting that managers should formally account for prey population dynamics when planning predator recovery.

Adult female survival was the most sensitive parameter to population growth. Large increases in adult female survival are needed to stabilize the population. Habitat and water management directed at improving adult survival should be considered to prevent future deer population declines. The use of prescribed fire and invasive vegetation management could reduce concealment cover, increase predator detection, and potentially improve deer survival. In the event that habitat management is not effective at increasing survival, managers should consider more drastic actions such as prey supplementation to alleviate predation pressure. Supplementation of the prey community through stocking programs could enhance prey abundances, potentially alleviating predation pressure on deer (Schortemeyer et al. 1991); however, reintroducing non-native species such as wild hogs would be highly controversial as it could negatively affect plant communities and possibly increase disease transmission. Additionally, although wildlife populations are only one consideration influencing decisions about water management in South Florida, adding more water to the northern units of BCNP, especially during fawning season, would likely negatively affect the deer population and the predators it supports.

My results suggest there may be an insufficient prey base to meet the long-term panther recovery goal within my study area for delisting as an endangered species. The current recovery goal is to achieve long-term viability of the Florida panther through a strategy that maintains the

viability of the current population in South Florida and expands the breeding portion of the population to areas north of the Caloosahatchee River. I recommend establishing a before-after-control-impact study to assess white-tailed deer population dynamics north of the Caloosahatchee River prior to the expansion of the Florida panther range. The analysis of prey population viability prior to large carnivore restoration efforts would allow managers to determine the degree to which habitat management of prey will be required for successful expansion of the panther population.

LITERATURE CITED

Bled, F., M. J. Cherry, E. P. Garrison, K. V. Miller, L. M. Conner, H. N. Abernathy, W. H. Ellsworth, L. L. S. Margenau, D. A. Crawford, K. N. Engebretsen, B. D. Kelly, D. B. Shindle, and R. B. Chandler. 2021. Impacts of large carnivore restoration on prey species with high economic and cultural value: A case study of Florida panther and white-tailed deer. Manuscript in review.

Chandler, R. B., and J. D. Clark. 2014. Spatially explicit integrated population models. Methods in Ecology and Evolution 5:1351–1360.

Chandler, R. B, K. Engebretsen, M. J. Cherry, E. P. Garrison, and K. V. Miller. 2018. Estimating recruitment from capture-recapture data by modeling spatio-temporal variation in birth and age-specific survival rates. Methods in Ecology and Evolution 9:2115–2130.

Dunning, J. B. Jr., D. J. Stewart, B. J. Danielson, B. R. Noon, T. L. Root, R. H. Lamberson, and E. E. Stevens. Spatially explicit population models: current forms and future uses. Ecological Application 5:3–11.

Gardner, B., J. Reppucci, M. Lucherini, and J. A. Royle. 2010. Spatially explicit inference for open populations: estimating demographic parameters from camera-trap studies. Ecology 91:3376–3383.

Gardner, B., R. Sollmann, N. S. Kumar, D. Jathanna, and K. U. Karanth. 2018. State space and movement specification in open population spatial capture-recapture models. Ecology and Evolution 8:10336–10344.

Gurevitch, J., G. A. Fox, N. L. Fowler, and C. H. Graham. 2016. Landscape demography: population change and its drivers across spatial scales. Quarterly Review of Biology 91:459-485.

Royle, J. A., A. K. Fuller, and C. Sutherland. 2017. Unifying population and landscape ecology with spatial capture-recapture. Ecography 40:1–12.

Schortemeyer, J. L. D. S. Maehr, J. W. McCown, E. D. Land, and P. D. Manor. 1991. Prey management for the Florida panther: a unique role for wildlife managers. Transactions of the North American Wildlife and Natural Resources Conference 56:512–526.